frontiers | Research Topics

Infectious diseases and hematology: Diagnosis and management

Edited by
Tomás José González-López and Pierpaolo Di Micco

Published in
Frontiers in Medicine
Frontiers in Public Health

ISSN 1664-8714
ISBN 978-2-8325-4676-5
DOI 10.3389/978-2-8325-4676-5

About Frontiers

Frontiers is more than just an open access publisher of scholarly articles: it is a pioneering approach to the world of academia, radically improving the way scholarly research is managed. The grand vision of Frontiers is a world where all people have an equal opportunity to seek, share and generate knowledge. Frontiers provides immediate and permanent online open access to all its publications, but this alone is not enough to realize our grand goals.

Frontiers journal series

The Frontiers journal series is a multi-tier and interdisciplinary set of open-access, online journals, promising a paradigm shift from the current review, selection and dissemination processes in academic publishing. All Frontiers journals are driven by researchers for researchers; therefore, they constitute a service to the scholarly community. At the same time, the *Frontiers journal series* operates on a revolutionary invention, the tiered publishing system, initially addressing specific communities of scholars, and gradually climbing up to broader public understanding, thus serving the interests of the lay society, too.

Dedication to quality

Each Frontiers article is a landmark of the highest quality, thanks to genuinely collaborative interactions between authors and review editors, who include some of the world's best academicians. Research must be certified by peers before entering a stream of knowledge that may eventually reach the public - and shape society; therefore, Frontiers only applies the most rigorous and unbiased reviews. Frontiers revolutionizes research publishing by freely delivering the most outstanding research, evaluated with no bias from both the academic and social point of view. By applying the most advanced information technologies, Frontiers is catapulting scholarly publishing into a new generation.

What are Frontiers Research Topics?

Frontiers Research Topics are very popular trademarks of the *Frontiers journals series*: they are collections of at least ten articles, all centered on a particular subject. With their unique mix of varied contributions from Original Research to Review Articles, Frontiers Research Topics unify the most influential researchers, the latest key findings and historical advances in a hot research area.

Find out more on how to host your own Frontiers Research Topic or contribute to one as an author by contacting the Frontiers editorial office: frontiersin.org/about/contact

Infectious diseases and hematology: Diagnosis and management

Topic editors

Tomás José González-López — Burgos University Hospital, Spain

Pierpaolo Di Micco — Ospedale Santa Maria delle Grazie, Italy

Citation

González-López, T. J., Di Micco, P., eds. (2024). *Infectious diseases and hematology: Diagnosis and management*. Lausanne: Frontiers Media SA. doi: 10.3389/978-2-8325-4676-5

Table of contents

frontiers | Frontiers in Medicine

TYPE Editorial
PUBLISHED 14 March 2024
DOI 10.3389/fmed.2024.1385874

OPEN ACCESS

EDITED AND REVIEWED BY
Eleni Gavriilaki,
Aristotle University of Thessaloniki, Greece

*CORRESPONDENCE
Tomás José González-López
✉ tjgonzalez@saludcastillayleon.es

RECEIVED 13 February 2024
ACCEPTED 04 March 2024
PUBLISHED 14 March 2024

CITATION
González-López TJ, Jarque I, Siniscalchi C and Di Micco P (2024) Editorial: Infectious diseases and hematology: diagnosis and management. *Front. Med.* 11:1385874. doi: 10.3389/fmed.2024.1385874

Editorial: Infectious diseases and hematology: diagnosis and management

Tomás José González-López[1]*, Isidro Jarque[2], Carmine Siniscalchi[3] and Pierpaolo Di Micco[4]

[1]Department of Hematology, Hospital Universitario de Burgos, Burgos, Spain, [2]Department of Hematology, Hospital Universitario y Politécnico La Fe, Valencia, Spain, [3]Department of Internal and Emergency Medicine, Parma University Hospital, Parma, Italy, [4]AFO MEDICA P.O. Santa Maria delle Grazie, ASL NA2 Nord, Naples, Italy

KEYWORDS

infections, hematology, diagnosis, management, vaccination

Editorial on the Research Topic
Infectious diseases and hematology: diagnosis and management

It is crucial to understand the immune status of hematological patients, as it significantly influences the severity and types of infections to which they are susceptible. Patients with neutropenia are at high risk of severe bacterial infections, and prolonged neutropenia increases the risk of fungal infections. Moreover, impaired T-cell function increases the likelihood of fungal and viral infections. Knowledge of local resistance patterns is essential to guide empirical antimicrobial therapies (1).

Regarding management, it is important to focus on prevention, diagnosis, and treatment. Thus, vaccines and anti-infective prophylaxis have improved survival rates for these patients. Having the best possible strategies for managing infections is fundamental for lowering the chances of illness and death for those who do get sick (2).

This compendium points to several issues. Thus, diverse novel aspects of the management and/or treatment of various infections, the validation of predictive risk models for infections in hematology, the COVID-19 behavior in certain populations, the optimal assessment of the response to some COVID-19 vaccinations, and atypical responses to treatments, e.g. antifungals such as voriconazole, are included here. This volume is completed by two articles focusing on other related aspects of hematology.

Pando-Caciano et al. address the management of refractory cytomegalovirus (CMV) infections in the context of pediatric haematopoietic stem cell transplantation (HSCT) highlighting the use of highly sensitive genetic tools to investigate virus resistance in a broader genome-wide range. This is the first reported case in Latin America of refractory CMV infection in a pediatric HSCT recipient without evidence of clinical symptoms and CMV genetic resistance.

Ge et al. report an intra-abdominal Mycobacterium syngnathidarum infection in an immunocompetent patient. This is the first report of Mycobacterium syngnathidarum infection in humans. This mycobacterium was detected by whole genome sequencing (WGS). Therefore, the authors suggest that WGS can serve as a high-resolution assay for the diagnosis of different subtypes of mycobacterial infection.

Cao et al. report a case of haemophagocytic lymphohistiocytosis (HLH) with detection of Rickettsia DNA in blood that met the diagnostic criteria of the Histiocyte Society's HLH-2004 guidelines. The patient was treated with antibiotics, glucocorticoid therapy and continuous renal replacement therapy (CRRT) temporarily improving his condition. However, the patient died 2 years later due to chronic renal failure caused by septic shock.

Zhou et al. address the risk of nosocomial infections with multi-drug resistant organisms (MDRO) in neonatal intensive care units (NICUs). Authors conducted a multicenter observational study at NICUs of two tertiary children's hospitals in China. This study is the first to construct a predictive risk model (PRM) for nosocomial infections with MDRO in NICUs.

Li et al. validate another PRM to establish the prognosis of hospitalized patients with severe fever with thrombocytopenia syndrome (SFTS) before reaching the critical illness stage and compare the predictive ability of groups with and without viral load. This PRM represents a convenient tool for early identification of critically ill patients in order to initiate better personalized treatment in time.

Huang et al. show their prediction of the risk of cytopenias during hospitalization in HIV/AIDS patients. The authors used artificial intelligence (five machine learning prediction models) to analyse the data and concluded hypoproteinaemia and cancer were the most important predictors in this context.

Ali et al. address the issue of COVID-19 in patients with chronic myeloid leukemia (CML). With respect to the controversy over whether CML patients have better outcomes than normal people or not, this review evaluates the outcome of CML patients with COVID-19 and attempts to address the missing area of knowledge.

Ghaffari et al. investigated human platelet antigen (HPA)-1 and HPA-3 (GPIIb/IIIa), HPA-2 (GPIb/IX), HPA-4 (GPIIIa), HPA-5 (GPIa/IIa) and HPA-15 (CD109) polymorphisms in 86 COVID-19-infected patients with thrombocytopenia and 136 COVID-19-infected patients without thrombocytopenia. The authors present here the first evidence suggesting the distinct association of specific combinations of HPA genotypes with thrombocytopenia in COVID-19 infected patients. They recommend evaluating the role of HPA polymorphisms as risk factors for thrombocytopenia in different COVID-19 populations.

Xie et al. present a rare case of a patient with systemic lupus erythematosus with a fungal infection who developed MDS-like adverse reactions after treatment with voriconazole. Because the patient's sputum culture showed Candida albicans infection, oral voriconazole was prescribed. After the use of voriconazole, drug-related adverse reactions such as visual disturbances, nausea, vomiting and others, as well as a gradual increase in serum creatinine and oliguria appeared. In addition, there was a decrease in peripheral blood cells, and MDS-like changes were observed in the bone marrow by bone marrow biopsy. After stopping voriconazole, drug-related adverse symptoms disappeared, while cytopenias and MDS changes improved significantly.

Szabó et al. show their results with 49 patients with hematological diseases (HD) and 46 healthy controls (HCs) enrolled to receive a full two-dose vaccination with three different SARS-CoV-2 vaccines (BNT162b2, or AZD1222, or BBIBP-CorV).

Although, humoral immune activity against SARS-CoV-2 can be highly evoked by the BNT162b2 mRNA-based vaccination compared to the other two, the authors demonstrate a significant weaker overall response to the vaccines in the immunologically deficient HD population against HCs, regardless of vaccine type.

Xu et al. investigate the feasibility and accuracy of liver iron concentration (LIC) quantification in thalassaemia (TM) patients using 1.5T and 3T T2* magnetic resonance imaging (MRI).

Li et al. confirm here that, in pediatric patients with hemophilia A, the US scoring system correlated well with the Hemophilia Joint Health Score (HJHS 2.1) for global and individual joint assessments, with excellent correlations for elbows, substantial correlations for knees and moderate correlations for ankles.

The articles of this Research Topic describe different and often insufficiently known aspects of the diagnosis and management of various infectious diseases in our hematological patients. Further studies following the results observed here will undoubtedly contribute to a better understanding of these issues.

Author contributions

TJG-L: Conceptualization, Formal analysis, Methodology, Supervision, Validation, Visualization, Writing – original draft, Writing – review & editing. IJ: Writing – original draft, Writing – review & editing. CS: Writing – original draft, Writing – review & editing. PD: Writing – original draft, Writing – review & editing.

Funding

The author(s) declare that no financial support was received for the research, authorship, and/or publication of this article.

Acknowledgments

The associate editors thank the authors, and all the reviewers and editors who undoubtedly contribute to the realization of this Research Topic.

Conflict of interest

The authors declare that the research was conducted in the absence of any commercial or financial relationships that could be construed as a potential conflict of interest.

The author(s) declared that they were an editorial board member of Frontiers, at the time of submission. This had no impact on the peer review process and the final decision.

Publisher's note

References

1. Blennow O, Ljungman P. Infections in hematology patients. *Con Guide Hematol.* (2019) 12:503–18. doi: 10.1007/978-3-319-97873-4_38

2. Khayr W, Haddad RY, Noor SA. Infections in hematological malignancies. *Dis Month.* (2012) 58:239–49. doi: 10.1016/j.disamonth.2012.01.001

frontiers | Frontiers in Medicine

TYPE Original Research
PUBLISHED 19 May 2023
DOI 10.3389/fmed.2023.1180614

OPEN ACCESS

EDITED BY
Tomás José Gonzalez López,
Burgos University Hospital, Spain

REVIEWED BY
Santosh Kumar Yadav,
Johns Hopkins Medicine, United States
Murtadha Al-Khabori,
Sultan Qaboos University, Oman

*CORRESPONDENCE
Peng Peng
✉ doublep@126.com

RECEIVED 06 March 2023
ACCEPTED 21 April 2023
PUBLISHED 19 May 2023

CITATION
Xu F, Peng Y, Xie H, Liang B, Yang G, Zhao F, Liu Y and Peng P (2023) A multicenter study on the quantification of liver iron concentration in thalassemia patients by means of the MRI T_2* technique. *Front. Med.* 10:1180614. doi: 10.3389/fmed.2023.1180614

A multicenter study on the quantification of liver iron concentration in thalassemia patients by means of the MRI T_2* technique

Fengming Xu[1], Yuzhao Peng[1], Hanhong Xie[1], Bumin Liang[2], Gaohui Yang[3], Fanyu Zhao[4], Yu Liu[5] and Peng Peng[1,6]*

[1]Department of Radiology, The First Affiliated Hospital of Guangxi Medical University, Nanning, Guangxi, China, [2]School of International Education, Guangxi Medical University, Nanning, Guangxi, China, [3]Department of Hematology, The First Affiliated Hospital of Guangxi Medical University, Nanning, Guangxi, China, [4]Department of Radiology, People's Hospital of Guangxi Zhuang Autonomous Region, Nanning, Guangxi, China, [5]Department of Radiology, The Affiliated Tumor Hospital of Guangxi Medical University, Nanning, Guangxi, China, [6]NHC Key Laboratory of Thalassemia Medicine, Guangxi Medical University, Nanning, Guangxi, China

Objective: To investigate the feasibility and accuracy of quantifying liver iron concentration (LIC) in patients with thalassemia (TM) using 1.5T and 3T T_2* MRI.

Methods: 1.5T MRI T_2* values were measured in 391 TM patients from three medical centers: the T_2* values of the test group were combined with the LIC (LIC_F) provided by FerriScan to construct the curve equation. In addition, the liver 3T MRI liver T_2* data of 55 TM patients were measured as the 3T group: the curve equation of 3T T_2* value and LIC_F was constructed.

Results: Based on the test group LIC_F (0.6–43 mg/g dw) and the corresponding 1.5T T_2* value, the equation was $LIC_F = 37.393T_2{*}^{\wedge}(-1.22)$ ($R^2 = 0.971$; $P < 0.001$). There was no significant difference between $LIC_{e-1.5T}$ and LIC_F in each validation group ($Z = -1.269, -0.977, -1.197$; $P = 0.204, 0.328, 0.231$). There was significant consistency (Kendall's $W = 0.991, 0.985, 0.980$; all $P < 0.001$) and high correlation ($r_s = 0.983, 0.971, 0.960$; all $P < 0.001$) between the two methods. There was no significant difference between the clinical grading results of $LIC_{e-1.5T}$ and LIC_F in each validation group ($\chi^2 = 3.0, 4.0, 2.0$; $P = 0.083, 0.135, 0.157$), and there was significant consistency between the clinical grading results (Kappa's K = 0.943, 0.891, 0.953; $P < 0.001$). There was no statistical correlation between the LIC_F (≥14 mg/g dw) and the 3T T_2* value of severe iron overload ($P = 0.085$). The LIC_F (2–14 mg/g dw) in mild and moderate iron overload was significantly correlated with the corresponding T_2* value ($r_s = -0.940$; $P < 0.001$). The curve equation constructed from LIC_F and corresponding 3T T_2* values in this range is $LIC_F = 18.463T_2{*}^{\wedge(-1.142)}$ ($R^2 = 0.889$; $P < 0.001$). There was no significant difference between LIC_F and LIC_{e-3T} in the mild to moderate range ($Z = -0.523$; $P = 0.601$), and there was a significant correlation ($r_s = 0.940$; $P < 0.001$) and significant consistency (Kendall's $W = 0.970$; $P = 0.008$) between them. LIC_{e-3T} had high diagnostic efficiency in the diagnosis of severe, moderate, and mild liver iron overload (specificity = 1.000, 0.909; sensitivity = 0.972, 1.000).

Conclusion: The liver iron concentration can be accurately quantified based on the 1.5T T_2* value of the liver and the specific LIC-T_2* curve equation. 3T T_2* technology can accurately quantify mild-to-moderate LIC, but it is not recommended to use 3T T_2* technology to quantify higher iron concentrations.

KEYWORDS

thalassemia, magnetic resonance imaging, iron overload, liver iron concentration, equation

1. Introduction

The liver is one of the major iron storage organs; LIC reflects the total iron load, which is an important clinical indicator for clinical monitoring, evaluation, and treatment of iron overload (1). Although the actual liver iron concentration provided by liver biopsy serves as the "gold standard" for clinical indicators, most scholars and medical centers prefer to use non-invasive MRI technology for LIC monitoring because biopsy provides only small samples and has the disadvantages of invasiveness and poor repeatability (2). The LIC (LIC_F), based on the MRI T_2/R_2 ($1000/T_2$) technique and reported by FerriScan (Resonance Health Limited, Burswood, WA, Australia), has been certified by the Food and Drug Administration (FDA) of the United States and has high reliability (3). However, there are many limitations to this technique (4): it requires patient-related MRI T_2/R_2 data to be sent to FerriScan for off-site post-processing and analysis. The off-site sending of patient data requires approval from the relevant center and involves time costs that will prolong the time to obtain LIC results. The additional cost of the analysis will also increase the cost of LIC monitoring at one time, which results in the use of FerriScan technology for liver iron quantification being limited to a few large medical centers, and the possibility of regular or long-term LIC monitoring in patients being greatly reduced.

The T_2^* technique, based on the gradient recalled echo (GRE) imaging sequence of MRI has been established as a non-invasive standard for quantifying tissue iron levels (5–7). Many centers have been using the T_2^* relaxation method and corresponding software technology to measure organ relaxation parameters, such as T_2^* and R_2^* ($1000/T_2^*$) values, to indirectly obtain the estimated value of organ iron concentration (8). Some studies have explored the relationship between liver 1.5T T_2^*/R_2^* and LIC in patients with iron overload and constructed the corresponding LIC-T_2^*/R_2^* curve equation (8–13). However, the equations constructed in these studies, which were partly based on liver iron concentrations obtained from small biopsy samples, have not been validated in multiple centers, and their reliability needs to be verified. Moreover, most of the current studies in this area are based on 1.5T MRI, while the studies based on 3T MRI are few and limited. many studies only discuss the correlation between 3T T_2^*/R_2^* and LIC and whether the diagnosis is liver iron overload, but there is less analysis of the cutoff value of clinical classification of mild, moderate, and severe iron overload (14, 15).

The aim of this study was to investigate the relationship between liver 1.5T, 3T T_2^* values and LIC_F in thalassemia (TM) patients based on large sample size and multicenter data and also to investigate the feasibility, reliability, and accuracy of 1.5T and 3T MRI T_2^* techniques in quantifying LIC in TM patients.

2. Materials and methods

2.1. Research data

Liver 1.5T MRI T_2^* data of thalassemia patients from three medical centers from January 2014 to June 2022 were retrospectively analyzed: 273 patients from the First Affiliated Hospital of Guangxi Medical University (Center 1), 54 from the Guangxi Zhuang Autonomous Region Ethnic Hospital (Center 2), and 64 from the Guangxi Medical University Affiliated Tumor Hospital (Center 3). In total, 13 patients underwent 1.5T MRI T_2^* liver scans at three centers (within 24 h of the same patient being scanned at different centers). In addition, 3T liver MRI T_2^* data of 55 TM patients from center 1 were collected. The inclusion criteria were: (1) patients diagnosed with thalassemia by genetic diagnosis, with a history of regular or irregular blood transfusion; (2) age $\geq$ 9 years old; (3) MRI for thalassemia was performed with liver T2 (as required by FerriScan) and T_2^* sequences. Exclusion criteria were: (1) the image data artifacts were large and did not meet the measurement requirements; (2) patients were complicated with other chronic liver diseases or neoplastic diseases. This study was conducted in accordance with the principles of the Declaration of Helsinki and approved by the Ethics Committee of the First Affiliated Hospital of Guangxi Medical University (2022-E457-01).

2.2. MR scanning methods

1.5T data: a Siemens 1.5T MRI scanner (MAGNETOM Avanto Fit & Altea, Siemens Healthcare, Erlangen, Germany), a Philips 1.5T MRI scanner (Achieva, Philips Medical Systems, Best, Netherlands), and the body coil were used. The images reported by FerriScan use a free-breathing two-dimensional multilayer spin-echo pulse sequence: rollover angle = 90°, repeat time (TR) = 1,000 ms, echo time (TE) = 6.0, 9.0, 12.0, 15.0, 18.0 ms, matrix = 256 × 256 mm^2, layer thickness = 5 mm, FOV = 400 mm × 400 mm. The scan time was 15 min. GRE scan sequence: the same level above the hepatic hilum was scanned with one breath hold at the end of exhalation. rotation angle = 20°, TR = 200.00 ms, TE = 1.29, 2.35, 3.43, 4.6, 5.68, 6.85, 7.93, 9.1, 10.18, 11.35, 12.43, 13.6 ms, matrix = 256 × 256 mm^2, layer thickness = 10 mm, FOV = 400 mm × 400 mm.

3T data: a Siemens 3T MRI scanner was used (Verio, Siemens Healthcare, Erlangen, Germany). TR = 200 ms, TE = 0.97, 2.38, 3.79, 5.20, 6.61, 8.02, 9.43, 10.84, 12.25, 13.66, 15.07, 16.48 ms; Rotation angle = 20°, matrix = 64 × 128 mm^2, layer thickness = 10 mm, FOV = 200 mm × 400 mm.

2.3. Data measurement and analysis

The 1.5T T2 image data was sent to FerriScan for post-processing and analysis. The LIC_F used in the study was obtained from the final FerriScan report (Figure 1A). The overall technical procedure of this study is shown in Figure 2.

All T_2^* image data were measured using CMRtools (CMRtools/Thalassemia Tools 2014, Cardiovascular Imaging Solutions, London, UK). Measurement procedure: T_2^* image data were exported from the PACS system and imported into a personal computer with CMRtools software installed. The "Thalassemia" function of CMRtools was used to draw a roughly similar ROI according to the range of liver levels measured by FerriScan, avoiding the visible intrahepatic vessels and bile ducts at the same liver level. The delineated ROIs and the fitted T_2^* values were then displayed in the post-processing software. The truncation method

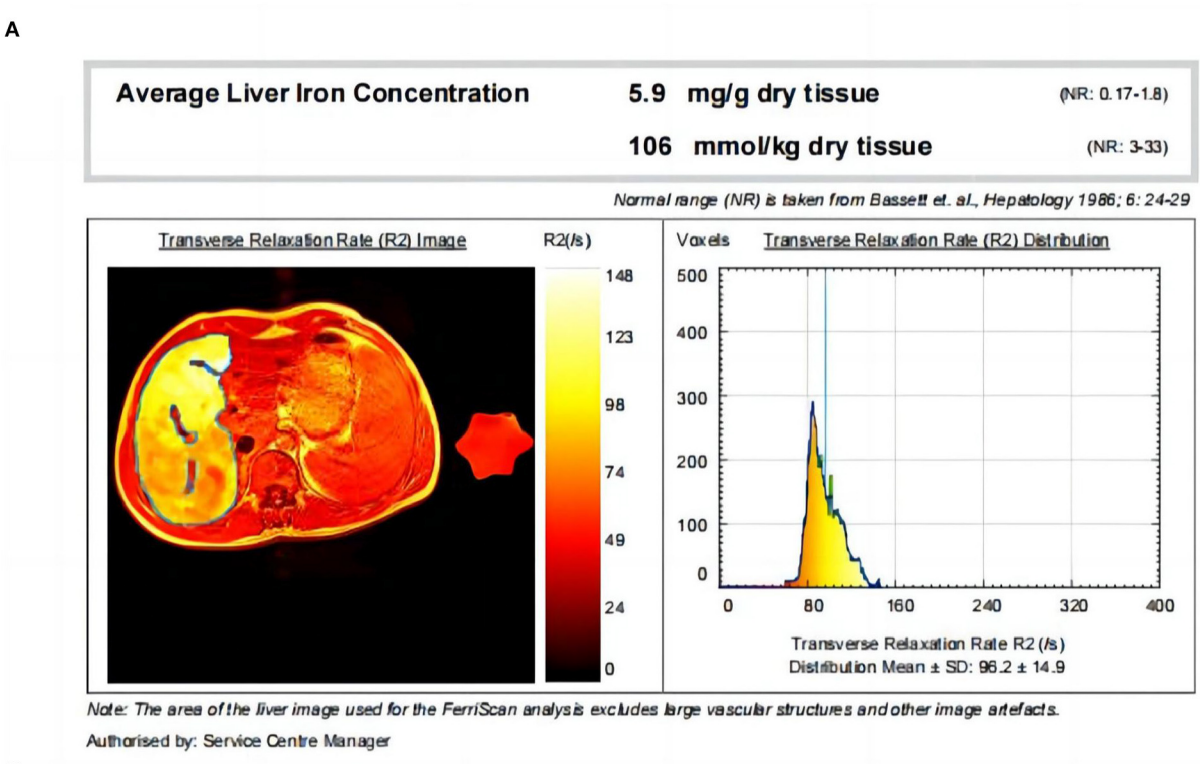

FIGURE 1
(A, B) A 35-year-old male thalassemia patient with an LIC_F of 5.9 mg/g dw **(A)** and mild iron overload in the liver; CMRtools showed a mean T_2^* of 3.81ms (the first seven echo signal intensities were included in the fitted curve, and the red "×" indicates the echo signal intensities of the removed offset curve) with an R^2 of 0.9999 **(B)**.

(14) was used to reject signal intensity values (SI) that deviated from the fitted curve one by one, and the T_2^* value was recorded when the goodness of fit (R^2) ≥ 0.98 (Figure 1B).

2.4. Statistical methods

SPSS 26.0 statistical software package was used for statistical analysis. All test results were statistically analyzed according to the test significance $\alpha = 0.05$. MedCalc 19.8.0 statistical software was used to analyze the consistency of T_2^* values measured by different MRI scanners.

The 1.5T data of 273 patients from center 1 were divided into 191 patients in the test group and 82 patients in the validation group 1 according to the ratio of 7:3 by random number method. The 1.5T data of 54 patients from Center 2 were used as validation group 2. The 1.5T data of 64 patients from Center 3 were used as validation group 3. The 3T data of 55 cases from Center 1 were taken as the 3T group (3T data were only self-verified due to a small amount of data and were not grouped).

The intraclass correlation coefficient (ICC) was used, according to the ratio of 7:3. The 1.5T T_2^* image data of 50 randomly selected patients from the test group ($n = 35$) and validation group 1 ($n = 15$) were measured to evaluate intra-observer and inter-observer agreement (independently performed by two radiologists with 5 years of experience in abdominal radiology diagnosis). The intra-observer ICC was calculated by comparing the T_2^* values measured by observer A twice. The inter-observer ICC was calculated by comparing the T_2^* values measured by observer B with the T_2^* values measured by observer A. The ICC between the different

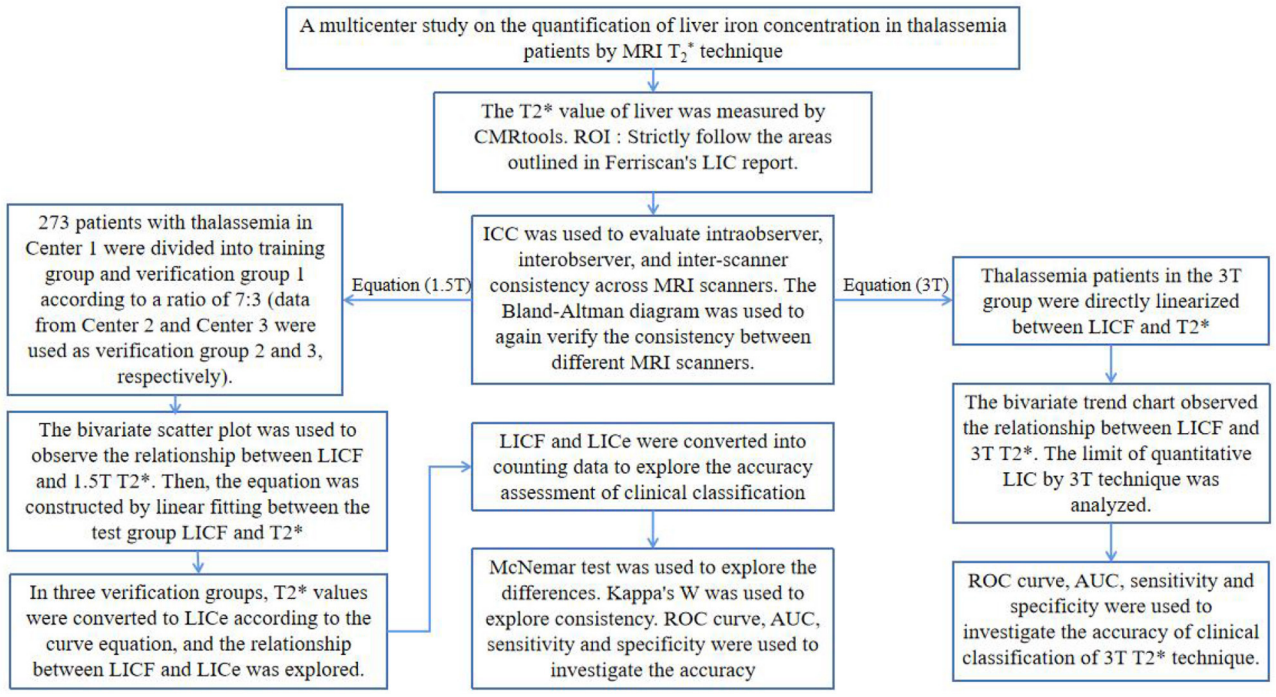

FIGURE 2
The overall technology roadmap.

MRI scanners was calculated by comparing the 1.5T T_2^* values of 13 patients at three centers. "Two-way random" was selected for "model" and "absolutely consistent" was selected for "type." When ICC > 0.75 and $P < 0.05$, the measured T_2^* values were considered to be highly consistent. The remaining T_2^* value measurements were performed by observer A. Bland–Altman plots were used to analyze the consistency of the 1.5T T_2^* values of 13 patients measured by different MRI scanners.

The age, LIC_F, and the measured liver T_2^* values of each group did not follow the normal distribution by the normality test ($P < 0.05$). The interquartile range ($P_{25\%}$, $P_{75\%}$) and median (M) were used as statistical descriptors. By curve fitting, the calibration curve equation was constructed between the T_2^* value of the test group and the LIC_F of the 3T group. The T_2^* values in each validation group and the 3T group were converted into $LIC_{e-1.5T}$ and LIC_{e-3T} by the constructed curve equation. Both $LIC_{e-1.5T}$ and LIC_{e-3T} did not conform to the normal distribution ($P < 0.05$). The Wilcoxon signed-rank test was used to examine the difference, and $P > 0.05$ was considered as no significant difference. Kendall's W coefficient was used to examine consistency. If the consistency coefficient $W > 0.75$ and $P < 0.05$, it indicated a high degree of consistency. Spearman rank correlation analysis was used to examine the correlation; if the correlation coefficient of $|r_s| > 0.75$ and $P < 0.05$, it indicated a high correlation.

LIC_e and LIC_F were graded according to the severity of clinical liver iron overload, which was divided into normal (<1.8 mg/g dw), mild (1.8–7.0 mg/g dw), moderate (7.0–14.0 mg/g dw), and severe (>14.0 mg/g dw) liver iron overload (12). The McNemar test was used to examine the difference in clinical grading results. When $P > 0.05$, there was no significant difference between the two. Kappa's coefficient (Kappa's K) was used to examine the consistency of clinical grading results. If K > 0.75 and $P < 0.05$, the two were highly consistent. With the LIC_F grading results as the reference standard, the area under the curve (AUC), sensitivity, and specificity of the receiver operating characteristic curve (ROC) was used to evaluate the accuracy of the $LIC_{e-1.5T}$ and LIC_{e-3T} clinical classification results in each validation group. The Youden index was used to evaluate the authenticity of the clinical classification results, and the cutoff values of different clinical classifications were recorded when the Youden index was maximum.

3. Results

3.1. Basic data information

In Center 1, there were 152 male subjects (55.68%) and 121 female subjects (44.32%), aged from 9 to 49 years (M = 19.00, $P_{25\%}$ = 12.00, $P_{75\%}$ = 27.00). In Center 2, there were 19 male subjects (35.19%) and 35 female subjects (64.81%), aged from 9 to 47 years (M = 13.00, $P_{25\%}$ = 12.00, $P_{75\%}$ = 21.25). In Center 3, there were 42 male subjects (65.63%) and 22 female subjects (34.37%), aged from 10 to 63 years (M = 15.50, $P_{25\%}$ = 11.00, $P_{75\%}$ = 25.00). In the 3T group, there were 33 males (60.00%) and 22 females (40.00%), aged from 9 to 25 years (M = 13.00, $P_{25\%}$ = 11.00, $P_{75\%}$ = 14.00).

3.2. Consistency analysis

The intra-observer ICC calculated based on the two measurements of observer A was 0.996 (95% confidence interval (CI) = 0.992–0.998) and $P < 0.001$. The inter-observer ICC between observers A and B was 0.978 (95%CI = 0.940–0.990), and

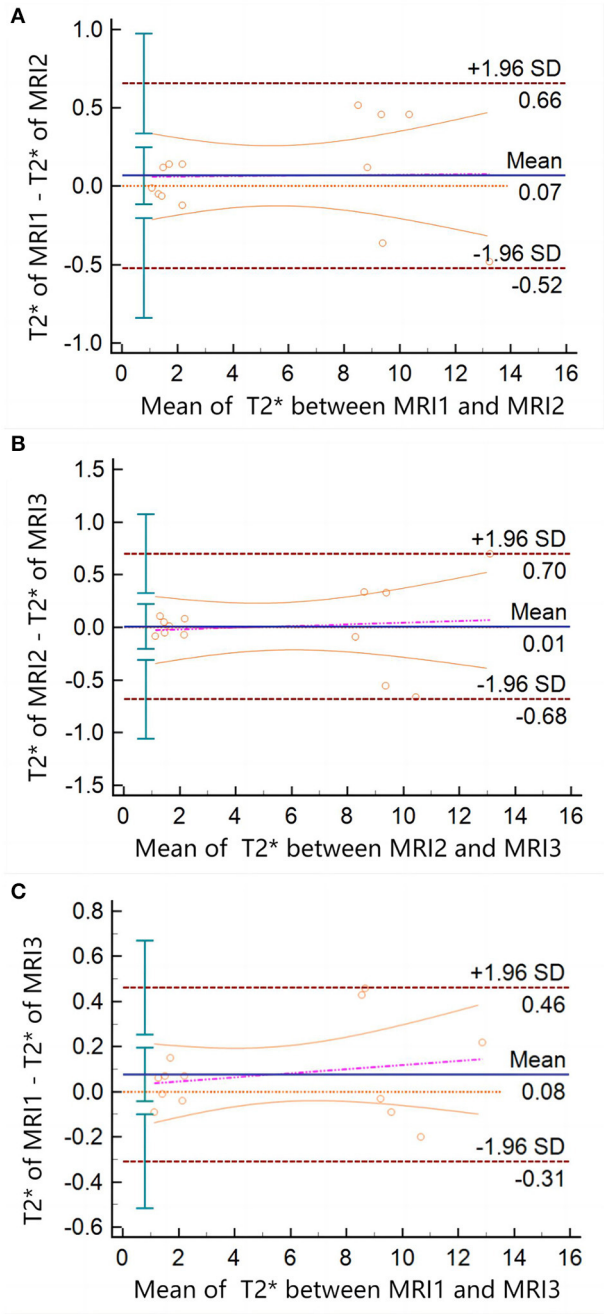

FIGURE 3
Bland–Altman plots of T_2^* measured between different MRI scanners. There is no data point exceeding 95%CI in **(A, B)**, or panel **(C)**. The arithmetic mean between the T_2^* values measured by the different MRI scanners was 0.06769 ($P = 0.4323$; 95%CI = −0.1138 to 0.2492), 0.009231 ($P = 0.9264$; 95%CI = −0.2040 to 0.2225), and 0.07692 ($P = 0.1832$; 95%CI = −0.04173 to 0.1956), respectively.

$P < 0.001$. The ICC between different MRI scanners was 0.999 (95%CI = 0.998–1) and $P < 0.001$. The results showed that the T_2^* values obtained by different MRI scanners were highly consistent with intra-observer and inter-observer. The Bland–Altman plots also showed significant consistency in the T_2^* values measured by different MRI scanners (Figure 3).

3.3. Formula construction

The trends of the relationships between LIC_F and T_2^* and LIC_F and LIC_e in each group are shown in Figure 4. According to the T_2^* value of the test group and LIC_F, the curve equation constructed was $LIC_F = 37.393T_2^{*\wedge}(-1.22)$ ($R^2 = 0.971$, $P < 0.001$) (Figure 4A). According to the T_2^* value of the 3T group and LIC_F (<14 mg/g dw) of mild-to-moderate iron overload, the curve equation was $LIC_F = 18.463T_2^{*\wedge}(-1.142)$ ($R^2 = 0.889$, $P < 0.001$) (Figure 4B). The liver T_2^*, LIC_F, $LIC_{e-1.5T}$, and LIC_{e-3T} values, and statistical description indicators of thalassemia patients in each group are shown in Table 1.

3.4. Formula verification

There was no significant difference between $LIC_{e-1.5T}$ and LIC_F in verification groups 1, 2, and 3 ($Z = -1.269, -0.977, -1.197$; $P = 0.204, 0.328, 0.231$). There was significant consistency between them (Kendall's $W = 0.991, 0.985, 0.980$; $P < 0.001$) and high correlation ($r_s = 0.983, 0.971, 0.960$; $P < 0.001$). There was no statistical difference between the clinical grading results of $LIC_{e-1.5T}$ and LIC_F in verification groups 1, 2, and 3 ($\chi^2 = 3.0, 4.0, 2.0$; $P = 0.083, 0.135, 0.157$), and the grading results are shown in Figure 5. There was significant consistency among the clinical grading results (Kappa's K = 0.943, 0.891, 0.953; $P < 0.001$). The accuracy indexes and corresponding cutoff values of the clinical classification results of $LIC_{e-1.5T}$ for the test group and each validation group are shown in Table 2.

In the 3T group, LIC_F in the mild-to-moderate range was significantly correlated with the corresponding T_2^* value ($r_s = -0.940$, $P < 0.001$). There was no statistically significant correlation between LIC_F and T_2^* values in the severe range ($P = 0.085$). Of the 36 patients with severe iron overload diagnosed by LIC_F, 1 (2.78%) was diagnosed with moderate iron overload by LIC_{e-3T}. Of the eight patients with moderate iron overload diagnosed by LIC_F, two (25%) were diagnosed with mild iron overload by LIC_{e-3T}. Of the 11 patients with mild iron overload diagnosed by LIC_F, one (9.10%) was diagnosed with moderate iron overload by LIC_{e-3T}. There was no significant difference between LIC_F and LIC_{e-3T} in the mild to moderate range ($Z = -0.523$, $P = 0.601$). There was a significant correlation between them ($r_s = 0.940$, $P < 0.001$) and significant consistency (Kendall's $W = 0.970$, $P = 0.008$). There was no significant difference between the clinical grading results of full range LIC_F ($\chi^2 = 1.333$, $P = 0.513$) and LIC_{e-3T} ($\chi^2 = 1.333$, $P = 0.513$). There was significant consistency among the clinical grading results (Kappa's K = 0.860, $P < 0.001$). The ROC curve of LIC_{e-3T} clinical grading results is shown in Figure 6, and the evaluation indices of diagnostic accuracy are shown in Table 2.

4. Discussion

As mentioned, magnetic resonance imaging has been widely considered the primary method for the non-invasive determination of liver iron concentration (6). FerriScan based on R_2 technology can generate reports including liver iron concentration, but it cannot be widely applied due to a variety of limiting factors,

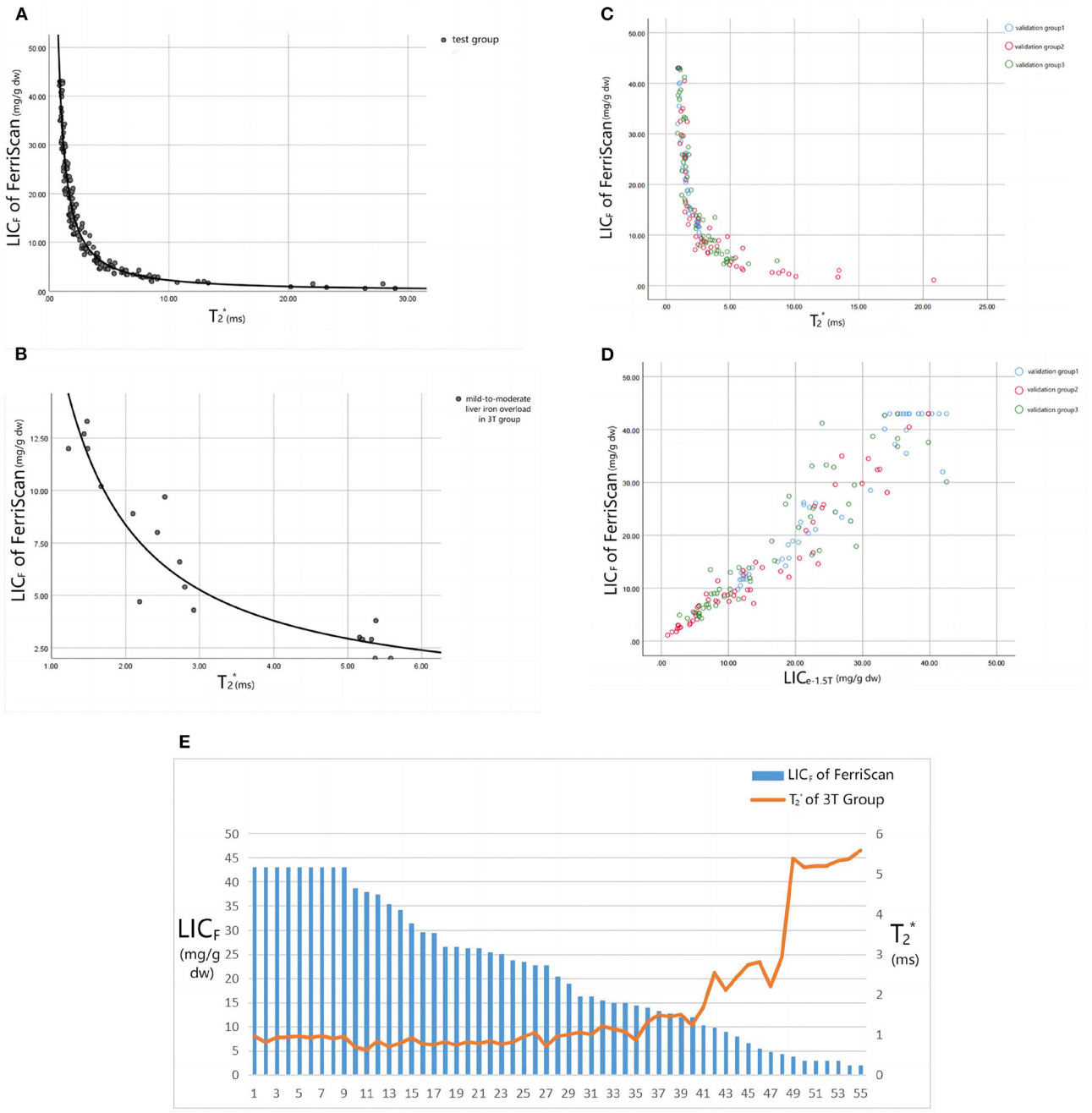

FIGURE 4
(A) Shows the fitting curve of LIC_F and 1.5T T_2^* value in the test group, and the fitting equation is $LIC_F = 37.393T_2^{*}\wedge(-1.22)$ ($R^2 = 0.971$, $P < 0.001$). **(B)** Shows the fitting curve of LIC_F and 3T T_2^* value for mild-to-moderate iron overload in the 3T group, and the fitting equation is $LIC_F = 18.463T_2^{*} \wedge (-1.142)$ ($R^2 = 0.889$, $P < 0.001$). **(C, D)** Show the trend scatter plots of the relationship between LIC_F and 1.5T T_2^* and LIC_F and $LIC_{e-1.5T}$ values in each validation group. **(E)** Shows the trend plot of the relationship between LIC_F and 3T T_2^* values in the 3T group: when $LIC_F > 14$ mg/g dw, the T_2^* value remained approximately 0.9 ms (the scanner could not accurately quantify the liver iron load in the range of $LIC_F > 14$ mg/g dw). Only when $LIC_F < 14$ mg/g dw did T_2^* values displayed a negative relationship with LIC_F.

especially for long-term and timely quantitative monitoring of LIC in patients (16). T_2^*/R_2^* image-based relaxometry and related measurement techniques have been developed in many centers. After years of research, many scholars have verified that the T_2^*/R_2^* value has an obvious linear relationship with LIC and partially constructed the curve equation of the relationship between them (8–13).

In the first quantitative study of liver iron overload using R_2^* relaxation measurement by Henninger et al. (8), the relevant parameters set were repetition time (TR) = 200 ms and initial echo time (TE) = 0.99 ms. Liver biopsy and MRI were performed on 17 patients with clinical suspicion of liver iron overload. The final regression model between R_2^* and LIC was constructed as follows: $LIC = 0.024R_2^* + 0.277$, correlation coefficient = 0.926,

TABLE 1 Statistical descriptive indicators of liver T_2^*, LIC_F, $LIC_{e-1.5T}$, and LIC_{e-3T} values of thalassemia patients in each group.

Group	Variable name	Number (N)	Min. ~ maximum value	Quartile ($P_{25\%}$)	Quartile ($P_{75\%}$)	Median (M)
Test group	T_2^* (ms)	191	0.86–28.92	1.19	4.25	2
	LIC_F (mg/g dw)	191	0.60–43.00	5.7	29.5	14.9
Validation group1	T_2^* (ms)	82	0.90–25.44	1.0875	4.4375	1.85
	LIC_F (mg/g dw)	82	0.90–43.00	6.025	35.925	14.6
	$LIC_{e-1.5T}$ (mg/g dw)	82	0.72–42.52	6.08	33.755	17.6
Validation group2	T_2^* (ms)	54	0.95–20.83	1.5075	5.155	2.625
	LIC_F (mg/g dw)	54	1.10–43.00	5.325	23.175	9.55
	$LIC_{e-1.5T}$ (mg/g dw)	54	0.92–39.81	5.2751	22.9435	12.1968
Validation group3	T_2^* (ms)	64	0.90–28.92	1.4725	4.76	2.885
	LIC_F (mg/g dw)	64	0.60–43.00	5.225	24.925	9.8
	$LIC_{e-1.5T}$ (mg/gdw)	64	0.62–42.52	5.2751	23.3285	10.2663
3T group (mild-to-moderate range)	T_2^* (ms)	19	1.23–5.58	1.67	5.2	2.73
	LIC_F (mg/g dw)	19	2.00–13.30	2.9	10.2	5.4
	LIC_{e-3T} (mg/g dw)	19	2.59–14.58	2.81	10.28	5.86
3T group (moderate-to-severe range)	T_2^* (ms)	46	0.61–2.80	0.8	1.2075	0.94
	LIC_F (mg/g dw)	46	5.40–43.00	14.375	37.55	24.4
	LIC_{e-3T} (mg/g dw)	46	5.70–32.47	14.8875	23.82	19.81

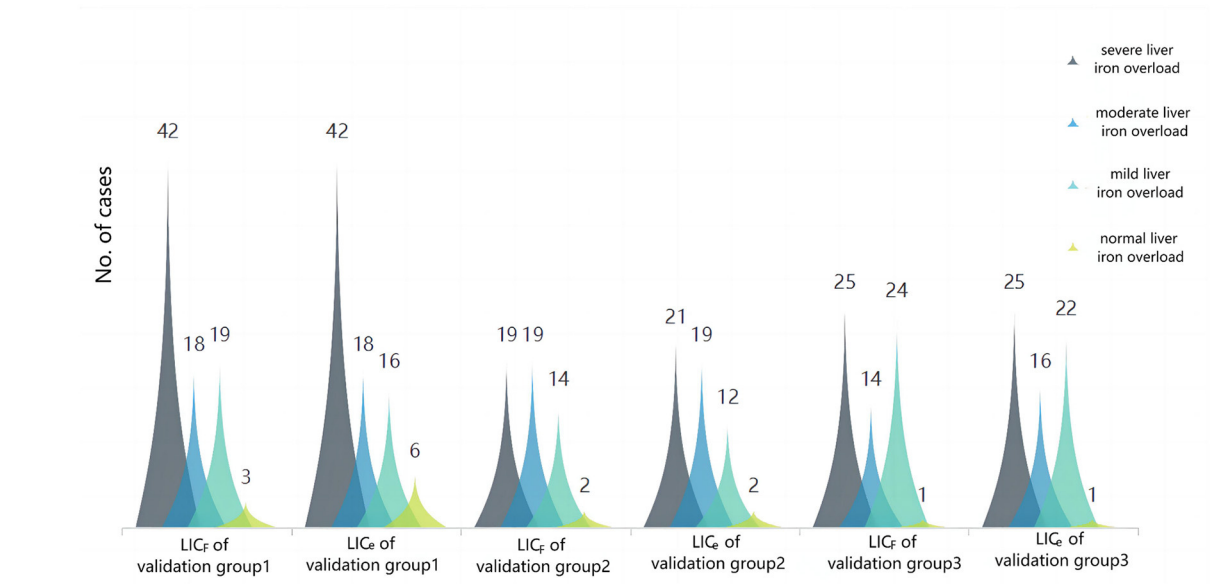

FIGURE 5
Cluster plot of the constituent ratio of clinical grades of liver iron overload in LIC_F and $LIC_{e-1.5T}$ for each validation group. The results showed that the overall distribution of the two methods was almost the same, and there were slight differences in some distributions: in validation group 1, three patients (3.66%) with liver iron overload were classified as mild according to LIC_F classification, and as normal according to LIC_e classification. In validation group 2, two patients (3.70%) had liver iron overload classified as mild according to LIC_F and moderate according to LIC_e. In total, two patients (3.70%) had moderate liver iron overload according to LIC_F and severe liver iron overload according to LIC_e. In validation group 3, two patients (3.13%) had mild liver iron overload according to LIC_F classification and moderate liver iron overload according to LIC_e classification.

TABLE 2 Accuracy indicators and clinical classification cutoff values of $LIC_{e-1.5T}$ clinical classification results in the validation group.

Group	Liver iron overload grading	AUC	95%CI	*P*	Specificity	Sensitivity	Youden index	Cut-off values (mg/g dw)
Test group-$LIC_{1.5T}$	Severe vs. moderate groups	0.991	0.983–0.999	<0.0001	0.967	0.94	0.907	16.005
	Moderate vs. mild groups	0.942	0.904–0.980	<0.0001	0.929	1	0.929	7.49
	Mild vs. normal group	0.999	0.995–1.000	<0.0001	0.989	1	0.989	2.3
Validation group 1-$LIC_{1.5T}$	Severe vs. moderate groups	1	1.000–1.000	<0.0001	1	1	1	15.425
	Moderate vs. mild groups	0.969	0.927–1.000	<0.0001	0.937	1	0.937	7.485
	Mild vs. normal group	0.988	0.963–1.000	0.019	0.987	1	0.987	1.225
Validation group 2-$LIC_{1.5T}$	Severe vs. moderate groups	0.995	0.985–1.000	<0.0001	1	0.947	0.947	19.814
	Moderate vs. mild groups	0.95	0.985–1.000	<0.0001	0.95	1	0.95	6.123
	Mild vs. normal group	1	0.963–1.000	0.019	0.981	1	0.981	2.302
Validation group 3-$LIC_{1.5T}$	Severe vs. moderate groups	1	1.000–1.000	<0.001	0.974	1	0.974	13.22
	Moderate vs. mild groups	0.972	0.923–1.000	<0.001	0.975	0.958	0.933	7.199
	Mild vs. normal group	1	1.000–1.000	0.008	0.984	1	0.984	2.182
3T group-LIC_{3T}	Severe vs. moderate groups	0.997	0.988–1.000	<0.001	1	0.972	0.972	14.785
	Moderate vs. mild groups	0.977	0.920–1.000	<0.001	0.909	1	0.909	6.13

slope = 0.024 (mg/g) [95% CI = 0.013–0.024], intercept = 0.277 (mg/g) [95% CI = 0.328–2.49]. In an early study by Wood et al. (9), the set TE was increased from the initial 0.8 ms to 4.8 ms at 0.25 ms intervals in a breath hold, and TR = 25 ms. After MRI evaluation of 102 patients with liver iron overload (the biopsy-measured LIC was evenly distributed between 1.3 mg/gdw and 32.9 mg/gdw, and one patient had a HIC of 57.8 mg/gdw), the final LIC-R_2* regression equation was constructed as follows: the correlation coefficient was 0.97, the slope was 37.4 Hz/mg/gdw, and the y-intercept was 23.7 Hz. In an early study by Hankins et al. (10), TE = 1.1–17.3 ms (20 echoes) was set, and 43 patients (32 with sickle cell anemia, six with major β-thalassemia, five patients with bone marrow failure) underwent MRI examination and liver biopsy (LIC range = 0.6 mg Fe/g to 27.6 mg Fe/g). The final LIC-R_2* regression model was constructed as follows: the intercept was −454.85, the slope was 28.02 ($P < 0.001$), the R^2 was 0.72, and the correlation coefficient was 0.98. In an early study by Christoforidis et al. (11), MRI was performed on 94 patients with β-thalassemia major with TE = 2.24–20.13 ms and TR = 200 ms. The relationship between liver–muscle ratio (MRI-LIC = 5–350 μmol/g) and R_2* (27.03–1,298.70 s^{-1}) was compared. The final LIC-R_2* regression model was R_2* = 0.851(MR-LIC) – 2.137 (correlation coefficient = 0.851). In the study by Garbowski et al. (12), TE was set as 0.93–16.0 ms. A total of 54 patients (36 cases of thalassemia major, seven cases of sickle cell anemia, four cases of myelodysplastic syndrome, three cases of Diamond-Blackfan anemia, two cases of red cell aplasia, two cases of pyruvate kinase deficiency anemia), and 31 healthy volunteers underwent liver biopsy (LIC = 1.7–42.3 mg/g dw) and MRI examination (R_2* range = 28.7–54.4 s^{-1}). The final regression models of LIC (biopsy) -T_2* and LIC (biopsy)-R_2* were constructed: (1) LIC = $31.94(T_2^*)^{-1.014}$, 95%CI of coefficient = 27.8–36.7 (87–115%), 95%CI of index = −1.118–0.91(110–90%). (2) LIC = $0.029(R_2^*)^{1.014}$, 95%CI of coefficient = 0.016–0.054 (55–186%), 95%CI of index = 0.910–1.118 (90–110%). Garbowski et al. (12) also constructed the correction relationship between LIC (Ferriscan)-R_2* and LIC-T_2*: (1) R_2-LIC = $0.83T_2^*$ – $LIC^{1.04}$,

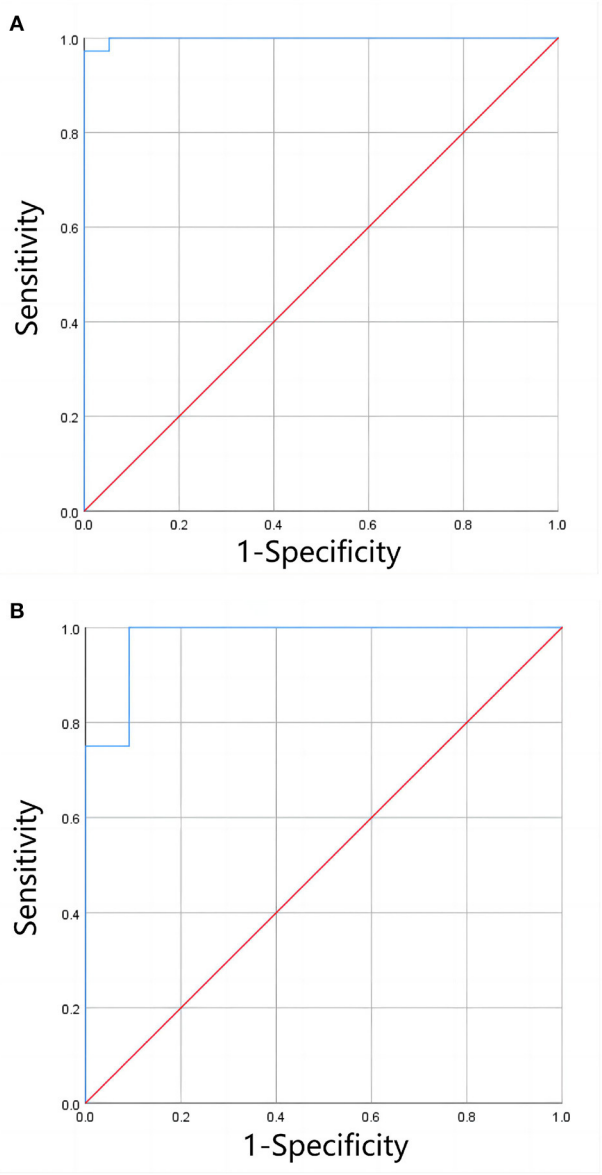

FIGURE 6
(A, B) Shows the ROC curves for clinical grading of moderate and severe liver iron overload, and of mild and moderate liver iron overload by LIC_{e-3T}, respectively. The results showed that LIC_{e-3T} had a high diagnostic efficiency for clinical grading of liver iron overload when only clinical grading diagnosis was performed (without precise quantification of LIC).

95%CI of coefficient = 0.96 ~ 1.11, 95%CI of index = 0.55 ~ 1.29. (2) R_2-LIC = $0.87R_2^*$ – LIC – 0.55, 95%CI of slope = 0.74–0.99, 95%CI of intercept = −0.01–1.19.

In this study, based on large sample size, multicenter validation, and complete statistical analysis, the equation $LIC_F = 37.393T_2^{*\wedge}$ (−1.22) was proposed to quantify LIC from 1.5T MRI T_2^*. For the 3T MRI quantification of liver iron overload, the relationship $LIC_F = 18.463T_2^{*\wedge}(-1.142)$ was proposed to quantify LIC in patients with mild-to-moderate iron overload. However, it is still not possible to accurately quantify LIC in patients with severe liver iron overload at 3T field strength. This also suggests that the 3T T_2^* technique should be avoided for the quantification of LIC in patients with severe iron overload, and 1.5T or other methods should be used instead. This conclusion is similar to that of d'Assignies (15). It is worth noting that this study found that when 3T T_2^* technology was used to quantify liver iron overload, although the T_2^* value of patients with severe liver iron overload was almost maintained at 0.9 ms, it was impossible to further accurately quantify the LIC value; however, if only the clinical classification of liver iron overload was performed, that is, only the classification of mild-to-moderate and severe iron overload was performed, the classification of liver iron overload would have high diagnostic efficacy.

The slope of the calibration curve proposed by different studies is different, and for the LIC calculated by the earlier calibration curve, Garbowski et al. (12) also proposed further calibration coefficients to calibrate the final LIC. The specific reasons for the differences are analyzed as follows: (1) the previous T_2^*/R_2^*-LIC calibration curve equation was based on liver biopsies, such as the study by Henninger et al. (8), Wood et al. (9), Hankins et al. (10), Christoforidis et al. (11), and Garbowski et al. (12). Although LIC provided by liver biopsy has been used as the "gold standard" for a long time, the materials and methods used in the process of liver biopsy, and the heterogeneity of iron in the liver will lead to differences between different studies; (2) The sample size used in some studies is small. A small sample size will not only increase the sampling error, but also limit the range of LIC used, and the final fitted calibration curve equation cannot be extended to quantify a wider range of LIC. For example, the LIC of 17 patients collected by Henninger et al. (8) through liver biopsy ranged from 0.917 mg/g to 11.646 mg/g. The authors believe that because the range of LIC studied is small, it is not appropriate to use the corresponding calibration curve to quantify a wider range of LIC; (3) Different models used to measure T_2^*/R_2^* will directly lead to differences in the final LIC. For example, Wood et al. (9) used an offset model, while Garbowski et al. (12) used a truncated model to measure R_2^*. Garbowski et al. (12) proposed that the R_2^* value measured by the offset model was high, while the R_2^* value measured by the truncated model was low, and emphasized the importance of using the appropriate measurement model to quantify T_2^*/R_2^* and the appropriate analysis techniques to construct the curve equation in clinical practice; (4) The high iron concentration corresponds to a very low T_2^* value, thus it is necessary to set a very short minimum echo time for more accurate measurement. However, due to the differences in the technique and scanning sequence used by different research centers, the different minimum echo time set obviously limits the lowest T_2^* value, which is the maximum value of LIC measured by the center. Some studies have shown that LIC with severe iron overload in the liver should be measured in combination with the signal intensity ratio between the liver and the paravertebral muscles (SIR) (17).

The shortcomings of this experiment are as follows: (1) the definition of the ROI. In this study, the delineated T_2^* image ROI was as close as possible to the T_2 image ROI delineated by FerriScan, but the artificial delineation of ROI was susceptible to various subjective and objective factors, and measurement error was inevitable; (2) In this study, the proportion of patients with moderate or severe liver iron overload was relatively large, and the proportion of patients with mild iron concentration was relatively

small, which had a certain bias. However, in general, this study was analyzed with large sample size and was validated in multiple centers, which makes the results reliable; (3) In this retrospective study, LIC_F was used as the reference standard, in other words, the T_2*-LIC calibration equation was constructed under the assumption that FerriScan based on T_2/R_2 technique was very reliable. Therefore, the equations obtained should not be extended to other techniques or organs for calculating iron concentration; (4) The sample size of 3T data is small, and it is difficult to perform grouping verification; (5) Accurate quantification of severe liver iron load by 3T T_2* technique still cannot be achieved due to the technical limitation of the 3T scanning sequence in this study.

5. Conclusion

This study explored the relationship between liver T_2* value and LIC_F provided by FerriScan in patients with thalassemia, and the related curve equation was constructed. After measuring the liver 1.5T T_2* value, the liver iron concentration could be accurately quantified, and liver iron concentration in patients with iron overload could be better monitored. An important reference for timely and better formulation of appropriate diagnosis and treatment plans can be made. 3T T_2* can be used to quantify liver iron concentration in patients with mild-to-moderate liver iron overload, while 1.5T T_2* or other methods are recommended for patients with severe liver iron overload.

Data availability statement

The original contributions presented in the study are included in the article/supplementary material, further inquiries can be directed to the corresponding author.

Ethics statement

The studies involving human participants were reviewed and approved by the Ethics Committee of the First Affiliated Hospital of Guangxi Medical University (2022-E457-01). Written informed consent from the participants' legal guardian/next of kin was not required to participate in this study in accordance with the national legislation and the institutional requirements.

Author contributions

PP contributed to the study's conception and design. Materials preparation and data collection were performed by FX, YP, HX, GY, FZ, and YL. Data analysis was performed by FX, HX, and YP. The first draft of the manuscript was written by FX and BL and all authors commented on earlier drafts of the manuscript. All authors have read and approved its final version.

Funding

This study was supported by grants from the National Natural Science Foundation of China (81760305 and 81641066) and the Innovation Project of Guangxi Graduate Education (YCSW2021135). At the same time, this study is supported by the Advanced Innovation Teams and Xinghu Scholars Program of Guangxi Medical University project.

Acknowledgments

The authors thank Meicheng Li, Hongxiu Zeng, and Yiling Huang for their technical support with MRI scanning. The authors also thank the Department of Hematology and Pediatrics of the First Affiliated Hospital of Guangxi Medical University for their support.

Conflict of interest

The authors declare that the research was conducted in the absence of any commercial or financial relationships that could be construed as a potential conflict of interest.

Publisher's note

All claims expressed in this article are solely those of the authors and do not necessarily represent those of their affiliated organizations, or those of the publisher, the editors and the reviewers. Any product that may be evaluated in this article, or claim that may be made by its manufacturer, is not guaranteed or endorsed by the publisher.

References

1. Labranche R, Gilbert G, Cerny M, Vu KN, Soulières D, Olivié D, et al. Liver iron quantification with MR imaging: a primer for radiologists. *Radiographics.* (2018) 38:392–412. doi: 10.1148/rg.2018170079

2. Xu F, Yi J, Liang B, Tang C, Feng Q, Peng P. Comparative study on the measurement of liver LICdw between Ferriscan and T_2* based licdw obtained by different software's. *Mediterr J Hematol Infect Dis.* (2022) 14:e2022072. doi: 10.4084/MJHID.2022.072

3. Jhaveri KS, Kannengiesser SAR, Ward R, Kuo K, Sussman MS. Prospective Evaluation of an R_2* Method for Assessing Liver Iron Concentration (LIC) against ferriscan: derivation of the calibration curve and characterization of the nature and source of uncertainty in the relationship. *J Magn Reson Imag.* (2019) 49:1467–74. doi: 10.1002/jmri.26313

4. Scott B. Reeder DH. *System and Method for Assessing Susceptibility of Tissue Using Magnetic Resonance Imaging.* USA: Wisconsin Alumni Research Foundation. (2018).

5. Henninger B, Plaikner M, Zoller H, Viveiros A, Kannengiesser S, Jaschke W, et al. Performance of different Dixon-based methods for MR liver iron assessment in comparison to a biopsy-validated R_2* relaxometry method. *Eur Radiol.* (2021) 31:2252–62. doi: 10.1007/s00330-020-07291-w

6. Khadivi Heris H, Nejati B, Rezazadeh K, Sate H, Dolatkhah R, Ghoreishi Z, et al. Evaluation of iron overload by cardiac and liver T_2* in β-thalassemia: Correlation with serum ferritin, heart function and liver enzymes. *J Cardiov Thor Res.* (2021) 13:54–60. doi: 10.34172/jcvtr.2021.18

7. Henninger B, Alustiza J, Garbowski M, Gandon Y. Practical guide to quantification of hepatic iron with MRI. *Eur Radiol.* (2020) 30:383–93. doi: 10.1007/s00330-019-06380-9

8. Henninger B, Zoller H, Rauch S, Finkenstedt A, Schocke M, Jaschke W, et al. R_2^* relaxometry for the quantification of hepatic iron overload: biopsy-based calibration and comparison with the literature. *RoFo.* (2015) 187:472–9. doi: 10.1055/s-0034-1399318

9. Wood JC, Enriquez C, Ghugre N, Tyzka JM, Carson S, Nelson MD, et al. MRI R2 and R2* mapping accurately estimates hepatic iron concentration in transfusion-dependent thalassemia and sickle cell disease patients. *Blood.* (2005) 106:1460–5. doi: 10.1182/blood-2004-10-3982

10. Hankins JS, McCarville MB, Loeffler RB, Smeltzer MP, Onciu M, Hoffer FA, et al. R_2^* magnetic resonance imaging of the liver in patients with iron overload. *Blood.* (2009) 113:4853–5. doi: 10.1182/blood-2008-12-191643

11. Christoforidis A, Perifanis V, Spanos G, Vlachaki E, Economou M, Tsatra I, et al. MRI assessment of liver iron content in thalassamic patients with three different protocols: comparisons and correlations. *Eur J Haematol.* (2009) 82:388–92. doi: 10.1111/j.1600-0609.2009.01223.x

12. Garbowski MW, Carpenter JP, Smith G, Roughton M, Alam MH, He T, et al. Biopsy-based calibration of T_2^* magnetic resonance for estimation of liver iron concentration and comparison with R2 Ferriscan. *J Cardiov Magn Reson.* (2014) 16:40. doi: 10.1186/1532-429X-16-40

13. Ouederni M, Ben Khaled M, Mellouli F, Ben Fraj E, Dhouib N, Yakoub IB, et al. Myocardial and liver iron overload, assessed using T_2^* magnetic resonance imaging with an excel spreadsheet for post processing in Tunisian thalassemia major patients. *Ann Hematol.* (2017) 96:133–9. doi: 10.1007/s00277-016-2841-5

14. Anwar M, Wood J, Manwani D, Taragin B, Oyeku SO, Peng Q. Corrigendum to "Hepatic iron quantification on 3 tesla (3 T) magnetic resonance (MR): technical challenges and solutions". *Radiol Res Pract.* (2018) 2018:8142478. doi: 10.1155/2018/8142478

15. d'Assignies G, Paisant A, Bardou-Jacquet E, Boulic A, Bannier E, Lainé F, et al. Non-invasive measurement of liver iron concentration using 3-Tesla magnetic resonance imaging: validation against biopsy. *Eur Radiol.* (2018) 28:2022–2030. doi: 10.1007/s00330-017-5106-3

16. Healy GM, Kannengiesser SAR, Espin-Garcia O, Ward R, Kuo KHM, Jhaveri KS. Comparison of Inline R_2^* MRI versus FerriScan for liver iron quantification in patients on chelation therapy for iron overload: preliminary results. *Eur Radiol.* (2021) 31:9296–305. doi: 10.1007/s00330-021-08019-0

17. Fernandes JL, Fioravante LAB, Verissimo MP, Loggetto SR. A free software for the calculation of T_2^* values for iron overload assessment. *Acta radiol.* (2017) 58:698–701. doi: 10.1177/0284185116666416

frontiers | Frontiers in Medicine

TYPE Original Research
PUBLISHED 26 June 2023
DOI 10.3389/fmed.2023.1193935

OPEN ACCESS

EDITED BY
Pierpaolo Di Micco,
Ospedale Santa Maria delle Grazie, Italy

REVIEWED BY
Gianluca Di Micco,
Ospedale Buon Consiglio Fatebenefratelli, Italy
Egidio Imbalzano,
University of Messina, Italy

*CORRESPONDENCE
Shuohui Chen
✉ chcsh2@zju.edu.cn

RECEIVED 26 March 2023
ACCEPTED 12 June 2023
PUBLISHED 26 June 2023

CITATION
Zhou J, Luo F, Liang J, Cheng X, Chen X, Li L and Chen S (2023) Construction and validation of a predictive risk model for nosocomial infections with MDRO in NICUs: a multicenter observational study.
Front. Med. 10:1193935.
doi: 10.3389/fmed.2023.1193935

Construction and validation of a predictive risk model for nosocomial infections with MDRO in NICUs: a multicenter observational study

Jinyan Zhou[1], Feixiang Luo[2], Jianfeng Liang[3], Xiaoying Cheng[4], Xiaofei Chen[5], Linyu Li[6] and Shuohui Chen[1]*

[1]Administration Department of Nosocomial Infection, Children's Hospital, Zhejiang University School of Medicine, National Clinical Research Center for Child Health, Hangzhou, China, [2]Neonatal Intensive Care Unit, Children's Hospital, Zhejiang University School of Medicine, National Clinical Research Center for Child Health, Hangzhou, China, [3]Statistics Office, Children's Hospital, Zhejiang University School of Medicine, National Clinical Research Center for Child Health, Hangzhou, China, [4]Quality Improvement Office, Children's Hospital, Zhejiang University School of Medicine, National Clinical Research Center for Child Health, Hangzhou, China, [5]Gastroenterology Department, Children's Hospital, Zhejiang University School of Medicine, National Clinical Research Center for Child Health, Hangzhou, China, [6]Hangzhou Children's Hospital, Hangzhou, Zhejiang, China

Objectives: This study aimed to construct and validate a predictive risk model (PRM) for nosocomial infections with multi-drug resistant organism (MDRO) in neonatal intensive care units (NICUs), in order to provide a scientific and reliable prediction tool, and to provide reference for clinical prevention and control of MDRO infections in NICUs.

Methods: This multicenter observational study was conducted at NICUs of two tertiary children's hospitals in Hangzhou, Zhejiang Province. Using cluster sampling, eligible neonates admitted to NICUs of research hospitals from January 2018 to December 2020 (modeling group) or from July 2021 to June 2022 (validation group) were included in this study. Univariate analysis and binary logistic regression analysis were used to construct the PRM. H-L tests, calibration curves, ROC curves and decision curve analysis were used to validate the PRM.

Results: Four hundred and thirty-five and one hundred fourteen neonates were enrolled in the modeling group and validation group, including 89 and 17 neonates infected with MDRO, respectively. Four independent risk factors were obtained and the PRM was constructed, namely: $P=1/(1+e^{-X})$, $X=-4.126+1.089\times$ (low birth weight) $+1.435\times$ (maternal age≥35years) $+1.498\times$ (use of antibiotics >7days)$+0.790\times$ (MDRO colonization). A nomogram was drawn to visualize the PRM. Through internal and external validation, the PRM had good fitting degree, calibration, discrimination and certain clinical validity. The prediction accuracy of the PRM was 77.19%.

Conclusion: Prevention and control strategies for each independent risk factor can be developed in NICUs. Moreover, clinical staff can use the PRM to early identification of neonates at high risk, and do targeted prevention to reduce MDRO infections in NICUs.

KEYWORDS

neonatal intensive care unit, multi-drug resistant organism, nosocomial infection, risk factor, predictive risk model

Introduction

Neonates in neonatal intensive care units (NICUs), especially low-birth-weight and premature infants, are more likely to develop nosocomial infections due to various invasive procedures, long hospital stays, and weak innate immunity (1). The study of 29 European countries showed that the nosocomial infection rate of NICUs was 10.7%, which was significantly higher than that of neonatal wards (3.5%) (2). Nosocomial infections in neonates can prolong hospitalization, increase treatment costs, and even lead to death (3). In recent years, the problem of bacterial resistance has become increasingly serious and is spreading globally (4, 5). According to the World Health Organization (WHO) global surveillance report (6), the proportion of *Escherichia coli*, *Klebsiella pneumoniae*, and *Staphylococcus aureus* resistant to some commonly used antimicrobial drugs exceeded 50%. Multi-drug resistant organism (MDRO) mainly refers to the bacterium resistant to three or more antibiotics clinically (7), which has brought great difficulties to clinical treatment of infections and posed great threats to the prognosis of neonates. Nosocomial infections with MDRO accounted for more than 30% of all nosocomial infections in the NICU (8), and was significantly associated with higher neonatal mortality (9).

As an important part of etiology in epidemiology, predictive risk models (PRMs) can identify risk factors related to disease and determine the effect of each risk factor on disease by establishing a multi-factor statistical model, so as to identify risk groups and achieve early prevention and intervention. At present, PRMs for nosocomial infections with MDRO are mainly aimed at the patients after liver transplantation (10), patients with biliary tract infection (11), adult critical patients (12) and emergency patients (13), and there is no PRM for nosocomial infections with MDRO in NICUs.

Therefore, this study aimed to construct and validate the PRM for nosocomial infections with MDRO in NICUs, in order to provide a scientific and reliable prediction tool, and to provide reference for clinical prevention and control of MDRO infections in NICUs.

Materials and methods

The research methods were determined in strict accordance with the 'Transparent reporting of a multivariable prediction model for individual prognosis or diagnosis (TRIPOD): the TRIPOD statement' (14).

Study design, research setting

We conducted a multicenter observational study at NICUs of two tertiary children's hospitals in Hangzhou, Zhejiang Province. The two NICUs have 30 and 50 beds respectively, mainly for the treatment of critical neonates with low birth weight, respiratory failure, complex congenital heart disease, severe brain injury, severe metabolic disorder, severe infection, and various congenital malformations. Since two research hospitals do not set up obstetrics, all neonates admitted to the two NICUs were born in other hospitals.

Participants

Using cluster sampling, neonates who were admitted to NICUs of two research hospitals from January 2018 to December 2020 (modeling group) or from July 2021 to June 2022 (validation group), were diagnosed with nosocomial infections during hospitalization, and had complete medical records were included in this study. In particular, if neonates had more than one nosocomial infection during hospitalization, only the first nosocomial infection was analyzed.

Data collection

In April 2021, 13 research variables including gestational age, birth weight, blood transfusion, duration of antibiotic use, breastfeeding, MDRO colonization, and maternal age were determined by systematic literature review and expert meeting method (see Supplementary material 1 for details and variable information). Modeling group data were collected retrospectively (January 2018 to December 2020) and validation group data were collected prospectively (July 2021 to June 2022). The data came from the critical care clinical information cloud system, hospital information system and hospital infection surveillance system. The data were entered independently by two people and reviewed by two others.

Sample size

A total of 13 independent variables were included in this study. In the logistic regression, the recommended empirical criterion is that events per variable (EPV) should be at least 10 to ensure stable results (15). The study (8) concluded that the proportion of nosocomial infections with MDRO in NICU was 31.29%. Therefore, the sample size of the modeling group was at least $13 \times 10 \div 31.29\% = 415$. A total of 435 neonates were included in the modeling group eventually.

The sample size of the validation group for external validation of the PRM was generally 1/4 ~ 1/2 of the sample size of the modeling group (16). So the sample size of the validation group was at least $435 \times 1/4 = 109$. A total of 114 neonates were included in the validation group actually.

Outcome variables

Nosocomial infections with MDRO refer to nosocomial infections whose pathogens are MDROs. MDROs mainly refer to bacteria resistant to three or more antibiotics clinically (7), including vancomycin-resistant *Enterococcus* (VRE), carbapenems-resistant *Enterobacteriacea* (CRE), methicillin-resistant *Staphylococcus aureus* (MRSA), carbapenem-resistant *Pseudomonas aeruginosa* (CRPA), carbapenem-resistant *Acinetobacter baumannii* (CRAB), and extended-spectrum beta-lactamases (ESBLs) -producing *Enterobacteriaceae* (e.g., *Escherichia coli* and *Klebsiella pneumoniae*), etc. According to the <Diagnostic criteria for nosocomial infections (trial)> (17) issued by the Ministry of Health, China, nosocomial infections refer to infections acquired in the hospital by hospitalized patients, including infections occurred during hospitalization or

acquired in the hospital and occurred after discharge (17). However, nosocomial infections do not include infections that occurred before admission or existed at admission (17).

Statistical analysis

SPSS 26.0 (IBM Corporation) and R 4.2.1 (R Core Team) were used for data analysis.

Statistical description and univariate analysis

The categorical variables were compared using the Fisher's exact test or χ^2 test and expressed as percentages. The continuous variables were tested for normal distribution by the Kolmogorov–Smirnov test, and Mann–Whitney *U* test or One-Way ANOVA was used according to their distribution. Continuous variables of normal distribution were expressed by mean ± standard deviation, and continuous variables of non-normal distribution were expressed by median (interquartile range). $p < 0.05$ was considered statistically significant.

Multivariate analysis

Binary logistic regression was performed on variables that were statistically significant ($p < 0.05$) in univariate analysis to explore the independent risk factors for nosocomial infections with MDRO in NICUs. The binary logistic regression adopted likelihood ratio (LR: forward), the inclusion probability was 0.05, and the exclusion probability was 0.10.

Model construction

The regression equation was obtained according to the partial regression coefficient β of each independent risk factor and the constant term in the binary logistic regression results, and the PRM was constructed, namely $P = 1/(1 + e\text{^}(-X))$, $X = \beta_0 + \beta_1 X_1 + \beta_2 X_2 + \beta_3 X_3 + \ldots + \beta_m X_m$. The R software was used to draw a nomogram based on the regression equation.

Model validation and evaluation

Hosmer-Lemeshow (H-L) test was used to evaluate the fitting degree of the model. $p > 0.05$ indicated that the PRM had a satisfactory fit (18). The calibration curve was used to reflect the calibration of the model. The discriminant validity of the model was usually tested by the area under the receiver operator characteristic curve (AUROC). It is generally believed that an AUROC value >0.70 indicates that the model has a relatively good discrimination (19). Decision curve analysis (DCA) was used to draw the DCA curves to evaluate the clinical effect of the model. The data of modeling group was resampled 1,000 times by Bootstrap method to validate the model internally. The data of the validation group were used to validate the model externally, and the accuracy of the model prediction was calculated.

Ethics approval

The Ethics Committee of Children's Hospital, Zhejiang University School of Medicine approved this study (2021-IRB-065). Informed consent has been obtained as required by the ethics committee.

Results

Basic characteristics of the research object

From January 2018 to December 2020, a total of 4,727 neonates were admitted to the two NICUs of research hospitals, with 459 cases of nosocomial infection, the incidence rate of nosocomial infection was 9.71%, including 24 cases with incomplete medical records. Therefore, the modeling group included 435 neonates. From July 2021 to June 2022, a total of 1,301 neonates were admitted to the two NICUs of research hospitals, with 114 cases of nosocomial infection, the incidence rate of nosocomial infection was 8.76%. Due to complete medical records, 114 neonates were included in the validation group. Basic characteristics of the modeling group and the validation group are shown in Table 1. The modeling group and validation group had 261 and 64 males, and 89 and 17 neonates infected with MDRO, respectively. The median gestational age of both groups was 29 weeks, the median birth weights were 1,230 g and 1,280 g, and the median ages of admission were 2 and 3 days, respectively. There is no significant difference in basic characteristics between the two groups. The pathogens of MDRO infections in the modeling and validation groups were mainly CRE and MRSA (Figure 1).

TABLE 1 Basic characteristics of the modeling group and the validation group.

Characteristic		Modeling group (*n*=435)	Validation group (*n*=114)	Z/χ^2	*p*
Gender, *n* (%)	Male	261 (60.00%)	64 (56.14%)	0.56	0.46
	Female	174 (40.00%)	50 (43.86%)		
Gestational age (weeks), Median (IQR)		29 (27, 32)	29 (27, 33)	1.25	0.21
Birth weight (g), Median (IQR)		1,230 (980, 1,640)	1,280 (943.75, 2351.25)	−0.29	0.77
With infectious diseases at admission, *n* (%)	Yes	100 (22.99%)	33 (28.95%)	1.75	0.19
	No	335 (77.01%)	81 (71.05%)		
Age of admission (days) Median (IQR)		2 (1，13)	3 (1，17.25)	1.01	0.31
Nosocomial infection with MDRO, *n* (%)	Yes	89 (20.46%)	17 (14.91%)	1.78	0.18
	No	346 (79.54%)	97 (85.09%)		

IQR, interquartile range, MDRO: multi-drug resistant organism.

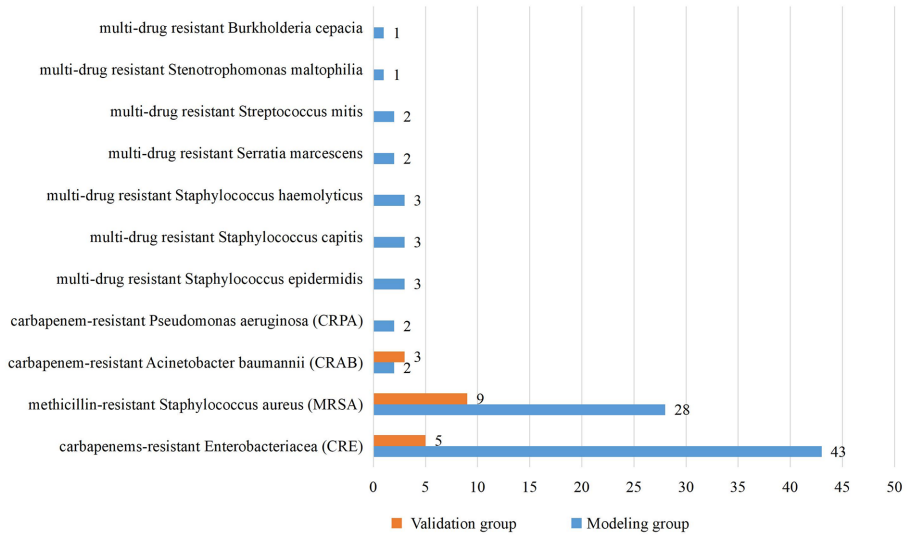

FIGURE 1
Pathogens of nosocomial infections with MDRO in NICUs.

Univariate analysis

The neonates in the modeling group were divided into the MDRO infection group and the non-MDRO infection group according to whether the pathogen was a MDRO. Univariate analysis of 13 variables was conducted to initially explore the differences between the two groups (Table 2). As can be seen from the table, there were 8 variables with statistically significant differences between the two groups. Compared with the non-MDRO infection group, the MDRO infection group was more likely to have the following characteristics: premature, low birth weight, maternal age ≥ 35 years, blood transfusion, blood collection >10 times, use of antibiotics >7 days, MDRO colonization and length of stay >10 days ($p < 0.05$).

Multivariate analysis

Collinearity diagnosis was performed on the above 8 variables that were significant in univariate analysis. The results showed that the tolerances of 8 variables were all >0.10, the variance inflation factors (VIFs) of 8 variables were all <10.0 (Specific results are presented in Supplementary material 2). It can be considered that there is no multicollinearity among the 8 variables (20), and logistic regression can be carried out. Binary logistic regression revealed that the independent risk factors of nosocomial infections with MDRO in NICUs were: low birth weight (OR: 2.97, 95%CI: 1.00 ~ 8.82, $p < 0.05$), maternal age ≥ 35 years (OR: 4.20, 95%CI: 2.43 ~ 7.26, $p < 0.01$), use of antibiotics >7 days (OR: 4.47, 95%CI: 2.45 ~ 8.17, $p < 0.01$) and MDRO colonization (OR: 2.20, 95%CI: 1.31 ~ 3.71, $p < 0.01$). The specific results of binary logistic regression are shown in Supplementary material 3.

PRM construction

According to the partial regression coefficient β of each independent risk factor and constant term in the logistic regression results, the logistic regression equation was obtained and the PRM was constructed, namely:

$P = 1/(1+e^{-X})$, $X = -4.126 + 1.089\times$ (low birth weight) $+1.435\times$ (maternal age ≥ 35 years) $+1.498\times$ (use of antibiotics >7 days) $+ 0.790\times$ (MDRO colonization).

In order to make the PRM more intuitive and more convenient for clinical application, the above logistic regression equation was drawn into a nomogram to visualize the PRM (Figure 2). The nomogram is used as follows. According to the actual situation of each risk factor of the neonate, the corresponding risk points (corresponding to the 'Points' line at the top of the nomogram) can be obtained by drawing a vertical line. Add up the risk points of each risk factor to get the total risk points (corresponding to the "Total points" line of the nomogram). Finally, the risk value (corresponding to the "Risk" line at the bottom of the nomograph) corresponding to the total points can be obtained by drawing a vertical line.

PRM validation

H-L test was conducted on the model in the modeling group and the validation group, and the p values were 0.61 and 0.49 (>0.05), respectively. It can be considered that there was no significant difference between the model predicted value and the actual value, and the model fit was good. The calibration curves were close to $y = x$, indicating that the predicted probability of the model was in good agreement with the actual probability (Figures 3A,D). The AUROC values of the modeling group and the validation group were 0.773 (95% CI: 0.718 ~ 0.828) and 0.788 (95% CI: 0.677 ~ 0.899) respectively, indicating that the model had a relatively good discrimination (Figures 3B,E). Using Bootstrap method, the data of modeling group was repeatedly sampled 1,000 times to calculate the corrected C-index, and the result was 0.766, indicating that the model was stable and the discrimination was good. The corresponding calibration curve was drawn, which was

TABLE 2 Univariate analysis of the modeling group (n=435).

Variable	MDRO infection group (n =89)	non-MDRO infection group (n =346)	Z/χ^2	p
Premature[a], n (%)	85 (95.51%)	284(82.08%)	9.91	<0.01
Low birth weight[b], n (%)	85 (95.51%)	284(82.08%)	9.91	<0.01
With infectious diseases at admission, n (%)	25 (28.09%)	75 (21.68%)	1.65	0.20
Maternal age ≥ 35 years[c], n (%)	40 (44.94%)	54 (15.61%)	35.97	<0.01
Breastfeeding, n (%)	63 (70.79%)	230 (66.47%)	0.60	0.44
Invasive mechanical ventilation, n (%)	65 (73.03%)	227 (65.61%)	1.77	0.18
Blood transfusion, n (%)	78 (87.64%)	246 (71.10%)	10.19	<0.01
Use of vascular catheter for ≥7 days[d], n (%)	50 (56.18%)	179 (51.73%)	0.56	0.45
Blood collection >10 times[e], n (%)	49 (55.06%)	134 (38.73%)	7.74	<0.01
Use of antibiotics >7 days[f], n (%)	72 (80.90%)	169 (48.84%)	29.44	<0.01
Combination of antibiotics, n (%)	56 (62.92%)	179 (51.73%)	3.57	0.06
MDRO colonization, n (%)	49 (55.06%)	138 (39.88%)	6.65	0.01
Length of stay >10 days[g], n (%)	81 (91.01%)	257 (74.28%)	11.44	<0.01

MDRO, multi-drug resistant organism.
[a]Preterm infants were defined as those born at a gestational age of < 37 weeks (≤259 days).
[b]Low birth weight infants were defined as those whose birth weight was < 2,500 g.
[c]Advanced maternal age is generally considered as maternal age ≥ 35 years, so the cut-off value was determined by this.
[d, f]The cut-off values were determined according to the relevant research results.
[e, g]The cut-off values were determined according to the ROC curves.

close to $y = x$, indicating that the predicted value fitted in well with the observed value (Figure 3C).

The prediction effect of the PRM

The ROC curve of the modeling group showed that the optimal cut-off value was when the predicted risk value was 0.27 (Figure 3B). Based on this, risk stratification was performed, that is, when the predicted probability was ≥0.27, the risk of nosocomial infections with MDRO was high, and when the predicted probability is <0.27, the risk of nosocomial infections with MDRO was low. According to the PRM, the prediction probability of nosocomial infections with MDRO of each neonate in the validation group was calculated, and the prediction effect of the model was tested. The results showed that in the validation group, the PRM predicted that 11 out of 17 cases of MDRO infection group were at high risk, and 77 out of 97 cases of non-MDRO infection group were at low risk. Compared with the actual results, the sensitivity of the prediction results was 64.71%, the specificity was 79.38%, the Jordan index was 0.44, the positive likelihood ratio was 3.14, the negative likelihood ratio was 0.44, and the prediction accuracy was 77.19%.

The clinical validity of the PRM

Decision curve analysis (DCA) was used to calculate the net benefit at each threshold probability in this study. The DCA curves of the modeling group and the validation group are shown in Figures 4A,B respectively. Suppose the PRM predicts that the probability of nosocomial infections with MDRO in neonate i is Pi. When Pi reaches a certain threshold (noted as Pt), it is considered that neonate i will have nosocomial infections with MDRO, and intervention measures will be taken. The abscissa is the threshold probability, and the ordinate is the net benefit of taking interventions. The black horizontal line and the blue slash line represented two extreme cases. The black horizontal line indicated that none of the neonates experienced nosocomial infections with MDRO and none received interventions, at which point the net benefit was zero. The blue slash line showed the net benefit when all neonates developed nosocomial infections with MDRO and all received interventions. The red curve represented the net benefit of performing interventions based on this study's PRM. The results showed that the red line was located above the black and blue lines when the threshold probabilities were 7% ~ 65 and 3% ~ 50% in the modeling group and the validation group, respectively. At this time, interventions based on the PRM can achieve greater net benefits, indicating that the PRM constructed in this study had certain clinical validity.

Discussion

With the rapid development of the Internet and the in-depth integration with the medical and health industry, relying on artificial intelligence and machine learning technology, the treatment, nursing and health management of patients gradually tend to be individualized and refined (21, 22). In this study, 13 research variables were identified through systematic literature review and expert meeting method. After univariate analysis and binary logistic regression analysis, 4 independent risk factors were attained. The PRM for nosocomial infections with MDRO in NICUs was constructed and a nomogram was drawn. The internal and external validation showed that the PRM had good calibration and discrimination, relatively accurate prediction, and had certain clinical validity, which can provide scientific basis for prevention and control of nosocomial infections with MDRO in NICUs.

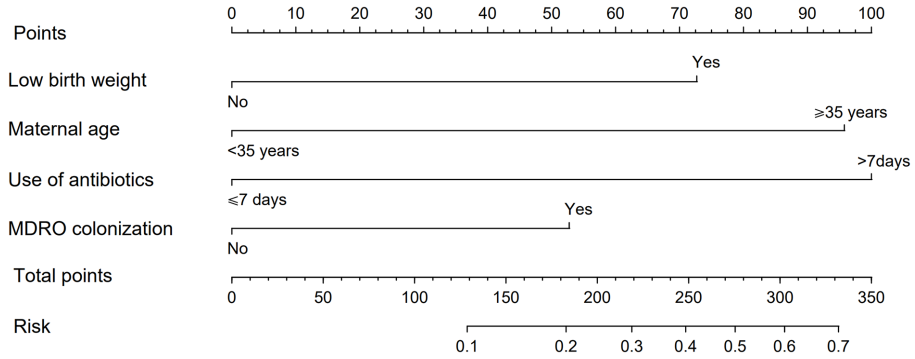

FIGURE 2
Nomogram of PRM for nosocomial infections with MDRO in NICUs. The method of using the nomogram was as follows: according to the actual situation of each risk factor in the neonate, the corresponding risk point was obtained through the vertical line (corresponding to the top of the nomogram), the risk point of each risk factor was summed to obtain the total risk points (corresponding to the total points line of the nomogram), and the risk value corresponding to the total points was obtained through the vertical line (corresponding to the bottom of the nomogram).

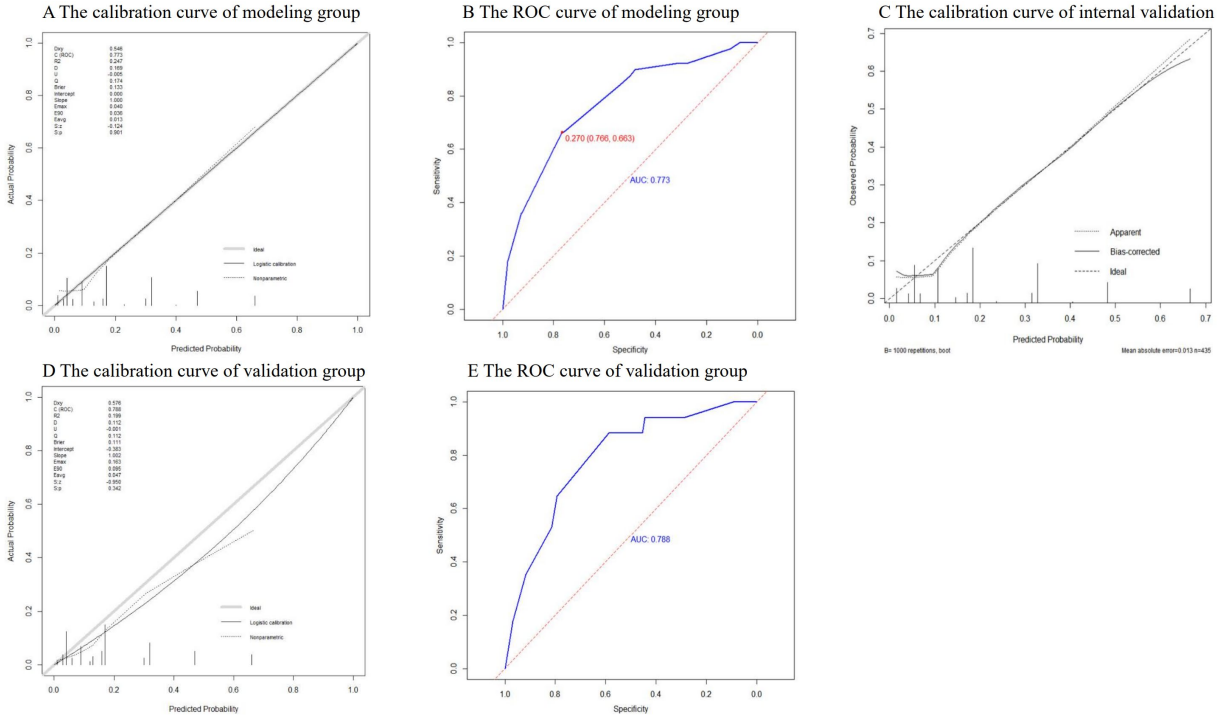

FIGURE 3
The results of internal and external validation.

The 4 independent risk factors obtained in this study were low birth weight, maternal age ≥ 35 years, use of antibiotics >7 days and MDRO colonization. Therefore, to reduce MDRO infections in NICUs, care for low birth weight infants should be enhanced. Appropriate marriage and childbearing should be advocated, and pregnant women, especially those with advanced maternal age, should take good prenatal care. Nursing staff should strengthen the postpartum care for elderly puerperae and closely observe their neonates. Rational use of antibiotics is particularly important to prevent MDRO infections. Doctors should administer antibiotics in strict accordance with the indications for the application of antibiotics, and nurses should feedback the effect of medication in time and cooperate with doctors to use drugs rationally. In addition, intensive MDRO surveillance of neonates should be undertaken in ways such as active screening, and prompt decolonization therapy should be offered to neonates with MDRO colonization.

In addition to guiding NICUs to carry out prevention and control strategies for each independent risk factor, based on the results of this study, clinical staff can use the PRM to identify high-risk neonates at an early stage, and give special attention to improve the effect of

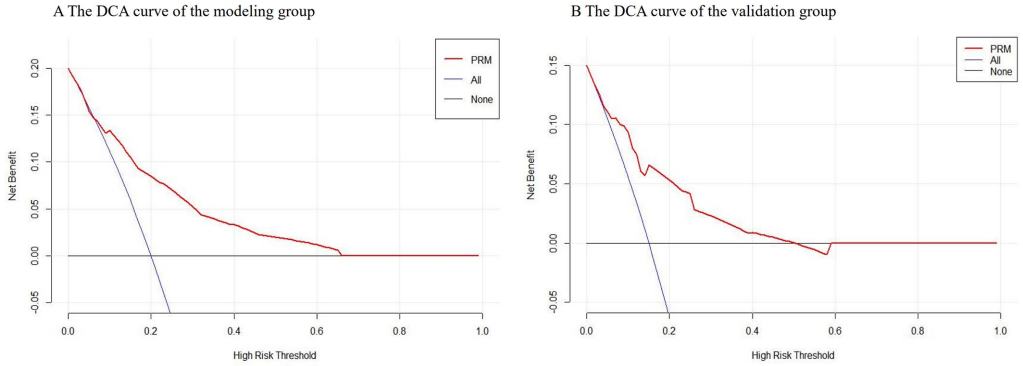

FIGURE 4
The DCA curves of the modeling group and the validation group.

infection prevention and control, reduce the incidence of infection, and ultimately improve the treatment effect and prognosis of neonates.

With the continuous development of global bacterial resistance, the situation of nosocomial infections with MDRO is becoming more and more serious. Nosocomial infections with MDRO greatly increase the difficulty of treatment, increase the financial burden on patients' families, and affect patient prognosis, even leading to patient death. In this context, constructing a PRM will help identify susceptible populations, achieve early prevention and intervention, so as to improve patient prognosis and medical quality. As far as we know, this study is the first to construct a PRM for nosocomial infections with MDRO in NICUs. This study provides a relatively scientific and relatively reliable prediction tool, and can provide reference for clinical prevention and control of MDRO infections in NICUs. However, there are some limitations to this study. Firstly, a retrospective design was adopted in the construction of the PRM, which may affect the accuracy of the results due to information bias. Secondly, since only two hospitals were selected, the study subjects were not sufficiently represented, and the generalizability of the findings needs to be further verified. Moreover, the external validation in this study selected research subjects from the same institutions in different periods rather than from different institutions, which makes it impossible to determine whether the model constructed in this study is applicable to other regions or other institutions. Finally, because the study sites of this study were tertiary children's hospitals, the applicability of the PRM to NICUs of other types of hospitals remains to be tested.

Conclusion

Our study constructed a PRM for nosocomial infections with MDRO in NICUs. After validating, the PRM had a good calibration degree and discriminant validity, relatively accurate prediction, and had some clinical application value. Based on the findings of this study, prevention and control strategies for each independent risk factor can be developed in NICUs. At the same time, clinical staff can take advantage of the PRM to enable early identification of neonates at high risk of MDRO infections, and thus do targeted prevention to reduce the occurrence of nosocomial infections with MDRO in NICUs.

Data availability statement

The original contributions presented in the study are included in the article/Supplementary material, further inquiries can be directed to the corresponding author.

Ethics statement

The studies involving human participants were reviewed and approved by the Ethics Committee of Children's Hospital, Zhejiang University School of Medicine (2021-IRB-065). Informed consent has been obtained as required by the ethics committee.

Author contributions

JZ conceptualized and designed the study, collected data, analyzed data, drafted the initial manuscript, and critically reviewed and revised the manuscript. FL conceptualized and designed the study, analyzed data, and critically reviewed and revised the manuscript. JL directed and supervised data analysis and critically reviewed and revised the manuscript. XYC reviewed data collection, and critically reviewed and revised the manuscript. XFC reviewed data collection, and critically reviewed and revised the manuscript. LL collected data and critically reviewed and revised the manuscript. SC conceptualized and designed the study, coordinated and supervised data collection and analysis, and critically reviewed and revised the manuscript for important intellectual content. All authors approved the final manuscript as submitted and agree to be accountable for all aspects of the work.

Acknowledgments

The authors would like to thank the doctors and nurses in NICUs for keeping patient records in detail, and thank Mingming Zhou for her guidance and help on microbiology in this study. Thanks to Linlin Cai and Xing Xin for helping with statistical analysis.

Conflict of interest

The authors declare that the research was conducted in the absence of any commercial or financial relationships that could be construed as a potential conflict of interest.

Publisher's note

All claims expressed in this article are solely those of the authors and do not necessarily represent those of their affiliated organizations, or those of the publisher, the editors and the reviewers. Any product that may be evaluated in this article, or claim that may be made by its manufacturer, is not guaranteed or endorsed by the publisher.

Supplementary material

The Supplementary material for this article can be found online at: https://www.frontiersin.org/articles/10.3389/fmed.2023.1193935/full#supplementary-material

References

1. Ponnusamy V, Venkatesh V, Clarke P. Skin antisepsis in the neonate: what should we use? *Curr Opin Infect Dis*. (2014) 27:244–0. doi: 10.1097/QCO.0000000000000064

2. Zingg W, Hopkins S, Gayet-Ageron A, Holmes A, Sharland M, Suetens C, et al. Health-care-associated infections in neonates, children, and adolescents: an analysis of paediatric data from the European Centre for Disease Prevention and Control point-prevalence survey. *Lancet Infect Dis*. (2017) 17:381–9. doi: 10.1016/S1473-3099(16)30517-5

3. Civardi E, Tzialla C, Baldanti F, Strocchio L, Manzoni P, Stronati M. Viral outbreaks in neonatal intensive care units: what we do not know. *Am J Infect Control*. (2013) 41:854–6. doi: 10.1016/j.ajic.2013.01.026

4. Laxminarayan R, Duse A, Wattal C, Zaidi AKM, Wertheim HFL, Sumpradit N, et al. Antibiotic resistance-the need for global solutions. *Lancet Infect Dis*. (2013) 13:1057–98. doi: 10.1016/S1473-3099(13)70318-9

5. Rhodes A, Evans LE, Alhazzani W, Levy MM, Antonelli M, Ferrer R, et al. Surviving Sepsis campaign: international guidelines for Management of Sepsis and Septic Shock: 2016. *Intensive Care Med*. (2017) 43:304–7. doi: 10.1007/s00134-017-4683-6

6. World Health Organization (WHO). *Antimicrobial resistance: global report on surveillance 2014*. Geneva: WHO (2014).

7. The Ministry of Health of China. Technical guidelines for the prevention and control of nosocomial infections with MDRO. (2011). available at: http://www.nhc.gov.cn/cmssearch/xxgk/getManuscriptXxgk.htm?id=50487 (Accessed January 1, 2023).

8. Xu L, Wang RY, Chen BB, et al. Risk factors and prevention measures of multiple drug-resistant infections in neonatal intensive care unit. *Chin J General Pract*. (2018) 16:1314–7.

9. Tsai MH, Chu SM, Hsu JF, Lien R, Huang HR, Chiang MC, et al. Risk factors and outcomes for multidrug-resistant gram-negative bacteremia in the NICU. *Pediatrics*. (2014) 133:e322–9. doi: 10.1542/peds.2013-1248

10. Giannella M, Freire M, Rinaldi M, Abdala E, Rubin A, Mularoni A, et al. Development of a risk prediction model for carbapenem-resistant Enterobacteriaceae infection after liver transplantation: a multinational cohort study. *Clin Infect Dis*. (2021) 73:e955–66. doi: 10.1093/cid/ciab109

11. Hu Y, Lin K, Lin K, Lin H, Chen R, Li S, et al. Developing a risk prediction model for multidrug-resistant bacterial infection in patients with biliary tract infection. *Saudi J Gastroenterol*. (2020) 26:326–6. doi: 10.4103/sjg.SJG_128_20

12. Wang Y, Lin Q, Chen Z, Hou H, Shen N, Wang Z, et al. Construction of a risk prediction model for subsequent bloodstream infection in intestinal carriers of carbapenem-resistant Enterobacteriaceae: a retrospective study in Hematology department and intensive care unit. *Infect Drug Resist*. (2021) 14:815–4. doi: 10.2147/IDR.S286401

13. On behalf of the INFURG-SEMES investigators (see addedum)González del Castillo J, Julián-Jiménez A, Gamazo-del Rio JJ, García-Lamberechts EJ, Llopis-Roca F, et al. A multidrug-resistant microorganism infection risk prediction model: development and validation in an emergency medicine population. *Eur J Clin Microbiol Infect Dis*. (2020) 39:309–3. doi: 10.1007/s10096-019-03727-4

14. Collins GS, Reitsma JB, Altman DG, Moons KGTRIPOD Group. Transparent reporting of a multivariable prediction model for individual prognosis or diagnosis (TRIPOD): the TRIPOD statement. The TRIPOD group. *Circulation*. (2015) 131:211–9. doi: 10.1161/CIRCULATIONAHA.114.014508

15. Gao YX, Zhang JX. Determination of sample size in logistic regression analysis. *J Evid Based Med*. (2018) 18:122–4.

16. Zhu XX. *Establishment and verification of risk prediction model of peristomal moisture-associated skin damage in patients with intestinal stoma*. Guangzhou: Southern Medical University (2021).

17. The Ministry of Health of China. Diagnostic criteria for nosocomial infections (trial). (2001). Available at: http://www.nhc.gov.cn/wjw/gfxwj/201304/37cad8d95582456d8907ad04a5f3bd4c.shtml (Accessed January 1, 2023).

18. Lemeshow S, Hosmer DW. A review of goodness of fit statistics for use in the development of logistic regression models. *Am J Epidemiol*. (1982) 115:92–6. doi: 10.1093/oxfordjournals.aje.a113284

19. Hanley JA, McNeil BJ. The meaning and use of the area under a receiver operating characteristic (ROC) curve. *Radiology*. (1982) 143:29–36. doi: 10.1148/radiology.143.1.7063747

20. Robert M, O'brien . A caution regarding rules of thumb for variance inflation factors. *Qual Quant*. (2007) 41:673–0. doi: 10.1007/s11135-006-9018-6

21. Imbalzano E, Orlando L, Sciacqua A, Nato G, Dentali F, Nassisi V, et al. Machine learning to calculate heparin dose in COVID-19 patients with active Cancer. *J Clin Med*. (2021) 11:219. doi: 10.3390/jcm11010219

22. Haug CJ, Drazen JM. Artificial intelligence and machine learning in clinical medicine, 2023. *N Engl J Med*. (2023) 388:1201–8. doi: 10.1056/NEJMra2302038

frontiers | Frontiers in Medicine

TYPE Original Research
PUBLISHED 17 July 2023
DOI 10.3389/fmed.2023.1176168

OPEN ACCESS

EDITED BY
Tomás José Gonzalez López,
Burgos University Hospital, Spain

REVIEWED BY
Kin Israel Notarte,
Johns Hopkins University, United States
Ferenc Uher,
Central Hospital of Southern Pest, Hungary
Gábor Barna,
Semmelweis University, Hungary

*CORRESPONDENCE
László G. Puskás
✉ laszlo@avidinbiotech.com
Gabor J. Szebeni
✉ szebeni.gabor@brc.hu

†These authors have contributed equally to this work and share first authorship

‡These authors have contributed equally to this work and share senior authorship

RECEIVED 28 February 2023
ACCEPTED 23 June 2023
PUBLISHED 17 July 2023

CITATION
Szabó E, Modok S, Rónaszéki B, Faragó A, Gémes N, Nagy LI, Hackler L Jr, Farkas K, Neuperger P, Balog JÁ, Balog A, Puskás LG and Szebeni GJ (2023) Comparison of humoral and cellular immune responses in hematologic diseases following completed vaccination protocol with BBIBP-CorV, or AZD1222, or BNT162b2 vaccines against SARS-CoV-2. *Front. Med.* 10:1176168. doi: 10.3389/fmed.2023.1176168

Comparison of humoral and cellular immune responses in hematologic diseases following completed vaccination protocol with BBIBP-CorV, or AZD1222, or BNT162b2 vaccines against SARS-CoV-2

Enikő Szabó[1†], Szabolcs Modok[2†], Benedek Rónaszéki[2], Anna Faragó[3,4], Nikolett Gémes[1,4], Lajos I. Nagy[3], László Hackler Jr.[3], Katalin Farkas[5], Patrícia Neuperger[1,4], József Á. Balog[1], Attila Balog[6], László G. Puskás[1,3,7*‡] and Gabor J. Szebeni[1,8,9*‡]

[1]Laboratory of Functional Genomics, Biological Research Centre, Szeged, Hungary, [2]Department of Medicine, Szent-Györgyi Albert Medical School-University of Szeged, Szeged, Hungary, [3]Avidin Ltd., Szeged, Hungary, [4]Doctoral School in Biology, Faculty of Science and Informatics, University of Szeged, Szeged, Hungary, [5]AstridBio Technologies Ltd., Szeged, Hungary, [6]Department of Rheumatology and Immunology, Faculty of Medicine, Albert Szent-Gyorgyi Health Centre, University of Szeged, Szeged, Hungary, [7]Avicor Ltd., Szeged, Hungary, [8]Department of Physiology, Anatomy and Neuroscience, Faculty of Science and Informatics, University of Szeged, Szeged, Hungary, [9]CS-Smartlab Devices, Kozarmisleny, Hungary

Background: Vaccination has proven the potential to control the COVID-19 pandemic worldwide. Although recent evidence suggests a poor humoral response against SARS-CoV-2 in vaccinated hematological disease (HD) patients, data on vaccination in these patients is limited with the comparison of mRNA-based, vector-based or inactivated virus-based vaccines.

Methods: Forty-nine HD patients and 46 healthy controls (HCs) were enrolled who received two-doses complete vaccination with BNT162b2, or AZD1222, or BBIBP-CorV, respectively. The antibodies reactive to the receptor binding domain of spike protein of SARS-CoV-2 were assayed by Siemens ADVIA Centaur assay. The reactive cellular immunity was assayed by flow cytometry. The PBMCs were reactivated with SARS-CoV-2 antigens and the production of activation-induced markers (TNF-α, IFN-γ, CD40L) was measured in $CD4^+$ or $CD8^+$ T-cells *ex vivo*.

Results: The anti-RBD IgG level was the highest upon BNT162b2 vaccination in HDs (1264 BAU/mL) vs. HCs (1325 BAU/mL) among the studied groups. The BBIBP-CorV vaccination in HDs (339.8 BAU/mL ***$p<0.001$) and AZD1222 in HDs (669.9 BAU/mL *$p<0.05$) resulted in weaker antibody response vs. BNT162b2 in HCs. The response rate of IgG production of HC vs. HD patients above the diagnostic cut-off value was 100% vs. 72% for the mRNA-based BNT162b2 vaccine; 93% vs. 56% for the vector-based AZD1222, or 69% vs. 33% for the inactivated vaccine BBIBP-CorV, respectively. Cases that underwent the anti-CD20 therapy resulted in significantly weaker (**$p<0.01$) anti-RBD IgG level (302 BAU/mL) than without CD20 blocking in the HD group (928 BAU/mL). The response rates of $CD4^+$

TNF-α^+, $CD4^+$ IFN-γ^+, or $CD4^+$ $CD40L^+$ cases were lower in HDs vs. HCs in all vaccine groups. However, the BBIBP-CorV vaccine resulted the highest $CD4^+$ TNF-α and $CD4^+$ IFN-γ^+ T-cell mediated immunity in the HD group.

Conclusion: We have demonstrated a significant weaker overall response to vaccines in the immunologically impaired HD population vs. HCs regardless of vaccine type. Although, the humoral immune activity against SARS-CoV-2 can be highly evoked by mRNA-based BNT162b2 vaccination compared to vector-based AZD1222 vaccine, or inactivated virus vaccine BBIBP-CorV, whereas the $CD4^+$ T-cell mediated cellular activity was highest in HDs vaccinated with BBIBP-CorV.

KEYWORDS

hematology diseases, SARS-CoV-2 vaccination, BBIBP-CorV, AZD1222, BNT162b2, COVID-19, protective immunity

1. Introduction

After the COVID-19 outbreak, it has rapidly become clear that SARS-CoV-2 infection is a higher threat with more severe clinical course to patients with hematological diseases (HD). Patients with HD suffer from higher mortality rate than the general population with COVID-19 or non-hematology COVID-19 patients (1–3) which can be explained by risk factors such as age, comorbidities and immunosuppressive therapies. After SARS-CoV-2 infection nearly one-third of the patients (31%) has been reported to be serologically negative for SARS-CoV-2 IgGs (4).

The vaccination against severe acute respiratory syndrome coronavirus 2 (SARS-CoV-2) emerged as the first line defense strategy in the fight against the global pandemic, and available vaccines have prevented COVID-19 related hospitalization, severe disease and death worldwide (5). SARS-CoV-2 vaccination improved the mortality rate of HD patients from 31% (pre-vaccination era) to 9% (6) which is still remarkably higher compared to the rate observed in the fully vaccinated overall population (7). A recent meta-analysis including 26 studies revealed that patients with HD had significantly lower seroconversion rate (33.3%) compared to healthy controls (74.9%) and despite the increase of seroconversion rates after the second dose, the significant difference between the two groups remained (65.3% vs. 97.8%) (8). A more recent meta-analysis of 150 studies with 20922 HD patients showed a pooled seroconversion rate after SARS-CoV-2 vaccination of 67.7% and the meta-regression analysis revealed that patients with lymphoid malignancies, but not myeloid malignancies, had lower seropositivity rates than those with solid tumors (9).

Multiple studies highlighted that patients with hematological malignancies receiving immunosuppressive therapies such as stem cell transplantation, anti-CD20 therapies, Bruton's tyrosine kinase (BTK) inhibitors and CAR-T cell treatments are at higher risk. Anti-CD20 monoclonal antibody therapy may result in prolonged depletion of normal B-cells and therefore markedly impaired humoral response to COVID-19 vaccination in HD patients with undetectable or decreased protective antibody titers (10–14).

There are several aspects of vaccination efficacy regarding this vulnerable group of patients which are rarely discussed in the literature. First, beyond the scope of humoral response to COVID-19 vaccination, the role of vaccine-induced cellular response is less explored. Minority of published articles incorporated the assessment of SARS-CoV-2-specific T-cell response after complete vaccination with detectable T-cell mediated immunity ranging between 29% and 88% of the HD patients (9, 10, 12, 15–17). Second, majority of the reports demonstrated the efficacy of mRNA and vector-based vaccines, although in many countries (including Hungary) inactivated vaccines are also approved.

To narrow down this knowledge gap, we conducted this complex study to compare the immunogenicity of mRNA (BNT162b2), vector-based (AZD1222) and inactivated (BBIBP-CorV) vaccine in a cohort of fully vaccinated patients with HD versus healthy individuals. Both humoral and cellular immunity was evaluated by measuring the neutralizing anti-SARS-CoV-2 antibody titers and by quantifying SARS-CoV-2 reactive T-cells with the help of multicolor flow cytometry.

2. Materials and methods

2.1. Ethical statement

The enrollment of patients was reviewed and approved by the Human Investigation Review Board of the National Public Health Center under Project Identification Code 47226-7/2019EÜIG. The patients provided their written informed consent to participate in this study. Subjects were informed about the study by a physician and acute SARS-CoV-2 infection was ruled out by RT-qPCR. Laboratory studies and interpretations were performed on coded samples lacking personal and diagnostic identifiers. The study adhered to the tenets of the most recent revision of the Declaration of Helsinki.

2.2. Study population

The main characteristics of the study participants (46 healthy controls, HCs and 49 hematologic disease patients, HDs) are summarized Table 1 and detailed demographic data of the enrolled HD patients vaccinated with BBIBP-CorV are summarized in Supplementary Table S1, vaccinated with AZD1222 are summarized in Supplementary Table S2, vaccinated with BNT162b2 are

TABLE 1 Demographic data of the enrolled HCs and HD patients vaccinated with anti-SARS-CoV-2 specific vaccines.

	Age (years, mean±SD)	Female	BBIBP-CorV	AZD1222	BNT162b2	Therapy: anti-CD20	Disease duration (years, mean±SD)
All HCs, $n=46$	43 ± 12	$n=30$ (65%)	$n=16$ (35%)	$n=14$ (30%)	$n=16$ (35%)	–	–
All patients with HDs, $n=49$	63 ± 14	$n=20$ (40%)	$n=15$ (30%)	$n=16$ (33%)	$n=18$ (37%)	$n=11$ (22%)	4.2 ± 3.2

summarized in Supplementary Table S3. All participants received two doses of the relevant vaccine in line with recommendations of the respective manufacturer of BBIBP-CorV (Sinopharm, Beijing Institute, Beijing, China); AZD1222 (ChAdOx1, University of Oxford and AstraZeneca, Cambridge, United Kingdom); and BNT162b2 (Comirnaty, Pfizer-BioNtech, Mainz, Germany). This prospective observational study was conducted at the Szent-Györgyi Albert Medical School-University of Szeged, Department of Medicine, Szeged, Hungary between October 2021 and February 2021. Adult patients with HDs were recruited who received two doses vaccination starting from February 2021 and completed by 1st June 2021. Peripheral blood and sera sampling was conducted after 4 months of the second vaccination event. The schematic cartoon of the project workflow is demonstrated in Supplementary Figure S1.

This study is a cross sectional analysis including a wide variety of hematology patients. Patients diagnosed with acute leukemia and aggressive lymphoma under induction chemotherapy were excluded. Treatment with tyrosine kinase inhibitors such as ibrutinib, ruxolitinib and dasatinib was allowed, similarly to any kind of anti-myeloma treatment including intermittent corticosteroids. A subgroup with known prior anti-CD20 moAb treatment was created. Patients with any sign of an acute infection, including confirmed acute SARS-CoV-2 infection were excluded. The distribution of vaccine types represents vaccine usage in the entire hematology patient population.

The withdrawal of 10 mL peripheral blood was carried-out into Lithium Heparin tubes (BD vacutainer, Beckton Dickinson). The primary endpoint was the humoral and cellular immunogenicity of homologous two doses of BBIBP-CorV or AZD1222, or BNT162b2, respectively. Secondary endpoints included: effect of anti-CD20 treatment and hematologic disease duration on the production of anti-RBD neutralizing antibodies in HD patients.

2.3. Measurement of anti-SARS-CoV-2 IgG antibodies

Measurement of SARS-CoV-2 anti-RBD (receptor binding domain) of spike (S) protein, the IgG-type antibodies was performed as described in detail previously by our group (18, 19). Briefly, quantitative measurement of neutralizing anti-RDB specific IgG-type antibody levels was performed with the Siemens Advia Centaur XPT system using the Siemens Healthineers SARS-CoV-2 IgG assay (sCOVG) (Siemens Healthineers, Munich, Germany). Irsara et al. (20), showed a proper correlation ($r=0.84$) of the positive sCOVG assay results with virus neutralization capacity. Measured index values were converted into WHO 20/136 approved international units of 1000 Binding Antibody Unit per milliliter (BAU/mL) using the following equation: (sCOVG index) × 21.8 = BAU/mL, where the diagnostic cut-off value was 21.8 BAU/mL), assay sensitivity was 10.9 BAU/mL (21).

2.4. Measurement of SARS-CoV-2 specific cellular immunity

Measurement of SARS-CoV-2 specific T-cell mediated immunity was performed as described in detail previously by our group (18, 19). Briefly, measurement of SARS-CoV-2 specific T-Cell memory was performed according to the instruction of the manufacturer using the SARS-CoV-2 Prot_S T Cell Analysis Kit (PBMC) (Miltenyi Biotec, Cat. No.: 130-127-586). The PBMCs were isolated by gradient centrifugation using Leucosep tubes (Greiner Bio-One, Cat. No.: 163288) following the instructions of the manufacturer. After the isolation of PBMCs and *in vitro* stimulation, staining with the antibodies, a minimum of 2×10^5 $CD3^+$ cells were acquired on CytoFLEX S FACS (Beckman Coulter). Manual gating was used to determine $CD4^+$ or $CD8^+$ T-cells within live $CD14^-/CD20^-$, $CD3^+$ lymphocytes in CytExpert (Beckman Coulter). Reactive cells were gated as $CD4^+$ TNF-α^+, $CD4^+$ IFN-γ^+, $CD4^+$ $CD40L^+$, $CD8^+$ TNF-α^+ and $CD8^+$ IFNγ^+ upon stimuli with the following pool of SARS-CoV-2 derived synthetic peptides: S-(spike, PepTivator SARS-CoV-2 Prot_S, Cat. No.: 130-126-701), M-(membrane, PepTivator SARS-CoV-2 Prot_M, Cat. No.: 130-126-702), N-(nucleocapsid, PepTivator SARS-CoV-2 Prot_N, Cat. No.:130-126-698) according to the instructions of the manufacturer (Miltenyi Biotec). The controls were the patient matched PBMCs left untreated. Gating was above the negative cells in the untreated control samples analyzed individually for each patient. The gating strategy has already been published by our group in the Supplementary Figure S1 in the reference Szebeni et al. (18). Cell numbers in the reporting gates were normalized to parental $CD4^+$ or $CD8^+$ T-cells (reactive cell number/parental cell number $\times 10^6$), then the background was normalized via subtraction of untreated from the stimulated. Finally, reactive cell numbers are shown in relation to 10^6 $CD4^+$ or $CD8^+$ T-cells (Mean ± SEM/1 × 10^6 parental $CD4^+$ T-cells, SD), the cut-off value was 400 reactive cells of 10^6 parental population.

2.5. Statistics

Data were analyzed with GraphPad Prism 8.0.1. Normality of distributions were tested with D'Agostino & Pearson test with an 0.05 alpha value. None of the groups were normally distributed datasets, so we used non-parametric Mann–Whitney test for two group comparisons and Kruskal–Wallis test was applied for three group comparisons. Dunn's test was used for multiple comparisons. Differences are considered significant at $^*p<0.05$, $^{**}p<0.01$, and $^{***}p<0.001$.

3. Results

3.1. SARS-CoV-2 specific humoral immunity in HDs following vaccination

The receptor binding domain (RBD) specific anti-spike (S) IgG isotype antibodies were measured in HDs versus healthy controls following complete vaccination after 4 months. Three types of SARS-CoV-2 specific vaccines were tested, the inactivated vaccine (BBIBP-CorV), or adenovirus vector-based (AZD1222), or mRNA (BNT162b2) technology-based vaccines (Figure 1A). Dunn's test was used for multiple comparisons and significant differences are marked in Figure 1. The humoral response rate corresponds to the percentage of subjects in one group in terms of the production of SARS-CoV-2 reactive IgG antibodies over the cut-off value 21.8 BAU/mL. The simple 'response' in Results 3.1 corresponds to SARS-CoV-2 reactive IgG production. The anti-RBD IgG level (mean of the BAU/mL ± SEM, SD) was the highest upon BNT162b2 vaccination in HDs (1264 ± 348.6, SD: 1479) vs. HCs (1325 ± 318.9, SD: 1276) among the studied groups. The BBIBP-CorV vaccination in HDs (339.8 ± 216.9, SD: 840 $^{***}p < 0.001$) and AZD1222 in HDs (669.9 ± 310.5, SD: 1242) $^{*}p < 0.05$) resulted in weaker antibody response vs. BNT162b2 in HCs (1325 ± 318.9, SD: 1276). The BBIBP-CorV in HCs showed less anti-RBD antibody production (41.09 ± 7.4, SD: 30 $^{*}p < 0.05$) vs. AZD1222 in HCs (211.8 ± 89.48, SD: 335), or vs. BNT162b2 in HCs (1325 ± 318.9, SD: 1242 $^{***}p < 0.001$) respectively (Figure 1A). The humoral response rate of HC vs. HD patients above the diagnostic cut-off value was 69% vs. 33% for the inactivated vaccine BBIBP-CorV; 93% vs. 56% for the vector-based AZD1222, or 100% vs. 72% for the mRNA-based BNT162b2 vaccine (Figure 1B), respectively.

Anti-CD20 therapy was given in the 22% ($n = 11$) of HDs (Table 1). The relatively low number of subjects (BBIBP-CorV:5; AZD1222:2, BNT162b2:4) receiving anti-CD20 therapy did not allow statistical comparisons of anti-RBD antibody levels between the vaccination groups. Although only one of eleven HD patients crossed the cut off 21.8 BAU/mL value in the anti-CD20 therapy group irrespectively of the type of vaccines. On the contrary, 27 of 38 HDs

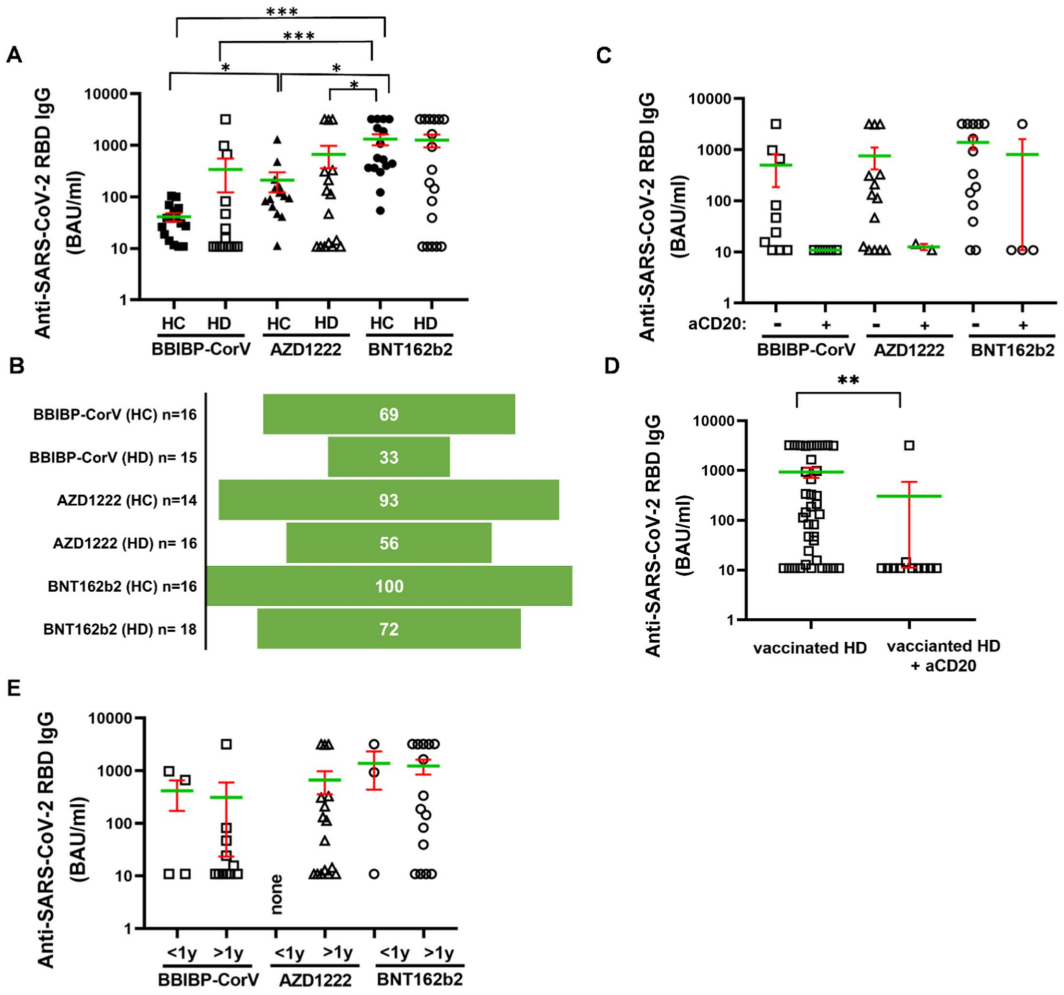

FIGURE 1
Humoral immune response to SARS-CoV-2 in HDs vs. HCs. The IgG-type anti-RBD (spike) antibodies were measured from the sera of the patients. **(A)** Subjects for studying BBIBP-CorV were n=16 (HC) and n=15 (HD), for AZD1222 were n=14 (HC) and n=16 (HD) for BNT162b2 were n=16 (HC) and n=18 (HD). **(B)** The response rate was calculated of the vaccination groups. Sub-group analysis was carried-out focusing on **(C,D)** anti-CD20 treatment or **(E)** disease duration. Mean (green line) and SEM (red whisker) values are demonstrated. *p<0.05, **p<0.01, and ***p<0.001.

(71%) showed positive response rate to vaccination without CD20 blocking therapeutics (Figure 1C). Pooling data of cases underwent the anti-CD20 therapy resulted in significantly weaker anti-RBD IgG level: 302 ± 291 (SD: 965) BAU/mL than 928 ± 215 (SD: 1324) BAU/mL without CD20 blocking in the HD group, $^{**}p < 0.01$ (Figure 1D). Eleven (73%), or sixteen (100%), or fifteen (83%) HD cases were diagnosed more than 1 year ago of the withdrawal of the blood. There was no statistical difference among the types of vaccines in terms of SARS-CoV-2 reactive IgG production due to disease duration following diagnosis (Figure 1E).

3.2. SARS-CoV-2 specific cellular immunity in HDs following vaccination

Next, the SARS-CoV-2 reactive cellular immunity was assayed by flow cytometry. The PBMCs were reactivated with SARS-CoV-2 antigens (S-, M-, N-peptide pools) and $CD4^+$ or $CD8^+$ T-cells were assayed to produce TNF-α, IFN-γ, and CD40L *ex vivo*. The cellular response rate corresponds to the percentage of subjects in one group in terms of the TNF-α, IFN-γ, or CD40L cytokine producing $CD4^+$ or $CD8^+$ T-cells over the cut off value that is 400 reactive cells of 10^6 parental population (Supplementary Figure S2). The simple "response" in Results 3.2 corresponds to the number of S-M-N-peptivator activated T-cells normalized to the background unstimulated controls. There was no statistical difference in the absolute number of reactive $CD4^+$ TNF-α T-cells in HDs versus HCs. However, as a trend HDs showed weaker $CD4^+$ TNF-α^+ T-cell activation, responsive cells (mean ± SEM/1×10^6 parental $CD4^+$ T-cells) were 814 ± 491 (SD: 1552) for HC versus 153 ± 73 (SD: 293) for HDs in the AZD1222 vaccinated group. The mRNA-based BNTB162b2 vaccination resulted in the activation of 382 ± 148 (SD: 591) reactive $CD4^+$ TNF-α T-cells in the HC group vs. 161 ± 55 (SD: 235) cells in HDs (Figure 2A). The number of CD4-TNF-α positive cells was highest in the BBIBP-CorV vaccine group: 2082 ± 1104 (SD: 3982) in HCs and 1955 ± 1655 (SD: 6079) in HDs (Figure 2A). Measurement of IFN-γ induction in $CD4^+$ T-cells showed also higher SARS-CoV-2 specific activation in HCs vs. HDs, detecting for BBIBP-CorV: 1767 ± 911 (SD: 3286) vs. 190 ± 57 (SD: 213) ($^*p < 0.05$); for AZD1222: 1619 ± 950 (SD: 3005) vs. 110 ± 33 (SD: 131); and for BNT162b2: 191 ± 75 (SD: 301) vs. 103 ± 31 (SD: 130) reactive $CD4^+$ IFNγ T-cells, respectively (Figure 2B). Then CD40L expression was significantly higher in $CD4^+$ T-cells in the HC vs. HDs for BBIBP-CorV: 2511 ± 849 (SD: 3062) vs. 323 ± 145 (SD: 543) $^{***}p < 0.001$; and for AZD1222: 1980 ± 912 (SD: 2884) vs. 193 ± 94 (SD: 377) $^{**}p < 0.01$, respectively (Figure 2C). The BNTB162b2 vaccine caused also higher CD40L activation in $CD4^+$ T-cells in HCs vs. HDs, namely 630 ± 224 (SD: 895) vs. 286 ± 123 (SD: 522) reactivated cells were detected, but it was not statistically significant difference (Figure 2C). Interestingly the inactivated virus vaccine BBIBP-CorV induced significantly higher CD40L response in HCs vs. BNT162b2: 2511 ± 849 (SD: 3062) vs. 630 ± 224 (SD: 895) $^*p < 0.05$ (Figure 2C).

The cellular response rate, the proportions of $CD4^+$ TNF-α^+ responder cases to vaccination in HC vs. HD for BBIBP-CorV were 61.5% vs. 35.7%; 40% vs. 12.5% for AZD1222, and 25% vs. 16.7% for BNT162b2. The proportions of $CD4^+$ IFN-γ^+ responders in HC vs. HD for BBIBP-CorV were 61.5% vs. 21.4%; for AZD1222 40% vs. 6.3%; for BNT162b2 18.8% vs. 5.6%. The proportions of $CD4^+$ $CD40L^+$ responders in HC vs. HD for BBIBP-CorV were 92.3% vs. 21.4%, for AZD1222 80% vs. 18.8%, and for BNT162b2 50% vs. 22.2% (Supplementary Figures S2A–C).

The cytotoxic $CD8^+$ T-cell mediated cellular immunity was measured for the induction of TNF-α or IFN-γ production. The HDs showed not significantly but tendentiously higher SARS-CoV-2 reactive $CD8^+$ TNF-α T-cell reactivation vs. HCs for AZD1222: 466 ± 183 (SD: 734) vs. 288 ± 213 (SD: 674); and for BNT162b2: 485 ± 327 (SD: 1387) vs. 169 ± 43 (SD: 171) (Figure 3A). In BBIBP-CorV vaccine group $CD8^+$ TNF-α positive cells were comparable in HCs and HDs: 277 ± 158 (SD: 561) vs. 225 ± 90 (SD: 337) (Figure 3A). The IFN-γ response in $CD8^+$ T-cells was also higher in HDs vs. HCs as a tendency for BBIBP-CorV: 265 ± 153 (SD: 593) vs. 86 ± 38 (SD: 139); for AZD1222: 733 ± 389 (SD: 1556) vs. 392 ± 189 (SD: 599); and for BNT162b2: 363 ± 101 (SD: 429) vs. 87 ± 41 (SD: 165) $^*p < 0.05$, respectively (Figure 3B).

The proportions of $CD8^+$ TNF-α^+ responder cases to vaccination in HC vs. HD for BBIBP-CorV were 23.1% vs. 21.4, 20% vs. 31.3% for AZD1222, and 12.5% vs. 16.7% for BNT162b2. The proportions of $CD8^+$ IFN-γ^+ responders in HC vs. HD for BBIBP-CorV were 7.7% vs. 14.3%; for AZD1222 30% vs. 37.5%; for BNT162b2 12.5% vs. 33.3% (Supplementary Figures S2D–E).

Next, we aimed to investigate the effect of anti-CD20 therapy on T-cell mediated peripheral immunity. Pooling cases both in the HC or HD groups irrespective of the vaccination type and dividing HDs based on anti-CD20 therapy status into two groups, the monoclonal antibody treatment in HDs tendentiously resulted in further weaker reactivation of $CD4^+$ T-cells upon SARS-CoV-2 antigen exposure. The numbers of $CD4^+$ TNF-α^+ reactive cells were 1060 ± 401 (SD: 2507) in HCs, 807 ± 587 (SD: 3668) in HDs without anti-CD20 therapy, or 134 ± 57 (SD: 170) in HDs with anti-CD20 therapy (Figure 4A). The numbers of $CD4^+$ IFN-γ^+ reactive cells were 1083 ± 397 (SD: 2481) in HCs, 144 ± 27 (SD: 169) in HDs without anti-CD20 therapy, or 74 ± 32 (SD: 97) in HDs with anti-CD20 therapy (Figure 4B). The numbers of $CD4^+$ $CD40L^+$ reactive cells were 1603 ± 391 (SD: 2443) in HCs, that was significantly reduced to 304 ± 83 (SD: 520) in HDs ($^{***}p < 0.001$) without anti-CD20 therapy, or further decreased in HDs with anti-CD20 therapy 101 ± 47 (SD: 141) ($^{***}p < 0.001$) (Figure 4C). The $CD8^+$TNF-α^+ or $CD8^+$ IFN-γ^+ reactive, SARS-CoV-2 specific T-cell numbers did not differ significantly among the HCs and HDs with no significant effect of anti-CD20 therapy (Figures 4D–E). The virus reactive $CD8^+$ IFN-γ cells were slightly increased in the anti-CD20-treated HD group compared to "untreated" HDs and HCs (Figure 4E).

4. Discussion

Patients with hematological malignancies represent a specifically susceptible population to COVID-19 with a heightened risk of severe disease and fatality (1–3). As the COVID-19 vaccination campaigns around the world unfolded and studies with large cohorts of HD patients arose, robust data was collected regarding vaccination efficacy and safety in HD patients. However, most trials investigated the effect of mRNA-and vector-based vaccines. Therefore, information on inactivated vaccines is limited. However, inactivated virus vaccines against SARS-CoV-2, such as BBIBP-CorV (Sinopharm, China), CoronaVac (Sinovac, China), Covaxin (India), COVIran Barekat (Iran), contributed significantly to worldwide vaccine coverage (22, 23). In Hungary, BBIBP-CorV was administered at large scales besides

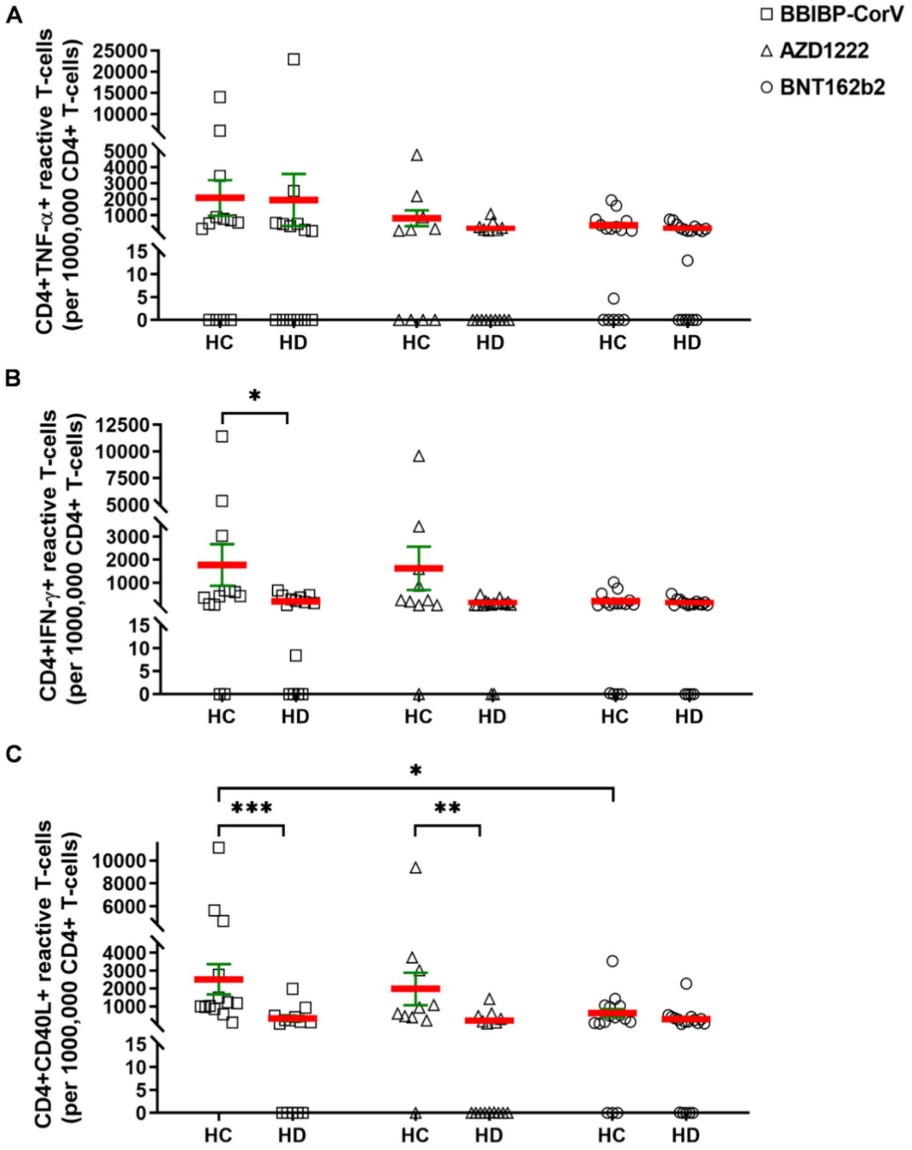

FIGURE 2
The CD4⁺ T-cells were assayed following ex vivo S/M/N peptide stimulation. Subjects in HCs vs. HDs were for BBIBP-CorV-2 n=13 vs. n=16; for AZD1222 n=vs. n=16; for BNT162b2 n=16 vs. n=18. The reactive TNF-α **(A)**, or IFN-γ **(B)**, or CD40L **(C)** producing CD4⁺ T-cells were quantified. Mean (red line) and SEM (green whisker) values are demonstrated. *p<0.05, **p<0.01, and ***p<0.001.

other vaccines, even to people at higher risk, like the elderly and patients with various cancers, including hematological malignancies. To the best of our knowledge, only one study addressed the efficacy of the BBIBP-CorV vaccine in cancer patients (24), and a comprehensive analysis of different vaccine types, including BBIBP-CorV in the context of HD is completely lacking. Here, we report our findings about the efficacy of the BBIBP-CorV vaccine compared to mRNA vaccine BNT162b2 (Pfizer BioNTech) and vector-based AZD1222 (AstraZeneca) vaccines to trigger humoral and cellular immunity in patients with hematological disease.

The receptor binding domain (RBD) specific anti-spike (S) IgG isotype antibodies were measured in HDs versus healthy controls following complete vaccination after 4 months. The highest antibody titers were attained in the BNT162b2 group (both controls and HDs), independent of disease status. Due to varying BAU/mL values within each group and the small size of the groups, no significant difference was observed between healthy controls and HDs in the case of any of the examined vaccine types (Figure 1A). The calculated seroconversion rates (Figure 1B) were more informative about the humoral response of HDs upon different vaccines than raw anti-RBD antibody values. Namely, seroconversion rates of HDs fell behind that of matching healthy controls: 33% vs. 69% (BBIBP-CorV), 56% vs. 93% (AZD1222), 72% vs. 100% (BNT162b2). This decreased performance of BNT162b2 and AZD1222 in HD patients is consistent with a pooled humoral response rate of 67.7% of HD patients found in the latest meta-analysis, where data was extracted mainly from articles on mRNA and adenoviral vaccines (9). The proportion of BBIBP-CorV vaccinated HDs mounting anti-S IgG response was only 33% which is

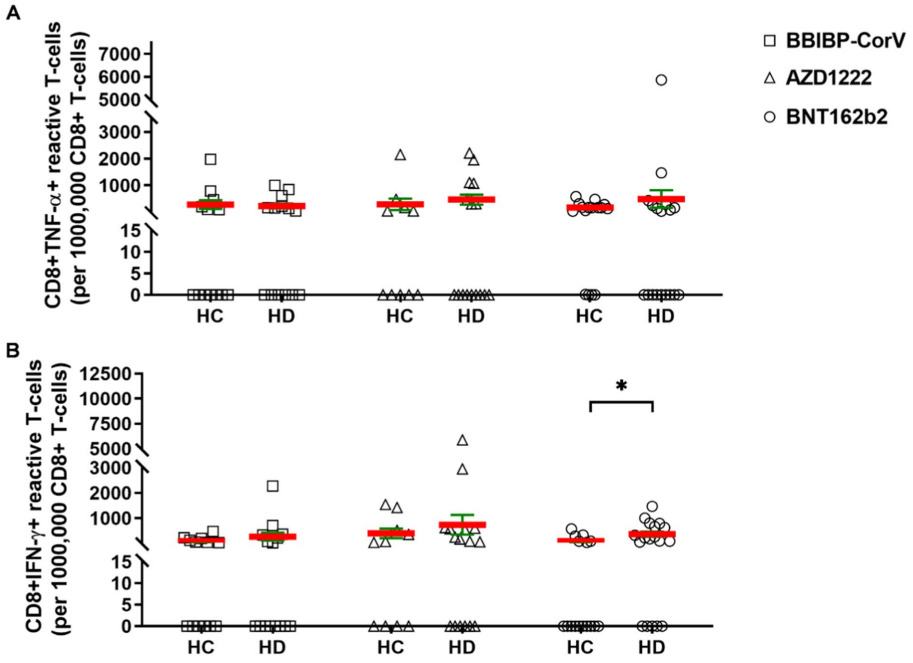

FIGURE 3
The CD8⁺ T-cell responses in HCs vs. HDs receiving different vaccines. The CD8⁺ T-cells were assayed following *ex vivo* S/M/N peptide stimulation. Subjects in HCs vs. HDs were for BBIBP-CorV-2 n=13 vs. n=16; for AZD1222 n=10 vs. n=16; for BNT162b2 n=16 vs. n=18. The reactive TNF-α **(A)**, or IFN-γ **(B)** producing CD8⁺ T-cells were quantified. Mean (red line) and SEM (green whisker) values are demonstrated. *p<0.05, **p<0.01, and ***p<0.001.

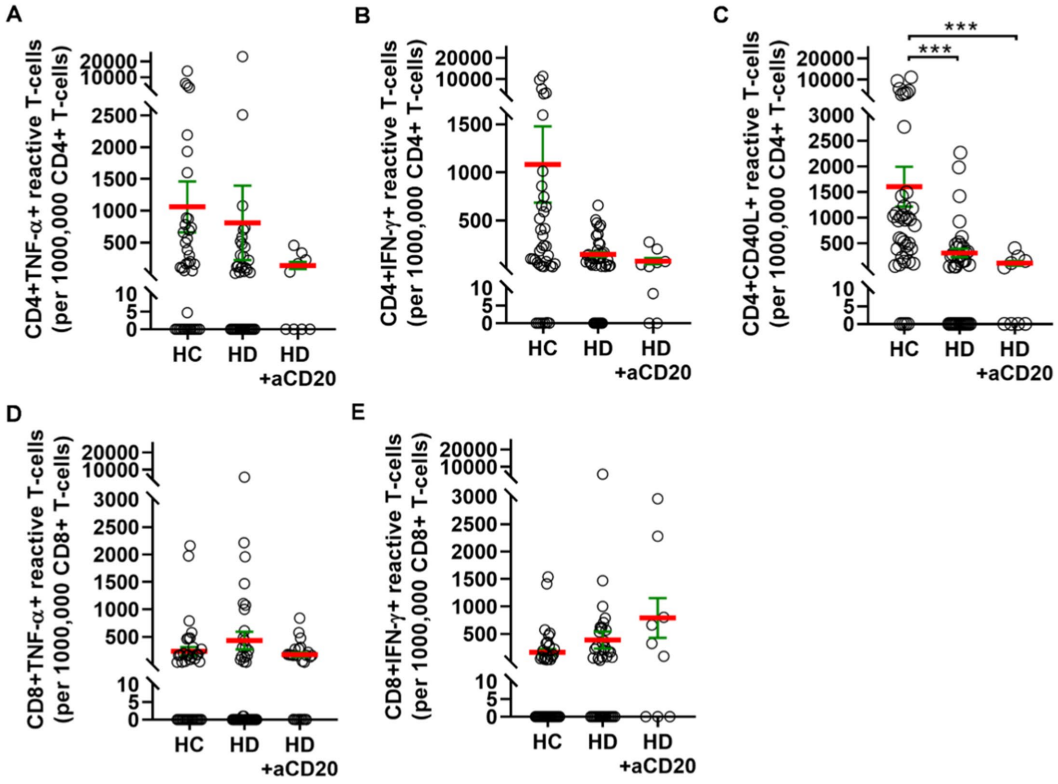

FIGURE 4
T-cell mediated SARS-CoV-2 specific peripheral immunity in HCs (n=39), HDs (n=39) or HDs that underwent anti-CD20 therapy (n=9). The reactive TNF-α **(A)**, or IFN-γ **(B)**, or CD40L **(C)** producing CD4⁺ T-cells were quantified. The reactive TNF-α **(D)**, or IFN-γ **(E)** producing CD8⁺ T-cells were quantified. Cases vaccinated with BBIBP-CorV, or AZD1222, or BNT162b2 were pooled to investigate the effect of anti-CD20 therapy on T-cell mediated immunity. **(C)** The anti-CD20 therapy significantly reduced the CD4⁺ CD40L⁺ reactive cell numbers in HDs.

comparable with the 38.1% from the only previous report by Ariamanesh and coworkers (24). The observed waning humoral response in HDs is in line with literature data affected by several patient factors such as age, sex, serostatus, treatments and comorbidities (25, 26). It should be noted that 5 out of 15 patients (33.3%) vaccinated with BBIBP-CorV received anti-CD20 therapy. On the other hand, 2 out of 16 (12.5%) and 4 out of 18 (22.22%) patients vaccinated with AZD1222 or BNT162b2 were on anti-CD20 therapy, respectively. Thus, anti-CD20 therapy was overrepresented in the BBIBP-CorV group, which could skew the vaccination response in this group. There is a clear consensus that immunosuppressive B-cell-directed treatments markedly impair immunogenicity in HD patients. Monoclonal anti-CD20 therapy in HD patients was associated with a considerably lower or undetectable humoral response due to prolonged B-cell depletion. Seroconversion of these patients was even poorer if the anti-CD20 was administered within 6–12 months before vaccination (10–14). Therefore, the impaired humoral response of HD patients undergoing anti-CD20 therapy in our cohort was expected, which manifested in significantly lower ($^{**}p < 0.01$) anti-RBD IgG levels in patients treated with anti-CD20 (Figure 1D). This effect was observed with all the studied vaccine types (Figure 1C), although the low number of subjects per vaccine type does not allow statistical comparison and drawing clear conclusions.

It has been emphasized that adding cellular response metrics to the gold standard antibody titer and neutralizing activity measurements would provide a better insight into the overall immune response to COVID-19 vaccination. However, cellular assays are more logistically complex to conduct compared to antibody measurements because they require viable PBMC samples with longer and more complex handling protocols (27). Both ELISpot (enzyme-linked immune absorbent spot) and flow cytometric assay are used to determine the magnitude of cellular response by measuring the ratio of cytokine-secreting cells within the PBMC population after antigen-specific activation. In contrast, flow cytometry has the extra advantage of providing additional information about the type of responding cells. Such studies incorporating flow cytometry assays to compare the cellular immune memory elicited by COVID-19 vaccines are limited, especially those with a simultaneous side-by-side comparison of multiple vaccine types.

Here, we compared SARS-CoV-2 specific T-cell responses induced by BNTB162b, AZD1222, and BBIBP-CorV in HD patients versus healthy individuals by flow cytometry. The strength of the current work is the separate enumeration of responsive $CD4^+$ and $CD8^+$ T-cells based on IFN-γ/TNF-α/CD40L expression. There was no significant difference in $CD4^+$ $TNF\text{-}\alpha^+$ or $CD4^+$ $IFN\text{-}\gamma^+$ T-cell frequencies between HCs and HDs except for higher $CD4^+$ $IFN\text{-}\gamma^+$ T-cells in HCs vs. HDs in BBIBP-CorV group (Figure 2B), although, in the HD group, the % of responders above the cut-off value of SARS-CoV-2 specific T-cells was lower in all vaccine groups. The frequency of $CD4^+$ $CD40L^+$ T-cells in HD patients was significantly lower compared to healthy volunteers in BBIBP-CorV and AZD1222 vaccine groups. In the case of BNTB162b, the proportion of $CD4^+$ $CD40L^+$ T-cells was also lower, but the difference was not significant (Figure 2C). The percentage of responders among healthy individuals was also highest in the $CD4^+$ $CD40L^+$ group in all vaccines, and in HDs, their proportion was reduced in all vaccine groups. The cytotoxic $CD8^+$ T-cell mediated immunity was measured by the induction of TNF-α or IFN-γ production. There was no significant difference in the number of reactive $CD8^+$ $TNF\text{-}\alpha^+$ T-cells between HCs and HDs, but interestingly, their number was higher in HDs vs. HCs in AZD1222 and BNTB162b group (Figure 3A). In HDs, tendentiously more responsive $CD8^+$ $IFN\text{-}\gamma^+$ T-cells were detected than in HCs in BBIBP-CorV and AZD1222 groups, and the difference was significant in the BNTB162b group (Figure 3B).

For comparison, we enlist the articles addressing SARS-CoV-2 specific T-cell response of people with hematological malignancies, which is only a tiny fragment of studies on mRNA or vector-based vaccines demonstrating cellular immunity after complete vaccination in 29%–88% of HD patients. Majority of the studies applied IFN-γ release assay (16, 17, 28, 29); IFN-γ ELISpoT (10, 12, 30–35); and IFN-γ/IL-2 FluoroSpot assay (36–38) or the combination of these (39). One study evaluated T-cell responses by immunosequencing the TCRβ chain (15). Some of these studies enrolled healthy controls as well and showed that the percentage of HD patients with SARS-CoV-2 reactive IFN-γ secreting T-cells is lower compared to that of healthy volunteers (10, 12, 28, 29, 32–35). Admittedly, our results are difficult to directly parallel with bulk anti-SARS-CoV-2 T-cell responses by these reports. The method used by Ehmsen and co-workers enabled the dissemination of $CD4^+$ restricted IFN-γ responses from $CD4^+$ plus $CD8^+$ IFN-γ responses in HD patients vaccinated with mRNA vaccines (16). Among patients with HD, 45% exhibited positive IFN-γ responses by T-cells, 81% of whom were positive for both $CD4^+$ and $CD8^+$ T-cells, and 18% only elicited a $CD8^+$ T-cell response (16). Furthermore, a report by Clemenceau and colleagues combined IFN-γ ELISpoT and flow cytometry for quantifying cellular immunity in AML and MDS patients receiving allogeneic stem cell therapy identifying spike-specific IFN-γ and TNF-α secreting cells within $CD4^+$ and $CD8^+$ T-cell populations. They found a higher percentage of SARS-CoV-2 specific $CD4^+$ $TNF\text{-}\alpha^+$ T-cells in allo-HSCT receiving patients than in healthy controls. However, after pooling the responses in CD4 and CD8 arms, only 78% of patients achieved cellular immunity compared to 100% of controls (40). Finally, another recent study focused on the analysis of SARS-CoV-2 specific $CD8^+$ T-cells in CLL and MDS patients after BNTB162b vaccination using DNA-barcoded peptide-MHC multimers covering the full SARS-CoV-2 Spike-protein they were able to map CD8 T-cell recognition sites and identified 59 antigen epitopes. Surprisingly, they also showed a higher frequency of vaccine-induced antigen-specific $CD8^+$ T-cells in the patient group than in healthy donors (41). This observation is consistent with our findings on increased SARS-CoV-2 specific CD8 T-cells in the HD group (Figure 3). Based on literature data, the authors may speculate that induction of T-cell mediated cellular responses by inactivated viral vaccine may rely at least partially, on the cross-presentation of viral antigens to MHC-I not exclusively demonstrated on MHC-II leading to $CD8^+$ T-cell activation, that is further boosted by the identified $CD4^+$ Th1 ($IFN\text{-}\gamma^+$and/or $TNF\text{-}\alpha^+$) helper T-cells (42, 43).'

The effect of anti-CD20 therapy on cellular immunity of hematological malignancy patients to SARS-CoV-2 is rarely presented in the related articles with divergent conclusions. The frequency of T-cell mediated responses were diminished in anti-CD20 treated chronic lymphocytic leukemia (CLL) patients (14%) compared to patients without the immunosuppressive therapy (29%) (32). In another study, majority of the lymphoma patients (75.3%) achieved cellular responses and their frequency was slightly lower (70%) in patients on anti-CD20 therapy (17). In a third study the rate of T-cell

responses was not reduced in HD patients on anti-CD20 monotherapy compared to HD patients without anti-CD20 (33). In our cohort, pooled HD patients on anti-CD20 therapy showed tendentiously lower number of SARS-CoV-2 reactive $CD4^+$ T-cells compared to HD patients with no anti-CD20 treatment (Figures 4A–C) and this result was further confirmed by the reduced or zero % of patients on anti-CD20 achieving the cut-off value of 400 responding CD4 T-cells in a million (data not shown). SARS-CoV-2 reactive $CD8^+$ IFN-γ T-cell numbers in HDs were slightly increased by anti-CD20 therapy but the difference was not significant (Figure 4E). Interestingly, after complete COVID-19 vaccination S-specific CD8 T-cell response rate was also higher in rheumatic disease patients receiving anti-CD20 therapy (81.8%) than in immunocompetent controls (66.7%) (44).

In summary, the present study is a side-by-side comparison of three different vaccine platforms (BNTB162b, AZD1222, and BBIBP-CorV) generating humoral and cellular immunity in a diverse cohort of participants with hematological diseases and in healthy volunteers. It has to be noted that our access to the control group was at younger age 43 ± 12 (median, y) while HD patients were 63 ± 14 (median, y) without significant difference. The humoral immunity to SARS-CoV-2 based on seropositivity values was impaired in patients with HDs in line with existing data in the literature. In HDs, the observed seroconversion rates imply the following order in vaccine efficacy inducing humoral immunity: BNTB162 ≫ AZD1222 ≫ BBIBP-CorV. Anti-CD20 therapy had a detrimental impact on the humoral responses regardless of vaccine type. On the other hand, the proportions of patients among HDs with sufficient SARS-CoV-2 specific T-cells above the cut-off value painted a different picture: CD4 T-cell responses in patients with hematological diseases were reduced, and CD8 T-cell responses were sustained or even elevated in all vaccine group compared to healthy controls. Bange et al. (45) have shown an increased CD8 T-cell mediated SARS-CoV-2 specific immunity in HDs as a compensatory mechanism to deficient humoral response. Vaccine performance hierarchy in HD patients generating CD4 TNF-α and CD4 IFN-γ responses was: BBIBP-CorV ≫ AZD1222 ≫ BNTB162b. Regarding CD4 CD40L responses in HDs based on frequency rates, the performance of the three vaccines was comparable. Furthermore, CD8 T-cell response rates of HDs were highest in the AZD1222 vaccine group. Although the CD20 is a classical B-cell marker, it has been recently elucidated that it can be a meaningful marker of pro-inflammatory T-cells (46–48). The anti-CD20 treatment significantly reduced the S-, M-, N-reactive $CD4^+$ $CD40L^+$ T-cell numbers in HDs.

Overall, patients with malignant hematologic disease have higher risk of mortality than the general population in the case of COVID-19 infection, which can be aggravated by other risk factors such as age, comorbidities, and immunosuppressive therapies. Despite of the clinically less severe latest variants of SARS-CoV-2, the best-case scenario in COVID-19 disease management is to prevent it, especially in vulnerable populations like hematology patients. In our study, we have demonstrated the significant weaker response to vaccines in immunologically impaired population such as hematology patients. Based on our results, the protective humoral immune activity of hematologic patients against SARS-CoV-2 can be best supported by mRNA-based vaccination with BNTb162b compared to other vaccines in this study. On the other hand, inactivated virus vaccine seems to be a better choice to elevate T-cell mediated cellular activity against SARS-CoV-2. It has to be noted that because of the already known decline in the humoral immune response over time, there is a high need for booster shots to prevent severe COVID-19 especially in immunocompromised patients (19, 49–51). However, data about the induction of humoral and cellular immunity followed by BBIBP-CorV vaccination with a side-by-side comparison of AZD1222 and BNT162b2 is restricted to few cited papers, limitations of the current research should be mentioned such as the followings. (1) The authors had access to patient-derived blood from heterogenous HDs, (2) our study lacks multi-center execution, (3) and the access to the HC group was with younger age median. (4) Latest Omicron subvariants displayed increased evasion of neutralizing antibodies induced by SARS-CoV-2 vaccination compared to the first Omicron and prior variants (52). Further research is warranted to investigate the effects of different SARS-CoV-2 vaccines on each HDs separately, with clear focus on the booster vaccination protocols also. The sequential combinations of different vaccine types could be the answer for the higher humoral and cellular SARS-CoV-2 protective immunity, but more studies need to be conducted to ensure safety and efficacy.

Data availability statement

The raw data supporting the conclusions of this article will be made available by the authors, without undue reservation.

Ethics statement

The studies involving human participants and The enrollment of patients were reviewed and approved by the Human Investigation Review Board of the National Public Health Center under Project Identification Code 47226-7/2019EÜIG. The patients/participants provided their written informed consent to participate in this study.

Author contributions

SM, LP, and GS conceived and designed the study, participated in data collection and analysis. SM supervised clinical data management and organized and supervised the vaccination protocol. NG, LN, AF, and KF performed experiments measuring SARS-CoV-2 specific T-cell responses. LN performed the measurement of SARS-CoV-2 specific neutralizing anti-RBD specific antibodies. SM and BR collected epidemiological and clinical data and assisted with the identification of SARS-CoV-2 infection and follow-up of patients. ES and GS analyzed the data, prepared the figures and wrote the manuscript. LP was responsible for laboratories. GS verified the data and had access to raw data. SM, LH, PN, AB, LP, and GS revised the manuscript. GS and LP had final responsibility for the decision to submit for publication. All authors contributed to the article and approved the submitted version.

Funding

This research was funded by the 2020-1.1.6-JÖVŐ-2021-00003 and 142877 FK22, KFI_16-1-2017-0105 grant from the National Research, Development, and Innovation Office (NKFI), Hungary. This work was

supported by the ÚNKP-22-5-SZTE-535 New National Excellence Program for GS, and by the KDP-2021 Program for NG (C1764415) of the Ministry for Innovation and Technology from the source of the National Research, Development and Innovation Fund. This work was supported by the János Bolyai Research Scholarship of the Hungarian Academy of Sciences BO/00582/22/8 (GS). This manuscript was prepared with the professional support of SZTE ÁOK-KKA Heténi Géza Scholarship_5S726 (AB). This manuscript was prepared with the support of the National Young Talent Scholarship for ES (NTP-NFTÖ-21-B-0164) by the Ministry of Culture and Innovation.

Conflict of interest

AF, LN, and HL were employed by Avidin Ltd. KF was employed by AstridBio Technologies Ltd. LP is the CEO of Avidin Ltd. and Avicor Ltd. GS was employed by CS-Smartlab Devices Ltd.

The remaining authors declare that the research was conducted in the absence of any commercial or financial relationships that could be construed as a potential conflict of interest.

Publisher's note

All claims expressed in this article are solely those of the authors and do not necessarily represent those of their affiliated organizations, or those of the publisher, the editors and the reviewers. Any product that may be evaluated in this article, or claim that may be made by its manufacturer, is not guaranteed or endorsed by the publisher.

Supplementary material

The Supplementary material for this article can be found online at: https://www.frontiersin.org/articles/10.3389/fmed.2023.1176168/full#supplementary-material

References

1. Fattizzo B, Giannotta JA, Sciume M, Cattaneo D, Bucelli C, Fracchiolla NS, et al (2020). Reply to "COVID-19 in persons with haematological cancers": a focus on myeloid neoplasms and risk factors for mortality. *Leukemia* 34:1957–60. doi: 10.1038/s41375-020-0877-y

2. Shah V, Ko Ko T, Zuckerman M, Vidler J, Sharif S, Mehra V, et al (2020). Poor outcome and prolonged persistence of SARS-CoV-2 RNA in COVID-19 patients with haematological malignancies; King's College Hospital experience. *Br J Haematol* 190:e279–82. doi: 10.1111/bjh.16935

3. Passamonti F, Cattaneo C, Arcaini L, Bruna R, Cavo M, Merli F, et al (2020). Clinical characteristics and risk factors associated with COVID-19 severity in patients with haematological malignancies in Italy: a retrospective, multicentre, cohort study. *Lancet Haematol* 7:e737–45. doi: 10.1016/S2352-3026(20)30251-9

4. Passamonti F, Romano A, Salvini M, Merli F, Porta MGD, Bruna R, et al (2021). COVID-19 elicits an impaired antibody response against SARS-CoV-2 in patients with haematological malignancies. *Br J Haematol* 195:371–7. doi: 10.1111/bjh.17704

5. Zheng C, Shao W, Chen X, Zhang B, Wang G, Zhang W (2022). Real-world effectiveness of COVID-19 vaccines: a literature review and meta-analysis. *Int J Infect Dis* 114:252–60. doi: 10.1016/j.ijid.2021.11.009

6. Pagano L, Salmanton-Garcia J, Marchesi F, Blennow O, Gomes da Silva M, Glenthoj A, et al (2022). Breakthrough COVID-19 in vaccinated patients with hematologic malignancies: results from the EPICOVIDEHA survey. *Blood* 140:2773–87. doi: 10.1182/blood.2022017257

7. Haas EJ, Angulo FJ, McLaughlin JM, Anis E, Singer SR, Khan F, et al (2021). Impact and effectiveness of mRNA BNT162b2 vaccine against SARS-CoV-2 infections and COVID-19 cases, hospitalisations, and deaths following a nationwide vaccination campaign in Israel: an observational study using national surveillance data. *Lancet* 397:1819–29. doi: 10.1016/S0140-6736(21)00947-8

8. Guven DC, Sahin TK, Akin S, Uckun FM (2022). Impact of therapy in patients with hematologic malignancies on seroconversion rates after SARS-CoV-2 vaccination. *Oncologist* 27:e357–61. doi: 10.1093/oncolo/oyac032

9. Uaprasert N, Pitakkitnukun P, Tangcheewinsirikul N, Chiasakul T, Rojnuckarin P (2022). Immunogenicity and risks associated with impaired immune responses following SARS-CoV-2 vaccination and booster in hematologic malignancy patients: an updated meta-analysis. *Blood Cancer J* 12:173. doi: 10.1038/s41408-022-00776-5

10. Lim SH, Stuart B, Joseph-Pietras D, Johnson M, Campbell N, Kelly A, et al (2022). Immune responses against SARS-CoV-2 variants after two and three doses of vaccine in B-cell malignancies: UK PROSECO study. *Nat Cancer* 3:552–64. doi: 10.1038/s43018-022-00364-3

11. Thakkar A, Gonzalez-Lugo JD, Goradia N, Gali R, Shapiro LC, Pradhan K, et al (2021). Seroconversion rates following COVID-19 vaccination among patients with cancer. *Cancer Cell* 39:e2:1081–1090.e2. doi: 10.1016/j.ccell.2021.06.002

12. Fendler A, Shepherd STC, Au L, Wilkinson KA, Wu M, Byrne F, et al (2021). Adaptive immunity and neutralizing antibodies against SARS-CoV-2 variants of concern following vaccination in patients with cancer: the CAPTURE study. *Nat Cancer* 2:1321–37. doi: 10.1038/s43018-021-00275-9

13. Addeo A, Shah PK, Bordry N, Hudson RD, Albracht B, Di Marco M, et al (2021). Immunogenicity of SARS-CoV-2 messenger RNA vaccines in patients with cancer. *Cancer Cell* 39:e2:1091–1098.e2. doi: 10.1016/j.ccell.2021.06.009

14. Herishanu Y, Avivi I, Aharon A, Shefer G, Levi S, Bronstein Y, et al (2021). Efficacy of the BNT162b2 mRNA COVID-19 vaccine in patients with chronic lymphocytic leukemia. *Blood* 137:3165–73. doi: 10.1182/blood.2021011568

15. Greenberger LM, Saltzman LA, Gruenbaum LM, Xu J, Reddy ST, Senefeld JW, et al (2022). Anti-spike T-cell and antibody responses to SARS-CoV-2 mRNA vaccines in patients with hematologic malignancies. *Blood Cancer Discov* 3:481–9. doi: 10.1158/2643-3230.BCD-22-0077

16. Ehmsen S, Asmussen A, Jeppesen SS, Nilsson AC, Osterlev S, Vestergaard H, et al (2021). Antibody and T cell immune responses following mRNA COVID-19 vaccination in patients with cancer. *Cancer Cell* 39:1034–6. doi: 10.1016/j.ccell.2021.07.016

17. Jimenez M, Roldan E, Fernandez-Naval C, Villacampa G, Martinez-Gallo M, Medina-Gil D, et al (2022). Cellular and humoral immunogenicity of the mRNA-1273 SARS-CoV-2 vaccine in patients with hematologic malignancies. *Blood Adv* 6:774–84. doi: 10.1182/bloodadvances.2021006101

18. Szebeni GJ, Gemes N, Honfi D, Szabo E, Neuperger P, Balog JA, et al (2022). Humoral and cellular immunogenicity and safety of five different SARS-CoV-2 vaccines in patients with autoimmune rheumatic and musculoskeletal diseases in remission or with low disease activity and in healthy controls: a single center study. *Front Immunol* 13:846248. doi: 10.3389/fimmu.2022.846248

19. Honfi D, Gemes N, Szabo E, Neuperger P, Balog JA, Nagy LI, et al (2022). Comparison of homologous and heterologous booster SARS-CoV-2 vaccination in autoimmune rheumatic and musculoskeletal patients. *Int J Mol Sci* 23:11411. doi: 10.3390/ijms231911411

20. Irsara C, Egger AE, Prokop W, Nairz M, Loacker L, Sahanic S, et al (2021). Clinical validation of the Siemens quantitative SARS-CoV-2 spike IgG assay (sCOVG) reveals improved sensitivity and a good correlation with virus neutralization titers. *Clin Chem Lab Med* 59:1453–62. doi: 10.1515/cclm-2021-0214

21. Saiag E, Goldshmidt H, Sprecher E, Ben-Ami R, Bomze D (2021). Immunogenicity of a BNT162b2 vaccine booster in health-care workers. *Lancet Microbe* 2:e650. doi: 10.1016/S2666-5247(21)00272-X

22. Mallapaty S (2021). China's COVID vaccines have been crucial - now immunity is waning. *Nature* 598:398–9. doi: 10.1038/d41586-021-02796-w

23. Dolgin E (2022). Omicron thwarts some of the world's most-used COVID vaccines. *Nature* 601:311. doi: 10.1038/d41586-022-00079-6

24. Ariamanesh M, Porouhan P, Peyro Shabany B, Fazilat-Panah D, Dehghani M, Nabavifard M, et al (2022). Immunogenicity and safety of the inactivated SARS-CoV-2 vaccine (BBIBP-Cor V) in patients with malignancy. *Cancer Investig* 40:26–34. doi: 10.1080/07357907.2021.1992420

25. Notarte KI, Ver AT, Velasco JV, Pastrana A, Catahay JA, Salvagno GL, et al (2022). Effects of age, sex, serostatus, and underlying comorbidities on humoral response post-SARS-CoV-2 Pfizer-bio NTech mRNA vaccination: a systematic

review. *Crit Rev Clin Lab Sci* 59:373–90. doi: 10.1080/10408363.2022.2038539

26. Notarte KI, Guerrero-Arguero I, Velasco JV, Ver AT, Santos de Oliveira MH, Catahay JA, et al (2022). Characterization of the significant decline in humoral immune response six months post-SARS-CoV-2 mRNA vaccination: a systematic review. *J Med Virol* 94:2939–61. doi: 10.1002/jmv.27688

27. Paramithiotis E, Sugden S, Papp E, Bonhomme M, Chermak T, Crawford SY, et al (2022). Cellular immunity is critical for assessing COVID-19 vaccine effectiveness in immunocompromised individuals. *Front Immunol* 13:880784. doi: 10.3389/fimmu.2022.880784

28. Marasco V, Carniti C, Guidetti A, Farina L, Magni M, Miceli R, et al (2022). T-cell immune response after mRNA SARS-CoV-2 vaccines is frequently detected also in the absence of seroconversion in patients with lymphoid malignancies. *Br J Haematol* 196:548–58. doi: 10.1111/bjh.17877

29. Yang LM, Costales C, Ramanathan M, Bulterys PL, Murugesan K, Schroers-Martin J, et al (2022). Cellular and humoral immune response to SARS-CoV-2 vaccination and booster dose in immunosuppressed patients: an observational cohort study. *J Clin Virol* 153:105217. doi: 10.1016/j.jcv.2022.105217

30. Ramasamy K, Sadler R, Jeans S, Weeden P, Varghese S, Turner A, et al (2022). Immune response to COVID-19 vaccination is attenuated by poor disease control and antimyeloma therapy with vaccine driven divergent T-cell response. *Br J Haematol* 197:293–301. doi: 10.1111/bjh.18066

31. Malard F, Gaugler B, Gozlan J, Bouquet L, Fofana D, Siblany L, et al (2021). Weak immunogenicity of SARS-CoV-2 vaccine in patients with hematologic malignancies. *Blood Cancer J* 11:142. doi: 10.1038/s41408-021-00534-z

32. Blixt L, Wullimann D, Aleman S, Lundin J, Chen P, Gao Y, et al (2022). T-cell immune responses following vaccination with mRNA BNT162b2 against SARS-CoV-2 in patients with chronic lymphocytic leukemia: results from a prospective open-label clinical trial. *Haematologica* 107:1000–3. doi: 10.3324/haematol.2021.280300

33. Liebers N, Speer C, Benning L, Bruch PM, Kraemer I, Meissner J, et al (2022). Humoral and cellular responses after COVID-19 vaccination in anti-CD20-treated lymphoma patients. *Blood* 139:142–7. doi: 10.1182/blood.2021013445

34. Schubert L, Koblischke M, Schneider L, Porpaczy E, Winkler F, Jaeger U, et al (2022). Immunogenicity of COVID-19 vaccinations in hematological patients: 6-month follow-up and evaluation of a 3rd vaccination. *Cancers* 14:14. doi: 10.3390/cancers14081962

35. Mellinghoff SC, Robrecht S, Mayer L, Weskamm LM, Dahlke C, Gruell H, et al (2022). SARS-CoV-2 specific cellular response following COVID-19 vaccination in patients with chronic lymphocytic leukemia. *Leukemia* 36:562–5. doi: 10.1038/s41375-021-01500-1

36. McKenzie DR, Munoz-Ruiz M, Monin L, Alaguthurai T, Lechmere T, Abdul-Jawad S, et al (2021). Humoral and cellular immunity to delayed second dose of SARS-CoV-2 BNT162b2 mRNA vaccination in patients with cancer. *Cancer Cell* 39:1445–7. doi: 10.1016/j.ccell.2021.10.003

37. Harrington P, Doores KJ, Saunders J, de Lord M, Saha C, Lechmere T, et al (2022). Impaired humoral and T cell response to vaccination against SARS-CoV-2 in chronic myeloproliferative neoplasm patients treated with ruxolitinib. *Blood Cancer J* 12:73. doi: 10.1038/s41408-022-00651-3

38. Shen Y, Freeman JA, Holland J, Solterbeck A, Naidu K, Soosapilla A, et al (2022). COVID-19 vaccine failure in chronic lymphocytic leukaemia and monoclonal B-lymphocytosis; humoural and cellular immunity. *Br J Haematol* 197:41–51. doi: 10.1111/bjh.18014

39. Haydu JE, Maron JS, Redd RA, Gallagher KME, Fischinger S, Barnes JA, et al (2022). Humoral and cellular immunogenicity of SARS-CoV-2 vaccines in chronic lymphocytic leukemia: a prospective cohort study. *Blood Adv* 6:1671–83. doi: 10.1182/bloodadvances.2021006627

40. Clemenceau B, Guillaume T, Coste-Burel M, Peterlin P, Garnier A, Le Bourgeois A, et al (2022). SARS-CoV-2 T-cell responses in allogeneic hematopoietic stem cell recipients following two doses of BNT162b2 mRNA vaccine. *Vaccines* 10:10. doi: 10.3390/vaccines10030448

41. Hernandez SPA, Hersby DS, Munk KK, Tamhane T, Trubach D, Tagliamonte M, et al (2022). Three doses of BNT162b2 COVID-19 mRNA vaccine establish long-lasting $CD8^+$ T cell immunity in CLL and MDS patients. *Front Immunol* 13:1035344. doi: 10.3389/fimmu.2022.1035344

42. Sanchez-Paulete AR, Teijeira A, Cueto FJ, Garasa S, Perez-Gracia JL, Sanchez-Arraez A, et al (2017). Antigen cross-presentation and T-cell cross-priming in cancer immunology and immunotherapy. *Ann Oncol* 28:xii74. doi: 10.1093/annonc/mdx727

43. Fu C, Peng P, Loschko J, Feng L, Pham P, Cui W, et al (2020). Plasmacytoid dendritic cells cross-prime naive CD8 T cells by transferring antigen to conventional dendritic cells through exosomes. *Proc Natl Acad Sci U S A* 117:23730–41. doi: 10.1073/pnas.2002345117

44. Madelon N, Lauper K, Breville G, Sabater Royo I, Goldstein R, Andrey DO, et al (2022). Robust T-cell responses in anti-CD20-treated patients following COVID-19 vaccination: a prospective cohort study. *Clin Infect Dis* 75:e1037–45. doi: 10.1093/cid/ciab954

45. Bange EM, Han NA, Wileyto P, Kim JY, Gouma S, Robinson J, et al (2021). CD8 T cells compensate for impaired humoral immunity in COVID-19 patients with hematologic cancer. *Res Sq*. 27:1280–1289. doi: 10.21203/rs.3.rs-162289/v1 [Preprint].

46. Lee AYS (2022). $CD20^+$ T cells: an emerging T cell subset in human pathology. *Inflamm Res* 71:1181–9. doi: 10.1007/s00011-022-01622-x

47. Vlaming M, Bilemjian V, Freile JA, Lourens HJ, van Rooij N, Huls G, et al (2021). CD20 positive CD8 T cells are a unique and transcriptionally-distinct subset of T cells with distinct transmigration properties. *Sci Rep* 11:20499. doi: 10.1038/s41598-021-00007-0

48. Shinoda K, Li R, Rezk A, Mexhitaj I, Patterson KR, Kakara M, et al (2023). Differential effects of anti-CD20 therapy on CD4 and CD8 T cells and implication of CD20-expressing CD8 T cells in MS disease activity. *Proc Natl Acad Sci U S A* 120:e2207291120. doi: 10.1073/pnas.2207291120

49. Notarte KI, Catahay JA, Velasco JV, Pastrana A, Ver AT, Pangilinan FC, et al (2022). Impact of COVID-19 vaccination on the risk of developing long-COVID and on existing long-COVID symptoms: a systematic review. *EClinicalMedicine* 53:101624. doi: 10.1016/j.eclinm.2022.101624

50. Notarte KI, de Oliveira MHS, Peligro PJ, Velasco JV, Macaranas I, Ver AT, et al (2022). Age, sex and previous comorbidities as risk factors not associated with SARS-CoV-2 infection for long COVID-19: a systematic review and meta-analysis. *J Clin Med* 11:11. doi: 10.3390/jcm11247314

51. Fernandez-de-Las-Penas C, Notarte KI, Peligro PJ, Velasco JV, Ocampo MJ, Henry BM, et al (2022). Long-COVID symptoms in individuals infected with different SARS-CoV-2 variants of concern: a systematic review of the literature. *Viruses* 14:14. doi: 10.3390/v14122629

52. Cao Y, Yisimayi A, Jian F, Song W, Xiao T, Wang L, et al (2022). BA.2.12.1, BA.4 and BA.5 escape antibodies elicited by omicron infection. *Nature* 608:593–602. doi: 10.1038/s41586-022-04980-y

frontiers | Frontiers in Medicine

TYPE Original Research
PUBLISHED 18 July 2023
DOI 10.3389/fmed.2023.1193830

OPEN ACCESS

EDITED BY
Pierpaolo Di Micco,
Ospedale Santa Maria delle Grazie, Italy

REVIEWED BY
Anil Pathare,
Sultan Qaboos University, Oman
Gianluca Di Micco,
Ospedale Buon Consiglio Fatebenefratelli, Italy
Kun Huang,
Capital Medical University, China

*CORRESPONDENCE
Dongxin Tang
✉ tangdongxintcm@163.com
Yang Liu
✉ ly7878@163.com

†These authors have contributed equally to this work

RECEIVED 25 March 2023
ACCEPTED 04 July 2023
PUBLISHED 18 July 2023

CITATION
Li Y, Wang F, Pan C, Zhang J, Zhang Q, Ban L, Song L, Wang J, He Z, Zeng X, Tang D and Liu Y (2023) Comparison of joint status using ultrasound assessments and Haemophilia Joint Health Score 2.1 in children with haemophilia. *Front. Med.* 10:1193830. doi: 10.3389/fmed.2023.1193830

Comparison of joint status using ultrasound assessments and Haemophilia Joint Health Score 2.1 in children with haemophilia

Yanju Li[1†], Feiqing Wang[2,3†], Chengyun Pan[1], Jing Zhang[1], Qian Zhang[1], Lingying Ban[1], Lingling Song[1], Jishi Wang[1], Zhixu He[4], Xiaojing Zeng[1], Dongxin Tang[2*] and Yang Liu[2,4*]

[1]Department of Hematology Oncology, Affiliated Hospital of Guizhou Medical University, Guiyang, China, [2]Clinical Medical Research Center, The First Affiliated Hospital of Guizhou University of Traditional Chinese Medicine, Guiyang, China, [3]Academy of Medical Engineering and Translational Medicine, Tianjin University, Tianjin City, China, [4]Key Laboratory of Adult Stem Cell Translational Research, Chinese Academy of Medical Sciences, Guizhou Medical University, Guiyang, China

Introduction: Ultrasound (US) has gained popularity in the evaluation of haemophilic joint diseases because it enables the imaging of soft-tissue lesions in the joints and bone-cartilage lesions. We aimed to determine the correlation between US evaluations and clinical assessments performed using HJHS 2.1 and to evaluate their respective characteristics in assessing early haemophilic arthropathy.

Methods: A total of 178 joints (32 knees, 85 elbows, and 61 ankles) in 45 haemophilia A patients (median age, 10 years; range, 6–15) were assessed using US and HJHS 2.1. Ultrasonographic scoring was performed in consensus assessments by one imager by using the US scores.

Results: The total HJHS 2.1 and US scores showed a strong correlation (rS=0.651, *P*=0.000, CI: 0.553–0.763), with an excellent correlation for the elbows (rS=0.867, *P*=0.000, CI: 0.709–0.941) and a substantial correlation for the knees (rS=0.681, *P*=0.000, CI: 0.527–0.797). The correlation for the ankles was relatively moderate (rS=0.518, P=0.000, CI: 0.308–0.705). Nine subjects (15.5%) without abnormalities, as indicated by HJHS 2.1, showed haemophilic arthropathy in US scoring. All nine joints showed moderate (1/9) to severe (8/9) synovial thickening in the ankle (5/9) and elbow joints (4/9). In contrast, 50 joints (50.5%) showed normal US scores and abnormal changes as indicated by HJHS 2.1. S scores correlated well with HJHS 2.1 for overall and individual joints.

Discussion: US could identify some early pathological changes in joints showing normal clinical findings, but still cannot replace the HJHS; however, it can serve as an imaging examination complementing HJHS 2.

KEYWORDS

Haemophilia Joint Health Score (HJHS), haemophilia, arthropathy, ultrasonography, children

1. Introduction

Haemophilia is a common sex-chromosome recessive hereditary haemorrhagic disease caused by a deficiency of coagulation factor VIII or IX. Joint bleeding is the most commonly reported type of haemorrhage in haemophilia patients, which could lead to synovial hypertrophy and direct bleeding-related osteochondral changes. The elbows, knees, and ankles are the most

affected among all joints in haemophilia. With the widespread use of prophylaxis, the onset of arthropathy has significantly reduced (1). However, because of many reasons, the prevention and treatment of haemophilia in China, especially in Guizhou Province, are lagging behind those in developed countries and the incidence of joint dysfunction is high, which seriously affects the quality of life of affected patients. Hence, early periodic monitoring of joint lesions in haemophilia patients is recommended, which is aimed at identifying early arthropathic changes and prevention of the development or progression of haemophilic arthropathy.

The Haemophilia Joint Health Score (HJHS 2.1) was developed to detect early joint changes in moderate or severe haemophilia in patients aged higher than 3 years; however, it did not consider normal childhood variations. Considering that physical examination assessment scores lack the sensitivity and specificity required for the identification of early and subclinical joint abnormalities, radiography has been recommended in addition to a clinical examination for assessing the joint status and disease progression in haemophilia patients.

Magnetic resonance imaging (MRI) is an accurate routine imaging method for joint lesions in haemophilia patients (2); however, its application is limited due to its high cost, the time required, and the possible requirement of sedative drugs. It can be used as a routine imaging examination method for screening and follow-up in only a few haemophilia patients with special needs. Ultrasound (US) examination, an imaging method that allows the imaging of soft-tissue lesions in the joints and bone-cartilage lesions, is becoming popular in the evaluation and examination of haemophilic joint diseases in recent years because it is convenient, economical, and safe (3, 4). Several previous studies have investigated the correlation between US findings and HJHS (5–7); however, the sample sizes in these studies were relatively small, and as of now, consensus on the issue is lacking. Hence, this study was aimed at assessing the value of US in the assessment of joint status in haemophilia by comparing it with HJHS 2.1 in children with haemophilia.

2. Materials and methods

2.1. Research object

A total of 178 knee joints of 45 children with haemophilia in the Affiliated Hospital of Guizhou Medical University in Guizhou Province were selected; all of the patients were male and aged between 6 and 15 years. All cases met the 2014 diagnostic criteria of the consensus of Chinese experts for the diagnosis and treatment of haemophilia A (8). Consent was obtained from all patients and/or their families prior to participation in this study.

2.2. Inspection method

Equipment: US: Low-speed blood flow conditions of the skeletal muscle were selected using the Philips iU22 colour US instrument with a high-frequency line array probe (5 ~ 12 MHz). Different positions were imaged according to the different joints of the patients. Images were obtained in the sitting position or by lying on the front and sides of the joint. The posterior parts of the joints were examined in the prone position. Random images of the joints were obtained in the sagittal and coronal views.

HJHS: Clinical function was assessed by a physiotherapist according to HJHS version 2.1. The HJHS 2.1 evaluates potential joint swelling (scale 0–3), swelling duration (scale 0–1), muscle atrophy (scale 0–2), crepitus during activity (scale 0–2), decreased curvature (scale 0–3), decreased stretch (scale 0–3), joint pain (scale 0–2), and loss of strength (scale 0–4). The HJHS for joint level ranges from 0 points, indicating perfect clinical function, to 20 points, indicating a severe loss of clinical function.

Ultrasound examination: US examination was performed on the same day by two imaging specialists. They observed for the following parameters: exudation (joint effusion or haemorrhage) (scale 0–3), fibrous septum (scale 0–1), synovial thickness (normal value: <1 mm) (scale 1–3), synovial thickening with synovial vascular hyperplasia (scale 1–2), hemosiderin deposition (scale 0–3), cartilage changes (scale 1–3), bone erosion (irregular bone mass destruction) (scale 0–1), osteophytes (formation of bone hyperplasia at the edge of the joint) (scale 0–1), and bone reconstruction (irregular and inconsistent joint surfaces) (scale 0–1). The total score possible is 18.

2.3. Statistical analysis

Data were analysed using SPSS l8.0 statistical software. Spearman's rank of correlation coefficient (rS) was used to study the correlations of the outcome measurement scores. A correlation was considered poor if rS was <0.4, moderate if rS was 0.4–0.6, good or substantial if rS was 0.6–0.8, and excellent if rS was >0.8.

3. Results

In our study, US-based scoring was performed for two of the three joints of the elbow, knee, and ankle of each patient. In total, 178 joints of 45 patients were assessed. Two joints (one knee and one ankle) could not be assessed because the data collected were incomplete. The median age of these patients was 10 years (range 6–15). The median HJHS and US score were 2 (range 0–17) and 0 (range 0–13) respectively. The baseline characteristics of the study joints are shown in Table 1.

Among these 178 joints, the HJHS 2.1 was positive for 120 joints (67.4%) and US scores for 79 joints (44.4%). There was a good correlation between HJHS 2.1 and US scores for all study joints (rS = 0.651, $p = 0.000$, CI: 0.553–0.763) (Figure 1). Nine subjects (15.5%, 9/58 joints) without abnormalities, as indicated by the HJHS 2.1, were found to have haemophilic arthropathy based on US scores (3 points for three patients, 4 points for four patients, 5 points for one patient and 6 points for one patient, respectively). Moderate (1/9) to severe (8/9) synovial thickening in the ankle joints (5/9) and elbow joints (4/9) was noted in all of these nine cases by using US. In seven of these cases, synovial thickening with synovial vascular proliferation in the ankle joints (3/7) and elbow joints (4/7) were noted. One case showed small changes in the cartilage of the elbow joint and the other case showed a small amount of hemosiderin deposition in the ankle joint, based on synovial thickening and synovial thickening with synovial vascular proliferation that were not detected by clinical examination. US scores according to HJHS 2.1 are shown in Table 2.

TABLE 1 Patients' baseline characteristics ($n = 45$ patients, 178 joints).

	Median (25th–75th percentile) or *n* (%)	Range
Age (years)	10 (6–15)	3–17
Elbow (n=32 joints)		
HJHS	2.5 (0–10)	0–16
US	4 (0–7)	0–12
Knee (n=85 joints)		
HJHS	2 (0–9.5)	0–17
US	0 (0–5)	0–13
Ankle (n=61 joints)		
HJHS	2 (0–5)	0–13
US	0 (0–4)	0–11
Total (n=178 joints)		
HJHS	2 (0–7)	0–17
US	0 (0–5)	0–13

HJHS, Haemophilia Joint Health Score; US, ultrasound.

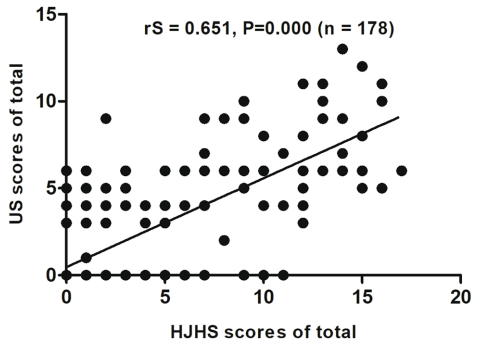

FIGURE 1
Scatter plot showing the correlation between the total clinical Hemophilia Joint Health Score (HJHS 2.1) and ultrasound (US) scores.

TABLE 2 Ultrasound findings according to HJHS 2.1 results at the joint level.

HJHS 2.1 score	Number of patients	Median US score (25th–75th percentile)	US score = 0 *n* (%)	US score = 18 *n* (%)
0	58	0 (0–0)	49 (84.5)	0 (0)
1-3	48	0 (0–3)	33 (68.8)	0 (0)
4-6	24	1.5 (0–4)	12 (50)	0 (0)
7-9	16	5.5 (2.5–8.5)	3 (18.8)	0 (0)
10-12	15	6.0 (4–8)	2 (13.3)	0 (0)
>12	17	9.0 (6–11)	2 (11.8)	0 (0)

HJHS, Haemophilia Joint Health Score, range 0–20; US, ultrasound, range 0–18.

Fifty joints (50.5%, 50/99 joints) had normal US scores but abnormal changes based on the HJHS 2.1 were found, which included 1 point for nine joints, 2 points for 17 joints, 3 points for seven joints, 4 points for seven joints, 5 points for two joints, 6 points for three joints, 7 points for two joints, 9 points for one joint 10 points for one joint, and 11 points for one joint. All of these patients had at least one with muscle atrophy, joint strength changes or swelling, partial joints with swelling for ≥6 months combined with or without joint pain, crepitus during activity, and decreased curvature or decreased stretch that could not be identified using the US scores.

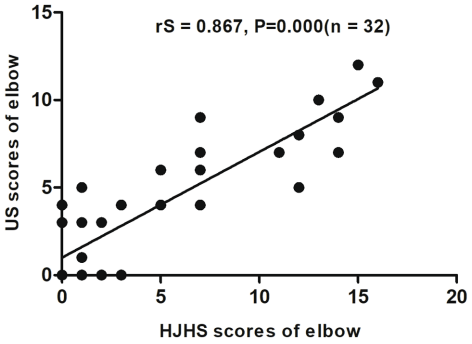

FIGURE 2
Scatter plot showing the correlation between the clinical Hemophilia Joint Health Score (HJHS 2.1) and ultrasound (US) score for the elbow.

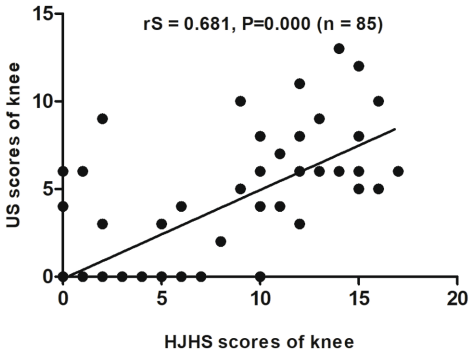

FIGURE 3
Scatter plot showing the correlation between the clinical Hemophilia Joint Health Score (HJHS 2.1) and ultrasound (US) score for the knee.

When different joints were evaluated separately, an excellent correlation was found between HJHS 2.1 and US scores for the elbows (rS = 0.867, $p = 0.000$, CI: 0.709–0.941) (Figure 2) and a substantial correlation was found for the knees (rS = 0.681, $p = 0.000$, CI: 0.527–0.797) (Figure 3). On the other hand, the correlation between the scores for the ankles was relatively moderate (rS = 0.518, $p = 0.000$, CI: 0.308–0.705) (Figure 4).

Five subjects (20.8%, 5/24 joints) had normal HJHS 2.1 for ankles but showed signs of haemophilic arthropathy in US assessments (3 points for two subjects, 4 points for two subjects, and 5 points for one subject). All of these five joints had a synovial thickness greater than 2.5 mm (scoring 3 points), of which two showed synovial vascular hyperplasia and one had both synovial vascular hyperplasia and hemosiderin deposition (Figure 4).

In contrast, 50 subjects (44.1%, 15/34 joints) had normal US ankle scores but showed abnormal findings in HJHS 2.1 assessments (1 point for four subjects, 2 points for three subjects, 3 points for one

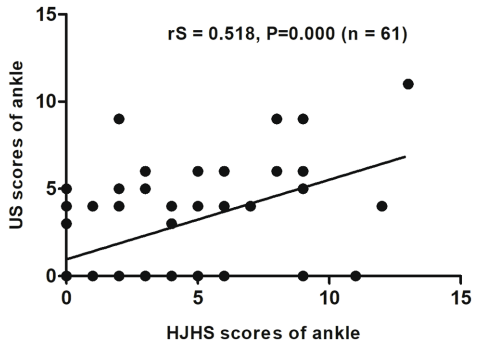

FIGURE 4
Scatter plot showing the correlation between the clinical Hemophilia Joint Health Score (HJHS 2.1) and ultrasound (US) score for the ankle.

subject, 4 points for three subjects, 5 points for one subject, 6 points for one subject, 9 points for one subject, and 11 points for one subject) (Figure 4). Six joints showed mild muscle atrophy while three had severe change. Among these, two joints showed crepitus during activity and decreased curvature, while one showed a decrease in extension and a change in joint strength based on the above changes. Mild and severe swelling was found in four joints each (three of these eight joints showed swelling in combination with muscle atrophy), of which seven had shown swelling for ≥6 months; one subject had a simple joint strength change that was not detected by US. Among the patients who reported a swelling duration of ≥6 months, one had joint pain and another had both joint pain and joint strength changes. Moreover, among the three patients with both muscle atrophy and swelling, one had joint pain, one experienced reduced stretching, and the third had a decreased curvature, decreased extension, and joint strength.

4. Discussion

Repeated joint bleeding in haemophilia often leads to joint deformity and dysfunction, which seriously affects the quality of life of patients (9), and with age, these lesions become more apparent (10). US has recently attracted growing interest as a potential tool to assess joint status and identify early arthropathic changes in haemophilia patients, which can ensure initiation of treatment as soon as possible and thereby prevent joint damage (11–13).

Previous studies showed a strong correlation between HJHS and US in the evaluation of the joints, and US could reveal a higher percentage of abnormalities than HJHS in both children and adults (7, 11, 14, 15). However, Poonnoose et al. (5) suggested that the correlation between HJHS and US for the osteochondral component was moderate (rS = 0.45) while that for the soft tissue component was poor (rS = 0.26).

In our study, we found a good correlation between HJHS 2.1 and US for all study joints (rS = 0.651, $p = 0.000$, CI: 0.553–0.763). This was consistent with the findings obtained by Altisent et al. (16). Early identification of synovial tissue thickening is important to prevent progression of haemophilic osteoarthrosis since the thickened synovial membrane and fragile neovascularization can increase the chance of joint bleeding and directly destroy articular cartilage, which further leads to the occurrence and progression of haemophilic arthropathy. In this study, the US scores for 15.5% of the joints that did not show abnormalities on HJHS 2.1 indicated haemophilic arthropathy, and synovial thickening was identified in all of these patients. The thickening was partial with small changes in the cartilage and hemosiderin deposition, which suggests that the US scoring system could identify early pathological changes in joints appearing normal in clinical examination and offers advantages over HJHS 2.1 in assessments of synovial thickening, hemosiderin deposition and cartilage changes. Due to the convenience of US, in the case of routine monitoring of joint function or even acute joint bleeding in hemophilia patients, US can provide clinical diagnosis and treatment with more rapid, convenient, and accurate therapeutic guidance value. Especially in the process of dynamic monitoring of joint disease changes in hemophiliacs, more sensitive intervention treatment can be given to hemophiliacs according to the results of dynamic changes in US, which can prevent further deterioration of the joint disease. However, our study also revealed changes with HJHS 2.1 that were not detected by the US scoring system and may require physical or drug intervention, which showed a higher percentage (50.5%) of positive points on HJHS 2.1 in relation to muscle atrophy, joint strength changes, or swelling while US scores for these findings were negative in previous studies (6, 16). This poor specificity of US in soft-tissue findings suggests that US is still lacking in the comprehensive evaluation of joint soft tissue changes and that the US scoring system and HJHS 2.1 would complement each other in order to ensure better assessment of joint status.

For a single joint US evaluation, Aspdahl et al. (14) suggested that a strong correlation exists between the HJHS and the US scores for elbows and knees (rS = 0.57, $p < 0.01$ and rS = 0.76, $p < 0.01$), but the correlation for ankles was substantially weaker (rS = 0.36, $p = 0.04$). In comparison with their results, our study showed a significant correlation between HJHS and US scores in all of the elbow, knee and ankle joints (rS = 0.867, $p = 0.000$; rS = 0.681, $p = 0.000$ and rS = 0.518, $p = 0.000$, respectively). This may be attributable to the size of our research sample. However, in our study, the correlation for the ankle joints was more moderate than that for the elbow and ankle joints, which was the same trend as that observed in their study. This suggests that when evaluating the osteoarticular lesions of the ankle joint, there is a strong need for a comprehensive evaluation that includes both US and HJHS assessments.

5. Conclusion

Our study confirmed that in paediatric patients with haemophilia A, the US scoring system correlated well with HJHS 2.1 assessments for overall and individual joint assessments, with the correlations being excellent for elbows, substantial for knees, and moderate for ankles. US could identify early pathological changes in apparently healthy joints and showed advantages over the HJHS 2.1 in terms of synovial thickening, hemosiderin deposition, and cartilage changes. However, it still had defects that prevented it from replacing the HJHS. Instead, it can serve as an imaging examination complementing HJHS 2.1 assessments.

Data availability statement

The original contributions presented in the study are included in the article/supplementary material, further inquiries can be directed to the corresponding authors.

Ethics statement

The studies involving human participants were reviewed and approved by Affiliated Hospital of Guizhou Medical University. Written informed consent to participate in this study was provided by the participants' legal guardian/next of kin.

Author contributions

YLi, FW, YLiu, and DT conceived of and designed the study. They had full access to all data in the study, and take responsibility for the integrity of the data, the accuracy of the data analysis, and the writing of the report. XZ, JW, and ZH critically revised the report. CP, JZ, QZ, LB, and LS performed the statistical analyses. YLi, FW, CP, JZ, QZ, LB, LS, JW, ZH, XZ, DT, and YLiu contributed to the data acquisition and analyses. All authors contributed to the article and approved the submitted version.

Funding

This study was supported by the National Natural Science Foundation of China (nos. 82160519 and 31660326); the Natural Science Foundation of Guizhou Province [nos. QianKeHe-ZK (2023) Key 042 and QianKeHe Support (2022)181]; and the Natural Science Foundation of Guiyang City [nos. (2022)4-3-2 and (2022)4-3-10]. The funders of the study had no role in study design, data collection, data analysis, data interpretation, or writing of the report.

Conflict of interest

The authors declare that the research was conducted in the absence of any commercial or financial relationships that could be construed as a potential conflict of interest.

Publisher's note

References

1. Nilsson IM, Berntorp E, Löfqvist T, Pettersson H. Twenty-five years' experience of prophylactic treatment in severe haemophilia A and B. *J Intern Med*. (1992) 232:25–32. doi: 10.1111/j.1365-2796.1992.tb00546.x

2. Kilcoyne RF, Nuss R. Radiological assessment of haemophilic arthropathy with emphasis on MRI findings. *Haemophilia*. (2003) 9:57–64. doi: 10.1046/j.1365-2516.9.s1.11.x

3. Zoica B, Petrescu C, Oprisoni A, Gafencu M, Bataneant M, Doros G, et al. Ultrasonography in the diagnosis and follow-up of hematologic emergencies of patients with hemophilia. *Ultraschall Med*. (2008) 29:S1. doi: 10.1055/s-2008-1079865

4. Di Minno MND, Pasta G, Airaldi S, Zaottini F, Storino A, Cimino E, et al. Ultrasound for early detection of joint disease in patients with hemophilic arthropathy. *J Clin Med*. (2017) 6:77. doi: 10.3390/jcm6080077

5. Poonnoose PM, Hilliard P, Doria AS, Keshava SN, Gibikote S, Kavitha ML, et al. Correlating clinical and radiological assessment of joints in haemophilia: results of a cross sectional study. *Haemophilia*. (2016) 22:925–33. doi: 10.1111/hae.13023

6. Foppen W, van der Schaaf IC, Fischer K. Value of routine ultrasound in detecting early joint changes in children with haemophilia using the 'Haemophilia Early Arthropathy Detection with Ultrasound' protocol. *Haemophilia*. (2016) 22:121–5. doi: 10.1111/hae.12769

7. Sigl-Kraetzig M, Bauerfeindt S, Amanda W, Axel S. Standardized joint-ultrasound for individualization of prophylaxis in hemophiliacs: easy-to-learn-ultrasonography (HEAD-US) of joints and correlation with function and clinics. *Ultraschall Med*. (2016) 37:S01. doi: 10.1055/s-0036-1587727

8. Thrombosis and Hemostasis Group, Chinese Society of Hematology, Chinese Medical Association/Hemophilia Treatment Center Collaborative Network of China. Chinese expert consensus on the diagnosis and treatment of acquired hemophilia A. *Zhonghua Xue Ye Xue Za Zhi*. (2014) 35:575–6. Chinese. doi: 10.3760/cma.j.issn.0253-2727.2014.06.026

9. Stephensen D, Rodriguez-Merchan EC. Orthopaedic co-morbidities in the elderly haemophilia population: a review. *Haemophilia*. (2013) 19:166–73. doi: 10.1111/hae.12006

10. Sari TT, Chozie NA, Gatot D, Tulaar ABM, Dharma R, Sukrisman L, et al. Clinical and ultrasound joint outcomes in severe hemophilia a children receiving episodic treatment in Indonesian National Hemophilia Treatment Center. *Med J Indones*. (2017) 26:47. doi: 10.13181/mji.v26i1.1494

11. Ligocki CC, Abadeh A, Wang KC, Adams-Webber T, Blanchette VS, Doria AS. A systematic review of ultrasound imaging as a tool for evaluating haemophilic arthropathy in children and adults. *Haemophilia*. (2017) 23:598–612. doi: 10.1111/hae.13163

12. Melchiorre D, Linari S, Innocenti M, Biscoglio I, Toigo M, Cerinic MM, et al. Ultrasound detects joint damage and bleeding in haemophilic arthropathy: a proposal of a score. *Haemophilia*. (2011) 17:112–7. doi: 10.1111/j.1365-2516.2010.02380.x

13. Doria AS, Keshava SN, Mohanta A, Jarrin J, Blanchette V, Srivastava A, et al. Diagnostic accuracy of ultrasound for assessment of hemophilic arthropathy: MRI correlation. *AJR Am J Roentgenol*. (2015) 204:W336–47. doi: 10.2214/AJR.14.12501

14. Aspdahl M, Viljakainen H, Petrini P, Ranta S. Comparison of joint status in children with haemophilia A using ultrasound and physical examination. *Eur J Phys*. (2018) 20:172–7. doi: 10.1080/21679169.2018.1438511

15. Timmer MA, Foppen W, Schutgens RE, Pisters MF, Fischer K. Comparing findings of routine Haemophilia Joint Health Score and Haemophlia early Arthropathy detection with UltraSound assessments in adults with haemophilia. *Haemophilia*. (2017) 23:e141–3. doi: 10.1111/hae.13147

16. Altisent C, Martorell M, Crespo A, Casas L, Torrents C, Parra R. Early prophylaxis in children with severe haemophilia A: clinical and ultrasound imaging outcomes. *Haemophilia*. (2016) 22:218–24. doi: 10.1111/hae.12792

frontiers | Frontiers in Public Health

TYPE Original Research
PUBLISHED 28 July 2023
DOI 10.3389/fpubh.2023.1184831

OPEN ACCESS

EDITED BY
Pierpaolo Di Micco,
Ospedale Santa Maria delle Grazie, Italy

REVIEWED BY
Alessandro Perrella,
Colli Hospital, Italy
Giuseppe Cardillo,
Medylab Advanced Biochemistry, Italy

*CORRESPONDENCE
Jiannan Lv
✉ gxaidscc@163.com
Yanling Hu
✉ ylhupost@163.com

†These authors have contributed equally to this work

RECEIVED 12 March 2023
ACCEPTED 14 July 2023
PUBLISHED 28 July 2023

CITATION
Huang L, Xie B, Zhang K, Xu Y, Su L, Lv Y, Lu Y, Qin J, Pang X, Qiu H, Li L, Wei X, Huang K, Meng Z, Hu Y and Lv J (2023) Prediction of the risk of cytopenia in hospitalized HIV/AIDS patients using machine learning methods based on electronic medical records. *Front. Public Health* 11:1184831. doi: 10.3389/fpubh.2023.1184831

Prediction of the risk of cytopenia in hospitalized HIV/AIDS patients using machine learning methods based on electronic medical records

Liling Huang[1†], Bo Xie[2†], Kai Zhang[1], Yuanlong Xu[1], Lingsong Su[1], Yu Lv[1], Yangjie Lu[1], Jianqiu Qin[3], Xianwu Pang[4], Hong Qiu[5], Lanxiang Li[6], Xihua Wei[4], Kui Huang[1], Zhihao Meng[1], Yanling Hu[2,4,5*] and Jiannan Lv[1,7*]

[1]Guangxi Clinical Center for AIDS Prevention and Treatment, Chest Hospital of Guangxi Zhuang Autonomous Region, Liuzhou, Guangxi, China, [2]School of Information and Management, Guangxi Medical University, Nanning, Guangxi, China, [3]Nanning Center for Disease Control and Prevention, Nanning, Guangxi, China, [4]Center for Genomic and Personalized Medicine, Guangxi key Laboratory for Genomic and Personalized Medicine, Guangxi Collaborative Innovation Center for Genomic and Personalized Medicine, Guangxi Medical University, Nanning, Guangxi, China, [5]Institute of Life Sciences, Guangxi Medical University, Nanning, Guangxi, China, [6]Basic Medical College of Guangxi Medical University, Nanning, Guangxi, China, [7]Department of Infection, Affiliated Hospital of the Youjiang Medical University for Nationalities, Baise, Guangxi, China

Background: Cytopenia is a frequent complication among HIV-infected patients who require hospitalization. It can have a negative impact on the treatment outcomes for these patients. However, by leveraging machine learning techniques and electronic medical records, a predictive model can be developed to evaluate the risk of cytopenia during hospitalization in HIV patients. Such a model is crucial for designing a more individualized and evidence-based treatment strategy for HIV patients.

Method: The present study was conducted on HIV patients who were admitted to Guangxi Chest Hospital between June 2016 and October 2021. We extracted a total of 66 clinical features from the electronic medical records and employed them to train five machine learning prediction models (artificial neural network [ANN], adaptive boosting [AdaBoost], k-nearest neighbour [KNN] and support vector machine [SVM], decision tree [DT]). The models were tested using 20% of the data. The performance of the models was evaluated using indicators such as the area under the receiver operating characteristic curve (AUC). The best predictive models were interpreted using the shapley additive explanation (SHAP).

Result: The ANN models have better predictive power. According to the SHAP interpretation of the ANN model, hypoproteinemia and cancer were the most important predictive features of cytopenia in HIV hospitalized patients. Meanwhile, the lower hemoglobin-to-RDW ratio (HGB/RDW), low-density lipoprotein cholesterol (LDL-C) levels, $CD4^+$ T cell counts, and creatinine clearance (Ccr) levels increase the risk of cytopenia in HIV hospitalized patients.

Conclusion: The present study constructed a risk prediction model for cytopenia in HIV patients during hospitalization with machine learning and electronic medical record information. The prediction model is important for the rational management of HIV hospitalized patients and the personalized treatment plan setting.

KEYWORDS

HIV, cytopenia, anemia, thrombocytopenia, leukopenia, electronic medical records, machine learning

1. Background

The human immunodeficiency virus (HIV) not only cause damage to the function of the immune system, but also have a negative impact on the body's hematopoietic system (1). Cytopenia is one of the common complications of HIV infection (2) and the common types are anemia, thrombocytopenia and leucopenia. Within the HIV patients, anemia is an independently influential factor in both the acceleration of disease progression and the decline in quality of life (3). The prevalence of anemia ranges from 1.3 to 95% (4). Currently there are relatively few reports on the prevalence of leukopenia and thrombocytopenia and their associated factors. The most common type of leukopenia is neutropenia. Neutropenia affects 5 to 30% of patients in the early stages of HIV infection. Whereas in patients with late-stage HIV infection, the prevalence of neutropenia can reach 57 to 76% (5–7). The prevalence of thrombocytopenia among HIV patients ranges from 4.1 to 40% (8). Cytopenia may negatively affect outcomes of treatment and accelerate disease progression in patients with HIV (9). The causes of cytopenia in HIV patients are complicated. Currently reported factors that have been correlated with the occurrence of cytopenias in HIV patients include the direct effects of HIV infection, the effects of drug therapy and OIs (10–12). And $CD4^+$ T cell counts as a marker of acquired immunodeficiency syndrome (AIDS) progression have also been proven to correlate with cytopenia (13).

Machine learning has had a wide range of applications in medicine in recent years, such as cancer diagnosis (14), medical imaging (15) and death prediction (16). Numerous machine learning algorithms have demonstrated their potential for application to large-scale biomedical and patient datasets. Machine learning can balance the deviation and variance of data. Machine learning can be utilized on datasets containing numerous multidimensional variables to identify high-dimensional, non-linear relationships between clinical features for the purpose of data-driven outcome prediction. This approach overcomes certain limitations of current risk prediction analysis methods. Machine learning models for medical big data based on electronic medical records will support doctors in clinical diagnosis and management.

Cytopenia continues to be a significant concern in numerous countries with limited resources. The severity of cytopenia and its associated factors can impact the effectiveness of highly active antiretroviral therapy (HAART). However, this issue has not received enough attention in many developing countries. Most reports on the prevalence and associated factors of cytopenias come from regions with high AIDS prevalence and developed countries. These data may be quite different from other regions in terms of patient characteristics, cytopenic status, and HAART, etc. (17–20). The main aim of the present study was to construct a predictive model that accurately predicts whether cytopenia would occur during hospitalization in people with HIV. To develop more appropriate treatment plans for HIV patients, it is essential to understand the profile of cytopenias and the relevant factors (21). However, there have been few reports on cytopenias among HIV patients in China. Thus, gaining insight into the risk factors that contribute to cytopenia in patients with HIV and developing an accurate predictive model for cytopenia could facilitate early intervention and prevent its progression in this patient population. For clinicians, the model could be used to screen HIV patients who may experience cytopenia in the future, and thus take a more appropriate treatment approach.

2. Materials and methods

2.1. Data collection

This study was carried out at Guangxi Chest Hospital. Guangxi Chest Hospital is located in Liuzhou, Guangxi. The hospital is the regional designated hospital for the treatment of serious infectious diseases. The study was carried out between June 2016 and October 2021 and enrolled a total of 6,220 hospitalized HIV infected patients. Through the hospital electronic medical record system identifying HIV patients with cytopenia. People with HIV who did not suffer from cytopenia on their admission were included as study participants. The diagnostic criteria for anemia is the same as that of the World Health Organization (WHO). A hemoglobin level < 110 g/L (women) or < 120 g/L (men) is defined as anemia. Anemia is graded as severe (hemoglobin <60 g/L), moderate (hemoglobin 60–89 g/L) and mild (hemoglobin 90–119 g/L for men or 90–109 g/L for women). Compared to anemia, leukopenia and thrombocytopenia do not have universally accepted cut-off values. We defined them using criteria that have been used in other studies (7, 22). The criterion for leukopenia was total leukocytes $<4.0 \times 103$/uL. Platelet counts $<150 \times 103$/uL were considered to be thrombocytopenia. The classification criteria for mild thrombocytopenia, moderate thrombocytopenia and severe thrombocytopenia were $100–150 \times 103$/uL, $50–100 \times 103$/uL and less than 50×103/uL, respectively, Gunda et al. (9). If a patient has multiple admissions to hospital, the data of the most recent admission will be included as a priority. The results of laboratory tests on the patient's blood first collected on admission to hospital were included in the study. The patient was discharged from hospital or died during hospitalization then observation was stopped. Patients younger than 18 years old, patients who received radiation therapy within the past 45 days, and pregnant women were excluded from the study. Because the underlying conditions of these patients themselves may induce or exacerbate cytopenias. All of the patients were confirmed to be HIV-positive by enzyme-linked immunosorbent assay and immunoblot detection laboratory tests, and the diagnosis was consistent with national HIV diagnostic criteria.

2.2. Data preprocessing

We extracted sociodemographic and clinical information, as well as blood examination records, from the medical electronic record system of Guangxi Chest Hospital to construct a structured dataset for the study participants. The structured dataset included 66 variables: 13 clinical comorbidity/co-infection variables (tuberculosis, pneumocystis, candida infection, cryptococcus, herpesvirus, cytomegalovirus, pneumonia, electrolyte disorders, hepatitis (B or C), hypoproteinemia, diabetes, hypertension, and cancer) 6 demographic indicators (gender, age, ethnicity, marital status, actual days in hospital and residence) 47 laboratory indicators ($CD8^+$ T cell count, $CD4^+$ T cell count and levels of ALP, ALT, AST, CEA, etc.).Excluding variables with missing data greater than 15%. Used Random Forest to fill in the missing values for the structured dataset (23). All the above data processing steps were done by the numpy, pandas and sklearn packages of Python 3.8.6.

2.3. Model construction and evaluation

Whether cytopenia had occurred in HIV patients at hospital discharge was used as a outcome of the prediction model. The data was divided randomly into two datasets using Scikit-learn, a Python package (24). 80% of the data was utilized for training the machine learning models and adjusting their parameters. 20% of the data were used to test the models and fine-tune the hyperparameters. We used five machine learning classifiers (artificial neural network (ANN), adaptive boosting (AdaBoost), k-nearest neighbour (KNN), support vector machine (SVM) and decision tree (DT)) to create five models for predicting outcomes. The five machine learning classification prediction models were all constructed based on the sklearn package from Python 3.8.6.

The predictive ability of the prediction models was evaluated using the area under the receiver operating characteristic (ROC) curve (AUC), specificity, accuracy, sensitivity, and F1 scores. The evaluation indicators were varied from 0 to 1, corresponding to the worst and best scores, respectively. Using these metrics together allowed a more comprehensive evaluation and comparison of the classification effectiveness of different machine learning methods. The prediction model with the most effective performance evaluation indicators was selected as the final model. To explain the outcome of the best-performing predictive model, we utilized the Shapley additive interpretation (SHAP) to calculate the contribution of each feature to the predicted outcome (25).

2.4. Statistical analysis

The analysis of data was conducted with Python version 3.8.6 and SPSS version 24 statistical software package (SPSS Inc., Chicago, IL). The descriptive statistics such as percentage, mean, median, IQR, and standard deviation were used as appropriate. Student's *t*-test was used to compare normally distributed continuous variables, while the Mann–Whitney U test was used for non-normally distributed continuous variables. The chi-square test was utilized to compare categorical variables. The tests were two-sided, and statistical significance was defined as p values less than 0.05.

2.5. Ethical statement

The Human Research Ethics Committee of Guangxi Medical University (ethical approval number: 20210172) and the Medical Ethics Committee of Chest Hospital (ethical approval number: 2022–011) approved this study. Informed consent was waived after review by the Chest Hospital Medical Ethics Committee. Patient information was de-identified, and confidentiality was maintained throughout the study.

3. Result

3.1. Sociodemographic characteristics of study participants

In this research, the prevalence of cytopenia in hospitalized HIV patients was 19.3% (1,201/6220). The study included 2,187 qualified people living with HIV. Figure 1 showed the selection process for the patients included in the present study. The study participants had a median age of 56 years (interquartile range (IQR): 45–66 years). The median number of days in hospital for study participants was 21 days (interquartile range (IQR): 12–33 days). Among the 2,187 study participants, 1,686 (77.1%) were male, 1,673 (76.5%) were from rural areas and 1,296 (59.3%) were married. Over half (55.0%) of the sample were from ethnic minority groups, with the Zhuang ethnic group comprising the majority (48.0%). The cytopenia and non-cytopenia groups differed significantly in demographic characteristics, including gender, ethnicity, marital status, and residence address ($p < 0.05$). The essential features of the study participants were listed in Table 1.

3.2. Clinical and laboratory characteristics of study participants

The most common clinical complication/co-infection in hospitalized HIV patients was Candida infection (56.8%, 1243/2187), followed by hypoproteinaemia (48.0%, 1049/2187), pneumonia (47.1%, 1030/2187), and tuberculosis (47.1%, 1030/2187). The prevalence of cytopenia was as high as 76.0% (190/250) in HIV patients with electrolyte disturbances, which was higher than 52.2% (1,011/1937) in HIV patients without electrolyte disturbances. The prevalence of cytopenia was 72.4% (760/1049) in HIV patients with hypoproteinaemia, which was higher than 38.8% (441/1138) in HIV patients without hypoproteinaemia. Table 2 showed detailed information about clinical complications/co-infections of the study participants.

We evaluated the median levels of important indicators in both cytopenic and non-cytopenic groups of patients with HIV. The hemocytopenic group had lower levels of $CD4^+$ T cell count, $CD45^+$ T cell count, $CD3^+$ T cell count, cholinesterase (CHE), creatinine clearance (Ccr), prealbumin (PA) and total cholesterol (CHOL). There were also some laboratory indicators of interest that were significantly different, such as serum cystatin (Cys-C), triglycerides (TG) and chlorine (Cl). Detailed characteristics of the laboratory indicators were shown in Table 3.

10.3389/fpubh.2023.1184831

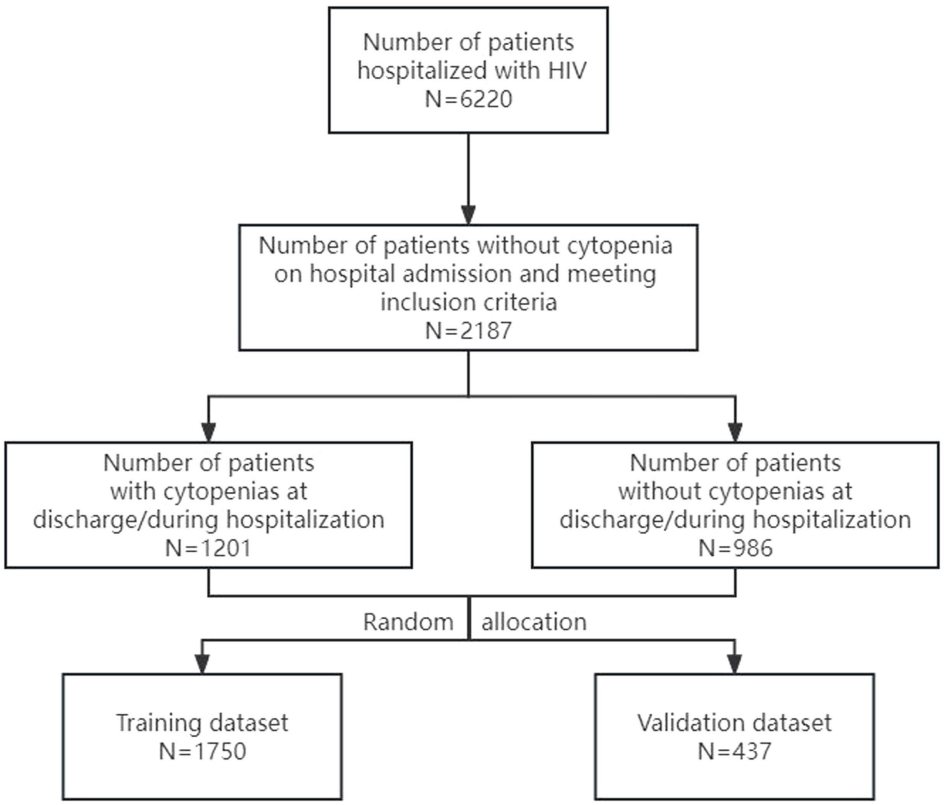

FIGURE 1
Flow diagram of the selection of participants included in the present study.

TABLE 1 Sociodemographic characteristics of HIV patients included in study.

Variables	Total (n = 2,187)	Outcome		Statistic	p-value
		Non-cytopenias (n = 986)	Cytopenias (n = 1,201)		
Age, years	56 (45,66)	56 (45,66)	55 (44,66)	−1.023	0.306
Days in hospital, days	21 (12,33)	22 (13, 32)	21 (12, 33)	−0.102	0.919
Sex				8.718	**0.003**
Female	501 (22.9%)	197 (39.3%)	304 (60.7%)		
Male	1,686 (77.1%)	789 (46.8%)	897 (53.2%)		
Ethnicity				8.586	**0.014**
Han	986 (45.0%)	415 (42.1%)	571 (57.9%)		
Zhuang	1,049 (48.0%)	507 (48.3%)	542 (51.7%)		
Other (minority)	152 (7.0%)	64 (42.1%)	88 (57.9%)		
Marital Status				7.289	**0.026**
Unmarried	485 (22.2%)	204 (42.1%)	281 (57.9%)		
Married	1,296 (59.3%)	615 (47.5%)	681 (52.5%)		
Divorce and widowhood	406 (18.6%)	167 (41.1%)	239 (58.9%)		
Residence				6.803	**0.009**
Urban	514 (23.5%)	206 (40.1%)	308 (59.9%)		
Rural	1,673 (76.5%)	780 (46.6%)	893 (53.4%)		

Numbers in bold represent significant groups ($p < 0.05$).

10.3389/fpubh.2023.1184831

TABLE 2 Characteristics of clinical complications/co-infections in HIV-positive patients included in study.

Variables	Total (*n* = 2,187)	Outcome		Statistic	*p*-value
		Non-cytopenias (*n* = 986)	Cytopenias (*n* = 1,201)		
Pneumonia				0.797	0.372
No	1,157 (52.9%)	532 (46.0%)	625 (54.0%)		
Yes	1,030 (47.1%)	454 (44.1%)	576 (55.9%)		
Tuberculosis				0.519	0.471
No	1,157 (52.9%)	530 (45.8%)	627 (54.2%)		
Yes	1,030 (47.1%)	456 (44.3%)	574 (55.7%)		
Pneumocystis				1.266	0.260
No	1,653 (75.6%)	734 (44.4%)	919 (55.6%)		
Yes	534 (24.4%)	252 (47.2%)	282 (52.8%)		
Candidiasis				9.435	0.002
No	944 (43.2%)	461 (48.8%)	483 (51.2%)		
Yes	1,243 (56.8%)	525 (42.2%)	718 (57.8%)		
Cryptococcus				12.046	0.001
No	2093 (95.7%)	960 (45.9%)	1,133 (54.1%)		
Yes	94 (4.3%)	26 (27.7%)	68 (72.3%)		
Herpesvirus				2.055	0.152
No	1972 (90.2%)	899 (45.6%)	1,073 (54.4%)		
Yes	215 (9.8%)	87 (40.5%)	128 (59.5%)		
Cytomegalovirus				10.781	0.001
No	2020 (92.4%)	931 (46.1%)	1,089 (53.9%)		
Yes	167 (7.6%)	55 (32.9%)	112 (67.1%)		
Electrolyte disturbances				50.684	<0.001
No	1937 (88.6%)	926 (47.8%)	1,011 (52.2%)		
Yes	250 (11.4%)	60 (24.0%)	190 (76.0%)		
Hypoproteinemia				250.351	<0.001
No	1,138 (52.0%)	697 (61.2%)	441 (38.8%)		
Yes	1,049 (48.0%)	289 (27.6%)	760 (72.4%)		
Hepatitis B/Hepatitis C				6.564	0.01
No	1903 (87.2%)	878 (46.1%)	1,025 (53.9%)		
Yes	284 (12.8%)	108 (38.0%)	176 (62.0%)		
Hypertension				0.272	0.602
No	2036 (93.1%)	921 (45.2%)	1,115 (54.8%)		
Yes	151 (6.9%)	65 (43.0%)	86 (57.0%)		
Diabetic Mellitus				0.792	0.373
No	2073 (94.8%)	930 (44.9%)	1,143 (55.1%)		
Yes	114 (5.2%)	56 (49.1%)	58 (50.9%)		
Cancer				214.099	<0.001
No	1954 (89.3%)	986 (50.5%)	968 (49.5%)		
Yes	233 (10.7%)	0 (0.0%)	233 (100.0%)		

10.3389/fpubh.2023.1184831

TABLE 3 Characteristics of the laboratory measures of the HIV patients included in the study.

Variables	Total (n = 2,187)	Outcome		p-value
		Non-cytopenias (n = 1,108)	Cytopenias (n = 1,079)	
$CD3^+$ T cell count (cell/ul)	493 (274,814)	550 (315,899)	456 (242,745)	<0.001
CD4/CD8 ratio	0.16 (0.06,0.36)	0.17 (0.07,0.39)	0.15 (0.06,0.33)	0.004
$CD4^+$ T cell count (cell/ul)	63 (18,167)	76 (20,214)	54 (15,143)	<0.001
$CD45^+$ T cell count (cell/ul)	743 (433,1,194)	843 (491,1,321)	681 (378,1,061)	<0.001
$CD8^+$ T cell count (cell/ul)	374 (217,617)	402 (245,665)	352 (191,578)	<0.001
(1–3)-β-D Glucan (pg/ml)	9.3 (7.3,77.4)	9.2 (7.2,58.0)	9.5 (7.4,105.4)	0.02
CEA (ng/mL)	3.9 (1.7,26.3)	4.1 (1.8,28.3)	3.8 (1.7,25.1)	0.162
ALB (g/L)	31.0 (26.5,35.4)	32.6 (27.8,36.6)	30 (25.3,34.1)	<0.001
HCO3std (mmol/L)	25.1 (22.5,27.1)	25.5 (23.3,27.2)	24.8 (21.6,26.9)	<0.001
CHE (U/L)	4643.0 (3165.0,6358.0)	5194.1 (3718.8,6936.3)	4233.0 (2804.0,5786.5)	<0.001
LDL-C (mmol/L)	2.2 (1.6,2.7)	2.4 (1.8,2.9)	2.0 (1.5,2.5)	<0.001
AMY (U/L)	93.0 (68.0,125.0)	91.9 (68.0,120.2)	94.0 (67.0,129.4)	0.311
Ca (mmol/L)	2.1 (1.9,2.2)	2.1 (2.0,2.2)	2.1 (1.8,2.2)	<0.001
TG (mmol/L)	1.4 (1.1,2)	1.5 (1.1,2.1)	1.4 (1.0,2.0)	0.041
HDL-C (mmol/L)	0.8 (0.6,1.1)	0.9 (0.7,1.1)	0.8 (0.5,1.1)	<0.001
GGT (U/L)	73 (39,139)	69.0 (38.8,127.0)	79.0 (40.0,150.0)	0.032
ALT (U/L)	20 (12,35)	21.5 (13.0,37.0)	19.0 (11.0,34.0)	0.001
AST/ALT	1.5 (1.0,2.2)	1.4 (0.9,2.0)	1.6 (1.1,2.3)	<0.001
AST (U/L)	28 (20,44)	27 (20,41)	29 (19,46)	0.306
Cys-C (mg/L)	1.19 (1.00,1.53)	1.14 (0.98,1.41)	1.24 (1.03,1.65)	<0.001
CREA (umol/L)	69 (56,88)	69 (56,85)	70 (55,92)	0.173
Ccr (ml/min)	63.2 (48.2,76)	66.2 (52.6,77.7)	60.5 (44.4,74.1)	<0.001
CK (U/L)	55.0 (34.0,95.5)	57.0 (36.0,99.0)	53.0 (33.0,92.0)	0.04
K (mmol/L)	3.7 (3.3,4.1)	3.7 (3.3,4.0)	3.7 (3.3,4.1)	0.928
IBIL (umol/L)	3.6 (2.4,5.6)	3.6 (2.4,5.6)	3.5 (2.4,5.6)	0.967
ALP (U/L)	99 (70,143)	92.0 (68.0,134.0)	105.0 (73.0,151.5)	<0.001
Cl (mmol/L)	102.9 (100.0,105.8)	102.0 (99.0,105.0)	102.9 (100.0,106.8)	<0.001
Mg (mmol/L)	0.8 (0.7,0.8)	0.77 (0.70,0.84)	0.75 (0.67,0.82)	<0.001
Na (mmol/L)	136 (133,139)	136 (133,139)	136 (133,139)	0.545
UREA (mmol/L)	4.1 (3.0,5.9)	4.0 (2.9,5.4)	4.3 (3.0,6.3)	0.001
UA (umol/L)	299 (217,416)	303 (227,430)	295 (211,409)	0.011
Glu (mmol/L)	6.8 (5.5,8.5)	6.9 (5.6,8.8)	6.7 (5.5,8.4)	0.008
PA (mg/L)	151 (91,218)	170 (109,237)	137 (78,205)	<0.001
GLOB (g/L)	37.4 (31.4,43.6)	36.9 (31.4,42.6)	37.8 (31.6,44.4)	0.031
LDH (U/L)	227 (179,307)	224 (179,296)	230 (179,315)	0.238
ADA (U/L)	22.6 (15.1,31.5)	22.3 (15.5,30.0)	22.8 (14.4,32.9)	0.359
DBIL (umol/L)	2.8 (1.7,5.6)	2.6 (1.6,4.8)	3.0 (1.7,6.5)	0.001
CHOL (mmol/L)	3.6 (2.9,4.4)	3.9 (3.1,4.6)	3.4 (2.7,4.1)	<0.001
TBIL (umol/L)	6.6 (4.4,11.1)	6.5 (4.4,10.3)	6.7 (4.5,12.0)	0.031
TBA (umol/L)	7.6 (3.8,15)	6.8 (3.5,13.2)	8.3 (4.1,17.0)	<0.001
TP (g/L)	69.2 (61.6,75.6)	70.1 (62.9,76.0)	68.5 (60.6,75.4)	0.001

TABLE 4 Performance of predictive models built by five machine learning algorithms.

Models	AUC	Sensitivity	Specificity	Accuracy	F1	Precision
SVC	0.844	0.730	0.787	0.758	0.753	0.779
KNN	0.831	0.735	0.767	0.751	0.740	0.745
ANN	0.858	0.745	0.798	0.772	0.766	0.788
AdaBoost	0.852	0.745	0.788	0.767	0.759	0.774
DT	0.647	0.634	0.661	0.648	0.624	0.615

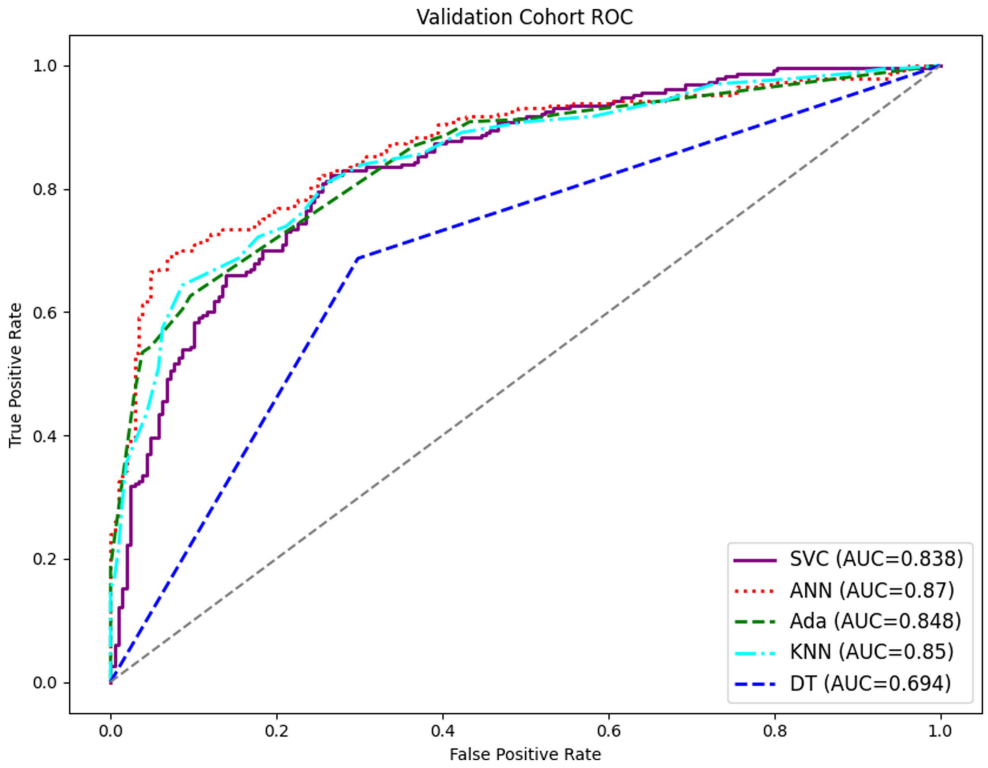

FIGURE 2
Evaluation of five machine learning algorithms based on the AUC of ROC curves.

3.3. Feature selection, model construction and evaluation

Using the sklearn package and the pandas package in Python 3.8.6 to achieve feature filtering of the data. We used recursive feature elimination (RFE) with random forest to select input features for a predictive model aimed at predicting the occurrence of cytopenia in HIV patients during hospitalization. Finally, 12 variables were selected from 66 variables as predictors of the risk of cytopenia in HIV patients. Among the 12 included indicators, 9 were laboratory examination indicators, including $CD4^+$ T cell count, serum cystatin (Cys-C), standard bicarbonate (HCO3std), low-density lipoprotein cholesterol (LDL-C), creatinine clearance (Ccr), chloride (Cl), glutamyltransferase (GGT), monocytes-to-lymphocites ratio (Mono/Lymph) and hemoglobin-to-RDW ratio (HGB/RDW), 3 clinical comorbidity/co-infection including electrolyte disturbances, hypoproteinemia and cancer.

The prediction models for the development of cytopenia in HIV patients during the hospitalization were constructed based on 12 features from the feature selection results. Table 4 displayed the prediction performance of the prediction models generated by the five machine learning algorithms. The ANN model demonstrated the highest sensitivity and specificity and therefore exhibited superior predictive power compared to other models. Figure 2 showed the ROC curves for the five models, with the ANN model displaying the most favorable results.

3.4. Explanation of risk factor

To better comprehend how the features integrated into the ANN prediction model contribute to the prediction results, we computed the SHAP values for each individual feature. The ANN prediction model generates a predictive value for each predicted sample. The SHAP value is a numerical score assigned to each feature in a given sample, indicating the degree of impact each feature has on the outcome and whether it is a positive or negative influence. The importance matrix diagram for the ANN model was shown in

Figure 3. The importance matrix ranks the features that affect cytopenias in hospitalized HIV patients, from most to least important. The importance matrix ranking results for the ANN prediction model were hypoproteinemia, HGB/RDW, cancer, LDL-C, $CD4^+$ T cell count, electrolyte disturbance, Cl, Ccr, HCO3std, Mono/Lymph, GGT and Cys-C. The SHAP summary plot showed how each variable had an impact on the predicted outcome of the occurrence of cytopenia in hospitalized HIV patients (Figure 4). Each patient was assigned a point, and features were color-coded based on attribute values, with red indicating higher values and blue indicating lower values. According to the SHAP summary plots, hypoproteinemia and cancer were identified as the most significant features. In hospitalized patients with HIV, these two features were strongly and positively correlated with cytopenia. HIV patients presenting with these two clinical comorbidities were at significantly increased risk of developing cytopenia during hospitalization compared to HIV patients not presenting with these two comorbidities. HGB/RDW, LDL-C, $CD4^+$ T cell count, Ccr, HCO3std and Mono/Lymph also had a significant effect on the occurrence of cytopenia in hospitalized patients with HIV. The risk of cytopenia increases as the value of these features decreases. The higher the value of Cl, GGT and Cys-C, the greater the risk of cytopenia. Hospitalized HIV patients with electrolyte disorders were more likely to develop cytopenia.

4. Discussion

This study conducted a retrospective analysis on a large sample size and identified Candida infection, hypoproteinemia, tuberculosis and pneumonia as the most frequent complications among hospitalized patients with HIV. This finding was similar to previous reports (26). The current study employed machine learning techniques and clinical features readily obtainable from electronic medical records to develop a predictive model for cytopenia risk in HIV patients during hospitalization. We evaluated and compared the predictive capabilities of five distinct machine learning models. The results showed that ANN models have the highest sensitivity and specificity. ANN model is widely used in clinical detection and pathology identification due to the good performance it has shown in recognition (27, 28). In comparison to other machine learning models, ANN are able to effectively process non-linear relationships, which is important in many real-world problems (29). ANN consist of multiple neurons and layers that enable them to learn and represent very complex relationships and have better capabilities for implicit pattern and feature extraction in data. The hidden layer structure of ANN enables them to capture and represent complex relationships between input features, thus better adapting to different types of data (30). As far as the authors know, the current research is the first published study to use ANN models to predict the occurrence of cytopenia in HIV patients during hospitalization.

The combination of electronic medical records and machine learning has contributed to the development of complex prediction models (31, 32). To enhance the transparency of the model's prediction process, we employed the SHAP method to compute the contribution of individual variables to the model's predicted outcome. The results showed that hypoproteinemia and cancer were important factors influencing the occurrence of cytopenia during hospitalization of HIV patients. We also identified HGB/RDW, LDL-C, $CD4^+$ T cell count and Ccr were the variables that had a greater impact.

Previous studies have demonstrated that hypoproteinemia is a potential predictor of disease progression and mortality among individuals with HIV (33). A cohort study in West Africa that investigated the nutritional status of HIV patients who received HAART for 1 year reported that low albumin was associated with anemia (34). It is not coincidental that serum albumin levels have been claimed to be independently associated with severe anemia and could influence mortality and the outcome of HAART in HIV patients (35). There is growing evidence that hypoproteinemia has a dramatic impact on cytopenia in HIV patients, particularly anemia. There are two possible reasons why people with cancer are more likely to develop anemia; cancer causes difficulty in the production of red blood cells and shortens the survival time of red blood cells (36). Furthermore, anti-cancer treatments may harm healthy blood cells. Our study discovered that hypoproteinemia and cancer were significant factors contributing to cytopenia in HIV patients during hospitalization.

After analyzing all features included in the model, we found that HGB/RDW, LDL-C, $CD4^+$ T cell count, and Ccr had the great impact on predicting the risk of cytopenia during hospitalization in HIV patients. Specifically, lower levels of HGB/RDW, LDL-C, $CD4^+$ T cell count, and Ccr were associated with an increased risk of cytopenia. HGB/RDW as a new comprehensive biomarker has gradually attracted widespread attention. The lower HGB/RDW levels have been demonstrated to be associated with cancer development and poor prognosis (37, 38). In the present case, HIV patients with lower levels of HGB/RDW had a higher risk of cytopenia during hospitalization. The lower HGB/RDW may represent abnormal erythrocyte homeostasis and deformed erythrocytes, leading to disturbed blood flow in the microcirculation (39), which may have contributed to the increased susceptibility of people living with HIV to cytopenias during hospitalization. Hemoglobin and RDW are easily accessible laboratory examination indicators. But HGB/RDW is rarely focused on during HIV treatment. The results of the present study showed that HGB/RDW is strongly associated with the development of cytopenias in people living with HIV and deserves greater attention.

Low LDL-C is often associated with long-term vegetarian diet (40), liver disease (41) and drug therapy (42). Low LDL-C has also been reported to be associated with chronic anemia (43). However, LDL-C has not been of particular concern in previous studies about risk factors associated with cytopenia in HIV patients. Although the mechanism of how lower LDL-C leads to cytopenia is not clear, there are some possible explanations. Possible explanations include erythrocyte fragility due to low cholesterol levels in the erythrocyte membrane (44), as well as LDL-related platelet activation and tissue factor expression (45). But the mechanism of how low LDL-C leads to cytopenia needs more further research to prove it.

As with previous studies, our research found that low $CD4^+$ T cell counts are a risk factor for cytopenia in HIV patients. $CD4^+$ T cell counts are closely correlated with HIV disease progression, and lower counts are typically indicative of advanced disease progression (46). The primary explanation for cytopenia, which results from low $CD4^+$ T cell counts in HIV patients, is likely HIV-mediated hematopoietic suppression and direct T cell infection (10). Moreover, research showed that improved $CD4^+$ T cell counts after HAART treatment have led to a reduction in the prevalence of cytopenia in HIV patients (47–49), indicating that HIV-related cytopenia is caused by HIV infection and immunosuppression (50).

10.3389/fpubh.2023.1184831

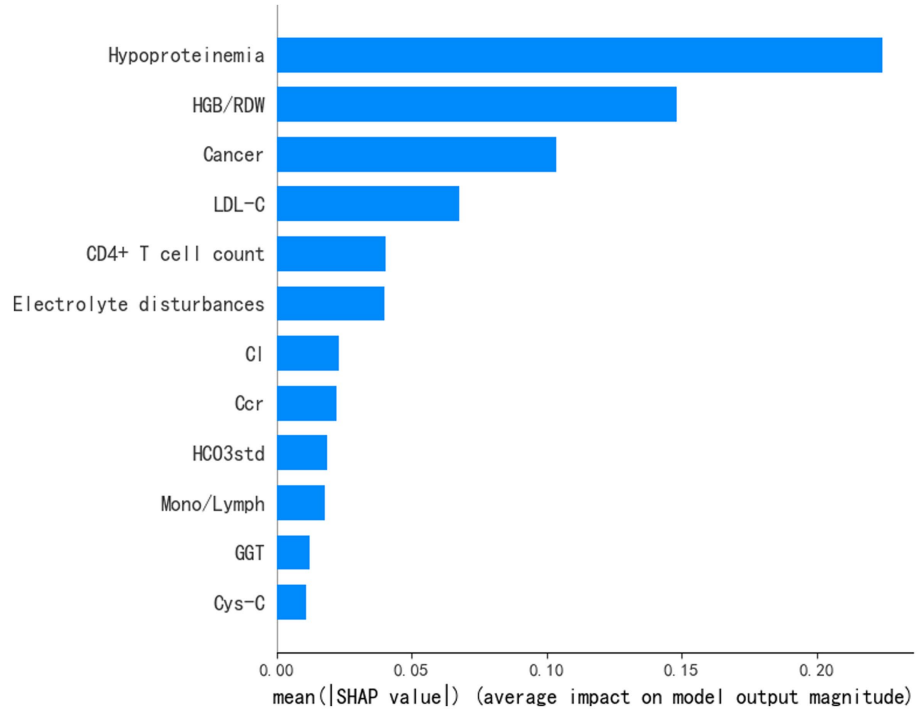

FIGURE 3
Importance matrix plot of the ANN model showing the contribution of each clinical feature to the predictive model of cytopenia in hospitalized HIV patients.

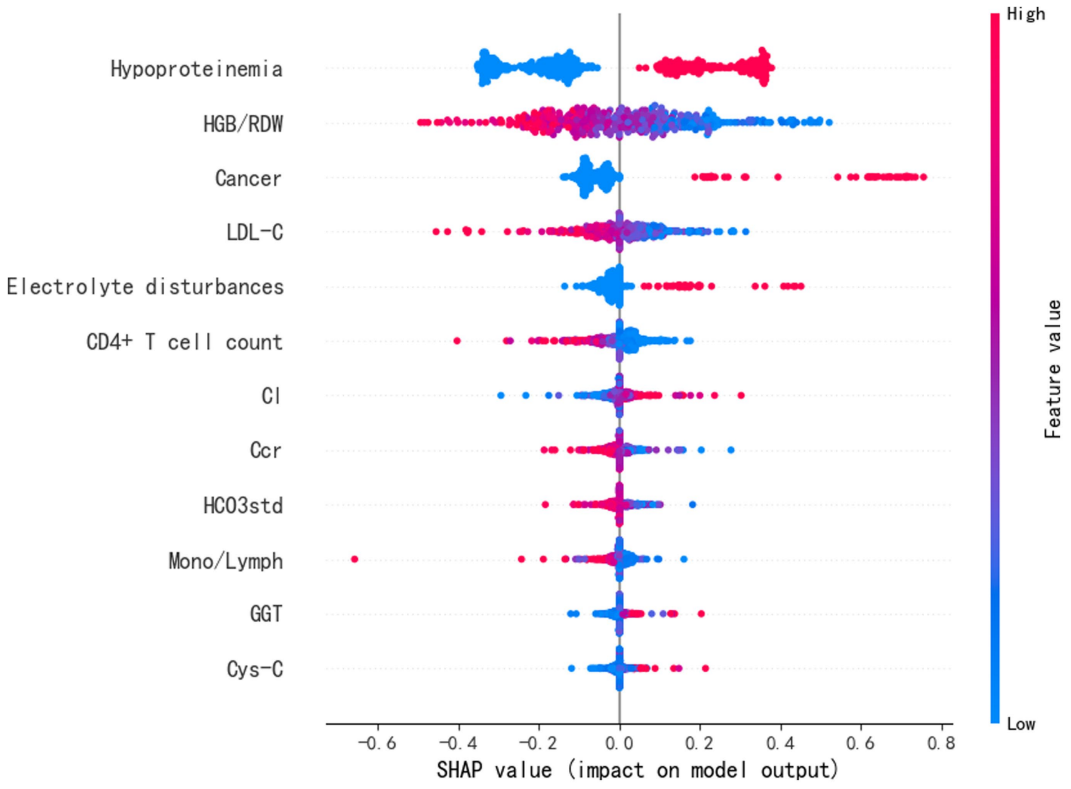

FIGURE 4
SHAP summary plot of the top 12 clinical features of the ANN model.

CCr is a sensitive marker of glomerular damage and an early indicator of kidney impairment. Lower CCr could lead to chronic kidney disease, and the common complications of chronic kidney disease include anemia (51). Concurrently, it has also been claimed that high serum creatinine is a significant predictor of anemia in HIV patients (52). GGT is an important indicator of liver function and an increased GGT level means impaired liver function. And abnormal liver function could cause a cytopenia (53). Both CCr and GGT reflect the organ function of HIV patients and the potential risk of cytopenia in HIV patients, but have not been focused on in previous studies. The levels of Cl, HCO3std and electrolytes provide valuable information about the body's metabolism, and their disturbances may indicate metabolic issues in HIV patients who were at a high risk of developing cytopenia. Mono/Lymph is demonstrated to be a predictor of the risk of developing tuberculosis in people living with HIV (54). And tuberculosis is one of the factors associated with the development of cytopenia in people living with HIV (9). Although Cys-C levels may be considered clinically insignificant and often overlooked, it is still important for predictive modeling purposes.

The present study used real-world data from electronic medical records to construct an ANN prediction model for predicting the risk of cytopenia in HIV patients during hospitalization using multiple clinical complications and clinical variables. We identified some risk factors associated with cytopenia in HIV patients that have not been focused on in previous studies. Finally, the predictive model can serve as a clinical screening tool to assess the risk of cytopenia in HIV patients during hospitalization, thus facilitating the development of more personalized and rational treatment plans. However, there were certain limitations in our study. Firstly, our study sample was predominantly limited to southern China and thus not indicative of the overall situation of individuals living with HIV throughout China. Secondly, the potential influence of medications and treatment regimens on the study outcomes was not taken into account during the data collection process. Thirdly, the prediction model in this study was not validated for stability using external data. Our model has been internally validated and demonstrates consistent and robust predictive ability for the results explored.

5. Conclusion

To sum up, this study utilized electronic medical records to gather demographic information, clinical complications, and laboratory test indicators of HIV patients. These clinical characteristics were then used to construct a predictive model to assess the risk of cytopenia in HIV patients. The predictive model has significant implications for improving the management of HIV patients and tailoring personalized treatment plans.

Data availability statement

The raw data supporting the conclusions of this article will be made available by the authors, without undue reservation.

Ethics statement

The Human Research Ethics Committee of Guangxi Medical University (ethical approval number: 20210172) and the Medical Ethics Committee of Chest Hospital (ethical approval number: 2022-011) approved this study. Informed consent was waived after review by the Chest Hospital Medical Ethics Committee. Patient information was de-identified, and confidentiality was maintained throughout the study. Written informed consent for participation was not required for this study in accordance with the national legislation and the institutional requirements.

Author contributions

YH, JL, LH, JQ, and KZ designed the study and provided the correlative knowledge. YX, LS, YL, YJL, ZM, and KH collected and provided the data. LL, XW, and BX extracted data and cleaned data. BX and LL constructed the prediction model. KZ, LS, YL, and BX generated the figures and tables. YX, YH, HQ, XP, and BX wrote and edited the manuscript. All authors contributed to the article and approved the submitted version.

Funding

This research was supported by several organizations, including the Guangxi Key Research and Development Program (2021AB12032), Research Projects for High-level Talents in Affiliated Hospital of Youjiang Medical College of Ethnic Minorities in 2022 (R202210308), Guangxi Medical and Health Appropriate Technology Development and Promotion Application Project (S2022042), Nanning Scientific Research and Technology Development Program (20206124), Guangxi Chinese Medicine Appropriate Technology Development and Promotion Project (GZSY22-71), and Major National Science and Technology Projects (2017ZX10202101-001-006). It is important to note that the funding bodies were not involved in the design of the study, data collection, analysis, interpretation or manuscript writing.

Acknowledgments

The authors would like to thank all participants of this study, financial supporters and Guangxi Chest Hospital for their support.

Conflict of interest

The authors declare that the research was conducted in the absence of any commercial or financial relationships that could be construed as a potential conflict of interest.

Publisher's note

References

1. Durandt C, Potgieter JC, Mellet J, Herd C, Khoosal R, Nel JG, et al. HIV and haematopoiesis. *S Afr Med J*. (2019) 109:40–5. doi: 10.7196/SAMJ.2019.v109i8b.13829

2. Fiseha T, Ebrahim H. Prevalence and predictors of cytopenias in HIV-infected adults at initiation of antiretroviral therapy in Mehal Meda hospital, Central Ethiopia. *J Blood Med*. (2022) 13:201–11. doi: 10.2147/JBM.S355966

3. Subbaraman R, Devaleenal B, Selvamuthu P, Yepthomi T, Solomon SS, Mayer KH, et al. Factors associated with anaemia in HIV-infected individuals in southern India. *Int J STD AIDS*. (2009) 20:489–92. doi: 10.1258/ijsa.2008.008370

4. Belperio PS, Rhew DC. Prevalence and outcomes of anemia in individuals with human immunodeficiency virus: a systematic review of the literature. *Am J Med*. (2004) 116:27–43. doi: 10.1016/j.amjmed.2003.12.010

5. Calenda V, Chermann JC. The effects of HIV on hematopoiesis. *Eur J Haematol*. (1992) 48:181–6. doi: 10.1111/j.1600-0609.1992.tb01582.x

6. Frontiera M, Myers AM. Peripheral blood and bone marrow abnormalities in the acquired immunodeficiency syndrome. *West J Med*. (1987) 147:157–60.

7. Fekene TE, Juhar LH, Mengesha CH, Worku DK. Prevalence of cytopenias in both HAART and HAART naïve HIV infected adult patients in Ethiopia: a cross sectional study. *BMC Hematol*. (2018) 18:8. doi: 10.1186/s12878-018-0102-7

8. Evans RH, Scadden DT. Haematological aspects of HIV infection. *Baillieres Best Pract Res Clin Haematol*. (2000) 13:215–30. doi: 10.1053/beha.1999.0069

9. Gunda DW, Godfrey KG, Kilonzo SB, Mpondo BC. Cytopenias among ART-naive patients with advanced HIV disease on enrolment to care and treatment services at a tertiary hospital in Tanzania: a cross-sectional study. *Malawi Med J*. (2017) 29:43–52. doi: 10.4314/mmj.v29i1.9

10. Koka PS, Reddy ST. Cytopenias in HIV infection: mechanisms and alleviation of hematopoietic inhibition. *Curr HIV Res*. (2004) 2:275–82. doi: 10.2174/1570162043351282

11. Opie J. Haematological complications of HIV infection. *S Afr Med J*. (2012) 102:465–8. doi: 10.7196/SAMJ.5595

12. Passos AM, Treitinger A, Spada C. An overview of the mechanisms of HIV-related thrombocytopenia. *Acta Haematol*. (2010) 124:13–8. doi: 10.1159/000313782

13. Vishnu P, Aboulafia DM. Haematological manifestations of human immune deficiency virus infection. *Br J Haematol*. (2015) 171:695–709. doi: 10.1111/bjh.13783

14. Chen Z, Wang M, de Wilde RL, Feng R, Su M, Torres-de la Roche LA, et al. A machine learning model to predict the triple negative breast Cancer immune subtype. *Front Immunol*. (2021) 12:749459. doi: 10.3389/fimmu.2021.749459

15. Ashour AS, Hawas AR, Guo Y. Comparative study of multiclass classification methods on light microscopic images for hepatic schistosomiasis fibrosis diagnosis. *Health Inf Sci Syst*. (2018) 6:7. doi: 10.1007/s13755-018-0047-z

16. Hu C, Liu Z, Jiang Y, Shi O, Zhang X, Xu K, et al. Early prediction of mortality risk among patients with severe COVID-19, using machine learning. *Int J Epidemiol*. (2021) 49:1918–29. doi: 10.1093/ije/dyaa171

17. Mocroft A, Kirk O, Barton SE, Dietrich M, Proenca R, Colebunders R, et al. Anaemia is an independent predictive marker for clinical prognosis in HIV-infected patients from across Europe. EuroSIDA study group. *AIDS*. (1999) 13:943–50. doi: 10.1097/00002030-199905280-00010

18. Sullivan PS, Hanson DL, Chu SY, Jones JL, Ward JW. Epidemiology of anemia in human immunodeficiency virus (HIV)-infected persons: results from the multistate adult and adolescent spectrum of HIV disease surveillance project. *Blood*. (1998) 91:301–8. doi: 10.1182/blood.V91.1.301

19. Turner BJ, Markson L, Taroni F. Estimation of survival after AIDS diagnosis: CD4 T lymphocyte count versus clinical severity. *J Clin Epidemiol*. (1996) 49:59–65. doi: 10.1016/0895-4356(95)00067-4

20. Choi SY, Kim I, Kim NJ, Lee SA, Choi YA, Bae JY, et al. Hematological manifestations of human immunodeficiency virus infection and the effect of highly active anti-retroviral therapy on cytopenia. *Korean J Hematol*. (2011) 46:253–7. doi: 10.5045/kjh.2011.46.4.253

21. Nassiri R. Avoiding antiretroviral-associated cytopenias. *J Am Osteopath Assoc*. (2006) 106:111–2.

22. Tamir Z, Seid A, Haileslassie H. Magnitude and associated factors of cytopenias among antiretroviral therapy naïve human immunodeficiency virus infected adults in Dessie, Northeast Ethiopia. *PLoS One*. (2019) 14:e0211708. doi: 10.1371/journal.pone.0211708

23. Tang F, Ishwaran H. Random Forest missing data algorithms. *Stat Anal Data Min*. (2017) 10:363–77. doi: 10.1002/sam.11348

24. Swami A, Jain R. Scikit-learn: machine learning in Python. *J Mach Learn Res*. (2013) 12:2825–30.

25. Tseng PY, Chen YT, Wang CH, Chiu KM, Peng YS, Hsu SP, et al. Prediction of the development of acute kidney injury following cardiac surgery by machine learning. *Crit Care*. (2020) 24:478. doi: 10.1186/s13054-020-03179-9

26. Pang W, Shang P, Li Q, Xu J, Bi L, Zhong J, et al. Prevalence of opportunistic infections and causes of death among hospitalized HIV-infected patients in Sichuan, China. *Tohoku J Exp Med*. (2018) 244:231–42. doi: 10.1620/tjem.244.231

27. Lugtu EJ, Ramos DB, Agpalza AJ, Cabral EA, Carandang RP, Dee JE, et al. Artificial neural network in the discrimination of lung cancer based on infrared spectroscopy. *PLoS One*. (2022) 17:e0268329. doi: 10.1371/journal.pone.0268329

28. Ganji Z, Aghaee Hakak M, Zare H. Comparison of machine learning methods for the detection of focal cortical dysplasia lesions: decision tree, support vector machine and artificial neural network. *Neurol Res*. (2022) 44:1142–9. doi: 10.1080/01616412.2022.2112381

29. Renganathan V. Overview of artificial neural network models in the biomedical domain. *Bratisl Lek Listy*. (2019) 120:536–40. doi: 10.4149/BLL_2019_087

30. Tian Y, Yang J, Lan M, Zou T. Construction and analysis of a joint diagnosis model of random forest and artificial neural network for heart failure. *Aging (Albany NY)*. (2020) 12:26221–35. doi: 10.18632/aging.202405

31. Damotte V, Lizée A, Tremblay M, Agrawal A, Khankhanian P, Santaniello A, et al. Harnessing electronic medical records to advance research on multiple sclerosis. *Mult Scler*. (2019) 25:408–18. doi: 10.1177/1352458517747407

32. Cheung M, Cobb AN, Kuo PC. Predicting burn patient mortality with electronic medical records. *Surgery*. (2018) 164:839–47. doi: 10.1016/j.surg.2018.07.010

33. Leal JA, Fausto MA, Carneiro M, Tubinambás U. Prevalence of hypoalbuminemia in outpatients with HIV/AIDS. *Rev Soc Bras Med Trop*. (2018) 51:203–6. doi: 10.1590/0037-8682-0093-2017

34. Sicotte M, Bemeur C, Diouf A, Zunzunegui MV, Nguyen VKfor the ATARAO initiative. Nutritional status of HIV-infected patients during the first year HAART in two west African cohorts. *J Health Popul Nutr*. (2015) 34:1. doi: 10.1186/s41043-015-0001-5

35. Sudfeld CR, Isanaka S, Aboud S, Mugusi FM, Wang M, Chalamilla GE, et al. Association of serum albumin concentration with mortality, morbidity, CD4 T-cell reconstitution among tanzanians initiating antiretroviral therapy. *J Infect Dis*. (2013) 207:1370–8. doi: 10.1093/infdis/jit027

36. Zucker S. Anemia in cancer. *Cancer Investig*. (1985) 3:249–60. doi: 10.3109/07357908509039786

37. Chi G, Lee JJ, Montazerin SM, Marszalek J. Prognostic value of hemoglobin-to-red cell distribution width ratio in cancer: a systematic review and meta-analysis. *Biomark Med*. (2022) 16:473–82. doi: 10.2217/bmm-2021-0577

38. Su YC, Wen SC, Li CC, Su HC, Ke HL, Li WM, et al. Low Hemoglobin-to-red cell distribution width ratio is associated with disease progression and poor prognosis in upper tract urothelial carcinoma. *Biomedicine*. (2021) 9:672. doi: 10.3390/biomedicines9060672

39. Salvagno GL, Sanchis-Gomar F, Picanza A, Lippi G. Red blood cell distribution width: a simple parameter with multiple clinical applications. *Crit Rev Clin Lab Sci*. (2015) 52:86–105. doi: 10.3109/10408363.2014.992064

40. Djekic D, Shi L, Brolin H, Carlsson F, Särnqvist C, Savolainen O, et al. Effects of a vegetarian diet on cardiometabolic risk factors, gut microbiota, and plasma metabolome in subjects with ischemic heart disease: a randomized, crossover study. *J Am Heart Assoc*. (2020) 9:e016518. doi: 10.1161/JAHA.120.016518

41. Jiang ZG, Mukamal K, Tapper E, Robson SC, Tsugawa Y. Low LDL-C and high HDL-C levels are associated with elevated serum transaminases amongst adults in the United States: a cross-sectional study. *PLoS One*. (2014) 9:e85366. doi: 10.1371/journal.pone.0085366

42. Ballantyne CM, Banach M, Mancini GBJ, Lepor NE, Hanselman JC, Zhao X, et al. Efficacy and safety of bempedoic acid added to ezetimibe in statin-intolerant patients with hypercholesterolemia: a randomized, placebo-controlled study. *Atherosclerosis*. (2018) 277:195–203. doi: 10.1016/j.atherosclerosis.2018.06.002

43. Shalev H, Kapelushnik J, Moser A, Knobler H, Tamary H. Hypocholesterolemia in chronic anemias with increased erythropoietic activity. *Am J Hematol*. (2007) 82:199–202. doi: 10.1002/ajh.20804

44. Yamori Y, Nara Y, Horie R, Ooshima A. Abnormal membrane characteristics of erythrocytes in rat models and men with predisposition to stroke. *Clin Exp Hypertens (1978)*. (1980) 2:1009–21. doi: 10.3109/10641968009037158

45. Rosenson RS, Lowe GD. Effects of lipids and lipoproteins on thrombosis and rheology. *Atherosclerosis*. (1998) 140:271–80. doi: 10.1016/S0021-9150(98)00144-0

46. Moir S, Chun TW, Fauci AS. Pathogenic mechanisms of HIV disease. *Annu Rev Pathol*. (2011) 6:223–48. doi: 10.1146/annurev-pathol-011110-130254

47. Deressa T, Damtie D, Workineh M, Genetu M, Melku M. Anemia and thrombocytopenia in the cohort of HIV-infected adults in Northwest Ethiopia: a facility-based cross-sectional study. *EJIFCC*. (2018) 29:36–47.

48. Woldeamanuel GG, Wondimu DH. Prevalence of thrombocytopenia before and after initiation of HAART among HIV infected patients at black lion specialized hospital, Addis Ababa, Ethiopia: a cross sectional study. *BMC Hematol*. (2018) 18:9. doi: 10.1186/s12878-018-0103-6

49. Levine AM, Karim R, Mack W, Gravink DJ, Anastos K, Young M, et al. Neutropenia in human immunodeficiency virus infection: data from the women's interagency HIV study. *Arch Intern Med*. (2006) 166:405–10. doi: 10.1001/archinte.166.4.405

50. Fan L, Li C, Zhao H. Prevalence and risk factors of cytopenia in HIV-infected patients before and after the initiation of HAART. *Biomed Res Int*. (2020) 2020:1–10. doi: 10.1155/2020/3132589

51. Jha V, Garcia-Garcia G, Iseki K, Li Z, Naicker S, Plattner B, et al. Chronic kidney disease: global dimension and perspectives. *Lancet*. (2013) 382:260–72. doi: 10.1016/S0140-6736(13)60687-X, Epub 2013 May 31. Erratum in: Lancet. 2013 Jul 20;382(9888):208

52. Tigabu A, Beyene Y, Getaneh T, Chekole B, Gebremaryam T, Sisay Chanie E, et al. Incidence and predictors of anemia among adults on HIV care at South Gondar zone public general hospital Northwest Ethiopia, 2020; retrospective cohort study. *PLoS One*. (2022) 17:e0259944. doi: 10.1371/journal.pone.0259944

53. Marks PW. Hematologic manifestations of liver disease. *Semin Hematol*. (2013) 50:216–21. doi: 10.1053/j.seminhematol.2013.06.003

54. Naranbhai V, Hill AV, Abdool Karim SS, Naidoo K, Abdool Karim Q, Warimwe GM, et al. Ratio of monocytes to lymphocytes in peripheral blood identifies adults at risk of incident tuberculosis among HIV-infected adults initiating antiretroviral therapy. *J Infect Dis*. (2014) 209:500–9. doi: 10.1093/infdis/jit494

frontiers | Frontiers in Medicine

TYPE Case Report
PUBLISHED 07 August 2023
DOI 10.3389/fmed.2023.1209174

OPEN ACCESS

EDITED BY
Pierpaolo di Micco,
Ospedale Santa Maria delle Grazie, Italy

REVIEWED BY
Bicky Thapa,
Medical College of Wisconsin, United States
Carmen Silvia Valente Barbas,
University of São Paulo, Brazil

*CORRESPONDENCE
Jing Wang
✉ wjeshospital@163.com

†These authors have contributed equally to this work and share first authorship

RECEIVED 20 April 2023
ACCEPTED 17 July 2023
PUBLISHED 07 August 2023

CITATION
Cao Y, Liu P, Song Q and Wang J (2023) Case report: A case of sepsis caused by rickettsial infection-induced hemophagocytic syndrome. *Front. Med.* 10:1209174.
doi: 10.3389/fmed.2023.1209174

Case report: A case of sepsis caused by rickettsial infection-induced hemophagocytic syndrome

Yanli Cao†, Peijun Liu†, Qiuling Song and Jing Wang*

Department of Respiratory and Critical Care Medicine, The Central Hospital of Enshi Tujia and Miao Autonomous Prefecture, Enshi, China

Hemophagocytic lymphohistiocytosis (HLH) is a rare histiocytic disorder characterized by reactive hyperplasia of the mononuclear phagocytic system, which is primarily caused by dysfunction of cytotoxic killer cells and natural killer cells, leading to antigen clearance barriers and the overactivation of the mononuclear phagocytic system due to continuous antigen stimulation. HLH encompasses a group of clinical syndromes marked by the overproduction of inflammatory cytokines. A 68-year-old Chinese man presented with persistent fever, chills, nausea, and vomiting; the patient had no history of any underlying conditions. Laboratory investigations revealed decreased levels of red blood cells, white blood cells, and platelets, along with reduced natural killer cell activity, increased CD25, hyperferritinemia, and the detection of Rickettsia DNA in his blood, meeting the diagnostic criteria of the Histiocyte Society HLH-2004 guidelines. The patient was treated with antibiotics, improving anemia, glucocorticoid therapy, and continuous renal replacement therapy (CRRT), temporarily improving his condition. However, the patient died after 2 years from chronic renal failure caused by septic shock.

KEYWORDS

Rickettsia, sepsis, multiple organ dysfunction, hemophagocytic syndrome, immune imbalance

Introduction

Rickettsiosis, a condition driven by transmission of intracellular gram-negative bacteria, is further categorized as spotted fever or typhus, generally resulting from arthropod infection in human populations (1, 2). Hemophagocytic lymphohistiocytosis (HLH), a rare and potentially fatal immune syndrome, is characterized by uncontrollable activation of cytotoxic lymphocytes and macrophages, leading to cytokine-mediated tissue damage and subsequent organ failure (3). Clinical and laboratory observations of HLH include fever, splenomegaly, organ failure, cytopenias, hypertriglyceridemia, hyperferritinemia, hemophagocytosis, and decreased NK cell activity (4, 5). Currently, HLH associated with rickettsial sepsis is an infrequent event. This article presents a unique case study for critical care and hematology specialists.

Case report

A 68-year-old Chinese male presented with a fever, with a temperature of up to 39.5°C, and continued to experience chills for more than 7 days. His red blood cell count (RBC), hemoglobin (Hgb), and platelet (Plt) count were all reduced (Table 1). He was admitted to the intensive care unit of Enshi Central Hospital in Hubei province. After the onset of the disease, the patient underwent antibiotic therapy at a local clinic, receiving a daily intravenous dose of 0.5 g levofloxacin for over 7 days. However, there was no significant improvement in the patient's condition. The patient was a farmer who lived in a karst mountain forest environment. Before this, he was in good health and had no other chronic diseases.

In the initial physical examination, the patient's body temperature was 36.3°C, pulse rate was 88 beats per minute, breathing rate was 18 breaths per minute, blood pressure was 100/60 mmHg, and both breathing and heart rate were regular. The patient exhibited a lean physique and a notably pale skin complexion while maintaining mental clarity. There was no rash or bleeding point all over his body. A scar of size 0.50*0.5 cm^2 was visible in the lower right abdomen, but there were no other apparent abnormalities.

Preliminary laboratory examination showed a significant decrease in white blood cells, lymphocytes, monocytes, red blood cells, hematocrit, platelets, and platelet volume. The neutrophil ratio was increased. Serum levels of alanine aminotransferase (ALT), aspartate aminotransferase (AST), alkaline phosphatase (ALP), lactate dehydrogenase (LDH), C-reactive protein (CRP), and procalcitonin (PCT) were significantly elevated. In addition, prothrombin time (PT) was increased, and D-dimer levels and fibrinogen degradation products (FDPs) were elevated (Table 1). All tests for viral respiratory pathogens, typical nuclear antibody spectrum, human immunodeficiency virus, and syphilis were negative. The patient was subjected to three distinct blood cell culture analyses, and all conclusively reported negative results. Concurrently, serological testing for antibodies associated with the Epstein–Barr Virus (EBV) and the Cytomegalovirus (CMV) was conducted, revealing negative outcomes. The nasal swab tested negative for the presence of COVID-19 RNA. Ferritin levels were extremely high, and the patient tested positive for hepatitis B virus antigen. Natural killer cell activity was 3.75%, and the activity was decreased. All inflammation markers associated with HLH were elevated, including CD25 (3,644 U/ml), ferritin (above 1,500 ng/ml, reference range: 23.9∼336.2 ng/ml), interleukin-6 (6.49 pg/L), and TNF-1(19 fmol/ml). Through high-throughput gene detection (NGS) of blood PMseq-DNA, we identified hepatitis B virus (HBV) and rickettsia presence in the samples (Supplementary Table S1, Supplementary Figure S1). The results of the HBV DNA were $9.35*10^4$ IU/ml. A regimen of 0.25 mg/day entecavir was used to treat patients with chronic hepatitis B.

The patient has a 0.5 × 0.5 cm^2 scar on his lower right abdomen, caused by a mosquito bite that occurred more than 10 days before hospital admission (Figure 1). The patient underwent cardiac and abdominal ultrasound imaging, which indicated right heart enlargement—the right atrium and ventricle transverse diameters were 5.1 cm and 4.8 cm, respectively. The left ventricular ejection fraction was 71%, and the left ventricle's short-axis fractional shortening was 40%. The liver was unremarkable, with clear intrahepatic vasculature. The spleen was normal, measuring 3.7 cm in thickness, with a smooth capsule and no splenic vein dilation. The renal parenchyma of both kidneys exhibited increased echogenicity, accompanied by the presence of small cysts. A chest CT scan revealed two inflammatory lung lesions and mild interstitial pulmonary edema (Figure 2A). Additionally, bilateral pleural effusion, lower pulmonary partial atelectasis, and bilateral pleural thickening were observed (Figure 2B). Aortic thickening was also observed, and some fluid was present in the pericardial cavity (Figure 2C). A peripheral blood smear was performed on the patient. The findings revealed that the white blood cell classification ratio and morphology were predominantly standard. There was variation in the size of red blood cells. Platelet distribution appeared satisfactory, and no blood parasites were observed (Supplementary Figure S2). The bone marrow puncture revealed significantly active proliferation of bone marrow nucleated cells, accompanied by erythrocyte hyperplasia and erythrocyte phagocytosis (Figure 3A). Most of the cells were granulomatous macrophages, and scattered platelet phagocytosis was also observed (Figure 3B). Granulocyte hyperplasia was characterized by immature neutrophils and band-shaped neutrophils (Figure 3C).

The patient presented with a diagnosis of HLH and multiple organ dysfunction syndrome (MODS), as he fulfilled seven out of the eight diagnostic criteria for HLH-2004 (6). These criteria include fever, peripheral blood cytopenia affecting at least three lineages, hypertriglyceridemia, the presence of hemophagocytic cells in the bone marrow without malignancy, decreased natural killer (NK) cell activity, hyperferritinemia, and CD25 levels above 2,400 U/ml. Furthermore, PMseq-DNA test results indicated the presence of septic shock caused by Rickettsia infection, a secondary complication of multiple organ dysfunction. Treatment consisted of fluid rehydration, blood transfusion, combination therapy with meropenem and minocycline, anti-inflammatory therapy with methylprednisolone sodium succinate, several sessions of renal replacement therapy (CRRT), and other supportive measures. The patient's condition improved over time, with the resolution of fever, and ultimately, he was discharged from the hospital.

Discussion

The significance of HLH is particularly relevant in the pediatric setting, with adult mortality rates ranging between 20 and 88% (7). HLH is typically classified into two types: (1) primary or familial HLH and (2) secondary HLH (8). It is a potentially fatal illness commonly precipitated by infection, autoimmune disorders, or malignancy (9). In clinical terms, HLH shares similarities with bacterial sepsis or systemic inflammatory response syndrome, with inflammatory overactivity and pathophysiological characteristics closely related to septic shock. Furthermore, clinical and laboratory features of septic shock are indistinguishable (10, 11).

The patient had septic shock, characterized by microbial infection causing fever, leukocyte imbalances, and multiple organ dysfunction syndrome (MODS) (12). He presented with persistent high fever, liver and kidney insufficiency, and effusion in multiple serous cavities. The lack of adequate circulating blood volume

TABLE 1 Laboratory result at admission.

Project	On admission	Before discharge	Reference range
White blood cell	2.39×10^9/L	3.31×10^9/L	4∼10 × 109/L
Neutrophil percentage	87.60%	48.90%	50∼70%
Lymphocyte	0.18×10^9/L	1.19×10^9/L	1∼4 × 109/L
Monocyte	0.11×10^9/L	0.4×10^9/L	$0.26∼0.8 \times 10^9$/L
Red blood cell	1.91×10^{12}/L	2.60×10^9/L	$4∼5.5 \times 10^9$/L
Hemoglobin	58 g/L	79 g/L	120∼160 g/L
Hematocrit	0.184	0.248	0.41∼0.49
Platelet	37×10^9/L	84×10^9/L	$90∼300 \times 10^9$/L
ALT	112 U/L	30 U/L	5∼40 U/L
AST	126 U/L	32 U/L	5∼40 U/L
Total bilirubin	9.5 umol/L	20 umol/L	2∼20 umol/L
Total protein	52.98 g/L	61.50 g/L	60∼82 g/L
Albumin	27.39 g/L	35.51 g/L	33∼48 g/L
Globulin	25.59 g/L	25.99 g/L	18∼35 g/L
Lactic dehydrogenase	332 U/L	155 U/L	109∼240 U/L
Procalcitonin	58.05 ng/ml	0.36 ng/ml	0∼0.5 ng/ml
C-reactive protein	122.81 mg/L	6.27 mg/L	0∼8 mg/L
Triglyceride	2.05 mmol/L	1.83 mmol/L	0.45∼1.7 mmol/L
Prothrombin time	12.2 s	13.0 s	9.4∼12.5 s
D-dimer levels	5.613 ug/ml	1.824 ug/ml	0∼0.243 ug/ml
FDP	30.896 ug/ml	14.542 ug/ml	0∼2.01 ug/ml
Fibrinogen	3.17 g/L	2.52 g/L	2.38∼4.98 g/L

was believed to cause MODS. Proper fluid management is crucial for resuscitation, as positive water balance is linked to more extensive organ failure and mortality (13). Our investigation revealed that the sepsis was caused by rickettsial infection, an intracellular, specialized gram-negative bacterium that can infect humans through arthropods such as ticks (14). A study by P. Aarthi et al. utilizing PCR-based DNA sequencing found that rickettsial infection could lead to neonatal sepsis (15). Tick-borne infections can cause a range of afflictions, including Rocky Mountain spotted fever, a severe tick-borne illness capable of inducing adult respiratory distress syndrome, septic shock, and myocarditis. Symptoms include elevated cardiac enzyme levels and declining myocardial function. However, the condition usually improves with antibiotic treatment (16).

A few reports of rickettsial infection causing hemophagocytic syndrome exist, though this condition occurs more frequently in children with an incomplete immune system (17, 18). The patient's condition must be distinguished from disorders such as thrombotic thrombocytopenic purpura (TTP) and hemolytic uremic syndrome (HUS). TTP is a rare thrombotic microvascular disease characterized by microvascular pathogenic hemolytic anemia (19). The patient had a trilineage decrease in red blood cells, white blood cells, and platelets. Significantly, there was no evidence of bleeding or clot development anywhere on the patient's body, prompting us to consider ruling out TTP from the differential diagnosis. HUS, predominantly observed in children, presents as a clinical triad of thrombocytopenia, anemia, and acute kidney injury. It is frequently associated with an *E. coli* infection (20). The patient did not exhibit symptoms such as diarrhea; thus, an intestinal disorder was not suspected. Considering the medical history, we can rule out the possibility of HUS. Despite the patient's slight rise in HBV DNA levels, an abdominal color Doppler ultrasonography scan clearly ruled out liver cirrhosis and liver injury. As a consequence, we ruled out the possibility of hepatitis B-related HLH.

Rickettsial infection is a zoonotic disease that is transmitted by arthropods. In this case, the patient resides in the mountains where arthropods are abundant. The diagnostic method for Rickettsia typically involves a combination of polymerase chain reaction (qPCR) and immunofluorescence detection. If collected early during the infection, specimens may not contain antibodies, but the probability of positive PCR increases (21). Rickettsial infection is usually treated with potent antibiotics such as doxycycline or minocycline. However, tigecycline has also been reported to treat Rickettsial meningitis since it increases drug concentrations in the blood (22). HLH is vulnerable to life-threatening complications such as multiple organ

FIGURE 1
Scar from a tick bite on the patient's lower right abdomen.

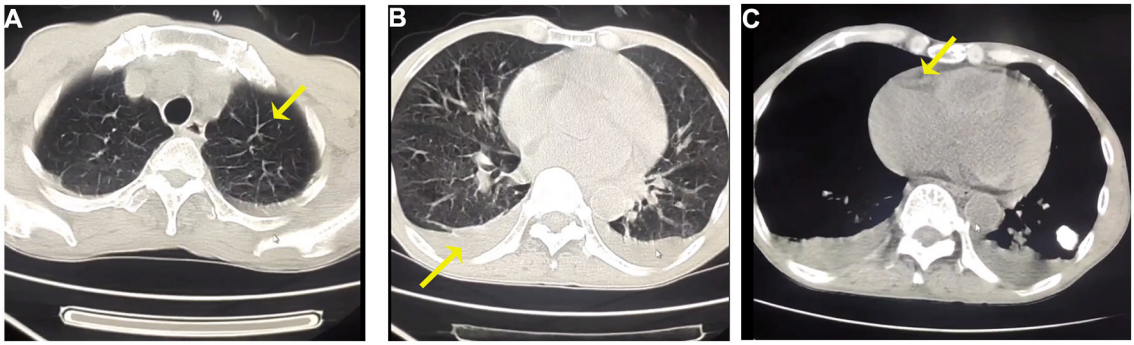

FIGURE 2
(A) Representative CT images of interlobular septal thickening at chest CT scan of both upper lungs. **(B)** Bilateral pleural effusions in the lower lungs. **(C)** The mediastinal window of the chest CT reveals a small amount of pericardial effusion.

dysfunction syndrome (MODS) and disseminated intravascular coagulation (23). Immediate identification and intervention are crucial for improving patient prognosis. Treatment options for this condition vary, including immunosuppressive agents, cytotoxic chemotherapy, and hematopoietic stem cell transplantation (24).

Initially, we planned to provide chemotherapy to the patient after his condition had improved, but he declined and left the hospital. Following his discharge, we conducted numerous follow-ups and discovered that the patient had fever for 2 years. However, his kidney function and mild anemia remained problematic. Sadly, the patient died 2 years later due to persistent kidney failure.

Conclusion

HLH is a rare yet potentially fatal disorder requiring high suspicion for prompt diagnosis and management. In the initial phases of secondary HLH, precise management of anti-infectives, shock prevention, and continuous renal replacement therapy have demonstrated positive effects of

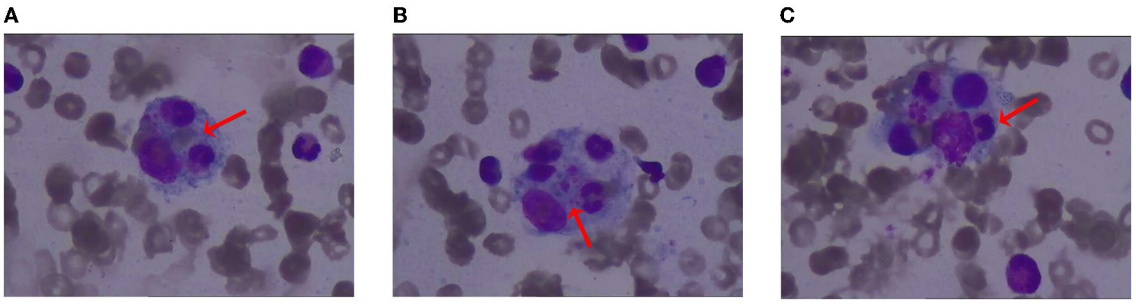

FIGURE 3
Illustration of bone marrow staining. **(A)** Erythrocyte phagocytosis; **(B)** platelet phagocytosis; **(C)** granulocyte phagocytosis.

patient treatment. Unfortunately, limited access to treatment options due to financial constraints and concerns over potential side effects of subsequent drug therapies often deter patients from seeking further medical interventions. Despite refusing additional treatment, the patient exhibited prolonged survival.

Data availability statement

The original contributions presented in the study are included in the article/Supplementary material, further inquiries can be directed to the corresponding author.

Ethics statement

The studies involving human participants were reviewed and approved by Ethics Committee of Enshi Tujia and Miao Autonomous Prefecture Central Hospital. The patients/participants provided their written informed consent to participate in this study. Written informed consent was obtained from the individual(s) for the publication of any potentially identifiable images or data included in this article.

Author contributions

YC contributed to the case collection, documentation, and writing of the manuscript. PL conducted extensive literature reviews and analysis of case studies. QS participated in image interpretation. JW contributed to the design aspect of the research and provided editorial support for the manuscript. All authors contributed to the article and approved the submitted version.

Acknowledgments

The authors thank the patient's family for approving this publication.

Conflict of interest

The authors declare that the research was conducted in the absence of any commercial or financial relationships that could be construed as a potential conflict of interest.

Publisher's note

All claims expressed in this article are solely those of the authors and do not necessarily represent those of their affiliated organizations, or those of the publisher, the editors and the reviewers. Any product that may be evaluated in this article, or claim that may be made by its manufacturer, is not guaranteed or endorsed by the publisher.

Supplementary material

The Supplementary Material for this article can be found online at: https://www.frontiersin.org/articles/10.3389/fmed.2023.1209174/full#supplementary-material

References

1. Stewart AG, Stewart AGA. An update on the laboratory diagnosis of rickettsia spp. *Infection Pathogens.* (2021) 10:1319. doi: 10.3390/pathogens10101319

2. Aita T, Sando E, Katoh S, Hamaguchi S, Fujita H, Kurita N. Serological cross-reactivity between spotted fever and typhus groups of rickettsia infection in Japan. *Int J Infect Dis.* (2023) 130:178–81. doi: 10.1016/j.ijid.2023.03.012

3. Griffin G, Shenoi S, Hughes GC. Hemophagocytic lymphohistiocytosis: an update on pathogenesis, diagnosis, and therapy. *Best Pract Res Clin Rheumatol.* (2020) 34:101515. doi: 10.1016/j.berh.2020.101515

4. Al-Samkari H, Berliner N. Hemophagocytic lymphohistiocytosis. *Annu Rev Pathol.* (2018) 13:27–49. doi: 10.1146/annurev-pathol-020117-043625

5. Ponnatt TS, Lilley CM, Mirza KM. Hemophagocytic lymphohistiocytosis. *Arch Pathol Lab Med.* (2022) 146:507–19. doi: 10.5858/arpa.2020-0802-RA

6. Henter JI, Horne A, Aricó M, Egeler RM, Filipovich AH, Imashuku S, et al. HLH-2004: diagnostic and therapeutic guidelines for hemophagocytic lymphohistiocytosis. *Pediatr Blood Cancer.* (2007) 48:124–31. doi: 10.1002/pbc.21039

7. Hayden A, Park S, Giustini D, Lee AY, Chen LY. Hemophagocytic syndromes (HPSs) including hemophagocytic lymphohistiocytosis (HLH) in adults: a systematic scoping review. *Blood Rev.* (2016) 30:411–20. doi: 10.1016/j.blre.2016.05.001

8. Esteban YM, de Jong JLO, Tesher MS. An overview of hemophagocytic lymphohistiocytosis. *Pediatr Ann.* (2017) 46:e309–13. doi: 10.3928/19382359-20170717-01

9. Bhatt NS, Oshrine B, An Talano J. Hemophagocytic lymphohistiocytosis in adults. *Leuk Lymphoma.* (2019) 60:19–28. doi: 10.1080/10428194.2018.1482543

10. Raschke RA, Garcia-Orr R. Hemophagocytic lymphohistiocytosis: a potentially underrecognized association with systemic inflammatory response syndrome, severe sepsis, and septic shock in adults. *Chest.* (2011) 140:933–8. doi: 10.1378/chest.11-0619

11. Castillo L, Carcillo J. Secondary hemophagocytic lymphohistiocytosis and severe sepsis/ systemic inflammatory response syndrome/multiorgan dysfunction syndrome/macrophage activation syndrome share common intermediate phenotypes on a spectrum of inflammation. *Pediatr Crit Care Med.* (2009) 10:387–92. doi: 10.1097/PCC.0b013e3181a1ae08

12. Hotchkiss RS, Moldawer LL, Opal SM, Reinhart K, Turnbull IR, Vincent JL. Sepsis and septic shock. *Nat Rev Dis Primers.* (2016) 2:16045. doi: 10.1038/nrdp.2016.45

13. Daulasim A, Vieillard-Baron A, Geri G. Hemodynamic clinical phenotyping in septic shock. *Curr Opin Crit Care.* (2021) 27:290–7. doi: 10.1097/MCC.0000000000000834

14. Zhang X, Geng J, Du J, Wang Y, Qian W, Zheng A, et al. Molecular identification of rickettsia species in haemaphysalis ticks collected from Southwest China. *Vector Borne Zoonotic Dis.* (2018) 18:663–8. doi: 10.1089/vbz.2017.2231

15. Aarthi P, Bagyalakshmi R, Mohan KR, Krishna M, Nitin M, Madhavan HN, et al. First case series of emerging rickettsial neonatal sepsis identified by polymerase chain reaction-based deoxyribonucleic acid sequencing. *Indian J Med Microbiol.* (2013) 31:343–8. doi: 10.4103/0255-0857.118874

16. Kushawaha A, Brown M, Martin I, Evenhuis W. Hitch-hiker taken for a ride: an unusual cause of myocarditis, septic shock and adult respiratory distress syndrome. *BMJ Case Rep.* (2013) 2013:bcr2012007155. doi: 10.1136/bcr-2012-007155

17. Jin YM, Liang DS, Huang AR, Zhou AH. Clinical characteristics and effective treatments of scrub typhus-associated hemophagocytic lymphohistiocytosis in children. *J Adv Res.* (2019) 15:111–6. doi: 10.1016/j.jare.2018.05.007

18. Cascio A, Pernice LM, Barberi G, Delfino D, Biondo C, Beninati C, et al. Secondary hemophagocytic lymphohistiocytosis in zoonoses. A systematic review. *Eur Rev Med Pharmacol Sci.* (2012) 16:1324–37.

19. Sukumar S, Lämmle B, Cataland SR. Thrombotic thrombocytopenic purpura: pathophysiology, diagnosis, and management. *J Clin Med.* (2021) 10:536. doi: 10.3390/jcm10030536

20. Cody EM, Dixon BP. Hemolytic uremic syndrome. *Pediatr Clin North Am.* (2019) 66:235–46. doi: 10.1016/j.pcl.2018.09.011

21. Robinson MT, Satjanadumrong J, Hughes T, Stenos J, Blacksell SD. diagnosis of spotted fever group rickettsia infections: the Asian perspective. *Epidemiol. Infect.* (2019) 147:e286. doi: 10.1017/S0950268819001390

22. Mastroianni A, Greco S, Urso F, Mauro MV, Vangeli V. Does tigecycline have a place in therapy for rickettsial infection of the central nervous system? *Infect Chemother.* (2022) 54:165–172. doi: 10.3947/ic.2021.0070

23. Morimoto A, Nakazawa Y, Ishii E. Hemophagocytic lymphohistiocytosis: pathogenesis, diagnosis, and management. *Pediatr. Int.* (2016) 58:817–25. doi: 10.1111/ped.13064

24. Rivière S, Galicier L, Coppo P, Marzac C, Aumont C, Lambotte O, et al. Reactive hemophagocytic syndrome in adults: a retrospective analysis of 162 patients. *Am. J. Med.* (2014) 127: 1118–25. doi: 10.1016/j.amjmed.2014.04.034

frontiers | Frontiers in Medicine

TYPE Case Report
PUBLISHED 05 October 2023
DOI 10.3389/fmed.2023.1265594

OPEN ACCESS

EDITED BY
Tomás José Gonzalez López,
Burgos University Hospital, Spain

REVIEWED BY
Masaki Fujita,
Fukuoka University, Japan
Jesús Navas,
University of Cantabria, Spain

*CORRESPONDENCE
Yan Yu
✉ hn-yuyan@kingmed.com.cn
Honglian Song
✉ 107541888@qq.com

RECEIVED 23 July 2023
ACCEPTED 15 September 2023
PUBLISHED 05 October 2023

CITATION
Ge H, Liang XW, Lu QR, He AX, Zhong PW, Liu J, Yu Y and Song HL (2023) Case report: Intraabdominal infection of *Mycobacterium syngnathidarum* in an immunocompetent patient confirmed by whole-genome sequencing. *Front. Med.* 10:1265594. doi: 10.3389/fmed.2023.1265594

Case report: Intraabdominal infection of *Mycobacterium syngnathidarum* in an immunocompetent patient confirmed by whole-genome sequencing

Hu Ge[1], Xiongwei Liang[1], Qiuran Lu[1], Aixiang He[2], Peiwen Zhong[3], Jun Liu[3], Yan Yu[1]*and Honglian Song[2]*

[1]Changsha KingMed Center for Clinical Laboratory, Changsha, Hunan, China, [2]Rucheng County People's Hospital, Rucheng, Hunan, China, [3]Guangzhou KingCreate Biotechnology Company Limited, Guangzhou, Guangdong, China

Background: The taxonomic group of non-tuberculous mycobacteria (NTM) encompasses more than 190 species and subspecies, some of which can cause pulmonary and extrapulmonary diseases across various age groups in humans. However, different subspecies exhibit differential drug sensitivities, and traditional detection techniques struggle to accurately classify NTM. Therefore, clinicians need more effective detection methods to identify NTM subtypes, thus providing personalized medication for patients.

Case presentation: We present the case of a 47-year-old female patient diagnosed with an intraabdominal infection caused by *Mycobacterium syngnathidarum*. Despite computed tomography of the chest suggesting potential tuberculosis, tuberculosis infection was ruled out due to negative TB-DNA results for ascites fluid and sputum and limited improvement of lung lesions after treatment. Additionally, acid-fast staining and Lowenstein–Jensen culture results revealed the presence of mycobacterium in ascites fluid. Subsequent whole-genome sequencing (WGS) confirmed the DNA sequences of *Mycobacterium syngnathidarum* in colonies isolated from the ascites fluid, which was further corroborated by polymerase chain reaction and Sanger sequencing. Ultimately, the patient achieved a complete recovery following the treatment regimen targeting *Mycobacterium syngnathidarum*, which involved clarithromycin, ethambutol hydrochloride, pyrazinamide, rifampicin, and isoniazid.

Conclusion: This is the first reported case of *Mycobacterium syngnathidarum* infection in humans. *Mycobacterium syngnathidarum* was detected by WGS in this case, suggesting that WGS may serve as a high-resolution assay for the diagnosis of different subtypes of mycobacterium infection.

KEYWORDS

intraabdominal infection, *Mycobacterium syngnathidarum*, non-tuberculous mycobacteria, pathogen diagnosis, whole-genome sequencing

Introduction

Non-tuberculous mycobacteria (NTM) are ubiquitous in the environment, present in water, soil, and aerosols, and can cause infections in humans and aquatic animals (1–4). NTM represent more than 190 species that can be classified as slow-growers including *M. avium Complex* (MAC), *M. kansasii*, and *M. gordonae*, and fast-growers, such as *M. abscessus complex*, *M. fortuitum*, and *M. chelonae*, according to whether colonies formed within 7 days (5–11). Despite worldwide recognition of the increasing prevalence and morbidity associated with NTM infection, assays to identify the species of NTM are still lacking (12, 13).

Whole-genome sequencing (WGS) can directly identify the sequences of pathogens and has been applied to the diagnosis of clinical infectious diseases (14, 15). In this study, we report a case of intraabdominal infection in a 47-year-old woman who was negative for TB-DNA in ascites fluid, while the yellow-green bacteria that were similar to *Mycobacterium tuberculosis* grew in Lowenstein–Jensen medium on the 3rd day. At the same time, a large number of DNA sequences of *Mycobacterium syngnathidarum* were identified by WGS. Following a 3 months treatment regimen consisting of ethambutol hydrochloride, pyrazinamide, rifampicin, isoniazid, and clarithromycin, the patient's condition improved.

To date, only one case of *Mycobacterium syngnathidarum* cultured from a clinically ill fish of the family Syngnathidae has been reported in PubMed (16). As far as we know, the present case represents the first case of intraabdominal infection caused by *Mycobacterium syngnathidarum* in humans.

Case description

A previously healthy 47-year-old female patient presented to the Rucheng County People's Hospital's urology department on September 26, 2022 with abdominal pain for 21 days and aggravation for 1 day. The patient had a medical history of thyroiditis and hypertension, denied any history of infectious diseases such as tuberculosis, and had no history of blood transfusion, surgery, or trauma.

On admission, the patient's respiratory rate and body temperature were 20 /min and 36.5°C, respectively. Physical examination revealed a symmetrical and normal chest appearance with clear breath sounds in both lungs. However, the patient exhibited significant tenderness and rebound pain in the lower abdomen. The results of laboratory tests were as follows: The white blood cell (WBC) count was 11.65×10^9/L, the percentages of neutrophils and lymphocytes were 89.6 and 5.10%, respectively, the C-reactive protein level was 34.03 mg/L, and the hemoglobin was 107.00 g/L. Procalcitonin concentration (PCT) and erythrocyte sedimentation rate (ESR) were normal. Color Doppler ultrasound showed a large amount of fluid in the abdominal cavity and a 57 × 52 mm cystic dark in the left adnexal area. At the same time, computed tomography (CT) of the chest and abdomen demonstrated patchy high-density lesions in both lungs. A large amount of effusion was observed in the abdominal cavity and pelvic cavity, along with a low-density cystic lesion of approximately 4.5 × 4.9 cm in the left adnexal area, along with an unclear and disarranged structure in the right adnexal area (Figure 1). These results suggested pulmonary tuberculosis and intraabdominal infection.

On the same day, the patient underwent laparoscopic exploration. Intraoperatively, it was found that the pelvic cavity contained approximately 400 mL of clear grass yellow fluid. The peritoneum, pelvic walls, and intestinal walls exhibited scattered grayish-yellow nodules. Adhesions were present between the intestinal duct, peritoneum, and the bilateral adnexa of the uterus. The left adnexa and the uterine basin wall formed an enveloped cyst with grass-yellow fluid inside. The surgeon aspirated fluid from the patient's abdomen, separated the adhesions, aspirated fluid from the cyst, and excised the nodules in the greater omentum. Amoxicillin and clavulanate potassium tablets were given after the operation. Ascites fluid examination results were as follows: total protein, 55.81 g/L, glucose, 4.62 mmol/L, lactate dehydrogenase, 364.00 U/L, adenosine deaminase, 19 U/L, chlorine 100.3 mmol/L, and positive acid-fast staining. For further diagnosis of tuberculosis, ascites fluid was collected for Lowenstein–Jensen medium, acid-fast staining, and TB-DNA analysis, and sputum for Lowenstein–Jensen medium culture and acid-fast staining.

On the 2nd day, the histopathology of the greater omentum showed hyperplasia of fibrous tissue with chronic granulomatous inflammation, but acid-fast staining was negative (Figure 2). TB-DNA and acid-fast staining of the ascites fluid and sputum were negative. Based on the results from CT, pathology, and microscopic examination, the patient was diagnosed with tuberculous peritonitis and secondary tuberculosis, and anti-tuberculosis treatment was initiated with ethambutol hydrochloride, pyrazinamide, rifampicin, and isoniazid. On the 15th day, the patient's condition improved and she was discharged from the hospital. Anti-tuberculosis treatment continued, and regular review was recommended.

On 14th October, the presence of yellow-green bacteria similar to *Mycobacterium tuberculosis* was observed in the ascites fluid culture after 12 days of incubation in the Lowenstein–Jensen medium (Figure 3A). The acid-fast staining was positive (Figure 3B), and single colonies were successfully grown after 3–4 days of bacteria isolation on blood agar plates and Lowenstein–Jensen medium. To gain further insight, WGS was performed on the cultures on 19th October, and the sequences of *Mycobacterium syngnathidarum* (ANI = 99.4282) were identified (Figure 3C). To validate the result of WGS, targeted PCR was performed on the bacteria isolated from the Lowenstein–Jensen medium using a pair of primers: forward 5′-ATGAGCGG TTCGGTGATGTT-3′, reverse 5′-CTACTCGCCAAATTCGCAGC-3′, targeting the genome of *Mycobacterium syngnathidarum*. The primers were designed and verified using Primer-BLAST[1] based on the reference genome sequence of *Mycobacterium syngnathidarum* available in NCBI.[2] The capillary electrophoresis technique (Qsep 100™; Bioptic) and Sanger sequencing confirmed the presence of *Mycobacterium syngnathidarum* (Figure 3D). However, due to the lack of reported pathogenicity with *Mycobacterium syngnathidarum* and the patient's symptoms being alleviated after anti-tuberculosis treatment during hospitalization, no immediate adjustment to the treatment plan targeting *Mycobacterium syngnathidarum* was made.

1 https://www.ncbi.nlm.nih.gov/tools/primer-blast/

2 https://www.ncbi.nlm.nih.gov/

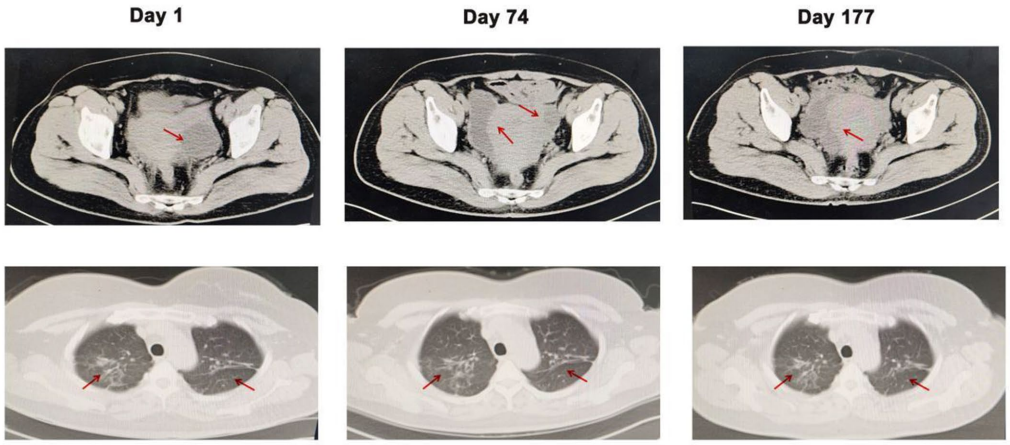

FIGURE 1
Computed tomography of the abdomen and chest on days 1, 74, and 177. Arrows indicate the lesions in the abdomen and lungs. Compared with the CT results on days 1 and 177, the low-density cystic lesion in the left adnexal area cavity disappeared, but patchy high-density lesions in both lungs did not improve.

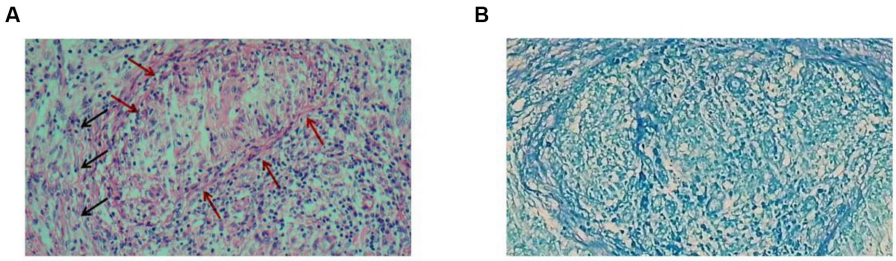

FIGURE 2
Histopathology of the nodular lesions on the greater omentum. **(A)** Hematoxylin–eosin staining shows hyperplasia of fibrous tissue (black arrows) with chronic granulomatous inflammation (red arrows). **(B)** Acid-fast staining was negative.

On 8th December, the patient came to the hospital for reexamination as scheduled, prompting a review of CT and Color Doppler ultrasound. Compared to the CT result on 26 September, the abdominal effusion and pelvic effusion were observed. The cystic lesion in the left adnexal area shrank, but the lesion on the right side was enlarged (Figure 1). Combined with the patient's symptoms and the previous results, the diagnosis of an intraabdominal infection caused by *Mycobacterium syngnathidarum* was made. Clarithromycin was added to the original treatment (ethambutol hydrochloride, pyrazinamide, rifampicin, and isoniazid) according to BacDive's guidance.[3] On March 21, 2023, the patient reported no abdominal discomfort and abdominal CT showed that the lesion in the left adnexal area disappeared (Figure 1). She continued eradication therapy for 6 months at home. In order to evaluate the sensitivity of *Mycobacterium syngnathidarum* to drugs, the drug susceptibility tests (Trek Diagnostic Systems Ltd., United Kingdom) of *Mycobacterium syngnathidarum* on August 29, 2023 showed that amikacin, ciprofloxacin, clarithromycin, doxycycline, linezolid, minocycline, and moxifloxacin were sensitive (Table 1).

Discussion and conclusion

NTM are ubiquitous and can survive in various environmental conditions, presenting challenges in their diagnosis and treatment (17, 18). However, clinical testing for drug susceptibility in NTM is lacking, and empiric therapy is not the best treatment according to the speed of NTM growth (19). Different strains of NTM have different susceptibilities to drugs, highlighting the importance of strain identification through molecular examination for devising appropriate treatment plans (19, 20). WGS aims to analyze the entire genome of a single bacterial colony, which provides better species identification than 16S RNA or other target genes (19, 21). In this study, we report the first case of intraabdominal infection caused by *Mycobacterium syngnathidarum* in humans.

Distinguishing between tuberculosis and non-tuberculosis infections remains a challenging aspect of clinical diagnosis. In this case, the patient presented with a 21 days history of lower abdominal pain, and

3 https://bacdive.dsmz.de/strain/158439

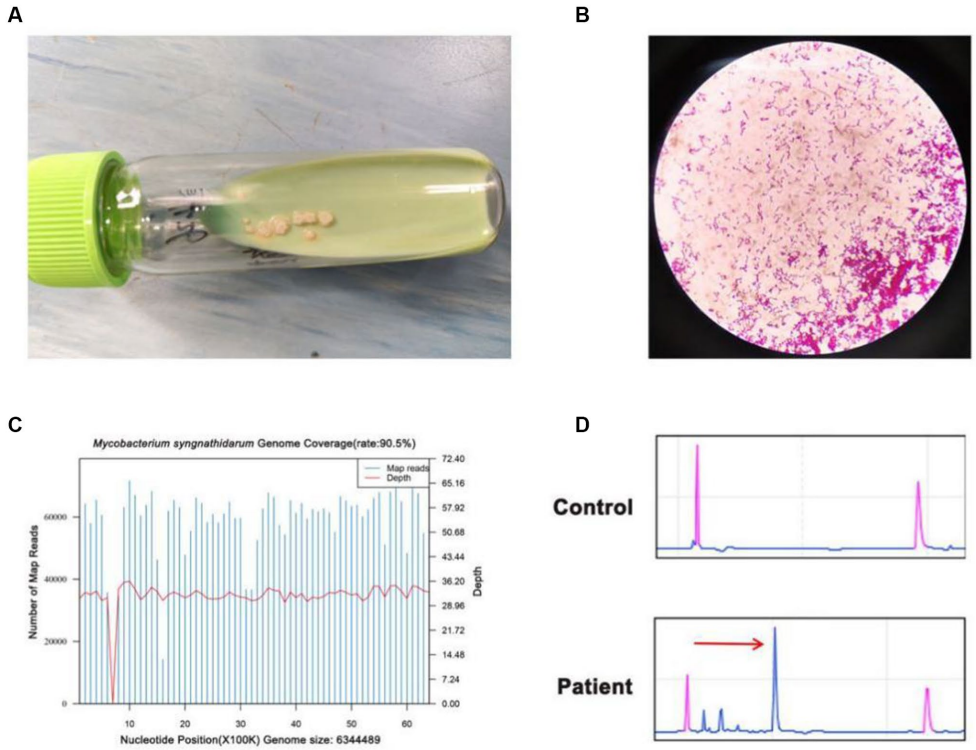

FIGURE 3
Identification of *Mycobacterium syngnathidarum* from the patient's ascites fluid. **(A)** *Mycobacterium tuberculosis* grew in the ascites fluid of Lowenstein–Jensen medium on the 12th day. **(B)** The acid-fast staining of *Mycobacterium syngnathidarum*. **(C)** The WGS result showed that the coverage of *Mycobacterium syngnathidarum* was 90.5%. **(D)** Polymerase chain reaction and the capillary electrophoresis technique confirmed the *Mycobacterium syngnathidarum* infection in the patient.

TABLE 1 **Drug susceptibility tests of *Mycobacterium syngnathidarum* by microtiter broth dilution method.**

Metabolite	Sensitivity (+/–)	MIC value
Amikacin	+	≤1 μg/mL
Cefoxitin	/	64 μg/mL
Ciprofloxacin	+	0.25 μg/mL
Clarithromycin	+	1 μg/mL
Doxycycline	+	0.25 μg/mL
Imipenem	/	16 μg/mL
Linezolid	+	8 μg/mL
Minocycline	+	1 μg/mL
Moxifloxacin	+	≤0.25 μg/mL
Tobramycin	–	8 μg/mL
Trimethoprim+Sulfamethoxazole	–	>8/152 μg/mL

Referring to the M24-A2 document of the Clinical and Laboratory Standards Institute (CLSI), the results were classified as sensitive (+), intermediate (/), and resistant (–). MIC stands for minimum inhibitory concentration.

the findings from abdomen computed tomography, acid-fast staining of ascites fluid, and histopathology of greater omental tubercles raised the possibility of tuberculosis infection. However, the identification of fast-growing *Mycobacterium syngnathidarum* through Lowenstein–Jensen medium, WGS, and targeted PCR, along with negative TB-DNA results in sputum and ascites fluid, indicated a potential intraabdominal infection caused by *Mycobacterium syngnathidarum*.

In this case, we first treated the patient with ethambutol hydrochloride, pyrazinamide, rifampicin, and isoniazid for anti-tuberculosis therapy. After 73 days, combined with the results of reexamination CT and Color Doppler ultrasound, *Mycobacterium syngnathidarum* was identified in ascites fluid by WGS and targeted PCR. Clarithromycin was added to the treatment for NTM. On March 21, 2023, the patient reported no abdominal discomfort and was advised to continue taking the medicine. It is worth noting that after 5 months of anti-TB treatment, the patient's pulmonary nodules did not change significantly. In addition, the patient had no symptoms of a respiratory infection or other evidence of etiology. At the same time, this study conducted drug susceptibility tests on *Mycobacterium syngnathidarum*, which further proved that the bacteria was sensitive to clarithromycin (Table 1). Ultimately, we concluded that the patient did not have a lung infection, but an intraabdominal infection caused by *Mycobacterium syngnathidarum*.

In conclusion, our study reports a patient with an intraabdominal infection caused by *Mycobacterium syngnathidarum* that was diagnosed using WGS. The patient showed successful recovery following treatment with clarithromycin, ethambutol hydrochloride, pyrazinamide, rifampicin, and isoniazid. WGS may be a high-resolution and sensitive assay for the diagnosis and surveillance of NTM infection.

Data availability statement

The original contributions presented in the study are included in the article/supplementary material, further inquiries can be directed to the corresponding authors.

Ethics statement

The studies involving humans were approved by Rucheng County People's Hospital ethics Association. The studies were conducted in accordance with the local legislation and institutional requirements. The participants provided their written informed consent to participate in this study. Written informed consent was obtained from the individual(s) for the publication of any potentially identifiable images or data included in this article.

Author contributions

HG: Writing – original draft, Writing – review & editing, Conceptualization, Data curation, Formal analysis, Investigation, Methodology, Software. XWL: Methodology, Writing – original draft. QRL: Conceptualization, Investigation, Writing – original draft. AXH: Conceptualization, Investigation, Software, Writing – original draft. PWZ: Data curation, Methodology, Writing – original draft. JL: Formal analysis, Visualization, Writing – original draft. YY: Conceptualization, Investigation, Software, Writing – review & editing. HLS: Conceptualization, Data curation, Formal analysis, Investigation, Methodology, Writing – review & editing.

Funding

The author(s) declare that no financial support was received for the research, authorship, and/or publication of this article.

Acknowledgments

The authors acknowledge the contributions of the staff at Changsha KingMed Center for Clinical Laboratory and colleagues at Rucheng County People's Hospital.

Conflict of interest

PWZ and JL were employed by Guangzhou KingCreate Biotechnology Company Limited.

The remaining authors declare that the research was conducted in the absence of any commercial or financial relationships that could be construed as a potential conflict of interest.

Publisher's note

References

1. Hill E, Wooten D. A patient with Mycobacteremia due to two different nontuberculous mycobacteria. *Open Forum Infect Dis*. (2022) 9:ofac519. doi: 10.1093/ofid/ofac519

2. Falkinham JO 3rd. Nontuberculous mycobacteria in the environment. *Clin Chest Med*. (2002) 23:529–51. doi: 10.1016/s0272-5231(02)00014-x

3. Zhang L, Li Y, Yang H, Mu Y, Jiang J, Duan X. *Mycobacterium chelonae* infection after a cat bite: a rare case report. *Clin Cosmet Investig Dermatol*. (2022) 15:1847–51. doi: 10.2147/CCID.S375826

4. Johnson MG, Stout JE. Twenty-eight cases of *Mycobacterium marinum* infection: retrospective case series and literature review. *Infection*. (2015) 43:655–62. doi: 10.1007/s15010-015-0776-8

5. Daley CL, Iaccarino JM, Lange C, Cambau E, Wallace RJ Jr, Andrejak C, et al. Treatment of nontuberculous mycobacterial pulmonary disease: an official ATS/ERS/ESCMID/IDSA clinical practice guideline. *Eur Respir J*. (2020) 56:2000535. doi: 10.1183/13993003.00535-2020

6. Alemayehu A, Kebede A, Neway S, Tesfaye E, Zerihun B, Getu M, et al. A glimpse into the genotype and clinical importance of non tuberculous mycobacteria among pulmonary tuberculosis patients: the case of Ethiopia. *PLoS One*. (2022) 17:e0275159. doi: 10.1371/journal.pone.0275159

7. Fraga K, Maireles M, Jordan M, Soldevila L, Murillo O. *Mycobacterium fortuitum* osteomyelitis of the cuboid bone treated with CERAMENT G and V: a case report. *J Bone Jt Infect*. (2022) 7:163–7. doi: 10.5194/jbji-7-163-2022

8. Go D, Lee J, Choi JA, Cho SN, Kim SH, Son SH, et al. Reactive oxygen species-mediated endoplasmic reticulum stress response induces apoptosis of *Mycobacterium avium*-infected macrophages by activating regulated IRE1-dependent decay pathway. *Cell Microbiol*. (2019) 21:e13094. doi: 10.1111/cmi.13094

9. Guo Y, Cao Y, Liu H, Yang J, Wang W, Wang B, et al. Clinical and microbiological characteristics of *Mycobacterium kansasii* pulmonary infections in China. *Microbiol Spectr*. (2022) 10:e0147521. doi: 10.1128/spectrum.01475-21

10. Niitsu T, Kuge T, Fukushima K, Matsumoto Y, Abe Y, Okamoto M, et al. Pleural effusion caused by *Mycolicibacterium mageritense* in an immunocompetent host: a case report. *Front Med (Lausanne)*. (2021) 8:797171. doi: 10.3389/fmed.2021.797171

11. Abdelaal HFM, Chan ED, Young L, Baldwin SL, Coler RN. *Mycobacterium abscessus*: it's complex. *Microorganisms*. (2022) 10:1454. doi: 10.3390/microorganisms10071454

12. Winthrop KL, McNelley E, Kendall B, Marshall-Olson A, Morris C, Cassidy M, et al. Pulmonary nontuberculous mycobacterial disease prevalence and clinical features: an emerging public health disease. *Am J Respir Crit Care Med*. (2010) 182:977–82. doi: 10.1164/rccm.201003-0503OC

13. Zhu YN, Xie JQ, He XW, Peng B, Wang CC, Zhang GJ, et al. Prevalence and clinical characteristics of nontuberculous mycobacteria in patients with bronchiectasis: a systematic review and Meta-analysis. *Respiration*. (2021) 100:1218–29. doi: 10.1159/000518328

14. Satta G, Lipman M, Smith GP, Arnold C, Kon OM, McHugh TD. *Mycobacterium tuberculosis* and whole-genome sequencing: how close are we to unleashing its full potential? *Clin Microbiol Infect*. (2018) 24:604–9. doi: 10.1016/j.cmi.2017.10.030

15. Brown AC. Whole-genome sequencing of *Mycobacterium tuberculosis* directly from sputum samples. *Methods Mol Biol*. (2021) 2314:459–80. doi: 10.1007/978-1-0716-1460-0_20

16. Fogelson SB, Camus AC, Lorenz W, Phillips A, Bartlett P, Sanchez S. *Mycobacterium syngnathidarum sp. nov.*, a rapidly growing mycobacterium identified in syngnathid fish. *Int J Syst Evol Microbiol*. (2018) 68:3696–700. doi: 10.1099/ijsem.0.002978

17. Prasla Z, Sutliff RL, Sadikot RT. Macrophage signaling pathways in pulmonary nontuberculous mycobacteria infections. *Am J Respir Cell Mol Biol*. (2020) 63:144–51. doi: 10.1165/rcmb.2019-0241TR

18. Zhu Y, Hua W, Liu Z, Zhang M, Wang X, Wu B, et al. Identification and characterization of nontuberculous mycobacteria isolated from suspected pulmonary tuberculosis patients in eastern China from 2009 to 2019 using an identification array system. *Braz J Infect Dis*. (2022) 26:102346. doi: 10.1016/j.bjid.2022.102346

19. Daley CL, Iaccarino JM, Lange C, Cambau E, Wallace RJ, Andrejak C, et al. Treatment of nontuberculous mycobacterial pulmonary disease: an official ATS/ERS/ESCMID/IDSA clinical practice guideline. *Clin Infect Dis*. (2020) 71:905–13. doi: 10.1093/cid/ciaa1125

20. Saxena S, Spaink HP, Forn-Cuní G. Drug resistance in nontuberculous mycobacteria: mechanisms and models. *Biology (Basel)*. (2021) 10:96. doi: 10.3390/biology10020096

21. Purushothaman S, Meola M, Egli A. Combination of whole genome sequencing and metagenomics for microbiological diagnostics. *Int J Mol Sci*. (2022) 23:9834. doi: 10.3390/ijms23179834

frontiers | Frontiers in Medicine

TYPE Original Research
PUBLISHED 06 November 2023
DOI 10.3389/fmed.2023.1265568

OPEN ACCESS

EDITED BY
Pierpaolo di Micco,
Ospedale Santa Maria delle Grazie, Italy

REVIEWED BY
Olga Scudiero,
University of Naples Federico II, Italy
Mamtha Balla,
ProMedica Toledo Hospital, United States

*CORRESPONDENCE
Ali Ghasemi
✉ a.qasemi2012@yahoo.com;
✉ a.ghasemi@semums.ac.ir

RECEIVED 23 July 2023
ACCEPTED 28 August 2023
PUBLISHED 06 November 2023

CITATION
Ghaffari K, Rad MA, Moradi Hasan-Abad A, Khosravi M, Benvidi A, Iraji M, Khargh HAH and Ghasemi A (2023) Association of the human platelet antigens polymorphisms with platelet count in patients with COVID-19.
Front. Med. 10:1265568.
doi: 10.3389/fmed.2023.1265568

Association of the human platelet antigens polymorphisms with platelet count in patients with COVID-19

Kazem Ghaffari [1,2], Mahsa Ashrafi Rad[3], Amin Moradi Hasan-Abad[4], Mersedeh Khosravi [5], Arefeh Benvidi [5], Mahsa Iraji[5], Heidar Ali Heidari Khargh[5] and Ali Ghasemi [3,6]*

[1]Student Research Committee, Khomein University of Medical Sciences, Khomein, Iran, [2]Department of Laboratory Sciences, Khomein University of Medical Sciences, Khomein, Iran, [3]Department of Biochemistry and Hematology, Faculty of Medicine, Semnan University of Medical Sciences, Semnan, Iran, [4]Autoimmune Diseases Research Center, Shahid Beheshti Hospital, Kashan University of Medical Sciences, Kashan, Iran, [5]Department of Biochemistry, Semnan University of Medical Sciences, Semnan, Iran, [6]Cancer Research Center, Semnan University of Medical Sciences, Semnan, Iran

Polymorphism in human platelet antigen (HPA)-1 and HPA-3 (GPIIb/IIIa), HPA-2 (GPIb/IX), HPA-4 (GPIIIa), HPA-5 (GPIa/IIa), & HPA-15 (CD109) was investigated in 86 COVID-19-infected patients with thrombocytopenia (Group A) and 136 COVID-19-infected patients without thrombocytopenia (Group B). HPA genotyping was done by the sequence-specific primers PCR method. Lower HPA-3a and higher HPA-3b (P = 0.028) allele frequencies were seen in Group A than in Group B, and homozygosity for HPA 3b (P = 0.038) alleles was more prevalent in Group A than in Group B. The allele and genotype distributions of the other HPA polymorphic variants were similar between the two groups. Univariate analysis identified the CCGGGC (P = 0.016) combined genotype to be negatively associated & the TCGGGC (P = 0.003) and CCGGGC (P = 0.003) to be positively associated with thrombocytopenia. The frequency of anti-HPA-1a and anti-HPA-3a antibodies was significantly higher in all patients compared to other anti-HPAs antibodies ($P < 0.05$). These results highlight the role of HPAs in the thrombocytopenia of COVID-19 infected patients. This is the first evidence demonstrating the differential association of the six common HPA gene variants and specific HPA genotype combinations with thrombocytopenia in COVID-19-infected patients.

KEYWORDS

coronavirus disease, thrombocytopenia, human platelet antigen polymorphisms, platelet count, PCR

Introduction

New coronavirus pneumonia is a new human respiratory disease developed by severe acute respiratory syndrome coronavirus 2 (SARS-CoV-2), officially named Coronavirus 2019 (COVID-19) by the World Health Organization (1). Severe patients often develop shortness of breath with or without hypoxemia, which eventually progresses to acute respiratory

distress syndrome, septic shock, coagulation dysfunction, incurable metabolic acidosis, and multiple organ failure (2). Patients with COVID-19 have similar hematologic changes as seen in patients with Middle East Respiratory Syndrome (MERS) (3). Thrombocytopenia and lymphopenia are common blood disorders in patients with COVID-19, indicating poor patient survival (4). The prevalence of thrombocytopenia in COVID-19 patients is highly variable (2). The exact causes of thrombocytopenia in patients with COVID-19 remain unknown, but some events such as increased platelet (PLT) destruction, reduced PLT production, and increased PLT consumption may lead to thrombocytopenia in patients with COVID-19 (5). PLT membrane glycoproteins express several antigenic features on their surface that have a polymorphism, known as human PLT antigens (HPAs) (6). To date, forty-one HPAs have been described in the Immuno Polymorphism Database (IPD)[1] (7). Among the types of HPAs, variants of HPA-1 to -5 and -15 are considered due to their high prevalence and clinical importance (8–11). HPAs have polymorphisms in populations and most of these polymorphisms are caused by the replacement of an amino acid in the structure of a protein by the replacement of a nucleotide in the structure of deoxyribonucleic acid (DNA) (12, 13). Association between some polymorphisms of the HPA system with some diseases such as post-transfusion purpura (PTP), fetal-neonatal alloimmune thrombocytopenia (NAIT) (14), myocardial infarction (15), stroke (16), venous thrombosis (17) and the progression of liver fibrosis (18) have been shown in some studies. The distribution of these gene variants is geographically and ethnically restricted (19, 20).

Based on a literature search, this is the first study that shows the association between polymorphisms of HPA-1 to -5 and -15 and the PLT count in patients with COVID-19, making this study unprecedented.

Materials and methods

Study population and laboratory methods

Two hundred and twenty-two patients with newly diagnosed COVID-19 who were referred to the Khordad Hospital, Varamin, Iran, were randomly included in the study. Informed consent was obtained from all patients who participated in this study. Patients were divided into group A; 86 COVID-19-infected patients with thrombocytopenia, and in group B, 136 COVID-19-infected patients without thrombocytopenia. The normal count of PLTs is 150–450 $\times$ 10^3 per mm^3. Thrombocytopenia is defined as a PLT count below 150 $\times$ $10^3/mm^3$ (21). Host and viral factors evaluated included gender, weight, age, age at infection, duration of infection, viral load, aspartate aminotransferase (AST), alanine aminotransferase (ALT), total bilirubin, prothrombin time (PT), PLT count, AST-to-PLT ratio index (APRI = [AST/upper limit of normal] $\times$ [100/PLTs, $\times$ 10^9/L]), albumin, fast blood sugar (FBS), triglycerides (TG), cholesterol & body mass index [(BMI); weight/height squared (kg/m2)]. Demographic and clinical findings were obtained from patients' records. We confirmed the diagnosis of COVID-19 via reverse transcriptase-polymerase chain reaction (RT-PCR) assays performed on nasopharyngeal swab specimens.

Inclusion criteria were: COVID-19 infection confirmed by serological testing and molecular assays. Exclusion criteria were as follow: acute and chronic liver diseases, fibrosis, cirrhosis, thrombotic thrombocytopenic purpura patients, heparin-induced thrombocytopenia, infections (such as hepatitis B virus, human immunodeficiency viruses, hepatitis C virus or coinfections), history of autoimmune disease, hypertension, splenomegaly/hypersplenism, pregnancy-related thrombocytopenia, gastrointestinal bleeding, cancer, transfusion of blood products, severe iron deficiency anemia, aplastic anemia, intravenous injection of human immunoglobulin, taking anti-PLT drugs such as aspirin, corticosteroids, and other diseases that cause thrombocytopenia. This study was approved by the Ethics Committee of Semnan University of Medical Sciences (Ethical committee code number: IR.SEMUMS.REC.1401.046). All experiments were performed by relevant guidelines and regulations.

DNA extraction

Five ml of patients' peripheral blood samples were collected on admission in sterile tubes containing EDTA anticoagulant. DNA extraction was performed using the Brasilica kit (LGC Biotecnologia, Brazil) kit using the standard manufacturer's protocol. Briefly, 200 µl of lysis solution was added to 200 µl of the patient's blood sample, and after adding 20 µl of proteinase K, it was placed at 60°C for 15 min. Then 100 µl of isopropanol was added and the solution was transferred to a DNA extraction column. After centrifugation, washing solutions 1 and 2 were added, and after the final centrifugation, 100 microliters of Elution buffer were added, and after centrifugation, DNA was extracted. DNA concentration was determined spectrophotometrically at 260 nm (A260) absorption using NanoDrop1000 (Thermo Scientific).

Sequence-specific primers PCR

Genotyping of the 6 HPA polymorphisms [HPA-1 T196C, HPA-2 T524C, HPA-3 T2622G, HPA-4 G526A, HPA-5 G1648A & HPA-15 A2108C (22)] was performed by Sequence-Specific Primers PCR (PCR–SSP), as described previously (23) with slight modifications. Briefly, to perform the PCR–SSP assay, the kit was used in such a way that 10 µl of Red master mix amplicon (Taq polymerase 2x and $Mgcl_2$ 1.5 µM) and 1 µl of forward primer, 1 µl of reverse primer, 4 µl of water and 4 µl of DNA Template were mixed and vortexed. Two sets of primers, each comprising an allele-specific and a common primer, were employed for the recognition of each allele. Negative control was carried out in all PCR runs.

Detection of PLTs associated antibodies

The frequency of target HPAs of anti-PLT antibodies in thrombocytopenic patients was assessed by Quantitative monoclonal immobilization of PLT antibodies (MAIPA). Since the

1 https://www.versiti.org/hpa

TABLE 1 Clinical characteristics of patients at admission.

Variable	Thrombocytopenic SARS-CoV-2 positive (*n* = 86)	Non-thrombocytopenic SARS-CoV-2 positive (*n* = 136)	*p*-value
Age, years [median (IQR)]	38.5 (27–69)	41.1 (24–65)	0.207
Gender (M/F)	45/41	79/57	0.409
Body weight (kg)*	76.1 ± 7.8	77.4 ± 4.9	0.142
Body mass index (*kg/m2*)*	32.7 ± 3.4	33.7 ± 2.4	0.118
Aspartate transaminase, U/l (IQR)	41.3 (16–83)	43.5 (21–89)	0.190
Alanine transaminase, U/L (IQR)	34.9 (7–129)	41.6 (11–165)	0.201
Platelet count, $\times 10^3/\mu L$*	110.4 ± 48.8	262.2 ± 53.6	**0.012**
AST-to-platelet ratio index (IQR)	0.49 (0.20–1.14)	0.44 (0.14–1.11)	**0.001**
Albumin, g/d*	4.2 ± 0.95	4.3 ± 0.93	0.846
SARS-CoV-2 RNA, UI/ml*	1238889.6 ± 1663703.3	1553931.2 ± 1979994.6	0.258
Fast blood sugar *	106.5 ± 17.4	110.6 ± 39.6	0.219
Cholesterol, mg/dl*	149.7 ± 34.7	150.1 ± 40.8	0.824
Triglyceride, mg/dl*	102 ± 31. 6	103.2 ± 33	0.826
Prothrombin time (s) (IQR)	12.1 (10–15)	12.2 (10–13)	0.967
Total bilirubin, mg/dl*	0.25 ± 0.16	0.28 ± 0.17	0.278
Creatinine, μmol/L	75.3 (62.4–89.8)	71.6 (60.5–86.7)	0.358
D-dimer, μg/mL	0.7 (0.5–6.2)	0.3 (0.1–1.4)	**0.021**
Death rate, *n* (%)	11 (12.8)	7 (5.2)	**0.042**
Lactate dehydrogenase	438.6 ± 231.4	394.6 ± 224.8	0.354
White blood cells ($\times 10^9$/L)	7.8 ± 1.9	8.1 ± 2.4	0.598
Absolute lymphocyte count ($\times 10^9$/L)	1.8 ± 2.7	2.1 ± 1.1	0.231
Platelet-to-lymphocyte ratio*	115.3 ± 125.1	231.7 ± 88.4	0.01
Time of hospitalization*, days	11.3 ± 5.2	8.6 ± 4.3	**0.03**

For quantitative variables, data are provided as the median (IQR) or, if marked with *, as the mean ± standard deviation. SARS-CoV-2 RNA: severe acute respiratory syndrome coronavirus 2 ribonucleic acid; n, number; IQR, interquartile range. Bold indicates $p < 0.05$.

frequencies of different HPA genes vary in different populations, MAIPA for different IgG antibodies against HPA-1, -2, -3, -4, -5, and -15 is needed. HPA-1, HPA-3, and HPA-4 are present on the GPIIb/IIIa, while HPA-2 is found on the GPIb/IX, HPA-5 is carried on the GPIa/IIa, and HPA-15 is localized to CD109 (22). MAIPA assay is an enzyme-linked immunosorbent assay (ELISA) technique for the detection and identification of HPA antibodies. The MAIPA assay was performed as described previously (24). In short, human PLT-Antibody Screening Cells and PLT-Antibody Identification Panel Cells (apDiaMed AG Kit, Switzerland) were incubated with the plasma of patients with COVID-19 and washed three times with phosphate-buffered saline (PBS) containing 0.05% EDTA. By adding PBS containing 1% Triton X-100, soluble PLT lysate was prepared and added to the pre-coated 96-well microtiter plates with Goat Anti-Mouse IgG Fc fragment specific (Jackson ImmunoResearch, West Grove, PA). After 1 hour (h) incubation, antibodies in the plasma of COVID-19 patients bound to HPA were detected with the final antibody (horseradish peroxidase-conjugated goat-antihuman IgG Fc fragment specific) and a substrate solution containing 3,3',5,5'-tetramethylbenzidine. The reaction is stopped by adding H_2SO_4. The absorbance of the plate was read at 450 nm on an automated microtiter plate reader. The optical density (OD) values above 0.2 were considered positive.

Statistical analysis

Pearson's χ2 test or Fisher's exact test was utilized to assess associations between the genotypic frequency of the HPA-1 to -5 and -15 systems with PLT count. Also, Pearson's χ2 test (or Fisher's exact test) and Student's *t*-test were utilized for qualitative variables and quantitative variables, respectively. Deviation from Hardy-Weinberg equilibrium was analyzed by Pearson's χ2 test. The multivariate logistic regression model was carried out to determine an independent association of HPA genotypes with thrombocytopenia. HPA combined genotype estimation was performed by the maximum-likelihood procedure. HPA genotype combinations were coded as per the allele (wild type or mutant) at each locus. The first letter refers to HPA-1 (T allele = 1a, C allele = 1b), the second to HPA-2 (T allele = 2a, C allele = 2b), the third to HPA-3 (T allele = 3a, G allele = 3b), the fourth to HPA-4 (G allele = 4a, A allele = 4b), the fifth to HPA-5 (G allele = 5a, A allele = 5b) and the sixth to HPA-15 (A allele = 15a, C allele = 15b). Odds ratios (OR) and 95% confidence intervals (CI) were determined by Univariate analysis. Statistical analysis was performed with the SPSS version 24.0 software (SPSS Inc., Chicago, IL, USA) and a genetic analyzer (ABI PRISM 310,

10.3389/fmed.2023.1265568

TABLE 2 HPA allele and genotype frequency.

HPAs	Allele/Genotype	Thrombocytopenic SARS-CoV-2 positive (n = 86)	Non-thrombocytopenic SARS-CoV-2 positive (n = 136)	p-value*	OR (95% CI)
	T allele	165 (95.9)	257 (94.5)	0.494	1
	C allele	7 (4.1)	15 (5.5)		0.727 (0.290–1.821)
HPA-1	T/T	79 (91.9)	121 (89)	0.483	1
	T/C	7 (8.1)	15 (11)		0.715 (0.279–1.831)
	C/C	0	0		
	T allele	122 (70.9)	205 (75.4)	0.301	1
	C allele	50 (29.1)	67 (24.6)		1.254 (0.816–1.927)
HPA-2	T/T	44 (51.2)	75 (55.1)	0.339	1
	T/C	34 (39.5)	55 (40.5)		1.054 (0.598–1.857)
	C/C	8 (9.3)	6 (4.4)		2.273 (0.740–6.980)
	T allele	118 (68.6)	212 (77.9)	**0.028**	1
	G allele	54 (31.4)	60 (22.1)		1.617 (1.051–2.488)
HPA-3	T/T	45 (52.3)	83 (61)	**0.038**	1
	T/G	28 (32.5)	46 (33.8)		1.123 (0.620–2.033)
	G/G	13 (15.2)	7 (5.2)		3.425 (1.275–9.199)
	G allele	172 (100)	272 (100)	1.000	
	A allele	0	0		
HPA-4	G/G	136 (100)	136 (100)	1.000	–
	G/A	0	0		
	A/A	0	0		
	G allele	172 (100)	272 (100)	1.000	
	A allele	0	0		
HPA-5	G/G	136 (100)	136 (100)	1.000	–
	G/A	0	0		
	A/A	0	0		
HPA-15	A allele	73 (42.4)	137 (50.4)	0.103	1
	C allele	99 (57.6)	135 (49.6)		1.376 (0.937–2.022)
	A/A	11 (12.7)	32 (23.6)	0.136	1
	A/C	51 (59.3)	73 (53.6)		2.032 (0.938–4.402)
	C/C	24 (28)	31 (22.8)		2.252 (0.946–5.365)

*Pearson's χ^2 test. Number (percent of total). Bold indicates $p < 0.05$.

Applied Biosystems). Statistical significance was set at a 0.05 level for all the tests.

Results

Demographic characteristics

There were a total of 222 patients admitted with a median age of 41.6 years old, ranging from 24 to 69 years. A total of 124 patients (55.8%) were male, and 98 (44.2%) were female. The demographic and clinical data of all the patients included are demonstrated in Table 1. No statistically significant differences were found between the patient groups about age, gender, BMI, AST, ALT, albumin, viral load, FBS, cholesterol, triglyceride, PT, total bilirubin, creatinine, LDH, WBCs, absolute lymphocyte count, and PLT-to-lymphocyte ratio. APRI, D-dimer, death rate, and duration of hospitalization were significantly higher in thrombocytopenic SARS-CoV-2 positive patients compared with non-thrombocytopenic patients ($P < 0.05$).

10.3389/fmed.2023.1265568

TABLE 3 The evaluation of the distribution of gene frequencies of HPA-1, HPA-2, HPA-3, and HPA-15 by Hardy–Weinberg equilibrium test.

Genotypes		ThrombocytopenicSARS-CoV-2 positive			Non-thrombocytopenicSARS-CoV-2 positive		
		EN	ON	*p*-value	EN	ON	*p*-value
HPA-1	T/T	79.1	79		121.4	121	
	T/C	6.7	7	0.793	14.2	15	0.925
	C/C	0.1	0		0.4	0	
	T/T	43.3	44		77.3	75	
HPA-2	T/C	35.5	34	0.582	50.5	55	0.929
	C/C	7.3	8		8.3	6	
	T/T	40.5	45		82.6	83	
HPA-3	T/G	37.0	28	0.981	46.8	46	0.076
	G/G	8.5	13		6.6	7	
	A/A	15.5	11		34.5	32	
HPA-15	A/C	42.0	51	0.691	68.0	73	0.140
	C/C	28.5	24		33.5	31	

ON, observed number; EN, expected number.

TABLE 4 Multivariate regression logistic of risk factors related to thrombocytopenia.

Variable			
HPA-3: T/T vs. G/G			
HPA-3: T/G vs. G/G	2.54	**0.011**	5.827 (1.504–22.575)
Age at infection	−0.35	0.720	0.982 (0.891–1.083)

Bold indicates $p < 0.05$.

Genotype and allele frequencies of HPAs

The HPA-1 to -5 and -15 genotypes and allele frequencies in patients with SARS-CoV-2 infection are summarized in Table 2. There were no significant differences in the genotype and allele frequency distribution for the HPA-1, -2, -4, -5, and -15 between thrombocytopenic SARS-CoV-2 positive patients and non-thrombocytopenic patients ($P > 0.05$). However, distributions of the genotype and allele frequency for HPA-3 were significantly different between the two groups. The allele frequency of HPA-3b [G allele] in the thrombocytopenic patients was found to be significantly higher than in the non-thrombocytopenic patients, and HPA-3a [T allele] in the thrombocytopenic patients was significantly lower than in the non-thrombocytopenic patients ($P = 0.028$). The genotype frequency of HPA-3bb [2622 G/G] was significantly higher in thrombocytopenic patients than that in non-thrombocytopenic patients, and the genotype frequency of HPA-3aa/ab [2622 T/T & T/G] was significantly lower in thrombocytopenic patients than that in the non-thrombocytopenic patients ($P = 0.038$). The OR of the HPA-3bb [2622 G/G] for thrombocytopenia was 3.425 (95% CI 1.275–9.199), and the OR of the HPA-3b [G allele] was 1.617 (95% CI 1.051–2.488). Genotypes did not deviate from the Hardy–Weinberg equilibrium in the HPA systems and revealed no indication of linkage disequilibrium (Table 3). Multivariate logistic regression showed an independent association between the genotype HPA-3aa ($P = 0.014$; OR [95% CI], 5.666 [1.412–22.737]) and HPA-3ab ($P = 0.011$; OR [95% CI], 5.827 [1.504–22.575]) with thrombocytopenia, when compared with genotype HPA-3bb, independent of the age at infection ($P = 0.720$) (Table 4).

HPA genotype combinations

Analysis of the six-locus HPA combined genotypes is shown in Table 5. Of the 62 HPA genotype combinations recognized, selected HPA genotype combinations were associated with thrombocytopenia. These included the TCGGGC ($P = 0.001$) & TTGGGC ($P = 0.029$) combined genotypes, which were higher, and the CCGGGC ($P = 0.001$) & TCTGGC ($P = 0.047$) combined genotypes, which were lower among thrombocytopenia patients compared to non-thrombocytopenic patients. Univariate analysis identified the CCGGGC ($P = 0.016$) combined genotype to be negatively associated & the TCGGGC ($P = 0.003$) and CCGGGC ($P = 0.003$) to be positively associated with thrombocytopenia (Table 6).

TABLE 5 HPA combined genotypes in thrombocytopenic and non-thrombocytopenic SARS-CoV-2 positive patients.

Combined genotype*	Thrombocytopenic SARS-CoV-2 positive (%)	Non-thrombocytopenic SARS-CoV-2 positive (%)	*p*-value
TTTGGA	73 (42.2)	137 (50.4)	0.119
TTTGGC	45 (26.2)	68 (25)	0.823
TCTGGC	0	7 (2.6)	**0.047**
TCGGGC	50 (29.1)	45 (16.5)	**0.001**
CCTGGC	0	15 (5.5)	**0.001**
TTGGGC	4 (2.3)	0	**0.029**

*HPA combined genotype (HPA-1, to -5, and -15) frequency determined by the maximum likelihood method. Fisher's exact test. Bold indicates $p < 0.05$.

Evaluation of PLT count

The mean PLT counts ± SD was significantly lower in thrombocytopenic SARS-CoV-2 positive patients compared to non-thrombocytopenic patients (110.4 ± 48.8 vs. 220.4 ± 48.8, × 10^3/μL; $P = 0.012$). The mean PLT counts did not differ among HPA-1, -2, -4, -5, and -15 genotypes (Figures 1A, B, D). However, the mean PLT counts of patients with the HPA-3bb genotype was significantly lower than patients with genotype HPA-3aa/ab ($P < 0.05$) (Figure 1C). In thrombocytopenic SARS-CoV-2 positive patients, 71.2% with HPA-3bb genotype had a low PLT count compared with 32.3% of those with HPA3aa/ab genotype. In non-thrombocytopenic patients, 57.4% with the HPA-3bb genotype had a low PLT count compared to only 27.6% of those with the HPA-3aa/ab genotype, using the normal cut-off of 150,000/μL. The mean ± SD time of hospitalization was 9.6 ± 4.8 days. Time of hospitalization was significantly and negatively correlated with the observed PLT count in two groups (Figure 2A). Also, correlation analysis showed that hospitalization time was significantly and negatively correlated with patients' PLTs based on HPA-3 genotype (Figure 2B). The duration of hospitalization was 8.5 ± 4.3 for HPA-3aa, 11.7 ± 5.1 for HPA-3ab, and 15.9 ± 3.5 for HPA-3bb.

MAIPA results in patients

Until now, the MAIPA assay was the specific method for PLT autoantibody detection. Thus we performed autoantibody detection in patient samples using the MAIPA method (25). In SARS-CoV-2 positive patients, MAIPA was positive in 54 of 222 (24.3%) (23/86 thrombocytopenic patients and 31/186 non-thrombocytopenic patients). The highest frequency of target HPAs of anti-PLT antibodies in thrombocytopenic patients was HPA-1a (12.7%), HPA-2a (6.9%), HPA-2b (3.4%), HPA-3a (13.9%), HPA-3b (9.3%), HPA-5a (5.8%), HPA-15a (4.6%), HPA-15b (3.4%), and all cases negative for HPA-1b, HPA-4a, and HPA-4b (Figure 3). The highest frequency of target HPAs of anti-PLT antibodies in non-thrombocytopenic patients was HPA-1a (16.9%), HPA-2a (6.6%), HPA-2b (3.6%), HPA-3a (13.9%), HPA-3b (5.1%), HPA-5a (6.6%), HPA-15a (5.1%), HPA-15b (5.8%), and all cases negative for HPA-1b, HPA-4a, and HPA-4b (Figure 3). The frequency of anti-HPA-1a and anti-HPA-3a antibodies was significantly higher in all patients compared to other anti-HPAs antibodies ($P < 0.05$).

TABLE 6 Distribution of HPA combined genotypes.

Combined genotype*	Univariate		
	Z score	*P*	OR (95%CI)
TTTGGA			1.00 (reference)
TTTGGC	0.847	0.397	1.242 (0.775–1.991)
TCTGGC	1.911	**0.056**	1.051 (1.013–1.091)
TCGGGC	2.967	**0.003**	0.480 (0.293–0.785)
CCTGGC	−2.967	**0.003**	1.109 (1.053–1.169)
TTGGGC	2.408	**0.016**	0.948 (0.900–0.999)

*HPA combined genotype (HPA-1, to -5, and -15) frequency determined by the maximum likelihood method. Combined genotypes were coded according to the allele (wild type or mutant) at each locus. Bold indicates $p < 0.05$.

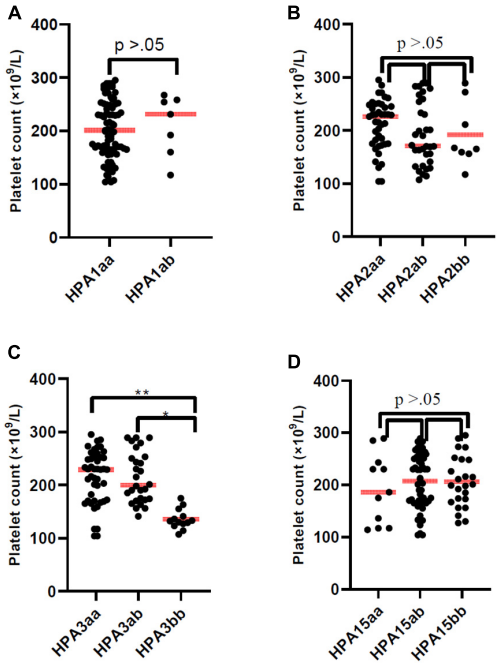

FIGURE 1
Platelet count of patients according to HPA-1, -2, -3, and -15 genotype. The line through the middle of the box is the median. Platelet count of patients with HPA-3bb genotype was significantly lower than patients with genotype HPA-3aa or HPA-3ab ($P < 0.05$).

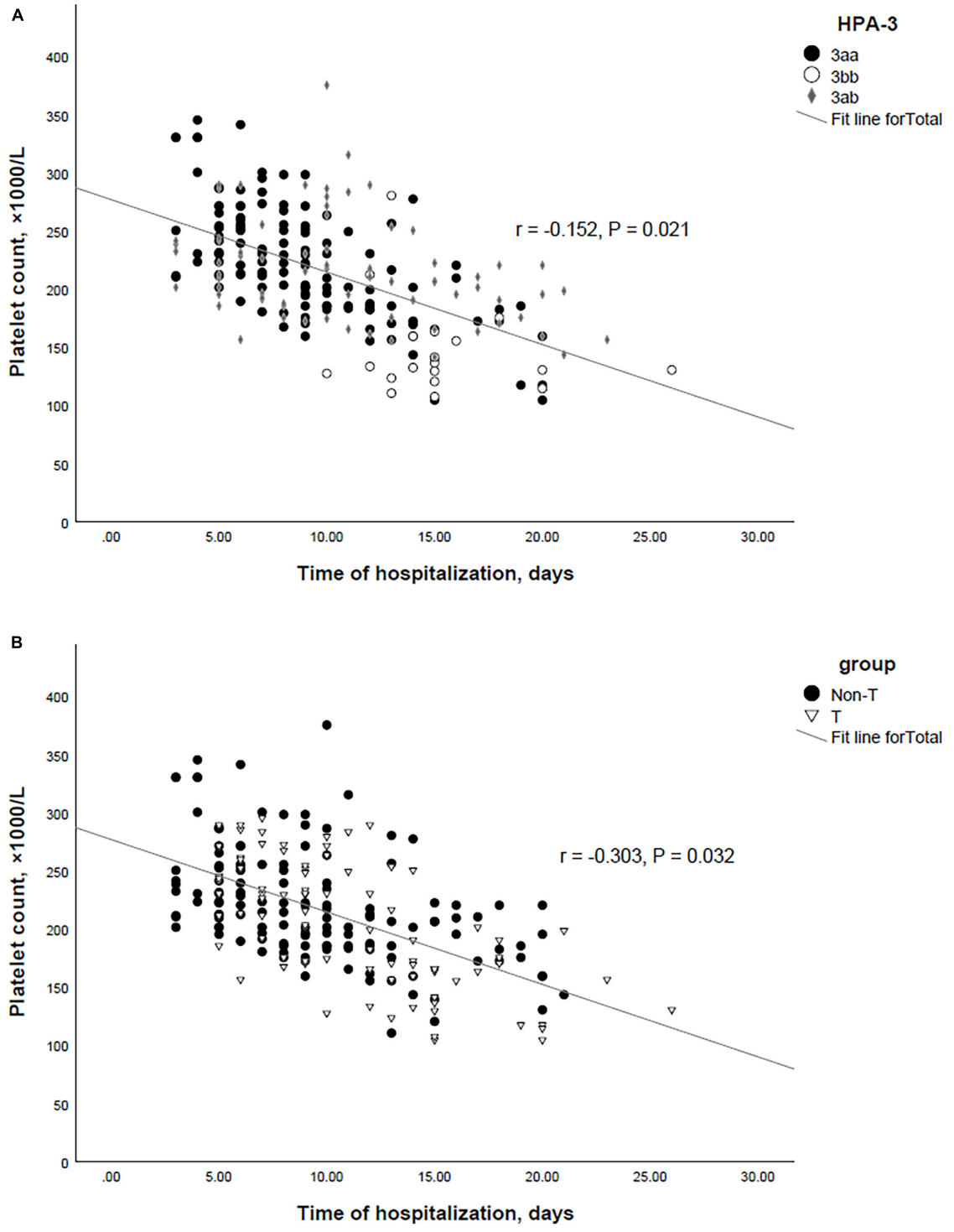

FIGURE 2
(A) Correlation between the HPA-3 and time of hospitalization in SARS-CoV-2 positive patients. **(B)** Correlation between the platelet count and time of hospitalization in SARS-CoV-2 positive patients.

Discussion

In this study, thrombocytopenia occurred in 38.7% of patients with COVID-19. In line with these findings, a study in China that included 1099 patients showed that 36.2% of patients had thrombocytopenia (26). In total, it has been determined that 5-41% of COVID-19 patients suffer from thrombocytopenia (27). Also, previous studies have shown that patients with severe COVID-19 disease present with thrombocytopenia and lymphopenia more than those with non-severe disease. These patients were more likely to develop acute respiratory distress syndrome (28, 29).

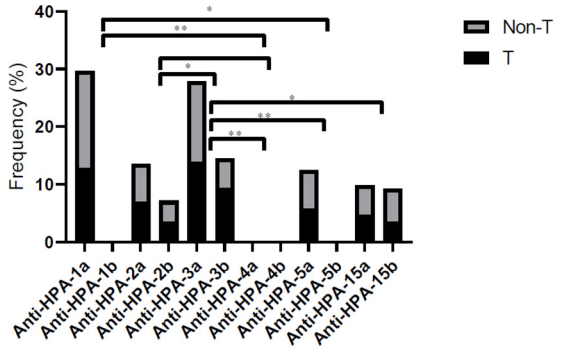

FIGURE 3
Comprehensive distribution of platelet-specific antibodies according to HPA-1, -2, -3, -4, -5, and -15 genotype in thrombocytopenic/non-thrombocytopenic SARS-CoV-2 positive. Statistical significance was set at a 0.05 level for all the tests. *$P < 0.05$, and **$P < 0.01$. T, thrombocytopenic; Non-T, non-thrombocytopenic.

Numerous studies have tried to determine the relationship between the severity of COVID-19 disease and the rate of disease progression by examining different variables to use the results along with other factors in diagnosing and determining the prognosis of patients and also managing treatment. Therefore, we studied the PLT count changes in patients with COVID-19 and the association between thrombocytopenia and the polymorphisms of HPA-1 to -5 and -15. To our knowledge, this is the first study to evaluate the association of HPA polymorphisms with PLT count in patients with COVID-19 infection.

Our study showed that in patients with COVID-19, the HPA-3bb genotype and HPA-3b allele are associated with a low PLT count. This study also identified HPA genotypic combinations associated with thrombocytopenia in COVID-19 patients. A significant finding was the reduction of PLT counts in TCGGGC and TTGGGC genotypes. While the combined genotypes TCTGGC and CCTGGC were not associated with a decrease in PLT count.

The HPA polymorphisms are related to a wide variety of clinical conditions (17, 18) and their pattern of distribution is affected by ethnicity (23, 30). Several previous studies have reported a possible association between the susceptibility to hepatitis C virus (HCV) infection and the gene frequencies of HPAs (18, 31). The association between HPA-1 polymorphic variants and fibrosis progression was previously reported by Silva et al. (31) in Brazilian HCV-infected patients.

The HPA-3 (T2622G, Ile843Ser) is present on the human PLT GPIIb. GPIIb is the alpha subunit of the PLT integrin GPIIb-IIIa receptor complex. The GPIIb/IIIa receptor complex performs various functions, including interaction with the endothelium and a role in the risk of myocardial infarction and thrombosis (12, 32–34). On the other hand, Hamaia et al. (35) reported that PLTs can act as carriers of HCV. There is not enough information about the direct interaction of HCV and COVID-19 with PLT. However, integrins such as glycoprotein or other adhesion molecules can play an important role in the interaction of viruses such as HCV or COVID-19 with PLTs.

The pathogenesis of thrombocytopenia in patients with COVID-19 is not fully understood. Severe changes in the immune response and autoimmunity have been reported in some viral infections, including HCV (36). From previous studies, it is known that antibodies against PLT surface antigens in patients with HCV can cause immunological destruction of PLTs (37). In a study about the role of immune mechanisms as a causative agent of thrombocytopenia in HCV hepatic patients, the authors found that PLT-associated GP antibodies cause thrombocytopenia in patients with chronic HCV infections. Also, Their results revealed that the highest frequency of target HPAs of anti-PLT antibodies in thrombocytopenic HCV-positive hepatic patients was HPA-1 (46.7%), HPA-2 (10%), HPA-3 (46.7%), HPA-4 (6.7%), HPA-5 (10%) and all cases negative for HPA-15 (38). These findings were to some extent similar to the results of this study. We detected PLT-specific antibodies in the patient's plasma to ensure a more accurate and credible conclusion of the relationship between PLT-specific antibodies and thrombocytopenia. These findings suggest an immune-based mechanism of thrombocytopenia in COVID-19-infected patients.

Moreover, we found a significant negative correlation between PLT count and time of hospitalization in SARS-CoV-2-positive patients. The average hospitalization day of patients with thrombocytopenia was longer than those without thrombocytopenia. In line with this finding, one study reported that patients with a higher platelet count had shorter hospitalization than patients with a lower platelet count at the time of admission (29).

Therefore, several hypotheses that lead to thrombocytopenia in patients with COVID-19 can be expressed as follows:

(a) Under normal physiological conditions, PLTs do not adhere to the vascular endothelium unless the PLT-endothelium interaction is disrupted (39, 40). The attachment of COVID-19 to platelets through HPA may cause the adhesion of platelets to the endothelium of blood vessels and subsequently thrombocytopenia by disrupting the PLT-endothelium interaction.
(b) In clinical trials and preclinical studies, it has been determined that GPIIb/IIIa receptor antagonists are effective inhibitors of platelet aggregation so that these antagonists reduce platelet half-life (41). The binding of COVID-19 to the GPIIb/IIIa receptor through HPA may cause the virus to act as an antagonist of this receptor and subsequently cause thrombocytopenia.
(c) PLT degradation may be due to the presence of anti-PLT antibodies with or without the presence of immune complexes that react with specific glycoproteins or HPAs.
(d) Binding of COVID-19 to PLTs via HPAs may lead to the formation of neo-antigens on the PLT surface, resulting in the formation and production of antibodies against target HPAs. In addition, it can be assumed that the immune complexes attached to the PLT surface may play an important role in PLT destruction, possibly through phagocytosis by macrophages of

the reticuloendothelial system. Therefore, HPA polymorphisms may play a role in the immune-mediated clearance of platelets in the reticuloendothelial system of patients with COVID-19.

To confirm these hypotheses, it is suggested to evaluate the glycoproteins of PLT levels and PLT-specific antibodies in patients with COVID-19.

Conclusion

These results highlight the role of HPAs in the thrombocytopenia of COVID-19-infected patients. Also, PLT-specific antibodies represent a common mechanism inducing thrombocytopenia in COVID-19-infected patients. We presented the first evidence suggesting the distinct association of specific HPA genotype combinations with thrombocytopenia in COVID-19-infected patients. Considering the population and ethnic heterogeneity in the distribution of HPA polymorphisms and their possible pathogenic capacity, it is recommended to evaluate the role of HPA polymorphisms as risk factors for thrombocytopenia in different populations with COVID-19.

Data availability statement

The original contributions presented in this study are included in the article/supplementary material, further inquiries can be directed to the corresponding author.

Ethics statement

The studies involving humans were approved by the Ethics Committee of Semnan University of Medical Sciences (Ethical Committee code number: IR.SEMUMS.REC.1401.046). The studies were conducted in accordance with the local legislation and institutional requirements. Written informed consent for participation in this study was provided by the participants' legal guardians/next of kin.

Author contributions

KG: Conceptualization, Writing—original draft. MR: Data curation, Investigation, Writing—original draft. MK: Funding acquisition, Software, Writing—original draft. AB: Data curation, Resources, Writing—original draft. MI: Resources, Software, Writing—original draft. HK: Software, Writing—original draft, Data curation. AG: Conceptualization, Project administration, Supervision, Validation, Visualization, Writing—review & editing.

Funding

The authors declare financial support was received for the research, authorship, and/or publication of this article. This study was supported by the Semnan University of Medical Sciences, Semnan, Iran.

Acknowledgments

We thank the Semnan University of Medical Sciences, Semnan, Iran, which has provided funding for this research.

Conflict of interest

The authors declare that the research was conducted in the absence of any commercial or financial relationships that could be construed as a potential conflict of interest.

Publisher's note

References

1. Abd El-Aziz TM, Stockand JD. Recent progress and challenges in drug development against COVID-19 coronavirus (SARS-CoV-2)-an update on the status. *Infect Genet Evol.* (2020) 83:104327. doi: 10.1016/j.meegid.2020.104327

2. Huang C, Wang Y, Li X, Ren L, Zhao J, Hu Y, et al. Clinical features of patients infected with 2019 novel coronavirus in Wuhan, China. *Lancet.* (2020) 395:497–506.

3. Al-Tawfiq J, Hinedi K, Abbasi S, Babiker M, Sunji A, Eltigani M. Hematologic, hepatic, and renal function changes in hospitalized patients with Middle East respiratory syndrome coronavirus. *Int J Lab Hematol.* (2017) 39:272–8. doi: 10.1111/ijlh.12620

4. Mishra AK, Sahu KK, George AA, Lal A. A review of cardiac manifestations and predictors of outcome in patients with COVID–19. *Heart Lung.* (2020) 49:848–52.

5. Xu P, Zhou Q, Xu J. Mechanism of thrombocytopenia in COVID-19 patients. *Ann Hematol.* (2020) 99:1205–8.

6. Bussel J, Kaplan C. The fetal and neonatal consequences of maternal alloimmune thrombocytopenia. *Baillière's Clin Haematol.* (1998) 11:391–408.

7. Al-Ouda S, Al-Banyan A, Abdel Gader A, Bayoumy N, Al-Gahtani F. Gene frequency of human platelet alloantigens-1 to-6 and-15 in Saudi blood donors. *Transfusion Med.* (2016) 26:220–4. doi: 10.1111/tme.12297

8. Ertel K, Al-Tawil M, Santoso S, Kroll H. Relevance of the HPA-15 (Gov) polymorphism on CD109 in alloimmune thrombocytopenic syndromes. *Transfusion.* (2005) 45:366–73. doi: 10.1111/j.1537-2995.2005.04281.x

9. Mechoulan A, Muller J, Branger B, Philippe H, Boscher C, Ville Y, et al. OP09.01: pregnancies with fetal and neonatal alloimmunization thrombocytopenia (FNAIT) in HPA-1 system: towards a less invasive management. *Ultrasound Obstetr Gynecol.* (2009) 34:88.

10. Socher I, Zwingel C, Santoso S, Kroll H. Heterogeneity of HPA-3 alloantibodies: consequences for the diagnosis of alloimmune thrombocytopenic syndromes. *Transfusion.* (2008) 48:463–72. doi: 10.1111/j.1537-2995.2007.01550.x

11. Kaplan C. Neonatal alloimmune thrombocytopenia: where do we stand? *ISBT Sci Ser.* (2007) 2:85–8.

12. Metcalfe P, Watkins N, Ouwehand W, Kaplan C, Newman P, Kekomaki R, et al. Nomenclature of human platelet antigens. *Vox Sanguinis.* (2003) 85:240–5.

13. Lucas G. Platelet and granulocyte glycoprotein polymorphisms. *Transfus Med.* (2000) 10:157–74.

14. Mueller-Eckhardt C, Kiefel V, Santoso S. Review and update of platelet alloantigen systems. *Transfus Med Rev.* (1990) 4:98–109.

15. Rosenberg N, Zivelin A, Chetrit A, Dardik R, Kornbrot N, Inbal A. Effects of platelet membrane glycoprotein polymorphisms on the risk of myocardial infarction in young males. *Isr Med Assoc J.* (2002) 4:411–4.

16. Reiner AP, Kumar PN, Schwartz SM, Longstreth W Jr., Pearce RM, Rosendaal FR, et al. Genetic variants of platelet glycoprotein receptors and risk of stroke in young women. *Stroke.* (2000) 31:1628–33. doi: 10.1161/01.str.31.7.1628

17. Ridker PM, Hennekens CH, Schmitz C, Stampfer MJ, Lindpaintner K. PIA1/A2 polymorphism of platelet glycoprotein IIIa and risks of myocardial infarction, stroke, and venous thrombosis. *Lancet.* (1997) 349:385–8. doi: 10.1016/S0140-6736(97)80010-4

18. Ghasemi A, Zadsar M, Shaiegan M, Samiei S, Namvar A, Rasouli M, et al. Human platelet antigens polymorphisms; association to the development of liver fibrosis in patients with chronic hepatitis C. *J Med Virol.* (2020) 92:45–52. doi: 10.1002/jmv.25423

19. Halle L, Bigot A, Mulen-Imandy G, M'bayo K, Jaeger G, Anani L, et al. HPA polymorphism in sub-Saharan African populations: beninese, cameroonians, congolese, and pygmies. *Tissue Antigens.* (2005) 65:295–8. doi: 10.1111/j.1399-0039.2005.00360.x

20. Yan L, Zhu F, He J, Sandler S. Human platelet alloantigen systems in three Chinese ethnic populations. *Immunohematology.* (2006) 22:6–10.

21. Izak M, Bussel JB. Management of thrombocytopenia. *F1000prime Rep.* (2014) 6:45.

22. Reiner AP, Aramaki KM, Teramura G, Gaur L. Analysis of platelet glycoprotein Ia (α2 integrin) allele frequencies in three North American populations reveals genetic association between nucleotide 807C/T and amino acid 505 Glu/Lys (HPA-5) dimorphisms. *Thromb Haemost.* (1998) 80:449–56.

23. Bhatti F, Uddin M, Ahmed A, Bugert P. Human platelet antigen polymorphisms (HPA-1,-2,-3,-4,-5 and-15) in major ethnic groups of Pakistan. *Transfus Med.* (2010) 20:78–87. doi: 10.1111/j.1365-3148.2009.00982.x

24. Brighton T, Evans S, Castaldi P, Chesterman C, Chong B. Prospective evaluation of the clinical usefulness of an antigen-specific assay (MAIPA) in idiopathic thrombocytopenic purpura and other immune thrombocytopenias. *Blood.* (1996) 88:194–201.

25. Porcelijn L, Van Beers W, Gratama JW, Van't Veer M, De Smet A, Sintnicolaas K. External quality assessment of platelet serology and human platelet antigen genotyping: a 10-year review. *Transfusion.* (2008) 48:1699–706. doi: 10.1111/j.1537-2995.2008.01748.x

26. Guan W-J, Ni Z-Y, Hu Y, Liang W-H, Ou C-Q, He J-X, et al. Clinical characteristics of 2019 novel coronavirus infection in China. *MedRxiv. [Preprint]* (2020) doi: 10.1101/2020.02.06.20020974

27. Zhang Y, Zeng X, Jiao Y, Li Z, Liu Q, Ye J, et al. Mechanisms involved in the development of thrombocytopenia in patients with COVID-19. *Thromb Res.* (2020) 193:110–5.

28. Chan AS, Rout A. Use of neutrophil-to-lymphocyte and platelet-to-lymphocyte ratios in COVID-19. *J Clin Med Res.* (2020) 12:448.

29. Qu R, Ling Y, Zhang YhZ, Wei LY, Chen X, Li XM, et al. Platelet-to-lymphocyte ratio is associated with prognosis in patients with coronavirus disease-19. *J Med Virol.* (2020) 92:1533–41.

30. Wu G-G, Tang Q-M, Shen W-D, Liao Y, Li H-C, Zhao T-M. DNA sequencing-based typing of HPA-1 to HPA-17w systems. *Int J Hematol.* (2008) 88:268–71. doi: 10.1007/s12185-008-0164-6

31. Zhou SH, Liang XH, Shao LN, Yu WJ, Zhao C, Liu M. Association of human platelet antigens polymorphisms with susceptibility to hepatitis C virus infection in Chinese population. *Int J Immunogenet.* (2017) 44:337–42. doi: 10.1111/iji.12341

32. Liu Y, Zhao F, Gu W, Yang H, Meng Q, Zhang Y, et al. The roles of platelet GPIIb/IIIa and αvβ3 integrins during HeLa cells adhesion, migration, and invasion to monolayer endothelium under static and dynamic shear flow. *J Biomed Biotechnol.* (2009) 2009:829243.

33. Lekakis J, Bisti S, Tsougos E, Papathanassiou A, Dagres N, Ikonomidis I, et al. Platelet glycoprotein IIb HPA-3 polymorphism and acute coronary syndromes. *Int J Cardiol.* (2008) 127:46–50. doi: 10.1016/j.ijcard.2007.04.039

34. Wu J-H, Zhang D-W, Cheng X-L, Shi H, Fan Y-P. Platelet glycoprotein IIb HPA-3 a/b polymorphism is associated with native arteriovenous fistula thrombosis in chronic hemodialysis patients. *Renal Fail.* (2012) 34:960–3. doi: 10.3109/0886022X.2012.706865

35. Hamaia S, Li C, Allain J-P. The dynamics of hepatitis C virus binding to platelets and 2 mononuclear cell lines. *Blood J Am Soc Hematol.* (2001) 98:2293–300. doi: 10.1182/blood.v98.8.2293

36. Pockros PJ, Duchini A, McMillan R, Nyberg LM, McHutchison J, Viernes E. Immune thrombocytopenic purpura in patients with chronic hepatitis C virus infection. *Am J Gastroenterol.* (2002) 97:2040–5.

37. Doi T, Homma H, Mezawa S, Kato J, Kogawa K, Sakamaki S, et al. Mechanisms for increment of platelet associated IgG and platelet surface IgG and their implications in immune thrombocytopenia associated with chronic viral liver disease. *Hepatol Res.* (2002) 24:23–33. doi: 10.1016/s1386-6346(02)00010-4

38. Aref S, Sleem T, El Menshawy N, Ebrahiem L, Abdella D, Fouda M, et al. Antiplatelet antibodies contribute to thrombocytopenia associated with chronic hepatitis C virus infection. *Hematology.* (2009) 14:277–81. doi: 10.1179/102453309X439818

39. Han J, Lim CJ, Watanabe N, Soriani A, Ratnikov B, Calderwood DA, et al. Reconstructing and deconstructing agonist-induced activation of integrin αIIbβ3. *Curr Biol.* (2006) 16:1796–806.

40. Jy W, Horstman LL, Park H, Mao WW, Valant P, Ahn YS. Platelet aggregates as markers of platelet activation: characterization of flow cytometric method suitable for clinical applications. *Am J Hematol.* (1998) 57:33–42. doi: 10.1002/(sici)1096-8652(199801)57:1<33::aid-ajh6>3.0.co;2-2

41. Weiss DJ, Mirsky ML, Evanson OA, Fagliari J, Mcclenahan D, Mccullough B. Platelet kinetics in dogs treated with a glycoprotein IIb/IIIa peptide antagonist. *Toxicol Pathol.* (2000) 28:310–6. doi: 10.1177/019262330002800211

frontiers | Frontiers in Medicine

TYPE Original Research
PUBLISHED 01 December 2023
DOI 10.3389/fmed.2023.1321490

OPEN ACCESS

EDITED BY
Pierpaolo Di Micco,
Ospedale Santa Maria delle Grazie, Italy

REVIEWED BY
Guanghua Zhai,
Nanjing Medical University, China
Gianluca Di Micco,
Ospedale Buon Consiglio Fatebenefratelli, Italy

*CORRESPONDENCE
Zhaoru Zhang
✉ zhangzhaoru168@163.com

RECEIVED 14 October 2023
ACCEPTED 16 November 2023
PUBLISHED 01 December 2023

CITATION
Li Z, Zhang Z and Chen C (2023) Novel nomograms to predict risk and prognosis in hospitalized patients with severe fever with thrombocytopenia syndrome.
Front. Med. 10:1321490.
doi: 10.3389/fmed.2023.1321490

Novel nomograms to predict risk and prognosis in hospitalized patients with severe fever with thrombocytopenia syndrome

Zhenxing Li, Zhaoru Zhang* and Chong Chen

Department of Infectious Diseases, The Affiliated Chaohu Hospital of Anhui Medical University, Hefei, China

Background: Severe fever with thrombocytopenia syndrome (SFTS) is an emerging and life-threatening infectious disease caused by SFTS virus. Although recent studies have reported the use of nomograms based on demographic and laboratory data to predict the prognosis of SFTS, no study has included viral load, which is an important factor that influences the prognosis, when compared with other risk factors. Therefore, this study aimed to develop a model that predicts SFTS prognosis before it reaches the critical illness stage and to compare the predictive ability of groups with and without viral load.

Methods: Two hundred patients with SFTS were enrolled between June 2018 and August 2023. Data were sourced from the first laboratory results at admission, and two nomograms for mortality risk were developed using multivariate logistic regression to identify the risk variables for poor prognosis in these patients. We calculated the area under the receiver operating characteristic curve (AUC) for the two nomograms to assess their discrimination, and predictive abilities were compared using net reclassification improvement (NRI) and integrated discrimination improvement (IDI).

Results: The multivariate logistic regression analysis identified four independent risk factors: age, bleeding manifestations, prolonged activated partial thromboplastin time, and viral load. Based on these factors, a final nomogram predicting mortality risk in patients with SFTS was constructed; in addition, a simplified nomogram was constructed excluding the viral load. The AUC [0.926, 95% confidence interval (CI): 0.882–0.970 vs. 0.882, 95% CI: 35 0.823–0.942], NRI (0.143, 95% CI, 0.036–0.285), and IDI (0.124, 95% CI, 0.061–0.186) were calculated and compared between the two models. The calibration curves of the two models showed excellent concordance, and decision curve analysis was used to quantify the net benefit at different threshold probabilities.

Conclusion: Two critical risk nomograms were developed based on the indicators for early prediction of mortality risk in patients with SFTS, and enhanced predictive accuracy was observed in the model that incorporated the viral load. The models developed will provide frontline clinicians with a convenient tool for early identification of critically ill patients and initiation of a better personalized treatment in a timely manner.

KEYWORDS

nomogram, fever, thrombocytopenia syndrome, SFTS virus, *Dabie bandavirus*

1 Introduction

Severe fever with thrombocytopenia syndrome (SFTS), commonly known as "tick disease," was first reported in China in 2011 (1). It is an emerging infectious disease caused by a new type of bunyavirus carried by ticks [originally named SFTS virus (SFTSV). In 2019, SFTSV was renamed *Dabie bandavirus* and reclassified into the genus *Bandavirus*, family *Phenuiviridae*, and order *Bunyavirales*] (2). Later on, the news of this syndrome reached Korea and Japan (3, 4). Cases of SFTS have also recently been recorded in Vietnam and Myanmar (5, 6), suggesting that the disease has spread more widely. The clinical manifestations of SFTSV include fever, thrombocytopenia, diarrhea, and even circulatory system-wide coagulation and multi-organ dysfunction in severe cases, with a fatality rate ranging from 2.8% to 47% (7, 8). Moreover, according to the World Health Organization's 2018 annual update of the Blueprint List of Priority Diseases, SFTS is one of the top 10 infectious diseases that demand priority attention (9). Because there is no effective treatment or vaccine to combat this disease, symptomatic and supportive care is essential for patient management, making it necessary for frontline clinicians to recognize patients at risk of life-threatening illness promptly.

It is well known that mathematical modeling of disease progression can help in predicting the success of clinical trials. The nomogram has gained acceptance as a trustworthy statistical tool in recent times. A nomogram is a simple visual graph that uses multiple key parameters to create a statistical model to quantify the risk of a clinical event (10, 11). Nomograms are frequently used in clinical settings to determine and decipher prognostic outcomes in various diseases, such as cancers and coronavirus disease (12–14). Although recent studies have reported the use of nomograms based on demographic and laboratory data to predict the prognosis of SFTS, no study has included viral load, which is more important in influencing the prognosis, compared with other risk factors. This study aimed to develop an accurate and simple model based on viral load and other factors, providing frontline clinicians with a convenient tool for early identification of critically ill patients and initiation of an optimal personalized treatment in a timely manner.

2 Materials and methods

2.1 Study participants

Between June 2018 and August 2023, 254 patients with SFTS confirmed by laboratory testing who were admitted to the Affiliated Chaohu Hospital of Anhui Medical University were included in this study. The inclusion criteria were as follows: (1) positive serum nucleic acid test and specific viral load and (2) hospitalization for at least 72 h. The exclusion criteria were as follows: (1) age < 18 years; (2) laboratory-confirmed infections with other pathogens, such as Hantaan virus, *Orientia tsutsugamushi*, and rickettsia; (3) history of hematological disorders; and (4) missing clinical data. Finally, 200 patients were enrolled in this study. Because this disease is prevalent in rural areas, many local medical institutions do not have relevant equipment to detect the viral load and have to send samples to the Centers for Disease Control and Prevention or large tertiary hospitals. Therefore, we divided the patients into two groups: with viral load and without viral load. Comparing the detection accuracy of the.

Two models will provide an extra choice and reference for locations where viral RNA load testing for SFTSV is unavailable (Figure 1). The patients were then divided into 165 survivors and 35 non-survivors based on their clinical outcome following admission. The study protocol complied with the Declaration of Helsinki and was approved by the hospital's ethics review board (No. KYXM-202303-025).

2.2 Data gathering

We gathered the patient demographic information (sex, age, illness duration, and outcome), presenting clinical signs, and results of initial post-admission laboratory tests [viral load, routine blood, liver and kidney functions, C-reactive protein (CRP), etc.] from an electronic system. The endpoints observed in this investigation were discharge on better terms or death.

2.3 Statistical analysis

Statistical analyses were performed using SPSS version 26 (SPSS Inc., Chicago, IL, United States) and R (version 4.2.2). Comparisons between groups were carried out using two independent samples *t*-tests on measurement data with a normal distribution, which are presented as mean ± standard deviation. Chi-square tests were used to assess categorical variables, which are reported as percentages (*n*, %). Measurement data with a non-normal distribution are presented as medians with interquartile ranges and compared using the Mann–Whitney *U* test. Independent risk factors were identified using univariate and multivariate logistic regression analyses to predict mortality rates. Statistical significance was set at $p < 0.05$.

Two nomograms were developed using independent risk factors for mortality prognosis. We calculated the area under the receiver operating characteristic curve (AUC) of the two nomograms to test model discrimination, and net reclassification improvement (NRI) and integrated discrimination improvement (IDI) were used to assess improvements in risk prediction and measure the usefulness of the new models (15, 16). The calibration curves of the two models indicated excellent concordance, and the net benefit at various threshold probabilities was measured using decision curve analysis.

3 Results

3.1 Demographic and laboratory indicators

In total, 200 patients met the inclusion criteria (53% female), 17.5% of whom died during hospitalization. The median age of all patients was 71 (range, 59–76) years, and the average time from

Abbreviations: APTT, Activated partial thromboplastin time; AUC, Area under the receiver operating characteristic curve; CI, Confidence interval; CK, Creatine kinase; CK-MB, CK-MB isoenzyme; CRP, C-reactive protein; IDI, Integrated discrimination improvement; NRI, Net reclassification improvement; OR, Odds ratio; PT, Prothrombin time; SFTS, Severe fever with thrombocytopenia syndrome; SFTSV, SFTS virus.

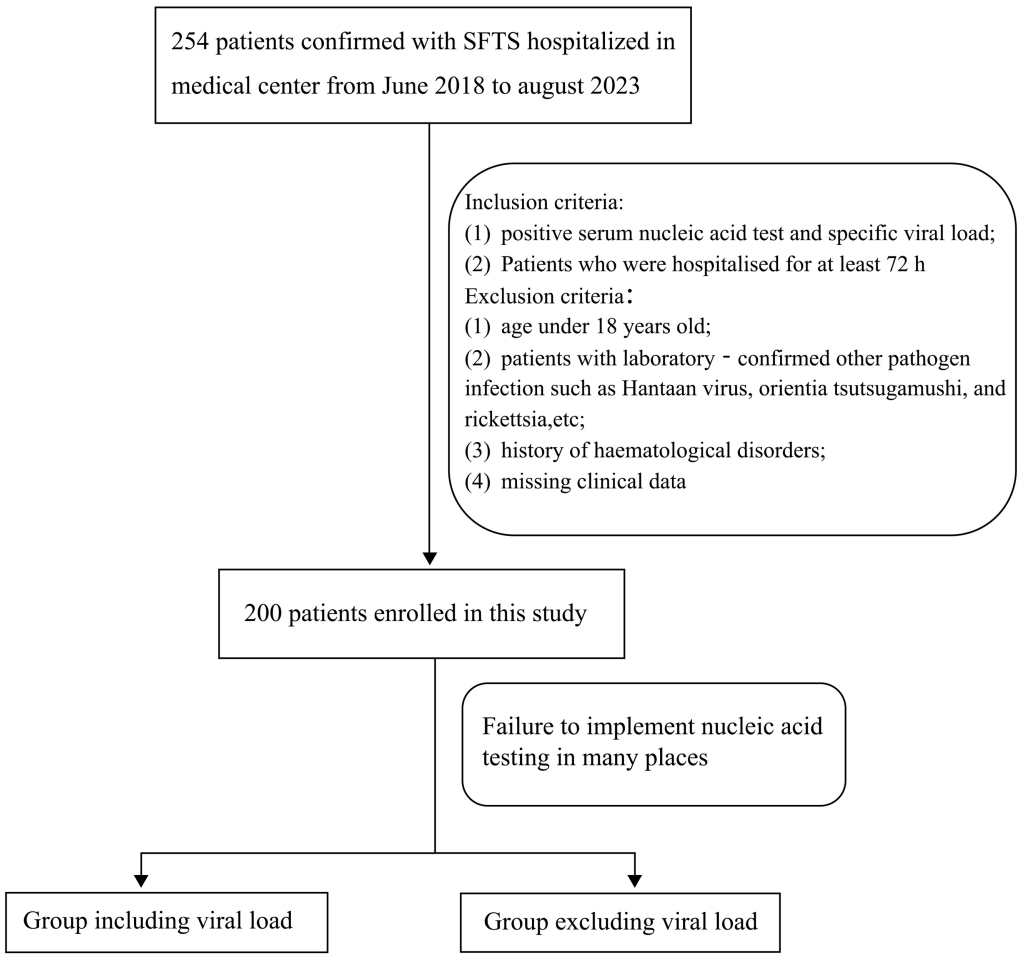

FIGURE 1
Flow diagram of study profile.

symptom onset to hospitalization was 4 (range, 3–5) days. The majority of the patients lived in rural areas (78%) and were farmers (76%). Approximately one-quarter (32.5%) had a clear history of tick bites, and less than half (46.5%) had underlying diseases such as hypertension, coronary heart disease, or chronic hepatitis at the time of admission. A high incidence of the SFTS was observed between April and October of each year. The patients were stratified into mortality and survival groups, with only age being significantly different between these groups ($p < 0.05$). Among all patients, 97.5% had fever, 66% fatigue, 74% anorexia, and 41% nausea or vomiting. Eleven clinical symptoms and indicators were compared between the survival and mortality groups. According to these findings, the incidence of bleeding manifestations was significantly higher in the mortality group than in the survival group [18/35 (51.4%) vs. 20/165 (12.1%), $p < 0.001$]. In contrast, the incidence of consciousness disorders was significantly higher in the mortality group than in the survival group [17/35 (48.6%) vs. 32/165 (19.4%), $p < 0.001$]. Bleeding manifestations included skin petechiae, as well as oral, gastrointestinal, and pulmonary bleeding. Consciousness disorders included drowsiness, blurred consciousness, and severe impairment of consciousness (no Glasgow Coma Score examination was performed). Fever, exhaustion, anorexia, and any other symptoms did not significantly differ between the two groups ($p > 0.05$) (Table 1).

3.2 Laboratory parameters

Most patients had leukopenia, thrombocytopenia, elevated liver enzyme levels, and myocardial impairment. Lymphocyte count, platelet count, and albumin level were significantly lower; levels of aspartate aminotransferase, creatine kinase (CK), CK-MB isoenzyme (CK-MB), lactate dehydrogenase, blood urea nitrogen, serum creatinine, uric acid, activated partial thromboplastin time (APTT), D-dimer, CRP, procalcitonin, and viral load were significantly higher; and prothrombin time (PT) was longer but within the normal range, in the mortality group than in the survival group, while the other biological indicators showed no differences between the two groups (Table 2).

3.3 Screening of predictors

Univariable logistic regression analysis revealed that older age; hemorrhagic manifestation; disturbance of consciousness; reduced platelet count; elevated levels of aspartate aminotransferase, CK, CK-MB, lactate dehydrogenase, blood urea nitrogen, serum creatinine, uric acid, PT, APTT, D-dimer, CRP, procalcitonin, albumin, and viral load were risk factors for mortality (Figure 2).

TABLE 1 Comparison of demographics and clinical characteristics between the two groups.

Variables	Total	Fatal		*p*-value
		No	Yes	
No.	200	165	35	
Age (years)	71(59–76)	70 (57–75)	76 (73–79)	<0.001
Days of onset (days)	4 (3–5)	4 (3–5)	4 (3–5)	0.332
Female (%)	106 (53)	89 (53.9)	17 (48.6)	0.563
Smoking (%)	32 (16)	24 (14.5)	8 (22.9)	0.223
Alcohol (%)	30 (15)	22 (13.3)	8 (22.9)	0.152
Operation history (%)	33 (16.5)	24 (14.5)	9 (25.7)	0.106
Epidemiology				
Residence, rural/urban, *n* (%)	156/44 (78/22)	126/39 (76.4/23.6)	30/5 (85.7/14.3)	(85.7/14.3) 0.225
Occupations, former/others *n* (%)	152/48 (76/24)	124/41 (75.2/24.8)	28/7 (80/20)	0.542
History of tick bite, *n* (%)	65 (32.5)	55 (33.3)	10 (28.6)	0.585
Underlying diseases, *n* (%)	93 (46.5)	72 (43.6)	21 (60)	0.078
Clinical symptoms, *n* (%)				
Fever	195 (97.5)	160 (97.0)	35 (100)	0.297
Fatigue	132 (66)	107 (64.8)	25 (71.4)	0.455
Anorexia	148 (74)	119 (72.1)	29 (82.9)	0.188
Nausea/vomiting	82 (41)	65 (39.4)	17 (48.6)	0.316
Myalgia	100 (50)	83 (50.3)	17 (48.6)	0.852
Diarrhea	80 (40)	64 (38.8)	16 (45.7)	0.447
Dizzy	35 (17.5)	29 (17.6)	6 (17.1)	0.951
Headache	30 (15)	23 (13.9)	7 (20)	0.362
Enlargement of lymph nodes	50 (25)	43 (26.1)	7 (20)	0.452
Bleeding manifestations	38 (19)	20 (12.1)	18 (51.4)	<0.001
Disturbance of consciousness	49 (24.5)	32 (19.4)	17 (48.6)	<0.001

Multivariable logistic regression analysis was performed to identify variables that could predict critical illness in patients with SFTS (Table 3). In the group with viral load, the variables associated with poor prognosis were older age, hemorrhagic manifestations, prolonged APTT, and viral load ($p \leq 0.001$ for all) (Table 3). In the group without viral load, the variables related to poor prognosis were older age, hemorrhagic manifestations, and prolonged APTT ($p < 0.001$ for all) (Table 3).

Based on the four factors identified in the group with viral load, a final nomogram predicting mortality risk in patients with SFTS was constructed (Figure 3A); another brief nomogram excluding the viral load was also constructed (Figure 3B). The AUC [0.926, 95% confidence interval (CI): 0.882–0.970 vs. 0.882, 95% CI: 0.823–0.942] and NRI (0.143, 95% CI: 0.036–0.285) were calculated and compared between the two models (Figure 4). In addition, we also calculated IDI (0.124, 95% CI, 0.061–0.186) between the two models. These results suggest that the former model is more accurate than the latter for predicting patient prognosis. Both calibration plots showed remarkable concordance between the predicted probability of mortality and actual observations, with mean absolute errors of 0.024 and 0.033, respectively (Figure 5). The decision curve analysis showed a potential net benefit with rather broad threshold probability distributions (Figure 6).

4 Discussion

SFTS is an emerging infectious disease caused by the *Dabie bandavirus* with a rapid progression and high fatality rate. Early identification of patients with poor prognosis is particularly important (8). Consequently, we conducted a retrospective examination of demographic data, clinical manifestations and symptoms, laboratory results, and indicators of mortality risk in 200 patients with SFTS. Since this disease is prevalent in rural areas and the cost of SFTSV testing equipment is high, many local healthcare facilities do not perform this test and thus, SFTSV results are not available in a timely manner. Therefore, we divided the patients into two groups based on whether the viral load was included and plotted nomograms. We aimed to compare the difference between the two groups regarding poor prognosis of SFTS and, at the same time, provide a reference for those who are unable to obtain viral load immediately. This study is the first to incorporate viral load into a model to predict the potential for poor prognosis in patients with SFTS, and better predictive accuracy was observed in the model that incorporated viral load (AUC: 0.926 vs. 0.882; NRI 0.143, 95% CI: 0.036–0.285; IDI 0.124, 95% CI: 0.061–0.186). According to Kwon et al. (17), there is a substantial difference in plasma viral RNA levels between survivors and non-survivors upon admission. Hayasaka et al. (18) performed a

TABLE 2 Comparison of laboratory test indicators between the two study groups.

Variables	Total	Fatal		*p*-value
		No	Yes	
No.	200	165	35	
Leukocytes, $\times 10^9$/L	2.36 (1.68–3.20)	2.36 (1.68–3.24)	2.39 (1.84–3.00)	0.953
Neutrophils, $\times 10^9$/L	1.49 (1.04–2.00)	1.44 (1.00–2.04)	1.76 (1.18–1.98)	0.177
Lymphocytes, $\times 10^9$/L	0.60 (0.44–0.83)	0.62 (0.45–0.86)	0.50 (0.39–0.64)	0.016
Monocytes, $\times 10^9$/L	0.15 (0.09–0.25)	0.16 (0.10–0.25)	0.12 (0.08–0.26)	0.417
Hemoglobin (g/L)	126.67 ± 17.92	126.90 ± 17.89	125.57 ± 18.23	0.602
Platelets, $\times 10^9$/L	60.75 ± 19.79	62.81 ± 19.92	51.03 ± 16.16	0.01
ALT (U/L)	54.0 (33.3–99.8)	52.0 (32.5–96.5)	64.0 (40.0–116.0)	0.242
AST (U/L)	135.5 (74.3–280.8)	122.0 (68.0–270.5)	208.0(143.0–512.0)	<0.001
GGT (U/L)	24.0 (16.0–40.8)	23.0 (15.5–38.5)	32.0 (19.0–45.0)	0.055
CK (U/L)	351 (147–844)	279 (142–644)	730 (226–1464)	0.002
CK-MB (U/L)	15.0 (6.4–30.0)	14.0 (5.0–25.1)	25.0 (15.0–51.8)	<0.001
LDH (U/L)	485 (313–853)	469.0 (311.5–822.5)	581 (423–1223)	0.0396
BUN (mmol/L)	7.0 (5.1–9.6)	6.7 (5.0–9.0)	10.0 (7.5–14.5)	<0.001
Creatinine (μmol/L)	77.0 (63.0–100.0)	74.0 (61.0–93.0)	100.0 (88.0–131.0)	<0.001
Uric acid (μmol/L)	275.5 (213.0–359.8)	269.0 (211.5–347.0)	347.0 (251.0–477.0)	0.001
PT (second)	11.83 ± 1.25	11.74 ± 1.26	12.24 ± 1.09	0.04
APTT (second)	45.36 ± 9.40	44.06 ± 8.87	51.53 ± 9.49	<0.001
Fibrinogen (g/L)	2.59 ± 0.62	2.60 ± 0.63	2.52 ± 0.58	0.726
D-dimer	2.71 (1.57–5.41)	2.38 (1.45–4.86)	4.85 (2.74–10.89)	0.001
Potassium (mmol/L)	3.74 ± 0.51	3.72 ± 0.52	3.83 ± 0.49	0.161
Sodium (mmol/L)	133.58 ± 3.91	133.58 ± 3.89	133.56 ± 4.09	0.776
Calcium (mmol/L)	1.98 ± 0.13	1.98 ± 0.13	1.95 ± 0.14	0.124
Albumin (g/L)	34.94 ± 4.28	35.44 ± 4.20	32.54 ± 3.89	<0.001
CRP (mg/L)	2.67 (0.67–7.42)	2.35 (0.50–5.32)	7.60 (3.26–9.56)	<0.001
PCT (ng/mL)	0.23 (0.11–0.54)	0.20 (0.11–0.44)	0.66 (0.29–2.27)	<0.001
Viral load (lg copy/mL)	4.77 (3.83–5.91)	4.50 (3.63–5.57)	6.15 (5.38–6.75)	<0.001

ALT, alanine transaminase; APTT, activated partial thromboplastin time; AST, aspartate aminotransferase; CRP, C-reactive protein; CK, creatine kinase; CK-MB, creatine kinase-MB isoenzyme; GGT, gamma-glutamyl transferase; LDH, lactate dehydrogenase; BUN, blood urea nitrogen; PCT, procalcitonin; PT, prothrombin time.

molecular imaging of SFTSV-induced infectious diseases in A129 mice infected with a lethal dose of the virus. The findings of this study support the idea that high viral load is a strong risk factor for catastrophic results in patients with SFTS. This may be related to the fact that high viral load induces higher levels of IFN-inducible protein-10 and macrophage inflammatory protein-1 while blocking the release of activated normal T cell-expressed and secreted factors, even more leading to severities or even death (19). Nevertheless, this investigation also indicated that advanced age was a significant contributor to SFTS mortality, consistent with previous reports. Qian et al. (20) constructed a risk model to forecast fatalities in patients with SFTS based on three high-risk variables: age, APTT, and CRP to lymphocyte ratio. According to research by Jung et al. (21), older age was linked to a higher 30 days mortality rate in patients with SFTS (adjusted hazard ratio: 1.10; 95% CI:1.04–1.17). This may be related to the prevalence of underlying disorders, reduced immunity, and higher incidence of morbidity and death in many older individuals. In addition, in ferrets with anatomical and physiological characteristics similar to those of humans, older ferrets infected with SFTSV were found to exhibit more severe clinical signs and higher mortality rates, than younger ferrets (22, 23). The three stages of the clinical course of SFTS are fever, multi-organ dysfunction, and convalescence. Jia et al. (24) discovered that APTT and thrombin time in patients that died were noticeably longer throughout the fever and multi-organ dysfunction stages and that APTT had high sensitivity and specificity in predicting mortality (84.85% and 81.65%, respectively). Song et al. (25) demonstrated a link between fatal outcomes in patients with SFTS and coma, pulmonary infection, high viral load, and prolonged APTT. In addition, Xu et al. (26) observed that prolonged APTT and bleeding manifestations were early independent warning factors for mortality, which is in line with our study. Additionally, we noticed that APTT was significantly prolonged in the mortality group ($p < 0.001$),

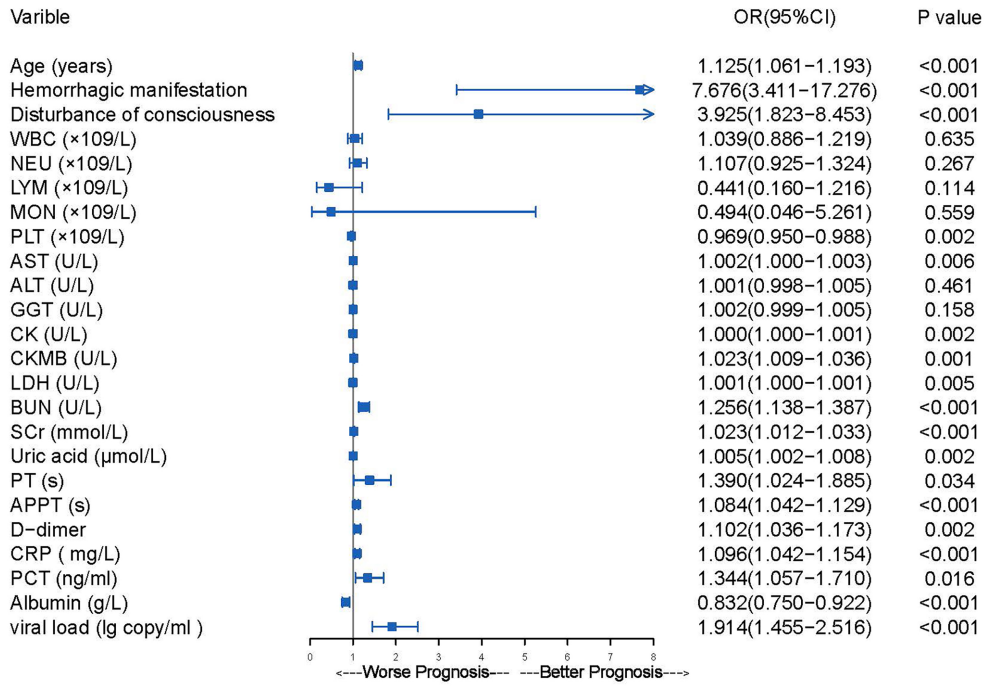

TABLE 3 Multivariable logistic regression analysis of the mortality risk in 200 patients with viral load.

(A) Group with viral load			
Variable	Coefficient (*B*)	OR (95% CI)	*p*-value
Age (years)	0.142	1.152 (1.058–1.255)	0.001
Hemorrhagic manifestations (Yes vs. No)	2.524	12.474 (3.894–39.955)	<0.001
APPT (s)	0.152	1.164 (1.088–1.246)	<0.001
Viral load (lg copy/mL)	0.778	2.178 (1.494–3.176)	<0.001

(B) Group without viral load			
Variable	Coefficient (*B*)	OR (95% CI)	*p*-value
Age (years)	0.140	1.150 (1.064–1.242)	<0.001
Hemorrhagic manifestations (Yes vs. No)	2.205	9.073 (3.259–25.260)	<0.001
APPT (s)	0.133	1.142 (1.079–1.208)	<0.001

APTT, activated partial thromboplastin time; OR, odds ratio; CI, confidence interval.

whereas PT was significantly different between the mortality and survival groups ($p = 0.034$); however, PT was within the normal range and not significantly prolonged. This may be related to the absence of coagulation factor XI, which Mizoe et al. (27) demonstrated to be the likely cause of APTT prolongation in SFTS. If APTT prolongation is triggered by coagulation factor deficits, plasma-derived or recombinant coagulation factors may serve as alternatives for the management of bleeding tendency (28, 29).

In line with the literature, our study revealed that bleeding symptoms were more frequent in the mortality group than in the survival group. This was the most significant risk factor of the parameters, both in the group with and without viral load [odds ratio (OR) 1 = 12.474; 95% CI: 3.894–39.955, OR 2 = 9.073; 95% CI: 3.259–25.260, respectively]. Li claimed that the emergence of hemorrhagic symptoms (adjusted OR = 2.79; $p < 0.001$) was a risk factor for SFTS mortality. The possible mechanisms of hemorrhagic signs as a risk factor for mortality may be thrombocytopenia and endothelial dysfunction (30). Patients with SFTS who experience severe thrombocytopenia may see a reduction in thrombin synthesis; in addition, SFTSV increases vascular permeability by destroying vascular endothelial cells, which are capable of causing extensive skin ecchymosis, as well as tissue and organ hemorrhages in patients with

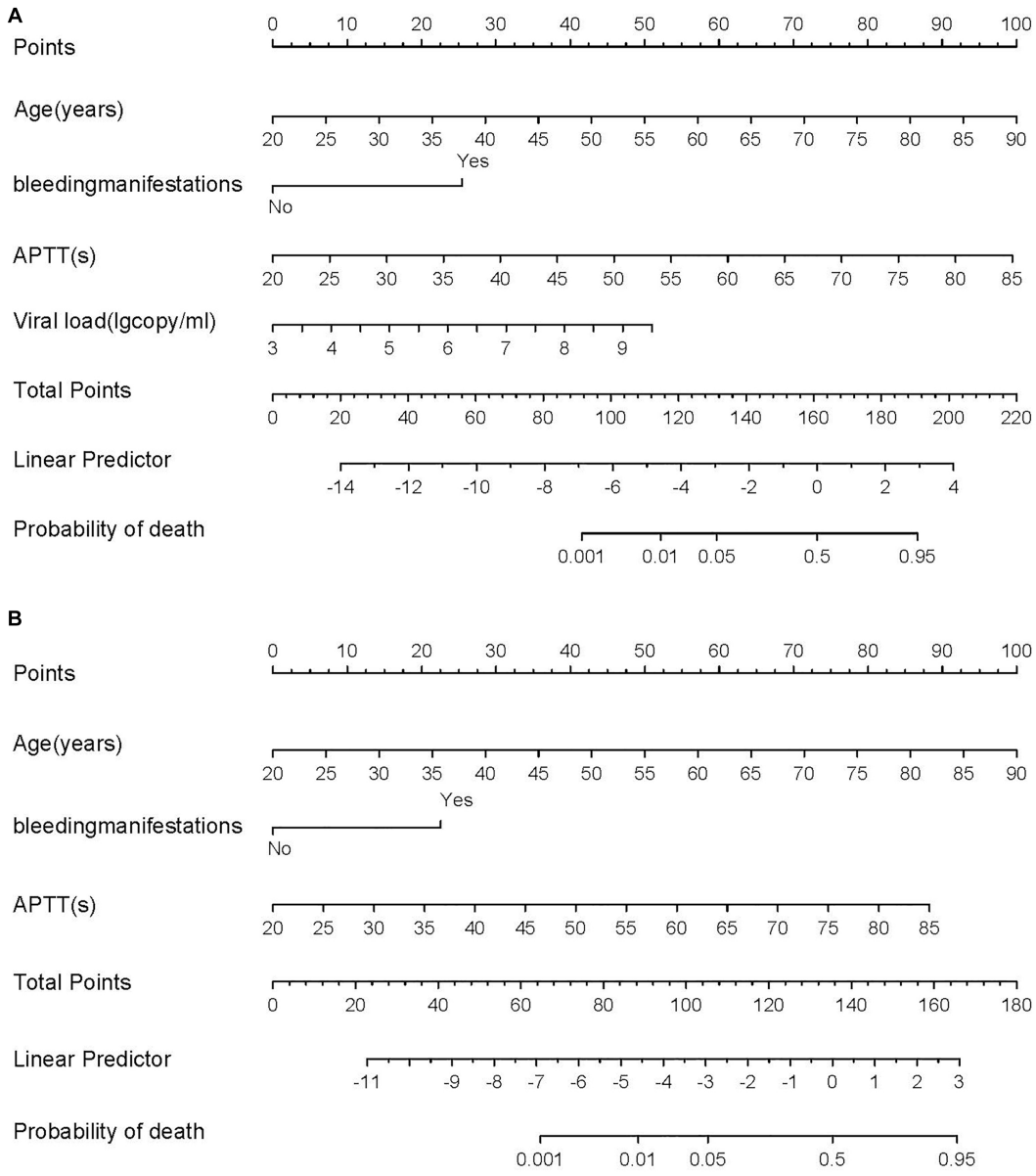

FIGURE 3
(A) The nomogram for predicting risk of death with SFTS. **(B)** The brief nomogram for predictor risk of death with SFTS.

SFTS (31, 32). Most importantly, practically all bleeding manifestations had a strong causal relationship with mortality, indicating the importance of regularly monitoring bleeding symptoms over the course of the illness.

This investigation established nomograms based on older age, presence of bleeding manifestations, prolonged APTT, and viral load. The models indicated the likelihood of critical illness in patients with SFTS, and our internal validation supported the model's efficacy. Analyzing risk factors can help predict severe illness, enabling proper care, and maximizing the use of available medical resources.

However, there are three limitations associated with the study design. First, because this was a single-center retrospective study, the quality and generalizability of the data may have been affected. Second, as APTT prolongation is a risk factor for predicting the prognosis of SFTS, SFTS in combination with other conditions that may cause APTT prolongation were not considered, such as antiphospholipid antibody syndrome, etc. Third, the models were not externally validated. For this reason, we are undertaking a prospective study in a larger cohort of patients with SFTS admitted to other healthcare facilities and after August 2023 to validate the predictive value of the model.

5 Conclusion

This study identified several risk variables for SFTS, including advanced age, presence of bleeding symptoms, prolonged APTT,

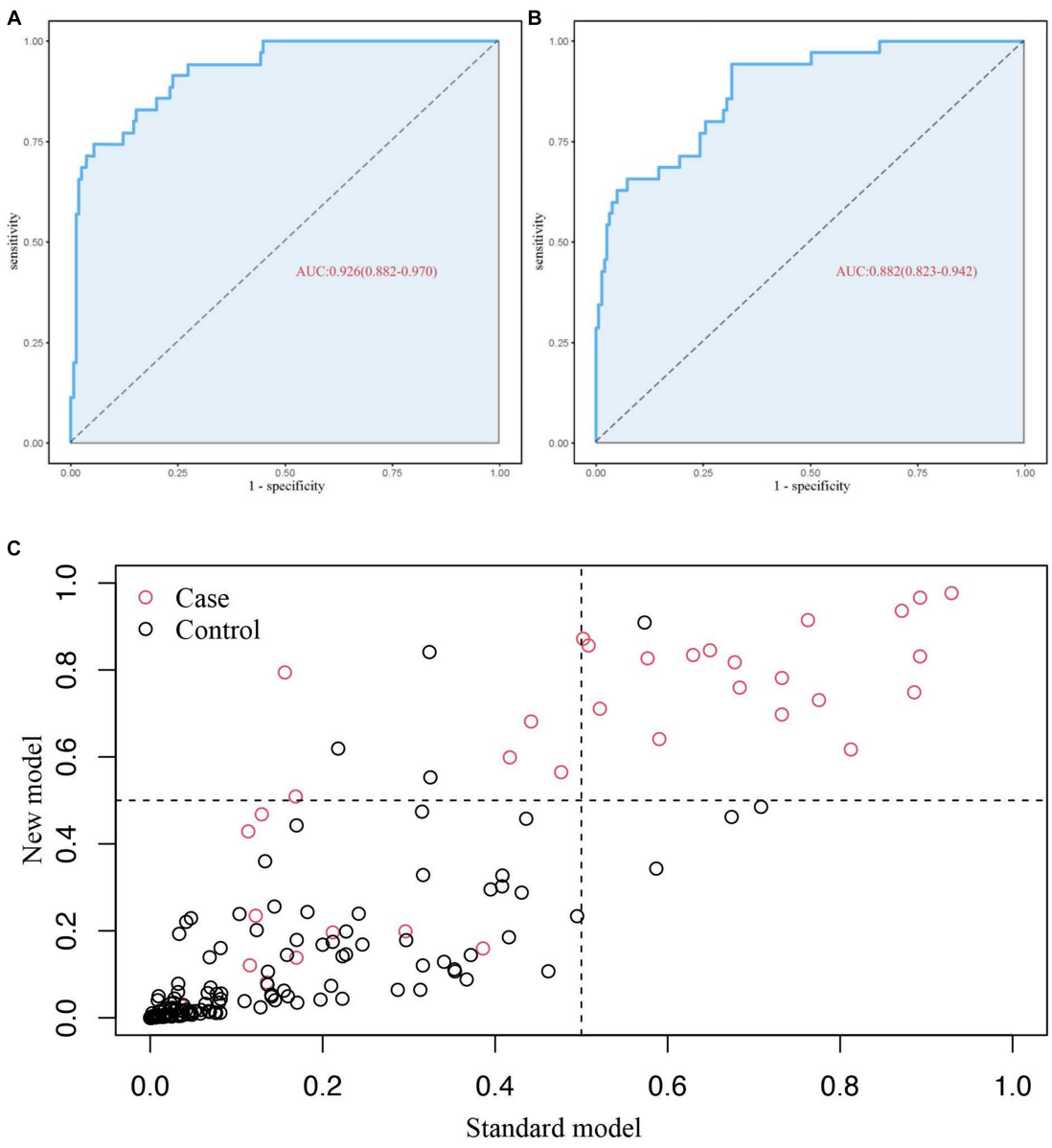

FIGURE 4
(A) ROC curve of 4 predictors, **(B)** ROC curve of 3 predictors, **(C)** the result graph NRI.

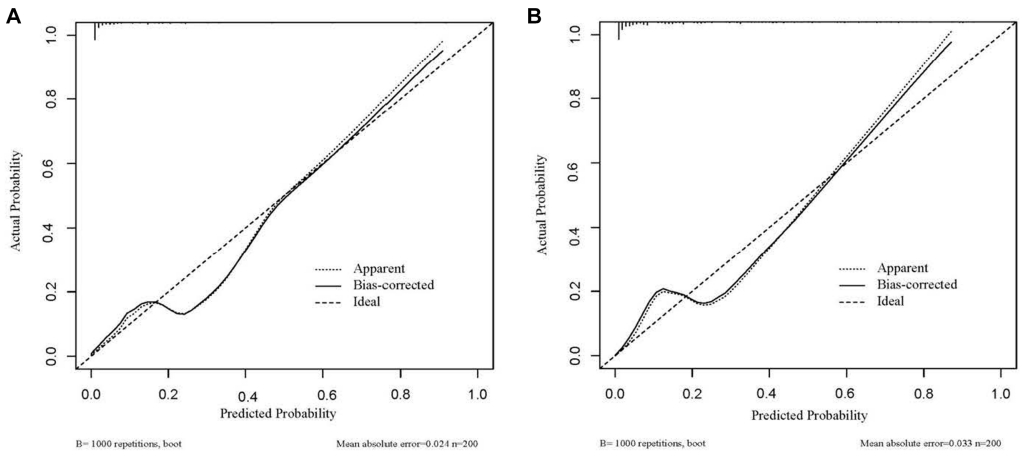

FIGURE 5
(A) The calibration curve of 4 predictors, **(B)** the calibration curve of 3 predictors.

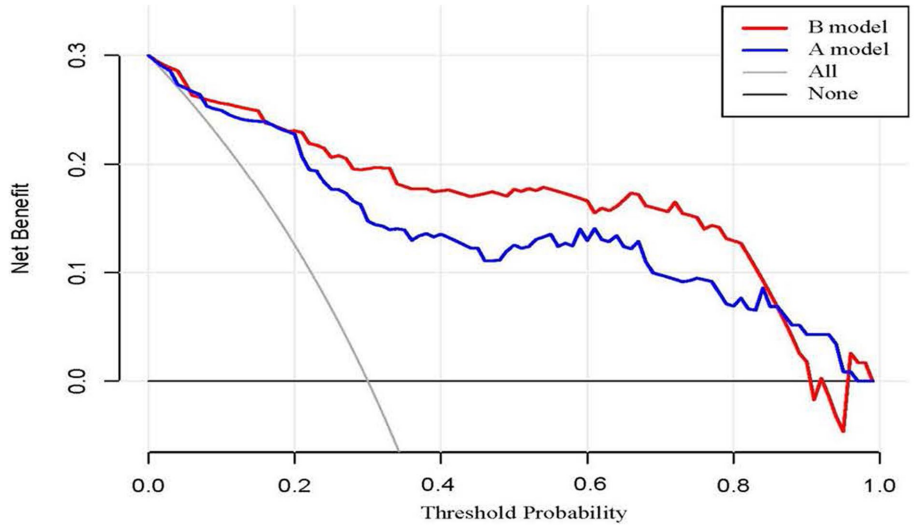

FIGURE 6
(A) DCA of 4 predictors, **(B)** DCA of 3 predictors.

and viral load. Two critical risk nomograms were developed based on these indicators for the early prediction of mortality risk in patients with SFTS, and enhanced predictive accuracy was observed in the model that incorporated viral load. The findings of this study may be of great significance for clinical applications.

Data availability statement

The original contributions presented in the study are included in the article/supplementary material, further inquiries can be directed to the corresponding author.

Ethics statement

The studies involving humans were approved by the Ethics Committee of the Affiliated Chaohu Hospital of Anhui Medical University (No. KYXM-202303-025). The studies were conducted in accordance with the local legislation and institutional requirements. The participants provided their written informed consent to participate in this study. Written informed consent was obtained from the individual(s) for the publication of any potentially identifiable images or data included in this article.

Author contributions

ZL: Writing – original draft, Writing– review & editing. ZZ: Writing – original draft, Writing – review & editing. CC: Data curation, Investigation, Writing – original draft.

Funding

The author(s) declare that no financial support was received for the research, authorship, and/or publication of this article.

Conflict of interest

The authors declare that the research was conducted in the absence of any commercial or financial relationships that could be construed as a potential conflict of interest.

Publisher's note

References

1. Yu XJ, Liang MF, Zhang SY, Liu Y, Li JD, Sun YL, et al. Fever with thrombocytopenia associated with a novel bunyavirus in China. *N Engl J Med*. (2011) 364:1523–32. doi: 10.1056/NEJMoa1010095

2. Hughes HR, Adkins S, Alkhovskiy S, Beer M, Blair C, Calisher CH, et al. ICTV virus taxonomy profile: *Peribunyaviridae*. *J Gen Virol*. (2020) 101:1–2. doi: 10.1099/jgv.0.001365

3. Kim KH, Yi J, Kim G, Choi SJ, Jun KI, Kim NH, et al. Severe fever with thrombocytopenia syndrome, South Korea, 2012. *Emerg Infect Dis*. (2013) 19:1892–4. doi: 10.3201/eid1911.130792

4. Takahashi T, Maeda K, Suzuki T, Ishido A, Shigeoka T, Tominaga T, et al. The first identification and retrospective study of severe fever with thrombocytopenia syndrome in Japan. *J Infect Dis*. (2014) 209:816–27. doi: 10.1093/infdis/jit603

5. Tran XC, Yun Y, Van An L, Kim SH, Thao NTP, Man PKC, et al. Endemic severe fever with thrombocytopenia syndrome, Vietnam. *Emerg Infect Dis*. (2019) 25:1029–31. doi: 10.3201/eid2505.181463

6. Win AM, Nguyen YTH, Kim Y, Ha NY, Kang JG, Kim H, et al. Genotypic heterogeneity of *Orientia tsutsugamushi* in scrub typhus patients and thrombocytopenia

syndrome co-infection, Myanmar. *Emerg Infect Dis*. (2020) 26:1878–81. doi: 10.3201/eid2608.200135

7. Li H, Lu QB, Xing B, Zhang SF, Liu K, Du J, et al. Epidemiological and clinical features of laboratory-diagnosed severe fever with thrombocytopenia syndrome in China, 2011–2017: a prospective observational study. *Lancet Infect Dis*. (2018) 18:1127–37. doi: 10.1016/S1473-3099(18)30293-7

8. Li J, Li S, Yang L, Cao P, Lu J. Severe fever with thrombocytopenia syndrome virus: a highly lethal bunyavirus. *Crit Rev Microbiol*. (2021) 47:112–25. doi: 10.1080/1040841X.2020.1847037

9. Mehand MS, Millett P, Al-Shorbaji F, Roth C, Kieny MP, Murgue B. World Health Organization methodology to prioritize emerging infectious diseases in need of research and development. *Emerg Infect Dis*. (2018) 24:e171427. doi: 10.3201/eid2409.171427

10. Park SY. Nomogram: an analogue tool to deliver digital knowledge. *J Thorac Cardiovasc Surg*. (2018) 155:1793. doi: 10.1016/j.jtcvs.2017.12.107

11. Pan Z, You H, Bu Q, Feng X, Zhao F, Li Y, et al. Development and validation of a nomogram for predicting cancer-specific survival in patients with Wilms' tumor. *J Cancer*. (2019) 10:5299–305. doi: 10.7150/jca.32741

12. Zhang W, Ji L, Wang X, Zhu S, Luo J, Zhang Y, et al. Nomogram predicts risk and prognostic factors for bone metastasis of pancreatic cancer: a population-based analysis. *Front Endocrinol*. (2021) 12:752176. doi: 10.3389/fendo.2021.752176

13. Massaccesi M, Dinapoli N, Fuga V, Rupe C, Panfili M, Calandrelli R, et al. A predictive nomogram for trismus after radiotherapy for head and neck cancer. *Radiother Oncol*. (2022) 173:231–9. doi: 10.1016/j.radonc.2022.05.031

14. Liu L, Xie J, Wu W, Chen H, Li S, He H, et al. A simple nomogram for predicting failure of non-invasive respiratory strategies in adults with COVID-19: a retrospective multicentre study. *Lancet Digit Health*. (2021) 3:e166–74. doi: 10.1016/S2589-7500(20)30316-2

15. Pencina MJ, D'Agostino RB Sr, Steyerberg EW. Extensions of net reclassification improvement calculations to measure usefulness of new biomarkers. *Stat Med*. (2011) 30:11–21. doi: 10.1002/sim.4085

16. Wu J, Zhang H, Li L, Hu M, Chen L, Xu B, et al. A nomogram for predicting overall survival in patients with low-grade endometrial stromal sarcoma: a population-based analysis. *Cancer Commun*. (2020) 40:301–12. doi: 10.1002/cac2.12067

17. Kwon JS, Kim MC, Kim JY, Jeon NY, Ryu BH, Hong J, et al. Kinetics of viral load and cytokines in severe fever with thrombocytopenia syndrome. *J Clin Virol*. (2018) 101:57–62. doi: 10.1016/j.jcv.2018.01.017

18. Hayasaka D, Nishi K, Fuchigami T, Shiogama K, Onouchi T, Shimada S, et al. 18F-FDG PET imaging for identifying the dynamics of intestinal disease caused by SFTSV infection in a mouse model. *Oncotarget*. (2016) 7:140–7. doi: 10.18632/oncotarget.6645

19. He Z, Wang B, Li Y, Hu K, Yi Z, Ma H, et al. Changes in peripheral blood cytokines in patients with severe fever with thrombocytopenia syndrome. *J Med Virol*. (2021) 93:4704–13. doi: 10.1002/jmv.26877

20. Qian F, Zhou W, Liu Y, Ge Z, Lai J, Zhao Z, et al. High C-reactive protein to lymphocyte ratio predicts mortality outcomes of patients with severe fever with thrombocytopenia syndrome: a multicenter study in China. *J Med Virol*. (2023) 95:e28546. doi: 10.1002/jmv.28546

21. Jung SI, Kim YE, Yun NR, Kim CM, Kim DM, Han MA, et al. Effects of steroid therapy in patients with severe fever with thrombocytopenia syndrome: a multicenter clinical cohort study. *PLoS Negl Trop Dis*. (2021) 15:e0009128. doi: 10.1371/journal.pntd.0009128

22. Kim YI, Kim SG, Kim SM, Kim EH, Park SJ, Yu KM, et al. Infection and rapid transmission of SARS-CoV-2 in ferrets. *Cell Host Microbe*. (2020) 27:704. doi: 10.1016/j.chom.2020.03.023

23. Park SJ, Kim YI, Park A, Kwon HI, Kim EH, Si YJ, et al. Ferret animal model of severe fever with thrombocytopenia syndrome phlebovirus for human lethal infection and pathogenesis. *Nat Microbiol*. (2019) 4:438–46. doi: 10.1038/s41564-018-0317-1

24. Jia B, Yan X, Chen Y, Wang G, Liu Y, Xu B, et al. A scoring model for predicting prognosis of patients with severe fever with thrombocytopenia syndrome. *PLoS Negl Trop Dis*. (2017) 11:e0005909. doi: 10.1371/journal.pntd.0005909

25. Song L, Zhao Y, Wang G, Huang D, Sai L. Analysis of risk factors associated with fatal outcome among severe fever with thrombocytopenia syndrome patients from 2015 to 2019 in Shandong, China. *Eur J Clin Microbiol Infect Dis*. (2022) 41:1415–20. doi: 10.1007/s10096-022-04506-4

26. Xu X, Sun Z, Liu J, Zhang J, Liu T, Mu X, et al. Analysis of clinical features and early warning indicators of death from severe fever with thrombocytopenia syndrome. *Int J Infect Dis*. (2018) 73:43–8. doi: 10.1016/j.ijid.2018.05.013

27. Mizoe A, Sakaue J, Takahara N. Why does activated partial thromboplastin time prolongation occur in severe fever with thrombocytopenia syndrome? *BMJ Case Rep*. (2020) 13:e235447. doi: 10.1136/bcr-2020-235447

28. Peters R, Harris T. Advances and innovations in haemophilia treatment. *Nat Rev Drug Discov*. (2018) 17:493–508. doi: 10.1038/nrd.2018.70

29. Menegatti M, Peyvandi F. Treatment of rare factor deficiencies other than hemophilia. *Blood*. (2019) 133:415–24. doi: 10.1182/blood-2018-06-820738

30. Li XK, Yang ZD, Du J, Xing B, Cui N, Zhang PH, et al. Endothelial activation and dysfunction in severe fever with thrombocytopenia syndrome. *PLoS Negl Trop Dis*. (2017) 11:e0005746. doi: 10.1371/journal.pntd.0005746

31. Yu CI, Becker C, Metang P, Marches F, Wang Y, Toshiyuki H, et al. Human CD141^{+} dendritic cells induce CD4^{+} T cells to produce type 2 cytokines. *J Immunol*. (2014) 193:4335–43. doi: 10.4049/jimmunol.1401159

32. Jeong EJ, Song JY, Lim CS, Lee I, Park MS, Choi MJ, et al. Viral shedding from diverse body fluids in a patient with severe fever with thrombocytopenia syndrome. *J Clin Virol*. (2016) 80:33–5. doi: 10.1016/j.jcv.2016.04.018

frontiers | Frontiers in Medicine

TYPE Case Report
PUBLISHED 07 December 2023
DOI 10.3389/fmed.2023.1286649

OPEN ACCESS

EDITED BY
Pierpaolo Di Micco,
Ospedale Santa Maria delle Grazie, Italy

REVIEWED BY
Apurva Patel,
Gujarat Cancer & Research Institute, India
Carmine Siniscalchi,
University of Parma, Italy

*CORRESPONDENCE
Xiangchen Gu
✉ gettygugu@126.com
Yan-Qiu Xu
✉ xuyanqiu1781@163.com

RECEIVED 31 August 2023
ACCEPTED 16 November 2023
PUBLISHED 07 December 2023

CITATION
Xie G-L, Wang X-S, Hu L-Y, Wang Y, Gu X and Xu Y-Q (2023) Myelodysplastic syndrome-like response after voriconazole treatment of systemic lupus erythematosus complicated with fungal infection: a case report.
Front. Med. 10:1286649.
doi: 10.3389/fmed.2023.1286649

Myelodysplastic syndrome-like response after voriconazole treatment of systemic lupus erythematosus complicated with fungal infection: a case report

Guang-Liang Xie[1], Xiao-Su Wang[2], Ling-Yan Hu[3], Yi Wang[1], Xiangchen Gu[1,4,5]* and Yan-Qiu Xu[1]*

[1]Department of Nephrology, Yueyang Hospital of Integrated Traditional Chinese Medicine and Western Medicine, Shanghai University of Traditional Chinese Medicine, Shanghai, China, [2]Department of Gastroenterology, Yueyang Hospital of Integrated Traditional Chinese Medicine and Western Medicine, Shanghai University of Traditional Chinese Medicine, Shanghai, China, [3]Department of Hematology, Yueyang Hospital of Integrated Traditional Chinese Medicine and Western Medicine, Shanghai University of Traditional Chinese Medicine, Shanghai, China, [4]Department of Nephrology, Ruijin Hospital, Shanghai Jiaotong University School of Medicine, Shanghai, China, [5]Department of Medicine, Shanghai Hospital of Civil Aviation Administration of China, Shanghai, China

Background: Voriconazole is mainly used to treat progressive and potentially life-threatening infections in immunocompromised patients. The adverse drug reactions related to voriconazole are varied. In some rare cases, the use of voriconazole can result in myelodysplastic syndrome (MDS)-like adverse reactions.

Case presentation: Here, we present a rare case of systemic lupus erythematosus patient with a fungal infection that developed MDS-like adverse reactions after treatment with voriconazole. The patient was admitted to the hospital because of 3 days of chest tightness and dyspnea. After the admission, the patient's sputum culture showed *Candida albicans* infection, and voriconazole was prescribed to be taken orally. After using voriconazole, drug-related adverse reactions such as visual impairment, nausea, vomiting, hiccup, middle and lower abdominal pain, disorders of consciousness, delirium, hallucination, slow response, and subcutaneous ecchymosis appeared, as well as the gradually increased serum creatinine, oliguria, and aggravated lower limb edema. In addition, there was a decrease in peripheral blood cells, and MDS-like changes in bone marrow were indicated by bone marrow biopsy. After discontinuing voriconazole, drug-related adverse symptoms disappeared, and hematocytopenia and the changes in MDS were significantly improved, which was confirmed by a subsequent bone marrow puncture at a 6 months interval.

Conclusion: This case reminded us that when using voriconazole for treatment, individual differences in patients should be considered, and the blood concentration of voriconazole should be closely monitored. Otherwise, potential drugs that affect voriconazole metabolism should be noted, and related adverse symptoms of patients should be closely observed during medication to reduce the occurrence of adverse drug events.

KEYWORDS

voriconazole, myelodysplastic syndrome, hematocytopenia, adverse drug reaction, case report, systemic lupus erythematosus

Introduction

Voriconazole is primarily used to treat progressive and potentially life-threatening infections in immunocompromised patients. As a broad-spectrum triazole antifungal drug, voriconazole prevents the biosynthesis of ergosterol and produces antifungal effects by inhibiting the demethylation of 14a-sterols which is mediated by cytochrome P450 in fungi. In the human body, voriconazole is primarily metabolized in the liver while inhibiting the liver cytochrome P450 system. 80% of the metabolites are excreted in the urine, and 20% are excreted in the feces. This medication is efficient in treating invasive fungal *Aspergillus* and *Candida* infections. Most patients have a high tolerance for triazole antifungal medications. The most frequent side events, which are often mild to moderate, are vision impairment, fever, rash, nausea, vomiting, diarrhea, headache, hallucinations, peripheral edema, and abdominal discomfort (1–3). The most frequent side effects associated with medication withdrawal include liver failure, rash, and vision impairment. Additionally, gastrointestinal issues, such as nausea, abdominal pain, vomiting, and diarrhea, are the most often reported adverse events in clinical settings. The most frequent side effects of voriconazole were transient visual impairment (23% of patients), fever (12%), diarrhea (9%), and vomiting (7%) in a randomized, double-blinded, multicenter safety and tolerability study (4). The rate of adverse responses associated with voriconazole treatment was 18.5% (22/119), in another multicenter observational study evaluating the treatment of invasive aspergillosis in adults with voriconazole. Serious adverse reactions include hallucinations, toxic nephropathy, neurotoxicity, hepatotoxicity, psychogenic encephalopathy, liver side effects (10.1%), and nephrotoxicity (3.4%) (5). Moreover, the most recent voriconazole instruction manual refers to "rare adverse reactions" involving various systems, including myelodysplastic syndrome (MDS). However, clinical reports of voriconazole-related MDS-like reactions were rare. Herein, we report a case of a patient with systemic lupus erythematosus who had a fungal infection and experienced MDS-like following voriconazole therapy.

Case presentation

A 73 years-old man was admitted to the hospital after experiencing dyspnea and chest tightness for 3 days. He has a 6 years history of gout, 5 years history of coronary heart disease, and a 2 years history of hypertension. He had long been treated for his disease with nifedipine GITS, clonidine, bisoprolol, and febuxostat. In addition, he received a diagnosis of systemic lupus erythematosus (SLE) due to skin erythema, photosensitivity, joint pain, positive for anti-dsDNA (228.65, normal <71 U/mL), anti-ANA (1.80), anti-Ro52 (99, normal <25), and decreases in complement C3 (0.574, normal 0.9–1.8 g/L) and C4 (0.088, normal 0.1–0.4 g/L) 2 years prior to admission and was taking prednisone 10 mg and hydroxychloroquine 100 mg daily, respectively. The patient's laboratory results are displayed in Table 1.

After admission, the pulmonary computer tomography (CT) scan was performed, and the results revealed pulmonary interstitial changes, pulmonary edema, and a small amount of pleural effusion on both sides, and his blood oxygen saturation was 75% (93% after oxygen inhalation), and the pulmonary infection was treated with cefminox sodium, piperacillin/tazobactam, and meropenem successively. Otherwise, a total of 120 grams of human immunoglobulin were administered to help improve the immune system of the patient.

The patient was given oral voriconazole (200 mg/day) for 25 days after the patient's sputum culture revealed *Candida albicans* infection and the serum (1,3)-β-D-glucan (+) (542 pg/mL, normal <60 pg/mL). Following the administration of voriconazole, we noticed a progressive decline in the patient's hemoglobin, leukocyte, and platelet counts in the patient's CBC test (Figure 1), accompanied by symptoms including visual impairment，nausea, vomiting, hiccups, middle and lower abdominal pain, disorders of consciousness, delirium, hallucination, slow response, and subcutaneous ecchymosis. AKI diagnosis criteria were also met by the patient's oliguria, gradually rising serum creatinine level, aggravated pleural effusion, and lower limb edema. The patient was treated with hemodialysis and intravenous methylprednisolone (40 mg) daily. When renal function, heart failure, pleural effusion, and edema rapidly improved and urine volume returned to above 1,000 mL per day, hemodialysis was discontinued. The patient's hemoglobin, leukocyte, and platelets gradually increased once the voriconazole was discontinued. At a follow-up of 14 days, we observed that these markers continued to improve.

During the course of the patient's treatment, red blood cells (600 mL), fresh frozen plasma (800 mL), and platelet concentrate (400 mL) were transfused. The blood alterations are depicted in Figure 1, but there was no discernible improvement in stopping the decreasing trend of blood cell count. We performed a bone marrow biopsy the day after discontinuing voriconazole to rule out any potential pathology that might cause hematopenia. Bone marrow aspirate showed active bone marrow hyperplasia. Nucleated cells proliferated actively, and the ratio of granulocytes to red blood cells was 0.387:1. Granular proliferation decreased, accounting for 27.5% of nuclear cells, with primitive cells accounting for 4.5%, the proliferation was mainly characterized by neutrophils, late promyelocytes, rod-shaped nuclei, and lobulated nuclei, with no abnormalities in morphology or size. Erythrocytosis was extremely active, accounting for 71% of nuclear cells, among them, primary red blood accounts for 5.5%, mainly consisting of proliferation of middle and late erythroblasts, imbalance in nuclear and cytoplasmic development, nuclear abnormalities, and megaloblastic transformation of erythroblasts could be observed, the size of mature red blood cells varies significantly, pathological hematopoiesis was very obvious. Megakaryocyte proliferation is very active with maturation disorders. Iron staining: external iron: 2 (+), internal iron: 80% iron granulosa erythrocytes. In addition, genetic testing was negative. Fluorescence *in situ* hybridization (FISH) was used to perform genetic testing on bone marrow aspirates and did not find any chromosomal abnormalities or gene deletions, including –7/7q–, +8, p53 (17p13.1), EGR1 (5q31), D20S108, etc. Flow cytometry detection of bone marrow (Figure 2A) showed that 1.6% of myeloid cells were primitive or immature. Microscope (Figures 2B,C) indicated that myelodysplastic syndrome (MDS) should be considered, erythroid hyperplasia is significantly active with megaloblastic transformation.

To ascertain whether the patient had fully recovered, we conducted another bone marrow puncture after a 6 months follow-up. The results of the second bone marrow aspiration revealed a significant reduction in the abnormal proliferation of erythroid, granulocytic, and megakaryocytic cells compared to the first, and no obvious MDS-like bone marrow abnormal proliferation was discovered. Flow cytometry

TABLE 1 Laboratory results of the patient.

Laboratory test	On admission	3 weeks after voriconazole treatment	2 weeks after voriconazole discontinuation
Hemoglobin (g/L)	84	48	71
WBC (×10^9/L)	2.4	1.4	3.9
Platelet (×10^9/L)	73	8	69
C-reactive protein (mg/L)	6.66	5.03	0.97
Creatinine (μmol/L)	290.0	580.1	218.8
Blood urea nitroge (mmol/L)	28.4	65.7	25.5
Uric acid (μmol/L)	405.5	421.0	366.2
ALT (U/L)	28	21	15
AST (U/L)	25	2	7
r-GT (U/L)	58	78	38.1
Anti-dsDNA (U/mL)	42	13	13
Complement C3 (g/L)	0.87	0.92	0.85
Anti-ANA	Negative	Negative	Negative

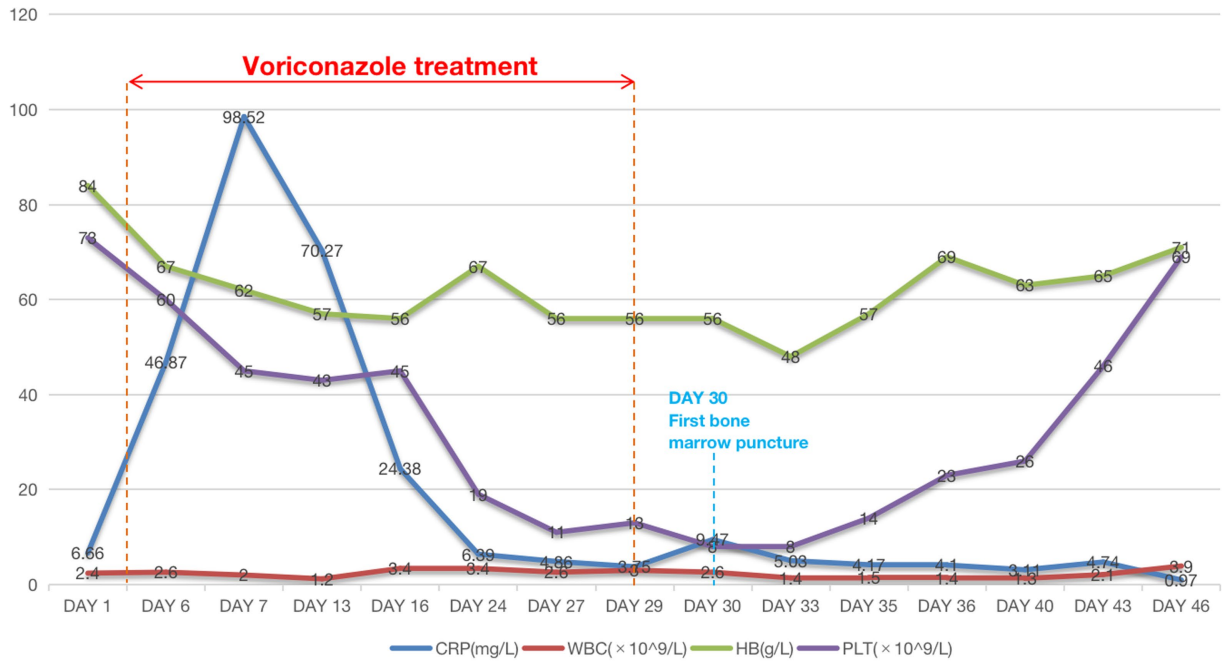

FIGURE 1
Changes in patient laboratory test results.

results (Figure 3A) demonstrated that no significant evidence of acute leukemia, NHL, or high-risk MDS-related immunophenotypic abnormalities were detected. Microscopic results bone marrow test was negative, no indication of MDS (Figures 3B,C).

Overall, when treating the patient with voriconazole during the first-hospital admission, we observed decreases in peripheral blood cells and diagnosed MDS-like changes in bone marrow by bone marrow puncture. After voriconazole withdrawal, drug-related side effects vanished, and the MDS alterations were significantly improved.

Discussion

The metabolism of voriconazole and the symptoms of adverse medication reactions differ dramatically between different races and individuals. Voriconazole metabolism *in vivo* exhibits a nonlinear pharmacokinetics characteristic, meaning that when the dosage is increased, the area under the drug time curve (AUC) increases sharply. The steady blood concentration was reached in about 5 days after intravenous or oral administration (6). In addition to being metabolized by liver cytochrome P450 Isozyme CYP2C19, CYP2C9,

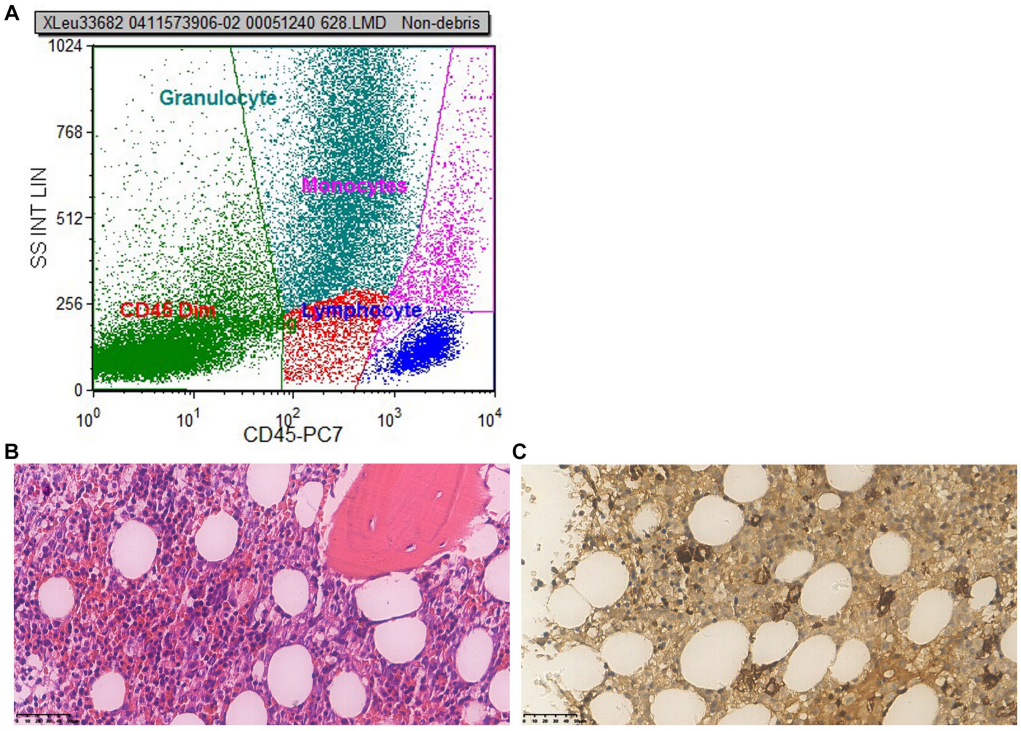

FIGURE 2
First bone marrow puncture results. **(A)** Flow cytometry: flow cytometry shows 1.6% of myeloid cells were primitive or immature. **(B)** Microscope (×400): the proliferation of nucleated red blood cells in the bone marrow is active, and primitive/immature cells are readily visible; the amount of erythrocytes increases, megaloblastic cells are easy to find; megakaryocytes are not decreased, no obvious collagen fibrosis in the bone marrow stroma. **(C)** Immunohistochemistry (×400): CD34 primitive/immature cells (+), accounting for 10%–15%, some of which are weak positive and tend to be erythroid precursor cells; megakaryocyte (+), small megakaryocytes and lymphoid small megakaryocytes are easily seen; MPO granulocyte (+); CD71 nucleated red blood cells (+); a small amount of CD20 B cells are scattered (+); CK (–); a small amount of NK cells in CD56 are scattered (+). Conclusion: myelodysplastic syndrome (MDS) should be taken into consideration, the erythroid hyperplasia is significantly active with megaloblastic transformation.

and CYP3A4, Voriconazole also inhibits these three enzymes. The pharmacokinetics of voriconazole vary significantly among individuals. *In vivo* studies have revealed that the main metabolic pathway, CYP2C19, exhibits genetic polymorphism with individual variations of up to 100 times. The population can be categorized into individuals with strong metabolism and individuals with weak metabolism based on the activity of this enzyme. While the prevalence of individuals with poor metabolisms ranges from 3% to 5% among Caucasians and African Americans, it can reach up to 15%–20% among Asians. In China, the phenotypes of people with weak CYP2C19 metabolism are nearly CYP2C19 * 2 and CYP2C19 * 3. According to research studies in healthy Caucasians and Japanese, the concentration of voriconazole in individuals with weaker metabolism within the same race was on average, four times greater in those with better metabolisms. The primary plasma metabolite of voriconazole is N-oxide, which accounts for approximately 72% of the total plasma. The half-life of voriconazole is around 6 h, and its distribution volume is 2–4.6 L/kg, indicating that it is broadly distributed in tissues. The genotype of CYP2C19 and the co-administration of medications that regulate the activity of CYP2C19, CYP2C9, and CYP3A4 could all have an impact on the blood concentration of voriconazole. The metabolism of CYP substrates may also be inhibited by voriconazole (7–10).

In this case, after taking voriconazole, this patient experienced symptoms of psychiatric encephalopathy, nausea, vomiting, hiccup, middle and lower abdominal pain, diarrhea, delirium, hallucinations, delayed response, and clinical signs such as progressive elevation of creatinine and renal toxicity, even blood cells counts and bone marrow also changed. These symptoms are consistent with the side effects listed in the instructions and early clinical studies. However, the majority of the side effects reported in previous clinical reports typically coexist with a few symptoms in a single patient. Nevertheless, in this case, the patient's use of voriconazole led to more complicated symptoms mentioned above, indicating the patient's susceptibility and intolerance to voriconazole's side effects.

It is important to highlight that this patient had a 2 years history of SLE. The phenomenon of SLE combined with hematological diseases has been widely reported in China. However, cases of combining with MDS are rare (11–13). The mechanism of bone marrow morphological changes in SLE patients is not yet elucidated. Some have suggested there are various antibodies against blood cells in the serum of SLE patients, which directly damage a certain lineage of hematopoietic progenitor cells or alter the bone marrow microenvironment, causing bone marrow dysplasia in SLE patients (14). MDS, which frequently arises during the active phase of SLE, has been linked to SLE in some studies (15, 16). Meanwhile, the patient

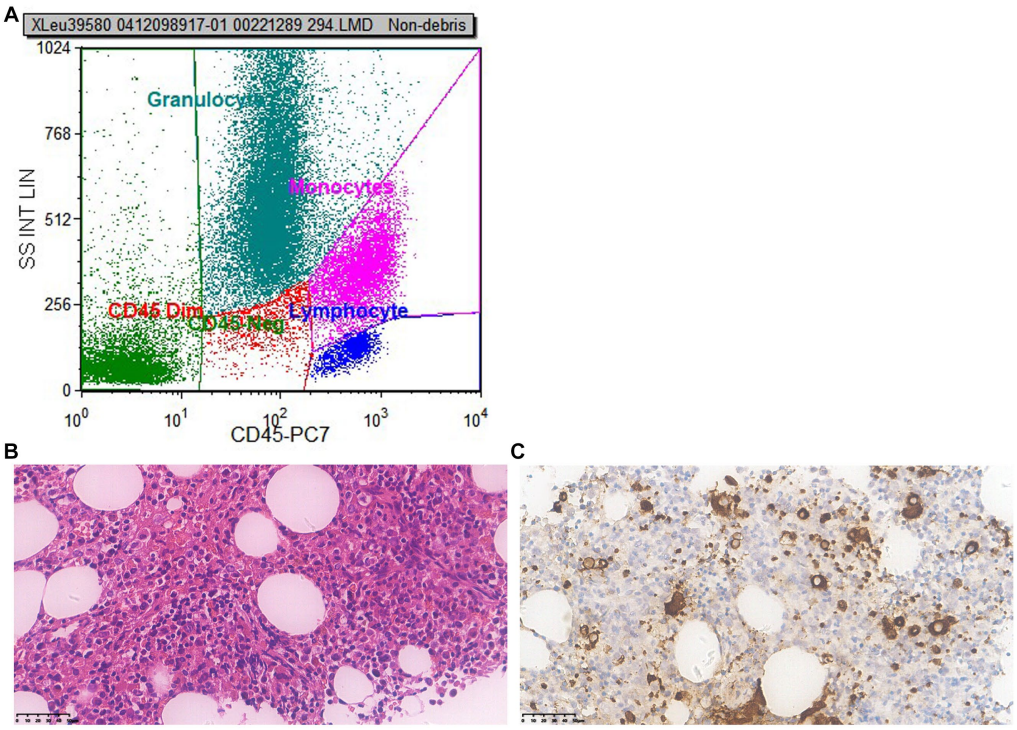

FIGURE 3
Second bone marrow puncture results 6 months later. **(A)** Flow cytometry: flow cytometry shows no significant evidence of acute leukemia, NHL, or high-risk MDS-related immunophenotypic abnormalities were detected. **(B)** Microscope (×400): the proliferation of nucleated red blood cells in the bone marrow is active; cells in all stages of the granulocyte lineage are visible, with the majority being cells in the more mature stage, while pale nucleus-like cells are easily visible; the number of red blood cells is small, mainly composed of middle to late-stage erythrocytes distributed in scattered and small clusters; the number of recognizable megakaryocytes is small, with varying sizes and scattered distribution; no obvious collagen fibrosis was observed between the bone trabeculae. **(C)** Immunohistochemistry (×400): CD34 primitive/immature cells (+), accounting for about 1%; CD117 primitive/immature cells (+), no increase observed; CD42b: megakaryocyte (+), increased in number, mainly small megakaryocytes; CK (–); CD71 nucleated red blood cells (+); MPO granulocyte (+); CD138 A few plasma cell were scattered (+). Conclusion: bone marrow test was negative, no indication of MDS.

was diagnosed with SLE for 2 years, but, there had been no significant reduction in his blood cells while receiving long-term steroid medication. In addition, there was no obvious increase in the levels of ANA, dsDNA antibody, rheumatoid factor, or decrease in C3 in the patient, and there was no joint swelling and pain, nor were there any other SLE symptoms like new erythra, indicating relevant performance during SLE flares. Although C-reactive protein (CRP) is also an indicator of SLE activity, the patient's CRP showed a transient spike. The increase in CRP was accompanied by exacerbation of pulmonary infection, indicating infection rather than SLE flare. It was unlikely related to SLE activity since it immediately returned to normal after the anti-infection and antifungal treatment. Based on the aforementioned findings, SLE activity and SLE-related triple decline or SLE-related MDS can be essentially ruled out.

We also took into account whether the patient developed primary MDS. MDS is a group of heterogeneous myeloid clonal diseases originating from hematopoietic stem cells, characterized by abnormal differentiation and development of myeloid cells, manifested as ineffective hematopoiesis, refractory hemocytopenia, hematopoietic failure, and high-risk transformation to acute myeloid leukemia (AML) (17, 18). The following conditions must be met for the MDS diagnosis: (1) continuous (≥6 months) reduction of one or more lineages of blood cells: red blood cells (Hb <110 g/L); neutrophils (ANC $< 1.5 \times 10^9$/L); platelets (BPC $< 100 \times 10^9$/L). (2) Exclude other hematopoietic and non-hematopoietic system diseases that can lead to reduced blood cells and pathological hematopoiesis. Determination criteria: (1) morbid hematopoiesis: bone marrow smear with at least 10% of any lines of red blood cell, neutrophil, or megakaryocyte; (2) the proportion of circular iron granulocytes occupying nuclear red blood cells is ≥15%; (3) primitive cells: 5%–19% in bone marrow smear; (4) chromosome abnormalities (19, 20). The literature indicates that MDS has multiple gene mutations, and spontaneous self-remission in *de novo* MDS is very rare (21, 22). The results of the patient's first bone marrow biopsy revealed MDS-like characteristics. Interestingly, the hemocytopenia resolved spontaneously after discontinuation of voriconazole and without any anti-MDS treatment. The bone marrow biopsy examined 6 months later revealed a notable improvement, indicating no MDS-like disease. Besides, no gene mutations were found in the two bone marrow biopsies with a 6 months interval before and after. Taken together, these findings rule out primary MDS, and conform to the characteristics of drug-related MDS.

The possibility of additional medications causing hemocytopenia during the treatment should also be taken into consideration. In the treatment of pulmonary infection, in addition to voriconazole, we also used cefminox sodium (4 days), piperacillin/tazobactam (3 days), and meropenem (29 days) successively for anti-infection. According to the instructions for these drugs, the side effect of

cefminox sodium is occasional pancytopenia (23); side effects of piperacillin/tazobactam include leukopenia, neutropenia, thrombocytopenia and other side effects (rare)，whole blood cell reduction (very rare) (24–26); side effects of meropenem include pancytopenia, agranulocytosis, hemolytic anemia (frequency unknown), leukopenia, thrombocytopenia (<1%) (27). The first two drugs have been used for a short period of time (only 3 and 4 days, respectively), and the incidence of side effects caused by drug-related hemocytopenia and MDS-like change in bone marrow is very low. Meropenem basically covered most of the course of inpatient treatment; among the three drugs, it seems to have the highest likelihood of causing the patients' hemocytopenia. Meropenem is a kind of carbapenem antibiotic, and carbapenem antibiotics usually have the characteristics of a broad spectrum and strong effect. The side effects of meropenem mainly include the following aspects: first, it may be prone to allergic reactions, such as skin erythema, itching, fever, redness, etc. In addition, it may have an impact on the blood system, and some patients may experience a decrease in granulocytes or platelets after use or may also experience an increase. However, the blood cells of the patient had decreased significantly before the use of meropenem, and the number of blood cells began to recover during the treatment without interrupting the use of it. Therefore, the evidence of hemocytopenia caused by meropenem is insufficient.

Figure 1 illustrates the patient's decreased blood cell count upon arrival. Following the discontinuation of voriconazole, the patient's blood cell count gradually increased but did not reach its pre-voriconazole values. The patient has a long-term history of SLE, as was already indicated, which may contribute to a decrease in blood cell count. The patient's condition, though, remained largely constant, and there had never before been an abrupt drop in blood cells. Following the administration of voriconazole, the patient's blood cell count dropped quickly and steadily, with platelets experiencing the greatest decline, dropping to a minimum of 8.0×10^9/L. After discontinuing voriconazole, the patient's blood cell count steadily improved until it reached the pre-disease level, though it was still lower than that of healthy individuals. Two possible explanations include the following: first, even though discontinuing voriconazole, the drug residue in the body was not immediately metabolized, and the drug side effects still played a role to some extent; secondly, although the patient's SLE condition remained stable, however, SLE continues to exist and will not disappear, and the objective phenomenon of cell reduction caused by it still exists.

The limitation of this case report is that we did not monitor the blood concentration of voriconazole to rule out the possibility of drug overdose. It is also important to understand the exact mechanism of voriconazole or its metabolites-induced bone marrow suppression in future studies.

Conclusion

Voriconazole was the cause of the patient's MDS-like bone marrow suppression. This case report reminds us that in clinical practice, when using voriconazole for anti-fungal infection treatment, individual differences in patients should be taken into consideration, and the serum concentration of voriconazole should be closely monitored. On the other hand, potential medications that affect voriconazole metabolism should also be noted, and patients should be carefully observed during medication to avoid the occurrence of adverse drug events.

Data availability statement

The original contributions presented in the study are included in the article/supplementary material, further inquiries can be directed to the corresponding authors.

Ethics statement

Ethical approval was not required for the studies involving humans because this is a retrospective case report, written informed consent was obtained from the individual(s) for the publication of any potentially identifiable images or data included in this article. The studies were conducted in accordance with the local legislation and institutional requirements. The human samples used in this study were acquired from this is a retrospective case report, all the data and images are based on previous medical treatment and examination results, and written informed consent was obtained from the individual(s) for the publication of any potentially identifiable images or data included in this article.

Author contributions

G-LX: Conceptualization, Formal analysis, Writing – original draft, Investigation. X-SW: Data curation, Investigation, writing – review & editing. L-YH: Data curation, Formal analysis, Writing – original draft. YW: Investigation, Writing – original draft. XG: Data curation, Project administration, Writing – review & editing. Y-QX: Methodology, Project administration, Resources, Writing – review & editing.

Funding

The author(s) declare financial support was received for the research, authorship, and/or publication of this article. This work was supported by the Shanghai Science and Technology Innovation Action Plan Medical Innovation Research Special Project (No. 21Y11922900), Shanghai Yueyang Hospital Program (No. 2201yyjm01), Shanghai Science and Technology Innovation Action Plan Biopharmaceutical Technology Support Particular Project (No. 23S11900500), and the Shanghai Jiao Tong University School of Medicine, 2022 Integrated Traditional Chinese and Western Medicine Research Platform (No. 2022zxy003).

Acknowledgments

The authors would like to thank the patient and their family for their great help in this report.

Conflict of interest

The authors declare that the research was conducted in the absence of any commercial or financial relationships that could be construed as a potential conflict of interest.

Publisher's note

References

1. Levine MT, Chandrasekar PH. Adverse effects of voriconazole: over a decade of use. *Clin Transpl*. (2016) 30:1377–86. doi: 10.1111/ctr.12834

2. Jin H, Wang T, Falcione BA, Olsen KM, Chen K, Tang H, et al. Trough concentration of voriconazole and its relationship with efficacy and safety: a systematic review and meta-analysis. *J Antimicrob Chemother*. (2016) 71:1772–85. doi: 10.1093/jac/dkw045

3. Kannan L, Raj R. Case report: Vancomycin-associated tubulointerstitial nephritis in clinical practice-case report and review of literature. *Front Med*. (2022) 9:899886. doi: 10.3389/fmed.2022.899886

4. Denning DW, Ribaud P, Milpied N, Caillot D, Herbrecht R, Thiel E, et al. Efficacy and safety of voriconazole in the treatment of acute invasive aspergillosis. *Clin Infect Dis*. (2002) 34:563–71. doi: 10.1086/324620

5. Jacobs F, Selleslag D, Aoun M, Sonet A, Gadisseur A. An observational efficacy and safety analysis of the treatment of acute invasive aspergillosis using voriconazole. *J Clin Microbiol Infect Dis*. (2012) 31:1173–9. doi: 10.1007/s10096-011-1425-5

6. Theuretzbacher U, Ihle F, Derendorf H. Pharmacokinetic/pharmacodynamic profile of voriconazole. *Clin Pharmacokinet*. (2006) 45:649–63. doi: 10.2165/00003088-200645070-00002

7. Dolton MJ, Ray JE, Chen SC, Ng K, Pont LG, McLachlan AJ. Multicenter study of voriconazole pharmacokinetics and therapeutic drug monitoring. *Antimicrob Agents Chemother*. (2012) 56:4793–9. doi: 10.1128/AAC.00626-12

8. Pascual A, Calandra T, Bolay S, Buclin T, Bille J, Marchetti O. Voriconazole therapeutic drug monitoring in patients with invasive mycoses improves efficacy and safety outcomes. *Clin Infect Dis*. (2008) 46:201–11. doi: 10.1086/524669

9. Moriyama B, Kadri S, Henning SA, Danner RL, Walsh TJ, Penzak SR. Therapeutic drug monitoring and genotypic screening in the clinical use of voriconazole. *Curr Fungal Infect Rep*. (2015) 9:74–87. doi: 10.1007/s12281-015-0219-0

10. Zonios D, Kadri S, Henning SA, Danner RL, Walsh TJ, Penzak SR. Voriconazole metabolism, toxicity, and the effect of cytochrome P450 2C19 genotype. *J Infect Dis*. (2014) 209:1941–8. doi: 10.1093/infdis/jiu017

11. Almuwaqqat Z, Roberts JW, Bashtawi Y. A rare and serious cause of pancytopenia in a patient with systemic lupus erythematosus: haemophagocytic lymphohistiocytosis. *BMJ Case Rep*. (2018) 2018:bcr2018226758. doi: 10.1136/bcr-2018-226758

12. Chalayer E, Costedoat-Chalumeau N, Beyne-Rauzy O, Ninet J, Durupt S, Tebib J, et al. Bone marrow involvement in systemic lupus erythematosus. *QJM*. (2017) 110:701–11. doi: 10.1093/qjmed/hcx102

13. Kiriakidou M, Ching CL. Systemic lupus erythematosus. *Ann Intern Med*. (2020) 172:ITC81–96. doi: 10.7326/AITC202006020

14. Voulgarelis M, Giannouli S, Tasidou A, Anagnostou D, Ziakas PD, Tzioufas AG. Bone marrow histological findings in systemic lupus erythematosus with hematologic abnormalities: a clinicopathological study. *Am J Hematol*. (2006) 81:590–7. doi: 10.1002/ajh.20593

15. Linabery AM, Roesler MA, Richardson M, Warlick ED, Nguyen PL, Cioc AM, et al. Personal history of autoimmune disease and other medical conditions and risk of myelodysplastic syndromes. *Cancer Epidemiol*. (2022) 76:102090. doi: 10.1016/j.canep.2021.102090

16. Yu H, Nagafuchi Y, Fujio K. Clinical and immunological biomarkers for systemic lupus erythematosus. *Biomol Ther*. (2021) 11:928. doi: 10.3390/biom11070928

17. Cazzola M. Myelodysplastic syndromes. *N Engl J Med*. (2020) 383:1358–74. doi: 10.1056/NEJMra1904794

18. Candelaria M, Dueñas-Gonzalez A. Therapy-related myelodysplastic syndrome. *Expert Opin Drug Saf*. (2015) 14:655–65. doi: 10.1517/14740338.2015.1014340

19. Hasserjian RP. Myelodysplastic syndrome updated. *Pathobiology*. (2019) 86:7–13. doi: 10.1159/000489702

20. Ghariani I, Braham N, Hassine M, Kortas M. Myelodysplastic syndrome classification. *Ann Biol Clin*. (2013) 71:139–44. doi: 10.1684/abc.2013.0804

21. Haferlach T. The molecular pathology of myelodysplastic syndrome. *Pathobiology*. (2019) 86:24–9. doi: 10.1159/000488712

22. Lee P, Yim R, Yung Y, Chu HT, Yip PK, Gill H. Molecular targeted therapy and immunotherapy for myelodysplastic syndrome. *Int J Mol Sci*. (2021) 22:10232. doi: 10.3390/ijms221910232

23. Wu S, Bi X, Lin Y, Yang L, Li M, Xie Y. Severe coagulopathy caused by cefminox sodium in a liver cirrhosis patient: a case report. *Infect Agent Cancer*. (2022) 17:30. doi: 10.1186/s13027-022-00446-y

24. Fry W, McCafferty S, Gooday C, Nunney I, Dhatariya KK. Assessing the effect of piperacillin/tazobactam on hematological parameters in patients admitted with moderate or severe foot infections. *Diabetes Ther*. (2018) 9:219–28. doi: 10.1007/s13300-017-0357-1

25. Lee KW, Chow KM, Chan NP, Lo AO, Szeto CC. Piperacillin/tazobactam induced myelosuppression. *J Clin Med Res*. (2009) 1:53–5. doi: 10.4021/jocmr2009.03.1227

26. Ruiz-Irastorza G, Barreiro G, Aguirre C. Reversible bone marrow depression by high-dose piperacillin/tazobactam. *Br J Haematol*. (1996) 95:611–2. doi: 10.1046/j.1365-2141.1996.d01-1952.x

27. Hussain K, Salat MS, Mohammad N, Mughal A, Idrees S, Iqbal J, et al. Meropenem-induced pancytopenia in a preterm neonate: a case report. *J Med Case Rep*. (2021) 15:25. doi: 10.1186/s13256-020-02632-1

frontiers | Frontiers in Medicine

TYPE Systematic Review
PUBLISHED 24 January 2024
DOI 10.3389/fmed.2023.1280271

OPEN ACCESS

EDITED BY
Tomás José Gonzalez López,
Burgos University Hospital, Spain

REVIEWED BY
Umut Yilmaz,
Istanbul University-Cerrahpasa, Türkiye
Kiana Shahzamani,
Lorestan University of Medical Sciences, Iran

*CORRESPONDENCE
Elrazi A. Ali
✉ razinho5@gmail.com

RECEIVED 19 August 2023
ACCEPTED 21 December 2023
PUBLISHED 24 January 2024

CITATION
Ali EA, Al-Sadi A, Al-maharmeh Q, Subahi EA, Bellamkonda A, Kalavar M, Panigrahi K, Alshurafa A and Yassin MA (2024) SARS-CoV-2 and chronic myeloid leukemia: a systematic review.
Front. Med. 10:1280271.
doi: 10.3389/fmed.2023.1280271

SARS-CoV-2 and chronic myeloid leukemia: a systematic review

Elrazi A. Ali[1]*, Anas Al-Sadi[2], Qusai Al-maharmeh[3], Eihab A. Subahi[2], Amulya Bellamkonda[1], Madhumati Kalavar[1], Kalpana Panigrahi[1], Awni Alshurafa[4] and Mohamed A. Yassin[4]

[1]Internal Medicine Department, Interfaith Medical Center/One Brooklyn Health, Brooklyn, NY, United States, [2]Internal Medicine Department, Hamad Medical Corporation, Doha, Qatar, [3]Internal Medicine Department, Saint Michael's Medical Center, Newark, CA, United States, [4]Department of Oncology-Hematology, National Center for Cancer Care and Research – Hamad Medical Corporation, Doha, Qatar

Introduction: Severe acute respiratory syndrome coronavirus 2 (SARS-CoV-2) is the virus causing the coronavirus disease of 2019. The disease has caused millions of deaths since the first pandemic at the end of 2019. Immunocompromised individuals are more likely to develop severe infections. Numerous mutations had developed in SARS-CoV-2, resulting in strains (Alfa Beta Delta Omicron) with varying degrees of virulence disease severity. In CML (chronic myeloid leukemia) patients, there is a lot of controversy regarding the effect of the treatment on the patient outcome. Some reports suggested potential better outcomes among patients with CML, likely due to the use of TKI; other reports showed no significant effects. Additionally, it is unknown how much protection immunization provides for cancer patients.

Method: In accordance with the Preferred Reporting Items for Systematic Reviews and Meta-Analyses (PRISMA) standards, we conducted a systematic review. Retrospective, prospective studies, reviews, case series, and case reports of chronic myeloid leukemia patients aged above 18 years who had SARS-CoV-2 infection were included. English literature was screened using PubMed, SCOPUS, and Google Scholar. Search terms include chronic myeloid leukemia, chronic myelogenous leukemia, and SARS-CoV-2 and Coronavirus disease 2019 (COVID-19). We searched the reference lists of the included studies for any new articles. The search included all articles published up to April 20, 2023. The review is registered in PROSPERO (registration number CRD42022326674).

Results: We reviewed 33 articles of available published literature up to April 2023 and collected data from a total of 682 CML patients with COVID-19. Most patients were in the chronic phase, seven were in the accelerated phase, and eight were in the blast phase. Disease severity was classified according to WHO criteria. Mortality was seen in 45 patients, and there were no reports of thrombotic events. Two hundred seventy-seven patients were in the era before vaccination; among them, eight were in the intensive care unit (ICU), and mortality was 30 (11%). There were 405 patients after the era of vaccination; among them, death was reported in 15 (4%) patients and ICU in 13 patients.

Limitations and conclusion: The major limitation of this review is the lack of details about the use or hold of TKIs during SARS-CoV-2 infection. Additionally, after the appearance of the different variants of the SARS-CoV-2 virus, few studies mentioned the variant of the virus, which makes it difficult to compare the outcome of the other variants of the SARS-CoV-2 virus in patients with CML. Despite the limitations of the study, CML patients with COVID-19 have no significant increase in mortality compared to other hematological malignancy.

Hematological cancers are associated with an increased risk of thrombosis, which is expected to increase in patients with COVID-19. However, patient with CML has not been reported to have a significant increase in thrombosis risk. The available data indicates that COVID-19's effect on patients with chronic myeloid leukemia (CML) still needs to be better understood due to the limited data.

Systematic review registration: https://www.crd.york.ac.uk/PROSPERO/display_record.php? RecordID:326674.

KEYWORDS

SARS-CoV-2 variants, COVID-19, SARS-CoV-2, chronic myelocytic leukemia (CML), chronic myeloid leukemia

Introduction

Chronic myeloid leukemia (CML) is a clonal myeloproliferative neoplasm with an overproduction of mature granulocytes. Nearly half of patients are asymptomatic and detected during routine screening or during routine blood work. Usually, patients present with abdominal distension, early satiety, and fatigue. Others may have atypical presentations and complications like priapism, eye symptoms or abdominal pain, and appendicitis (1–3). After the introduction of tyrosine kinase inhibitors, the treatment goals of CML have changed dramatically, and Patients with CML are expected to have a normal life expectancy, and treatment aims for a better quality of life (4). Worldwide, SARS-CoV-2 has caused millions of deaths. Mortality is higher for patients with multiple medical conditions, such as diabetes mellitus and hypertension (5, 6). Besides the respiratory manifestation, COVID-19 can present with liver renal cutaneous manifestations (7–9). Recently, the overall mortality of COVID-19 has improved with time due to improvements in preventive measures, the presence of vaccination, and effective antiviral medications. What the exact risk is for CML patients infected with SARS-CoV-2 is unclear, though. Additionally, the real mortality impact of immunization, ideal treatment options, and interactions with CML and COVID-19 therapy need to be explored. Many studies suggested a potentially higher risk of mortality among CML patients from COVID-19, while other studies reported lower mortality with a presumed protective effect from TKI. Additionally, the impact of SARS-CoV-2 on CML patients and the outcome with the different strains is poorly understood.

Methods

Following the PRISMA (preferred reporting items for systematic reviews and meta-analyses) guidelines, PubMed, Scopus, and Google Scholar databases were searched for published articles through April 20, 2023, for qualified studies. The search included Retrospective, prospective studies, randomized control trial, reviews, case series, and case reports. The inclusion criteria were English literature with CML patients above 18 years who had SARS-CoV-2 infection. Articles in a language other than English articles about patients less than 18 years and articles with non-sufficient information were excluded, and patients with bone marrow transplants were excluded. Search terms were (chronic myeloid leukemia) OR (chronic myelogenous leukemia) AND (SARS-CoV-2) OR (COVID-19). Two independent reviewers (EA and A.E.) evaluated the studies for inclusion in the review by looking through the titles and abstracts of the search records they had retrieved to see which ones were eligible. If there was ever a disagreement between the independent reviewers over a research's eligibility, it was usually resolved via careful consideration and evaluation of the study in question, a third reviewer, was consulted in case consensus could not be established. Excluded studies were those that did not fit the predetermined qualifying requirements. We searched the reference lists of the included studies for any new articles. The search included all articles published up to April 20, 2023. The review is registered in PROSPERO (registration number CRD42022326674).

Results

We reviewed 33 articles of available published literature (Figure 1) up to April 2023 and collected data from a total of 682 CML patients with COVID-19 (35–70). Most of the reports were from the United States, Europe (United Kingdom, Italy, Germany), and China. Twenty-four studies were reported before and 12 after the introduction of vaccination. Most patients were in the chronic phase, seven patients were in the accelerated phase, and eight patients were in the blast phase. Disease severity was classified as per WHO criteria (10), severe disease if a patient requires oxygen or, has saturation below 94% or requires ventilatory support. SARS-CoV-2 infection was reported in both patients with a recent diagnosis of CML and in patients diagnosed with CML for months to years (up to 14 years). Twenty-seven patients were managed at home, and 21 patients were in ICU (intensive care unit) during the hospital course. Forty-one patients required oxygen therapy; among them, seven patients required mechanical intubation, and six patients required non-invasive ventilation. Mortality was seen in 45 patients, and there were no reports of thrombotic events. In the pre-vaccination era (Supplementary Tables 1, 2), five patients were intubated, four required NIV, and nine required oxygen. In the post-vaccination era (Supplementary Tables 1, 2), 32 (8.1%) patients out of 407 required oxygen; among them, two were intubated, and 3 required NIV. Two hundred seventy-seven patients were in the era before vaccination; among them, eight were in ICU, and mortality was 30 (11%). There were 405 patients after the era of vaccination; among them, death was reported in 15 (4%) patients and ICU in 13 (3.19%) patients. This is expressed as a Z score of 3.5614 with a p value of 0.00038. The result is significant at $p < 0.05$. For patients admitted to ICU, the mortality

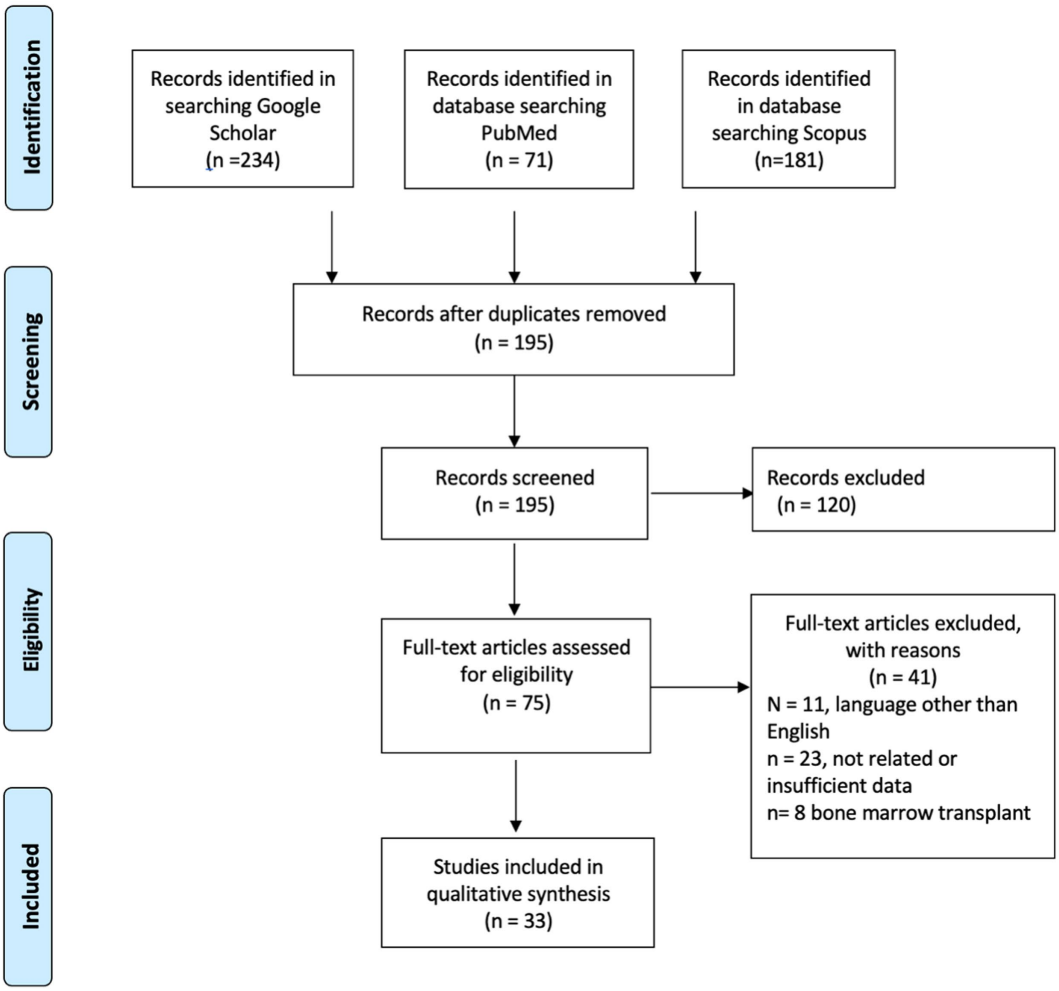

FIGURE 1
The PRISMA flow diagram detailing articles screening of chronic myleid leukemia patient with SARS-CoV-2.

was 4/8 in the pre-vaccination era and 9/13 in the post-vaccination era. For the vast majority of the patients, there was no clear documentation if treatment of CML was continued or held during COVID-19. The first COVID-19 vaccine was the Pfizer-BioNTech COVID-19 Vaccine, which was first available on December 11, 2020, followed by other vaccines like Moderna. Also, there was no documentation about prior vaccination for cases reported after introducing COVID-19 vaccines. Many patients had comorbidities, including diabetes mellitus, hypertension, chronic kidney disease, coronary artery disease, hypothyroidism, obesity, dyslipidemia, prostate cancer, and gastroesophageal reflux disease. There was no report of thrombotic events; however, some patients developed AKI, autoimmune hemolytic anemia, rhabdomyolysis, DIC and possible HLH, cranial nerve palsy, and DKA during COVID-19.

Discussion

The primary factor in mortality from COVID-19 is often ARDS; other factors include cardiac arrhythmia, cardiac arrest, and pulmonary embolism. The average mortality for the general population from COVID-19 varies; during the first wave, there were no vaccines, and the mortality was around 4.3% (11). However, after the emergence of vaccination, worldwide mortality went down. The availability of resources plays a major role; in limited-resource countries, the mortality was reported to be extremely high, up to 48% (12). Patients with hematological malignancies have a high rate of mortality with SARS-CoV-2 infection. In a study with over 300 hematology patients (70% myeloma, acute leukemia, and active lymphoma), the mortality was 26%, which is markedly higher than our findings in CML patients (13). The same study showed a mortality of 83% for patients with critical illness. Our review showed that for ICU-admitted CML patients, the mortality exceeds 50%: 4/8 (50%) in the pre-vaccination era and 9/13 (69%) in the post-vaccination era. This data showed a three-times drop in overall mortality in CML patients in the post-vaccination era, 11 to 4%, but high ICU mortality. This would suggest that COVID-19 immunization and treatment are effective in reducing illness severity but have little impact on lowering fatality rates for critical patients with CML. On the other hand, mortality in the general population varied significantly during the different waves of the pandemic, but the ICU mortality did not change substantially; most reports show mortality around 23 to 28% (14).

Fortunately, the majority of SARS-CoV-2 mutations have no effect on viral function. Only a few mutations resulted in new variants with

10.3389/fmed.2023.1280271

TABLE 1 Shows a comparison between the different variants of SARS-CoV-2.

Variant	Timeline and region	Global dominance	Characteristics
Delta	India in December 2020	dominant globally until emergence of the Omicron variant.	High risk of transmission and severe disease and hospitalization.
Alpha	UK in late 2020	globally dominant, until the emergence of the Delta variant	might be associated with greater disease severity.
Beta	South Africa in late 2020	no	immune evasion: convalescent plasma did not neutralize viral constructs with Beta spike protein
Gamma	Japan and Brazil in December 2020	no	Possible increased transmissibility and an impact on immunity
Omicron	Botswana and South Africa in November 2021	globally dominant variant	High risk of transmission, immune evasion, but low risk for severe disease

Source: https://www.who.int/en/activities/tracking-SARS-CoV-2-variants/

significant effects on transmission and clinical implications on populations. It resulted in different strains, some of which have increased spread but low severity of illness like Omicron (Table 1). Omicron infections were reported to be milder than other strains. Omicron differs from other SARS-CoV-2 strains in three ways: high rate of replication (15), capacity to avoid the humoral immune response, and high rate of reinfection (15). In CML patients, Omicron infection was reported to cause mild infection (16). A similar outcome was also observed in other groups of patients, such as acute leukemia, polycythemia Vera, essential thrombocythemia, and chronic lymphocytic leukemia (17–19).

Unfortunately, few studies regarding SARS-CoV-2 virus infection in CML patients have been done after the introduction of vaccines and the emergence of different strains. Our review included 24 studies that were reported before December 2020. Considering that the first vaccine was available in December 2020, it is less likely that studies published before 2021 included patients who received vaccines. The data showed that there was a significant drop in mortality for patients with CML after the vaccination from 11 to 4%, which is a drop by three times in mortality. The improvement in mortality after vaccination could be attributed to several factors. First, it might be related to the different strains that have different virulence; for example, infections with milder strains like Omicron resulted in a lower mortality rate compared to other strains (Table 1). Additionally, the availability of effective treatment and medications with antiviral activity that were not available initially during the first waves. Similarly, ICU admission rates are probably lower due to the effect of vaccination on preventing fatal illness and severe illness (20). Besides vaccination, adherence to preventive measures, start of new medications, and experience with treating COVID-19 (21).

Generally, Interruption of TKI therapy was found to be associated with poor long-term outcomes. The real question is, is TKI continuation during COVID-19 beneficial or harmful? Few studies reported the status of TKI if it was continued during COVID-19 treatment or was held. For patients who had the TKI continued ($n = 9$), there were no mortality or serious adverse events. Few patients reported that TKIs were held due to prolonged QT, namely with imatinib ($n = 1$) and with nilotinib ($n = 2$). One patient out of the nine patients who continued TKI had the dose of imatinib reduced due to interaction with ritonavir, which resulted in an increased effect of imatinib. It seems that the decision to continue or to hold TKI should be individualized and weigh benefits and risks. For patients with expected serious side effects, it might be reasonable to hold TKI for a few days and then reassess the risks and benefits.

Initial reports showed that CML patients on TKI are noted to have a favorable outcome against severe COVID-19, after noticing that patients on TKI including CML have a favorable outcome. *In vitro* studies showed that gilteritinib, nintedanib, and imatinib pose antiviral activity, and they vary in their potency, likely depending on the host-targeted tyrosine kinase by suppressing viral replication (22). Additionally, It was therapeutically possible to use gilteritinib at a concentration that would result in 90% virus suppression (22). TKI might have a protective effect against SARS-CoV-2 through different mechanisms; firstly, TKI inhibits viral cell entry and fusion with cell membranes and the formation of endosomes (23). Also, Imatinib and other TKI inhibit Abl2 protein expression, which is required for viral growth (24). On the other hand, there is a theoretical risk of increased severe infection in CML patients taking TKI due to targeted inhibition of kinases involved in immune cell function. This might result in suppressed cellular immune response that facilitates viral replication.

Generally, patients with cancer usually have poor outcomes with SARS-CoV-2 infection, particularly lung cancer and hematological cancer (25). Moreover, patients with cancer have an increased risk of thrombosis compared to the non-cancer population. CML is not known to be at high risk for thrombosis compared to other cancers like pancreatic and gastric cancers. Compared to other MPNs like polycythemia vera and essential thrombocythemia, CML has a lower risk of thrombotic events (26). The heparinase, which is associated with angiogenesis and the development of cancer, may provide a mechanistic explanation for the decreased thrombosis in CML. When compared to ET and JAK2-positive MPN, CML, and Jak2-negative, MPN expresses less heparinase in the bone marrow and has fewer thrombosis (27). The reported thrombosis in CML is mainly arterial (myocardial infarction, cerebrovascular accidents, and peripheral artery disease) and mostly linked to the use of different TKI more often reported with the second-generation TKIs nilotinib, dasatinib, and ponatinib (28). TKI use is associated with endothelial dysfunction and vascular toxicity that lead to accelerated atherosclerosis and thrombosis (28). However, previous studies demonstrated no significant increased risk of arterial thrombosis (29). Paradoxically, TKI is associated with an increased risk of bleeding that is related to TKI-associated thrombocytopenia and is seen in dasatinib more than the other TKIs and platelet dysfunction (30). Platelet dysfunction with TKI use was demonstrated with impaired platelet aggregation with epinephrine *in vitro* (31). Overall, TKIs are associated with bleeding and an increased risk of arterial thrombosis; this might explain the lower risk of thrombotic events in CML patients. Considering their increased risk of thrombosis

compared to the general population, CML patients with COVID-19 interestingly are not reported to develop additional risk thrombotic events as might be expected. This finding is supported by the Sweden study (32), the study with the longest follow-up for patients with CML and COVID-19, starting from March 2020 to April 2023, showed that there is no significant adverse outcome when compared imatinib to the newer TKI, also the study showed CML patients with no vaccination, had a slightly higher risk of hospitalization compared to their controls (32). The study also raised the finding that few events were reported among these patients. Our review showed that the mortality rate in CML covid patients improved significantly in the post-vaccination era. This could be explained by the improvement of our understanding of COVID-19, the protective effect of vaccines, and the change in the virulence of the recent strains. A similar finding is seen in a systematic review comparing COVID-19 among hematological malignancies; most cases before the vaccination were available (March 10, 2021) showed that CML patients reported no dyspnea, diarrhea, or respiratory distress compared to other cancers like ALL, MPN lymphoma (33).

In this review, there are important limitations; the testing of CML patients for COVID-19 may change from region to region, where patients with mild disease are less likely to be diagnosed with COVID-19 in resource-limited settings, creating a potential bias that results in higher-than-actual mortality rates among these cases as mild cases are not reported. Additionally, the indications for COVID-19 testing changed multiple times and may not have been the same before and after vaccination, which creates a bias when comparing the two eras in terms of mortality and severe disease. Moreover, the availability of vaccines was not synchronous throughout the world, and some of the reported patients in the post-vaccine era may not have had vaccines locally available. On the other hand, during the initial pandemic, there were no clear treatment guidelines. Many studies have tried to find an effective treatment that can reduce the mortality of COVID-19. Currently, there are many medications that have been shown to prove survival benefit in patients with severe COVID-19 pneumonia (32).

Conclusion

The COVID-19 mortality rates among CML patients did not appear to be extremely high compared to the general population and were lower than most reports calculating COVID-19 mortality among patients with more severe hematologic diseases. Our review showed that the mortality of CML patients with COVID-19 has significantly improved from 11% in the pre-vaccination period to 4% in the post-vaccination era. However, for CML patients with severe infection requiring ICU admission, the mortality remains high. The available data indicates that COVID-19's effect on patients with chronic myeloid leukemia (CML) still needs to be better understood due to the limited data.

Data availability statement

The original contributions presented in the study are included in the article/Supplementary material, further inquiries can be directed to the corresponding author.

Author contributions

EA: Conceptualization, Data curation, Investigation, Methodology, Project administration, Validation, Visualization, Writing – original draft, Writing – review & editing. AA-S: Data curation, Investigation, Writing – review & editing. QA-m: Data curation, Writing – review & editing. ES: Validation, Writing – review & editing, Data curation. MK: Supervision, Validation, Writing – review & editing. KP: Writing – review & editing, Validation, Visualization. AB: Writing – review & editing, Validation. AA: Validation, Writing – review & editing, Visualization. MY: Writing – review & editing, Conceptualization, Data curation, Investigation, Project administration, Supervision.

Funding

The author(s) declare financial support was received for the research, authorship, and/or publication of this article. Open access payment by Qatar National Library.

Acknowledgments

I wish to show my gratitude to the Internal medicine residency program, to Panigrahi for the scientific support.

Conflict of interest

AA-S was employed by the company Hamad Medical Corporation. AA and MY were employed by the company National Center for Cancer Care and Research – Hamad Medical Corporation.

The remaining authors declare that the research was conducted in the absence of any commercial or financial relationships that could be construed as a potential conflict of interest.

The author(s) declared that they were an editorial board member of Frontiers, at the time of submission. This had no impact on the peer review process and the final decision.

Publisher's note

Supplementary material

The Supplementary material for this article can be found online at: https://www.frontiersin.org/articles/10.3389/fmed.2023.1280271/full#supplementary-material

References

1. Ali E, Soliman A, De Sanctis V, Nussbaumer D, Yassin MA. Priapism in patients with chronic myeloid leukemia (CML): a systematic review. *Acta Bio Medica: Atenei Parmensis*. (2021) 92.:e2020164. doi: 10.23750/abm.v92i3.10796

2. Ahmad R, Ali E, Okar L, Elaiwy O, Abdelrazek M, Mulikandathil Y, et al. Acute appendicitis revealing a diagnosis of chronic myelogenous leukemia. *Clinical Case Reports*. (2021) 9:1913–6. doi: 10.1002/ccr3.3902

3. Yassin MA, Ata F, Mohamed SF, Alkhateeb A, Naeem U, Al-Qatami AI, et al. Ophthalmologic manifestations as the initial presentation of chronic myeloid leukemia: a review. *Surv Ophthalmol*. (2022) 67:530–43. doi: 10.1016/j.survophthal.2021.07.001

4. Gambacorti-Passerini C, Antolini L, Mahon FX, Guilhot F, Deininger M, Fava C, et al. Multicenter independent assessment of outcomes in chronic myeloid leukemia patients treated with imatinib. *J Natl Cancer Inst*. (2011) 103:553–61. doi: 10.1093/jnci/djr060

5. Soliman A, Nair AP, Al Masalamani MS, De Sanctis V, Khattab MA, Alsaud AE, et al. Prevalence, clinical manifestations, and biochemical data of type 2 diabetes mellitus versus nondiabetic symptomatic patients with COVID-19: a comparative study. *Acta Bio Medica: Atenei Parmensis*. (2020) 91:e2020010. doi: 10.23750/abm.v91i3.10214

6. Iqbal F, Soliman A, De Sanctis V, Mushtaq K, Nair AP, Al Masalamani MA, et al. Prevalence, clinical manifestations, and biochemical data of hypertensive versus normotensive symptomatic patients with COVID-19: a comparative study. *Acta Bio Medica: Atenei Parmensis*. (2020) 91. doi: 10.23750/abm.v91i4.10540

7. Ali E, Ziglam H, Kohla S, Ahmed M, Yassin M. A case of fulminant liver failure in a 24-year-old man with coinfection with hepatitis B virus and SARS-CoV-2. *American J Case Reports*. (2020) 21:e925932–1. doi: 10.12659/AJCR.925932

8. Ali E, Badawi M, Ahmed A, Abdelmahmuod E, Ibrahim W. Severe SARS-CoV-2 infection presenting with acute kidney injury and diabetic ketoacidosis complicated by pancreatitis in a 53-year man with hypertension. *Clinical Case Reports*. (2021) 9:1202–6. doi: 10.1002/ccr3.3731

9. Ali E, Mohamed A, Abuodeh J, Albuni MK, Al-Mannai N, Salameh S, et al. SARS-CoV-2 and guttate psoriasis: a case report and review of literature. *Clinical Case Reports*. (2021) 9:e04568. doi: 10.1002/ccr3.4568

10. COVID-19 Treatment Guidelines Panel. Coronavirus Disease(2019) (COVID-19) Treatment Guidelines. National Institutes of Health. Available at: https://www.covid19treatmentguidelines.nih.gov/

11. Wang D, Hu B, Hu C, Zhu F, Liu X, Zhang J, et al. Clinical characteristics of 138 hospitalized patients with 2019 novel coronavirus–infected pneumonia in Wuhan, China. *JAMA*. (2020) 323:1061–9. doi: 10.1001/jama.2020.1585

12. Pagnano KB, Kok CH, Mauro MJ, Cortes JE, Evans N, Jiang Q, et al. COVID-19 in patients with chronic myeloid leukemia: poor outcomes for patients with comorbidities, older age, advanced phase disease, and those from low-income countries: an update of the candid study. *Blood*. (2021) 138:634. doi: 10.1182/blood-2021-150026

13. Civriz Bozdağ S, Cengiz Seval G, Yönal Hindilerden İ, Hindilerden F, Andıç N, Baydar M, et al. Clinical characteristics and outcomes of COVID-19 in Turkish patients with hematological malignancies. *TurkishJ Haematol: Official J Turkish Society Haematol*. (2022) 39:43–54. doi: 10.4274/tjh.galenos.2021.2021.0287

14. Vahidy FS, Drews AL, Masud FN, Schwartz RL, Boom ML, Phillips RA. Characteristics and outcomes of COVID-19 patients during initial peak and resurgence in the Houston metropolitan area. *JAMA*. (2020) 324:998–1000. doi: 10.1001/jama.2020.15301

15. Pulliam JR, van Schalkwyk C, Govender N, von Gottberg A, Cohen C, Groome MJ, et al. Increased risk of SARS-CoV-2 reinfection associated with emergence of omicron in South Africa. *Science*. (2022) 376:eabn4947. doi: 10.1126/science.abn4947

16. Qi F, Bao M, Gao H, Zhang X, Zhao S, Wang C, et al. Patients with chronic myeloid leukemia and coronavirus disease 2019 in the omicron era. *Ann Hematol*. (2023) 102:2707–16. doi: 10.1007/s00277-023-05413-0

17. Ali EA, Alamin MA, Abu-Tineh M, Ahmed K, Alshurafa A, Rozi W, et al. A case series of SARS-CoV-2 omicron variant in patients with acute leukemia. *Cureus*. (2022) 14:e25196. doi: 10.7759/cureus.25196

18. Ali EA, Khamees I, Alshurafa A, Qasim H, Abu-Tineh MA, Ahmed K, et al. Severe acute respiratory syndrome coronavirus 2 omicron variant in patients with Philadelphia-negative myeloproliferative neoplasm: a single center experience. *Oncology*. (2022) 100:460–6. doi: 10.1159/000525750

19. Khamees I, Ali EA, Malkawi L, Rozi W, Yassin MA. SARS-CoV-2 omicron variant in patients with chronic lymphocytic leukemia: case series. *Cureus*. (2022) 14:e32041. doi: 10.7759/cureus.32041

20. Baden LR, El Sahly HM, Essink B, Kotloff K, Frey S, Novak R, et al. Efficacy and safety of the mRNA-1273 SARS-CoV-2 vaccine. *N Engl J Med*. (2021) 384:403–16. doi: 10.1056/NEJMoa2035389

21. Kurtz P, Bastos LS, Dantas LF, Zampieri FG, Soares M, Hamacher S, et al. Evolving changes in mortality of 13,301 critically ill adult patients with COVID-19 over 8 months. *Intensive Care Med*. (2021) 47:538–48. doi: 10.1007/s00134-021-06388-0

22. Boytz R, Słabicki M, Ramaswamy S, Patten JJ, Zou C, Meng C, et al. Anti-SARS-CoV-2 activity of targeted kinase inhibitors: repurposing clinically available drugs for COVID-19 therapy. *J Med Virol*. (2023) 95:e28157. doi: 10.1002/jmv.28157

23. Sisk JM, Frieman MB, Machamer CE. Coronavirus S protein-induced fusion is blocked prior to hemifusion by Abl kinase inhibitors. *J Gen Virol*. (2018) 99:619–30. doi: 10.1099/jgv.0.001047

24. Coleman CM, Sisk JM, Mingo RM, Nelson EA, White JM, Frieman MB. Abelson kinase inhibitors are potent inhibitors of severe acute respiratory syndrome coronavirus and Middle East respiratory syndrome coronavirus fusion. *J Virol*. (2016) 90:8924–33. doi: 10.1128/JVI.01429-16

25. Fernandes GA, Feriani D, IL ES, DR ES, Arantes PE, Da Silva Canteras J, et al. Differences in mortality of cancer patients with COVID-19 in a Brazilian cancer center. *InSeminars in Oncology*. (2021) 48:171–80. doi: 10.1053/j.seminoncol.2021.01.003

26. Tefferi A, Elliott M. Thrombosis in myeloproliferative disorders: prevalence, prognostic factors, and the role of leukocytes and JAK2V617F. *InSeminars in thrombosis and hemostasis*. (2007) 33:313–20. doi: 10.1055/s-2007-976165

27. Kogan I, Chap D, Hoffman R, Axelman E, Brenner B, Nadir Y. JAK-2 V617F mutation increases heparanase procoagulant activity. *Thromb Haemost*. (2016) 115:73–80. doi: 10.1160/TH15-04-0320

28. Haguet H, Bouvy C, Delvigne AS, Modaffari E, Wannez A, Sonveaux P, et al. The risk of arterial thrombosis in patients with chronic myeloid leukemia treated with second and third generation BCR-ABL tyrosine kinase inhibitors may be explained by their impact on endothelial cells: an in-vitro study. *Front Pharmacol*. (2020) 11:1007. doi: 10.3389/fphar.2020.01007

29. Hekmatjou H, Roboz GJ, Ritchie EK, Lee S, Desai P, Scandura JM, et al. Arterial thrombotic complications are uncommon in patients without cardiovascular risk factors and occur at equivalent rates in chronic myeloid leukemia (CML) patients treated with imatinib and nilotinib. *Blood*. (2014) 124:1811. doi: 10.1182/blood.V124.21.1811.1811

30. Quintás-Cardama A, Kantarjian H, Ravandi F, O'Brien S, Thomas D, Vidal-Senmache G, et al. Bleeding diathesis in patients with chronic myelogenous leukemia receiving dasatinib therapy. *Cancer*. (2009) 115:2482–90. doi: 10.1002/cncr.24257

31. Quintás-Cardama A, Han X, Kantarjian H, Cortes J. Tyrosine kinase inhibitor–induced platelet dysfunction in patients with chronic myeloid leukemia. *Blood J American Society of Hematol*. (2009) 114:261–3. doi: 10.1182/blood-2008-09-180604

32. Dahlén T, Flygt H, Lübking A, Olsson-Strömberg U, Wennström L, Dreimane A, et al. The impact of Covid-19 in patients with chronic myeloid leukemia—a nationwide population-based study. *Leukemia*. (2023) 37:1156–9. doi: 10.1038/s41375-023-01893-1

33. Naimi A, Yashmi I, Jebeleh R, Imani Mofrad M, Azimian Abhar S, Jannesar Y, et al. Comorbidities and mortality rate in COVID-19 patients with hematological malignancies: a systematic review and meta-analysis. *J Clin Lab Anal*. (2022) 36:e24387. doi: 10.1002/jcla.24387

34. Chokkalingam AP, Hayden J, Goldman JD, Li H, Asubonteng J, Mozaffari E, et al. Association of remdesivir treatment with mortality among hospitalized adults with COVID-19 in the United States. *JAMA Netw Open*. (2022) 5. doi: 10.1001/jamanetworkopen.2022.44505

frontiers | Frontiers in Medicine

TYPE Case Report
PUBLISHED 02 February 2024
DOI 10.3389/fmed.2024.1335969

OPEN ACCESS

EDITED BY
Pierpaolo Di Micco,
Ospedale Santa Maria delle Grazie, Italy

REVIEWED BY
Nopporn Apiwattanakul,
Mahidol University, Thailand
Nicolina Capoluongo,
Hospital of the Hills, Italy

*CORRESPONDENCE
Alejandra Pando-Caciano
✉ alejandra.pando@upch.pe

RECEIVED 09 November 2023
ACCEPTED 15 January 2024
PUBLISHED 02 February 2024

CITATION
Pando-Caciano A, Escudero-Ramirez KA, Torres-Rodríguez JC and Maita-Malpartida H (2024) Refractory human cytomegalovirus infection without evidence of genetic resistance in the UL-54 and UL-97 genes in a pediatric hematopoietic stem cell transplant recipient: a case report. *Front. Med.* 11:1335969. doi: 10.3389/fmed.2024.1335969

Refractory human cytomegalovirus infection without evidence of genetic resistance in the UL-54 and UL-97 genes in a pediatric hematopoietic stem cell transplant recipient: a case report

Alejandra Pando-Caciano[1]*, Ketty Adid Escudero-Ramirez[1], Jackeline Carol Torres-Rodríguez[2] and Holger Maita-Malpartida[1,3]

[1]Department of Cellular and Molecular Sciences, School of Science and Philosophy, Universidad Peruana Cayetano Heredia, Lima, Peru, [2]Sub Unidad Integral Especializada del Paciente de Progenitores Hematopoyéticos, Instituto Nacional de Salud del Niño San Borja, Lima, Peru, [3]Sub Unidad de Investigación e Innovación Tecnológica, Instituto Nacional de Salud del Niño San Borja, Lima, Peru

Cytomegalovirus (CMV) infection is a common complication in patients undergoing hematopoietic stem cell transplantation (HSCT). Management of refractory CMV infections, especially in developing countries, can be challenging due to the limited availability of second and third-line antiviral drugs or alternative treatments. Here, we present a case of an 8 years-old patient diagnosed with acute myeloid leukemia. Eight months post-diagnosis, the patient underwent TCR-$\alpha\beta^+$/CD19$^+$-depleted haploidentical HSCT. Both the donor and recipient tested positive for anti-CMV IgG and negative for IgM antibodies. Before transplantation, the patient received CMV prophylaxis in the form of intravenous ganciclovir. Post-transplantation, the patient exhibited oscillating CMV viral loads and was diagnosed with a refractory infection. Treatment with ganciclovir, foscarnet, and cidofovir was unsuccessful. Sequencing of UL-54 and UL-97 genes was performed to rule out potential resistance to first-line treatment. Ten months after the HSCT, the child died from hypovolemic shock due to gastrointestinal bleeding. This is the first case reported in Peru and Latin America of a refractory CMV infection in a pediatric HSCT recipient without evidence of clinical symptoms and CMV genetic resistance. This case demonstrates the need for alternative treatments to manage refractory CMV infections, especially in haploidentical HSCT cases where drug resistance is frequent (~15%). Furthermore, this case highlights the importance of using highly sensitive genetic tools to detect mutations associated with virus resistance in a broader range of the viral genome.

KEYWORDS

HSCT, cytomegalovirus infection, antiviral resistance, ganciclovir, foscarnet, cidofovir, case report

Introduction

Human herpesvirus 5 or human cytomegalovirus (CMV) is a member of the Herpesviridae family (1). CMV seroprevalence in Latin America (60%–90%) is significantly higher than in Europe or North America (2). The infection among immunocompetent individuals is usually asymptomatic, but among transplanted individuals, CMV can cause fatal diseases such as pneumonia, enteritis, cystitis, and encephalitis (3). Additionally, infection can cause graft failure due to the inhibition of the myelopoiesis (4).

Post-transplant CMV infection monitoring relies on weekly qPCR-based detection and quantification of blood viral load (5). This approach enables preemptive antiviral therapy to prevent end-stage organ disease (5). Approved antiviral agents for CMV infections include ganciclovir, valganciclovir, foscarnet, cidofovir, letermovir, and maribavir (6, 7).

One main challenge in managing CMV infection in transplant recipients is refractory infections, which may be related to genetic or non-genetic mechanisms (8). The significant incidence of resistant CMV, especially among haploidentical HSCT recipients (~15%) (9), makes the need for quick and accurate detection of resistant cases evident. Typically, the choice of therapeutic approaches is adjusted according to the specific resistance profile of the virus with the aim of achieving early remission of the infection. CMV drug resistance is evaluated by conventional PCR and sequencing of the UL-54 (phosphotransferase) and UL-97 (DNA polymerase) genes (10).

We report here the case of a high-risk pediatric patient with acute myeloid leukemia who developed a refractory CMV infection. Despite treatment with ganciclovir, valganciclovir, foscarnet, and cidofovir, the infection persisted. This is the first case reported in Peru and Latin America of refractory CMV infection in a pediatric HSCT recipient without evidence of clinical symptoms or genetic resistance.

This case highlights the need for highly sensitive genetic tests to characterize mutations associated with CMV resistance to drugs and for alternative treatments to manage refractory CMV infections in order to extend the survival chances of individuals undergoing HSCT.

Case report

We present the case of an 8 years-old male patient who underwent haploidentical hematopoietic stem cell transplantation (HSCT) for acute myeloid leukemia. The procedure was carried out on November 18th, 2019, at the Instituto Nacional de Salud del Niño San Borja in Lima, Peru. The patient received an allograft from his mother with a 3/6 HLA match after depleting $CD19^+$ and $TCR\alpha\beta^+$ cells.

The patient received chemotherapy according to the ALL-BFM 2009 protocol and achieved complete remission after four blocks of consolidation (11). The conditioning regimen involved the administration of fludarabine, antithymocyte globulin, cyclophosphamide, and total body irradiation. No prophylaxis for graft-versus-host disease (GvHD) was provided before transplantation. The histocompatibility study showed haploidentical compatibility with his mother at the HLA-B and HLA-DQ loci, resulting in the selection of the mother as the transplant donor.

The patient had no active CMV infection prior to transplantation. However, both the recipient and donor tested positive for anti-CMV IgG. Anti-CMV prophylaxis was started 16 days prior to transplantation, with the initial administration of ganciclovir at a dose of 5 mg/kg/12 h for 6 days, suspension of treatment for 7 days, and restart of ganciclovir treatment at a dose of 5 mg/kg/12 h for 3 days.

No immunosuppressive therapy was administered following transplantation. At day +14, immune reconstitution was assessed by absolute neutrophil count, which was greater than 0.5×10^9 cells/L (neutrophil count = 0.6×10^9 cells/L). Recovery of $CD8^+$, $CD19^+$, and NK cells was faster than $CD4^+$ cells. $CD4^+$ recovery occurred at 6 months post-HSCT, while $CD8^+$, $CD19^+$, and NK recovery occurred during the first trimester (Table 1). At day +35, the patient presented complete chimerism with >95% donor cells for all three cell lineages (T, B, and myeloid cells), confirming engraftment without GvHD.

The viral load of CMV was quantified by real-time PCR (targeting the 4 IE antigen gene) in peripheral blood (PB) samples. Reactivation of CMV infection was observed on day +32, with the presence of 688 DNA copies/mL. The kinetics of the viral load showed a pattern consistent with a CMV infection refractory to the administered drugs, observing an increase in viral load, accompanied by a fall and a new increase, throughout the post-HSCT period (see Figure 1).

Because of infection reactivation, preemptive treatment was started with intravenous ganciclovir (5 mg/kg/12 h) for 7 days, followed by foscarnet (180 mg/kg/day) for 10 days, ganciclovir (5 mg/kg/12 h) for 46 days, foscarnet (180 mg/kg/day) for 15 days, and cidofovir (5 mg/kg/week) for 4 weeks. The highest viral load (2.5×10^5 copies/mL) was recorded on day +67 during the application of the antiviral treatment and gradually decreased until it reached 223 copies/mL on day +123. An invasive pulmonary infection with small pseudo-nodules in the right lung was also recorded. No causative agents were identified, and the infection was managed with amphotericin B and voriconazole.

On day +127, an increase in viral load from 223 copies/mL to 1,452 copies/mL was observed, restarting treatment with foscarnet (180 mg/kg/day) for 18 days, cidofovir (5 mg/kg/week) for 2 weeks, ganciclovir (5 mg/kg/12 h) for 3 days and foscarnet (180 mg/kg/day) for 80 more days, until day +273. On the fourteenth day after the administration of foscarnet (day +207), the viral load fell below the detection limit (equivalent to 120 copies/mL). However, 4 days later

TABLE 1 Immune recovery after HSCT.

Cell lineage	Cell count (cells/μL)			Reference values (cells/μL)
	2 months post-HSCT	3 months post-HSCT	6 months post-HSCT	
$CD4^+$	59	286	455	300–2,000
$CD8^+$	196	466	541	300–1,800
$CD19^+$	655	1,102	1,123	200–1,600
NK	1,225	892	725	90–900

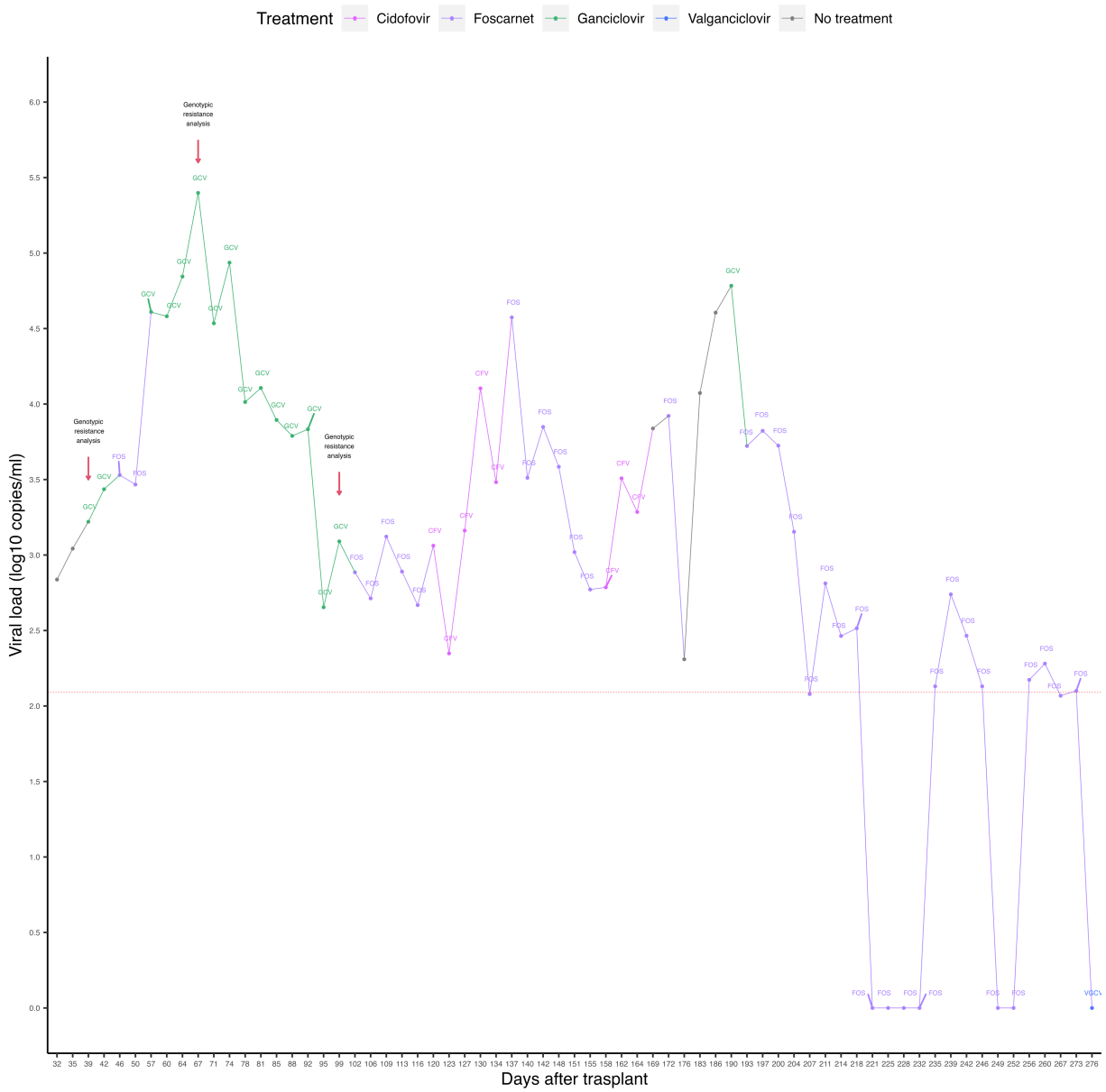

FIGURE 1
Timeline representing CMV viral loads and antiviral treatments of the case. The dashed red horizontal line represents the limit of detection of the qPCR assay. The red arrows indicate the time points of genotypic resistance analysis. GCV, ganciclovir; FOS, foscarnet; CFV, cidofovir; VGCV, valganciclovir.

(day +211), an increase in the viral load to 649 copies/ml was observed during the application of foscarnet. The viral load then became negative at day +221, remaining undetectable until day +232. Three days later, virus reactivation was observed with a viral load of 135 copies/mL (day +235), which increased to 549 copies/mL, then decreased to 292 copies/mL, 135 copies/mL, and finally became negative on day +249. The last reactivation was observed on day +256, with a viral load of 149 copies/mL. On day +275, the patient started treatment with oral valganciclovir (15–18 mg/kg/day) for 9 days. After the last reactivation, the viral load became undetectable on day +276, coinciding with the administration of valganciclovir.

Due to our suspicion of a refractory CMV infection, PB samples were analyzed by Sanger sequencing to identify mutations, deletions, insertions, or substitutions in the UL-54 and UL-97 genes known to confer genetic resistance to drugs. Nevertheless, genotypic analyses performed on days +39, +67, and +99 failed to detect modifications compatible with genetic drug resistance.

During the post-HSCT period, the patient showed coinfection with adenovirus and BK polyomavirus, detected by quantitative PCR in plasma and serum. These infections were detected on days +11 and +18 and successfully cleared at days +148 and +188, respectively.

On day +245 of HSCT, the patient was diagnosed with disease relapse by flow cytometry and PCR of bone marrow samples (7.49% of pathological myeloid blasts and 11.14% of AML1-ETO$^+$ cells). The biopsy of the pterygoid mass confirmed infiltration of blasts in the right sphenoid maxillary sinus, which extended from the right pterygoid to invade the intracranial extra-axial space at the level of the temporal fossa and right choana. Intravenous cytarabine (30 mg every 24 h) was started for 8 days, and intrathecal cytarabine (30 mg every 24 h) for 3 days, with no effect on disease remission. Chimerism tests revealed mixed

chimerism greater than 94%, with donor T, B, and myeloid cell populations greater than 95%, 94%, and 95%, respectively. The patient presented volume growth of the right side of the face, palpebral ptosis, and visual loss of the right eye due to infiltration of blasts. On day +276, the patient was discharged with parental consent and received palliative therapy for pain management with morphine administration.

On day +290, the patient was admitted to the emergency department due to hematemesis followed by fainting. Laboratory tests revealed severe anemia, acute kidney disease due to tumor lysis, leukocytosis with blastemia, and thrombocytopenia. The patient was discharged 2 days later with a poor short-term prognosis. On day +308, the patient was readmitted to the emergency department due to hematemesis. On physical examination, he presented poor general condition, with paleness, tachycardia, hypotension, fever, sunken eyes, multiple ecchymoses, increased volume of the left arm, and chronic malnutrition. Laboratory studies revealed leukocytosis due to the presence of blasts, thrombocytopenia, anemia, high levels of C-reactive protein (354.6 mg/L), urea (80.2 mg/dL), urea nitrogen (37.45 mg/dL), and procalcitonin (86.17 ng/mL). One day after readmission, the patient died of hypovolemic shock due to intestinal bleeding.

Discussion

This is the first case reported in Peru and Latin America describing persistent CMV infection in a pediatric haploidentical HSCT recipient. CMV infection significantly increases morbidity in transplant patients and represents a major risk factor for survival (12). The incidence of CMV infection in individuals undergoing haploidentical HSCT is significantly higher than in those with matched sibling donors (MSD) or matched unrelated donors (MUD) (85.7%, 39.0%, 55.6%, respectively; $p < 0.001$) (13). Among haploidentical HSCT patients, CMV reactivation occurs in 55% of cases, leading to CMV disease in 5% (14). Receiving a haploidentical HSCT is considered a risk factor for CMV infection development (OR = 4.24, $p = 0.007$) (15).

Refractory infections in HSCT recipients are usually common (12%) (12). Refractory CMV infection is characterized by a viremia increase of more than 1-$\log_{10}$ after at least 2 weeks of antiviral treatment (8). It is important to note that some drugs used to treat the CMV infection in the present case could not be administered on time due to shortage at the institution.

The presence of refractory infection constitutes a significant risk for the survival of infected patients (3 years event-free survival: 53% in cases of resistant CMV vs. 87% in cases of susceptible CMV; $p < 0.001$) (12). In the present case, a persistent viral load was observed during the 9 months post-HSCT, with an increase of 2.5-$\log_{10}$ compared to the initial viral load of 688 copies/mL. The highest viral load was 2.5×10^5 copies/mL on day +67. These findings confirmed the presence of a refractory CMV infection, which is characterized by fluctuating viral loads.

Initial treatment for CMV infection among HSCT recipients consists of ganciclovir or valganciclovir for at least 2 weeks (3). In case of adverse events (neutropenia or thrombocytopenia) or intolerance, using foscarnet for 2–3 weeks or cidofovir for 2 weeks is recommended (3). Foscarnet administration as a first-line treatment has been suggested for adult patients presenting bone marrow function (16). In cases of mutations conferring high resistance to foscarnet and cidofovir, such as the C592G mutation in the UL97 gene, a switch to ganciclovir is recommended, expecting virus clearance within 14 days (16, 17).

In addition to conventional pharmacological approaches, CMV-specific T-cell therapy (CMV-TCT) has been suggested as a promising treatment option for CMV infections following HSCT. The therapy is suggested for cases of refractory CMV with progressive viral disease such as pneumonitis and colitis (18). Donor-derived CMV-TCT has been proven to be effective in treating CMV infections in pediatric patients undergoing HSCT, with an overall response rate of 89.5% (19). Combining CMV-TCT with foscarnet has demonstrated efficacy in resolving CMV-associated retinitis in a pediatric recipient of haploidentical TCR$\alpha\beta^+$/CD19$^+$ cell-depleted HSCT (20). Notably, this therapeutic strategy has not been reported for HSCT recipients in Peru. Challenges related to logistics and the cost of the T-cell separation process may pose significant obstacles to the future implementation of this therapy in developing countries.

Previous reports suggest combining viral load monitoring with genetic screening to detect mutations in the UL-97 and UL-54 genes for treatment adjustment based on the specific viral resistance profile (21). However, in the presented case, genetic resistance testing during the first 3 months post-HSCT did not reveal any known mutations associated with drug resistance. Contrarily, the highest viral load observed during the entire post-transplant period occurred at day +67 (2.5×105 copies/ml), approximately 2 months after the transplant.

Known drug resistance in CMV results primarily from mutations in the UL-97 and UL-54 genes. UL-97 mutations affect ganciclovir activation but do not impact susceptibility to foscarnet or cidofovir (22). UL-54 mutations confer resistance to all available drugs, and their combination with UL-97 mutations results in high-level resistance to multiple drugs (23). Additionally, in transplant recipients, rare mutations associated with letermovir resistance have also been reported in the UL-56 gene, which encodes a component of the viral terminase complex responsible for the cleavage and packaging of viral genome into nascent viral capsids (24–26). Among solid organ transplant recipients, mutations in the UL-97 and UL-54 genes account for 26% of drug resistance cases, whereas mutations in UL-56 account for only 3% of cases (27).

The case presented here is exceptional since there was no response to treatment with ganciclovir, foscarnet, and cidofovir despite the absence of mutations associated with CMV resistance. The last measurement of viral load before the patient's discharge at day +276, suggested virus clearance by foscarnet, although no additional tests were performed to confirm a possible new reactivation. A similar case of an older adult with chronic myelomonocytic leukemia who underwent HSCT with an MUD donor was previously reported in 2022. The patient presented four episodes of CMV infection with no mutations on the UL-97 and UL-54 genes. Intriguingly, however, analysis of the UL-56 gene revealed an unknown mutation (R246C). This mutation was associated with a superior replicative capacity but did not necessarily lead to a reported increase drug resistance (27). The combination of enhanced replicative capacity and the absence of mutations in UL-97 and UL-54 genes may explain persistent viral loads in cases like the one presented here, suggesting the importance of including the analysis of the UL-56 gene in addition to UL-97 and UL-54 genes in similar cases.

On day +308, the patient died of gastrointestinal bleeding, possibly caused by CMV colitis, similar to a previous report (28). Since gastrointestinal biopsies were not performed, the diagnosis of a probable CMV infection of the gastrointestinal tract could not be verified. Upper and lower gastrointestinal tract infections are more frequent in transplant recipients with underlying hematological conditions than in transplant patients with solid tumors ($p = 0.02$) (29). Therefore, it is essential that

healthcare institutions managing transplanted patients have access to tests permitting CMV detection and quantification in the gastrointestinal tract (30). In the case reported here, despite the availability of these laboratory tests, signs of gastrointestinal involvement in the patient did not manifest themselves in the final month before death. During this period, no further testing was performed to confirm probable CMV gastrointestinal disease, as the patient was in palliative care.

In transplant patients, the initial episode of DNAemia is usually asymptomatic (>80%). However, approximately 15% of these individuals have CMV disease when the first viremia is detected, which includes CMV syndrome, pneumonia, and gastrointestinal disease (31). Gastrointestinal bleeding in haploidentical HSCT recipients may occur from day +1 to +892 post-transplantation, with clinical presentations that include rectal bleeding (69%), hematemesis (20%) and melena (9%) (32). Timely treatment is crucial to increase the chances of survival in transplant patients, especially in HSCT patients, as mortality from CMV-induced gastrointestinal can be as high as 42% (29). Hence, monitoring the potential development of CMV disease in transplant patients with persistent viral loads is of critical importance.

Documented cases of HSCT recipients with refractory or resistant CMV infections are scarce worldwide and more typically involve adult solid organ transplants (26, 33–35). In Latin America, only one case of a heart transplant recipient with suspected genetic resistance has been reported, involving a 12 years-old pediatric patient initially treated with ganciclovir upon diagnosis of CMV-DNAemia. As viral loads persisted, foscarnet was administered, resulting in remission of the infection (36). Genetic resistance tests were not conducted, presumably due to the absence of this type of testing in the healthcare institution.

The case reported here highlights the importance of actively monitoring the development of CMV disease in patients with asymptomatic CMV DNAemia and considering alternative therapeutic options. It also highlights the need for more sensitive genetic tests, such as next-generation sequencing (NGS), since standard sequencing fails to detect relevant mutations in 9% of cases (37). The need for this approach is exemplified by the case of an 8 months-old who received an HSTC from an MSD. NSG detected the D588N mutation in the UL-54 gene, while standard sequencing failed to detect it. This mutation is clinically relevant due to its association with resistance to foscarnet, ganciclovir, and cidofovir (38).

In summary, this report described the case of a patient diagnosed with acute myeloid leukemia who underwent haploidentical HSCT and subsequently developed CMV infection refractory to first, second, and third-line treatment. The infection had an atypical asymptomatic presentation with no evidence of genetic resistance in the UL-97 and UL-54 genes. Although thrombocytopenia may have caused gastrointestinal bleeding, it cannot be ruled out that CMV colitis caused this episode.

Data availability statement

The original contributions presented in the study are included in the article/supplementary material, further inquiries can be directed to the corresponding author.

Ethics statement

The study was approved by the Comité Institucional de Ética en Investigación, Instituto Nacional de Salud del Niño San Borja. Written informed consent was obtained from the minor(s)' legal guardian/next of kin for the publication of any potentially identifiable images or data included in this article.

Author contributions

AP-C: Conceptualization, Formal analysis, Methodology, Writing – original draft. KE-R: Investigation, Writing – original draft. JT-R: Supervision, Writing – review & editing. HM-M: Supervision, Writing – review & editing, Conceptualization, Funding acquisition.

Funding

The author(s) declare financial support was received for the research, authorship, and/or publication of this article. This research was funded by PROCIENCIA—CONCYTEC within the framework of the call "Proyecto Investigación Básica, 2018-01" (Contract number 107-2018-FONDECYT). The funder had no role in study design, data collection and analysis, decision to publish, or preparation of the manuscript.

Acknowledgments

We would like to express our gratitude to the parents of the child whose case was reported for granting us permission to publish their child's case. We would also like to thank K. Marshall McNagny for taking the time to review the manuscript and providing valuable suggestions that greatly improved it.

Conflict of interest

The authors declare that the research was conducted in the absence of any commercial or financial relationships that could be construed as a potential conflict of interest.

Publisher's note

References

1. Gugliesi F, Coscia A, Griffante G, Galitska G, Pasquero S, Albano C, et al. Where do we stand after decades of studying human cytomegalovirus? *Microorganisms*. (2020) 8:685. doi: 10.3390/microorganisms8050685

2. Fowler K, Mucha J, Neumann M, Lewandowski W, Kaczanowska M, Grys M, et al. A systematic literature review of the global seroprevalence of cytomegalovirus: possible implications for treatment, screening, and vaccine development. *BMC Public Health*. (2022) 22:1659. doi: 10.1186/s12889-022-13971-7

3. Cho S-Y, Lee D-G, Kim H-J. Cytomegalovirus infections after hematopoietic stem cell transplantation: current status and future immunotherapy. *Int J Mol Sci*. (2019) 20:2666. doi: 10.3390/ijms20112666

4. Renzaho A, Podlech J, Kühnapfel B, Blaum F, Reddehase MJ, Lemmermann NAW. Cytomegalovirus-associated inhibition of hematopoiesis is preventable by cytoimmunotherapy with antiviral CD8 T cells. *Front Cell Infect Microbiol*. (2020) 10:138. doi: 10.3389/fcimb.2020.00138

5. Jakharia N, Howard D, Riedel DJ. CMV infection in hematopoietic stem cell transplantation: prevention and treatment strategies. *Curr Treat Options Infect Dis*. (2021) 13:123–40. doi: 10.1007/s40506-021-00253-w

6. Panda K, Parashar D, Viswanathan R. An update on current antiviral strategies to combat human cytomegalovirus infection. *Viruses*. (2023) 15:1358. doi: 10.3390/v15061358

7. Yong MK, Shigle TL, Kim Y-J, Carpenter PA, Chemaly RF, Papanicolaou GA. American Society for Transplantation and Cellular Therapy Series: #4—cytomegalovirus treatment and management of resistant or refractory infections after hematopoietic cell transplantation. *Transplant Cell Ther*. (2021) 27:957–67. doi: 10.1016/j.jtct.2021.09.010

8. Sassine J, Khawaja F, Shigle TL, Handy V, Foolad F, Aitken SL, et al. Refractory and resistant cytomegalovirus after hematopoietic cell transplant in the letermovir primary prophylaxis era. *Clin Infect Dis*. (2021) 73:1346–54. doi: 10.1093/cid/ciab298

9. Shmueli E, Or R, Shapira MY, Resnick IB, Caplan O, Bdolah-Abram T, et al. High rate of cytomegalovirus drug resistance among patients receiving preemptive antiviral treatment after haploidentical stem cell transplantation. *J Infect Dis*. (2014) 209:557–61. doi: 10.1093/infdis/jit475

10. Recio V, González I, Tarragó D. Cytomegalovirus drug resistance mutations in transplant recipients with suspected resistance. *Virol J*. (2023) 20:153. doi: 10.1186/s12985-023-02127-7

11. Instituto Nacional de Salud del Niño San Borja. *Guía de Práctica Clínica de Leucemia Linfoblastica Aguda*. Lima, Peru (2016). Available at: https://www.insnsb.gob.pe/guia-clinica-sub-unidad-de-atencion-integral-especializada-de-tph-2/. (Accessed September 4, 2023)

12. Szmit Z, Frączkiewicz J, Salamonowicz-Bodzioch M, Król A, Ussowicz M, Mielcarek-Siedziuk M, et al. The impact of high CMV viral load and refractory CMV infection on pediatric HSCT recipients with underlying non-malignant disorder. *J Clin Med*. (2022) 11:5187. doi: 10.3390/jcm11175187

13. Lin C-H, Su Y-J, Hsu C-Y, Wang P-N, Teng C-LJ. Haploidentical allogeneic hematopoietic stem cell transplantation increases the risk of cytomegalovirus infection in adult patients with acute leukemia. *Transpl Infect Dis*. (2019) 21:e13096. doi: 10.1111/tid.13096

14. Yeh T-J, Yang C-I, Huang C-T, Wang M-H, Chuang T-M, Ke Y-L, et al. Revisit of the association between cytomegalovirus infection and invasive fungal infection after allogeneic hematopoietic stem cell transplantation: a real-world analysis from a high CMV Seroprevalence area. *J Fungi*. (2022) 8:408. doi: 10.3390/jof8040408

15. Jaing T-H, Chang T-Y, Chen S-H, Wen Y-C, Yu T-J, Lee C-F, et al. Factors associated with cytomegalovirus infection in children undergoing allogeneic hematopoietic stem-cell transplantation. *Medicine*. (2019) 98:e14172. doi: 10.1097/MD.0000000000014172

16. Einsele H, Ljungman P, Boeckh M. How I treat CMV reactivation after allogeneic hematopoietic stem cell transplantation. *Blood*. (2020) 135:1619–29. doi: 10.1182/blood.2019000956

17. Springer KL, Chou S, Li S, Giller RH, Quinones R, Shira JE, et al. How evolution of mutations conferring drug resistance affects viral dynamics and clinical outcomes of cytomegalovirus-infected hematopoietic cell transplant recipients. *J Clin Microbiol*. (2005) 43:208–13. doi: 10.1128/JCM.43.1.208-213.2005

18. Kállay K, Kassa C, Réti M, Karászi É, Sinkó J, Goda V, et al. Early experience with CliniMACS prodigy CCS (IFN-gamma) system in selection of virus-specific T cells from third-party donors for pediatric patients with severe viral infections after hematopoietic stem cell transplantation. *J Immunother*. (2018) 41:158–63. doi: 10.1097/CJI.0000000000000197

19. Ruan Y, Luo T, Liu Q, Liu X, Chen L, Wen J, et al. Features of cytomegalovirus infection and evaluation of cytomegalovirus-specific T cells therapy in children's patients following allogeneic hematopoietic stem cell transplantation: a retrospective single-center study. *Front Cell Infect Microbiol*. (2022) 12:1027341. doi: 10.3389/fcimb.2022.1027341

20. Seo S, Smith C, Fraser C, Patheja R, Shah SP, Rehan S, et al. Adoptive T-cell therapy for pediatric cytomegalovirus-associated retinitis. *Blood Adv*. (2019) 3:1774–7. doi: 10.1182/bloodadvances.2019000121

21. El Chaer F, Shah DP, Chemaly RF. How I treat resistant cytomegalovirus infection in hematopoietic cell transplantation recipients. *Blood*. (2016) 128:2624–36. doi: 10.1182/blood-2016-06-688432

22. Hakki M, Chou S. The biology of cytomegalovirus drug resistance. *Curr Opin Infect Dis*. (2011) 24:605–11. doi: 10.1097/QCO.0b013e32834cfb58

23. Hantz S, Garnier-Geoffroy F, Mazeron M-C, Garrigue I, Merville P, Mengelle C, et al. Drug-resistant cytomegalovirus in transplant recipients: a French cohort study. *J Antimicrob Chemother*. (2010) 65:2628–40. doi: 10.1093/jac/dkq368

24. Kleiboeker SB. Prevalence of cytomegalovirus antiviral drug resistance in transplant recipients. *Antivir Res*. (2023) 215:105623. doi: 10.1016/j.antiviral.2023.105623

25. Chou S. Rapid *in vitro* evolution of human cytomegalovirus UL56 mutations that confer letermovir resistance. *Antimicrob Agents Chemother*. (2015) 59:6588–93. doi: 10.1128/AAC.01623-15

26. Cherrier L, Nasar A, Goodlet KJ, Nailor MD, Tokman S, Chou S. Emergence of letermovir resistance in a lung transplant recipient with ganciclovir-resistant cytomegalovirus infection. *Am J Transplant*. (2018) 18:3060–4. doi: 10.1111/ajt.15135

27. Santos Bravo M, Tilloy V, Plault N, Palomino SS, Mosquera MM, Navarro Gabriel M, et al. Assessment of UL56 mutations before letermovir therapy in refractory cytomegalovirus transplant recipients. *Microbiol Spectr*. (2022) 10:e0019122. doi: 10.1128/spectrum.00191-22

28. Bhat V, Joshi A, Sarode R, Chavan P. Cytomegalovirus infection in the bone marrow transplant patient. *World J Transplant*. (2015) 5:287–91. doi: 10.5500/wjt.v5.i4.287

29. Torres HA, Kontoyiannis DP, Bodey GP, Adachi JA, Luna MA, Tarrand JJ, et al. Gastrointestinal cytomegalovirus disease in patients with cancer: a two decade experience in a tertiary care cancer center. *Eur J Cancer*. (2005) 41:2268–79. doi: 10.1016/j.ejca.2005.07.011

30. Suárez-Lledó M, Marcos MÁ, Cuatrecasas M, Bombi JA, Fernández-Avilés F, Magnano L, et al. Quantitative PCR is faster, more objective, and more reliable than immunohistochemistry for the diagnosis of cytomegalovirus gastrointestinal disease in allogeneic stem cell transplantation. *Biol Blood Marrow Transplant*. (2019) 25:2281–6. doi: 10.1016/j.bbmt.2019.07.016

31. Lodding IP, da Cunha Bang C, Sørensen SS, Gustafsson F, Iversen M, Kirkby N, et al. Cytomegalovirus (CMV) disease despite weekly preemptive CMV strategy for recipients of solid organ and hematopoietic stem cell transplantation. *Open Forum Infect Dis*. (2018) 5:ofy080. doi: 10.1093/ofid/ofy080

32. Sun X, Su Y, Liu X, Zhang Y, He Y, Han W, et al. Overt gastrointestinal bleeding following haploidentical haematopoietic stem cell transplantation: incidence, outcomes and predictive models. *Bone Marrow Transplant*. (2021) 56:1341–51. doi: 10.1038/s41409-020-01187-5

33. Chon WJ, Kadambi PV, Xu C, Becker YT, Witkowski P, Pursell K, et al. Use of leflunomide in renal transplant recipients with ganciclovir-resistant/refractory cytomegalovirus infection: a case series from the University of Chicago. *Case Rep Nephrol Dial*. (2015) 5:96–105. doi: 10.1159/000381470

34. Paolucci S, Campanini G, Cassaniti I, Tebaldi A, Novazzi F, Fratini A, et al. Emergence of letermovir-resistant HCMV UL56 mutant during rescue treatment in a liver transplant recipient with ganciclovir-resistant infection HCMV: a case report. *BMC Infect Dis*. (2021) 21:994. doi: 10.1186/s12879-021-06694-4

35. Gómez Valbuena I, Alioto D, Serrano Garrote O, Ferrari Piquero JM. Uso de leflunomida en infección de citomegalovirus resistente: a propósito de un caso. *Farm Hosp*. (2016) 40:52–4. doi: 10.7399/fh.2016.40.1.10161

36. Rojas-Contreras C, De la Cruz-Ku G, Vilcarromero S, Villacaqui Ayllon R, Valcarcel-Valdivia B. Reporte de caso de resistencia al ganciclovir en enfermedad por citomegalovirus postrasplante cardiaco: case report. *Rev Peru Med Exp Salud Publica*. (2018) 35:145–9. doi: 10.17843/rpmesp.2018.351.3562

37. López-Aladid R, Guiu A, Mosquera MM, López-Medrano F, Cofán F, Linares L, et al. Improvement in detecting cytomegalovirus drug resistance mutations in solid organ transplant recipients with suspected resistance using next generation sequencing. *PLoS One*. (2019) 14:e0219701. doi: 10.1371/journal.pone.0219701

38. Mousavi-Jazi M, Schloss L, Drew WL, Linde A, Miner RC, Harmenberg J, et al. Variations in the cytomegalovirus DNA polymerase and phosphotransferase genes in relation to foscarnet and ganciclovir sensitivity. *J Clin Virol*. (2001) 23:1–15. doi: 10.1016/s1386-6532(01)00160-3

Frontiers in Medicine

Translating medical research and innovation into improved patient care

A multidisciplinary journal which advances our medical knowledge. It supports the translation of scientific advances into new therapies and diagnostic tools that will improve patient care.

Discover the latest Research Topics

See more →

Frontiers

Avenue du Tribunal-Fédéral 34
1005 Lausanne, Switzerland
frontiersin.org

Contact us

+41 (0)21 510 17 00
frontiersin.org/about/contact